Universitat Autònoma de Barcelona

The source of interleukin-6 in the central nervous system determines its effects on body weight and behavior

Olaya Fernández Gayol

ADVERTIMENT. L'accés als continguts d'aquesta tesi queda condicionat a l'acceptació de les condicions d'ús establertes per la següent llicència Creative Commons: http://cat.creativecommons.org/?page_id=184

ADVERTENCIA. El acceso a los contenidos de esta tesis queda condicionado a la aceptación de las condiciones de uso establecidas por la siguiente licencia Creative Commons: http://es.creativecommons.org/blog/licencias/

WARNING. The access to the contents of this doctoral thesis it is limited to the acceptance of the use conditions set by the following Creative Commons license: https://creativecommons.org/licenses/?lang=en

Institut de Neurociències
Facultat de Biociències
Departament de Biologia Cel·lular, Fisiologia i Immunologia
Universitat Autònoma de Barcelona

The source of interleukin-6 in the central nervous system determines its effects on body weight and behavior

Olaya Fernández Gayol
2017

Memòria de tesis presentada per
Olaya Fernández Gayol per tal d'optar al grau de
Doctor en Neurociències per la
Universitat Autònoma de Barcelona.

Aquest treball ha estat realitzat sota la direcció del
Doctor **Juan Hidalgo Pareja**, catedràtic d'universitat del
Departament de Biologia Cel·lular, Fisiologia i
Immunologia de la Universitat Autònoma de Barcelona.

Director de tesi — Doctoranda

Dr. Juan Hidalgo Pareja — Olaya Fernández Gayol

I’m only human after all

Rag‘n’bone man

Human

Esta tesis doctoral ha sido realizada con financiación de las siguientes entidades:

- UAB (PIF 456-02-1/2011) y Ministerio de Educación, Cultura y Deporte (FPU2012-00365).
- Ministerio de Economía, Industria y Competitividad (SAF2011-23272) y Fondo Europeo de Desarrollo Regional.

AGRADECIMIENTOS

Es un tópico que todo el mundo repite en los agradecimientos de su tesis (*data not shown*) que esta sección es la que más les ha costado escribir. Pero después de muchos meses redactando los cientos de páginas que se encuentran a continuación, me veo el último día con no más que una lista de gente a la que no quería olvidarme de agradecer y poca idea de cómo ligar sus nombres a su contribución a esta tesis.

Porque si bien las personas más próximas, empezando por mi director de tesis el Dr. Juan Hidalgo, y todas mis colegas de grupo: las Dras. Mercè Giralt y Amalia Molinero, y mis compañeras de penurias (perdón, doctorandas) Gemma Comes, Anna Escrig y Paula Sanchis, han participado en el día a día de mi formación como investigadora, hay otras muchas personas que desde más cerca o más lejos han contribuido también (aunque algunas no lo sepan).

Todas las ya doctoras con las que coincidí en el laboratorio en mis primeras etapas, Bea, Yas y María, me enseñaron desde a hacer PCRs, destetar ratones, dar mis primeros con ImageJ, a hablar por los codos en el despacho (aunque en esto ya tenía experiencia previa). Y quiero creer que yo también les devolví algo, y me siento especialmente orgullosa de haber hecho de Bea una *musical geek* como yo, aunque no haya podido hacer nada para curar su termogénesis deficiente.

También han aportado su granito de arena al día a día todos los compañeros de "ratas", pasados y presentes, y quiero mencionar especialmente a Jordi "Ninja", que alimentó y contribuyó de forma crítica a mi pasión por escribir macros en ImageJ.

Camino, mi pescadito fuera del agua, vivió conmigo la entrada al laboratorio y la vida de norteña en un clima adverso, e hizo con nuestros fines de semana y escapadas varias que pudiese mantener la salud mental en los momentos más duros.

También me han ayudado varios estudiantes de carrera o máster, a los que debo, entre infinidad de cosas, el ahorrarme muchas PCRs (aunque total, "sólo son dos horas") y la práctica de la paciencia y la reformulación de conceptos, muchas gracias Ajna, Adam, Jesús, Neli, Alberto y Alicia. Especialmente a Ali, mi mini-yo, compañera de comilonas y compras.

Nuestra secretaria, Paqui, se merece una sección entera por su constante alegría y efectividad, que sólo se empieza a apreciar completamente cuando se notan las consecuencias de su inexistencia.

Mis agradecimientos también cruzan el charco. Todo el equipo del Dr. Richard Palmiter en la UW en Seattle me acogió como una más, y agradezco enormemente el privilegio de pasar con ellos tres fantásticos meses de ciencia y actividades extra-académicas. Estoy especialmente agradecida a la Dra. Stephanie Padilla, a quien sólo conocía como el nombre detrás de mis sondas de *in situ*, y que resultó ser una fantástica amiga y mentora durante mi estancia allí. Y por supuesto, quiero agradecer a Albert y Eli acogerme en su casa mientras encontraba mi zulillo.

También quisiera, sin entrar en política, mencionar a las entidades o personas que han permitido otros aspectos más mundanos de esta tesis. Por un lado, las causantes de que pudiera comer, siempre manteniendo el nivel que se espera de mi *tupper*, durante estos seis años en el laboratorio: la UAB y el Ministerio de Educación, Cultura y Deporte. Y por otro, Alexandra Elbakyan, sin la cual mucha de mi investigación no hubiera sido posible.

Finalmente, agradecer a mi madre su integridad, y la enseñanza de que cada día hay que hacer las cosas lo mejor posible por la simple satisfacción de hacer bien el trabajo. Un trabajo que, como me decía mi profesor de guitarra, es un 10% de inspiración y un 90% de transpiración.

Muchas gracias a todos ellos y también a todas las personas que se han cruzado en mi camino a lo largo de los años y que, a pesar de no poderlas mencionar aquí, han puesto su granito de arena en formar la persona que soy hoy.

CONTENTS

LIST OF FIGURES

LIST OF TABLES

ACRONYMS

α-MSH	alpha melanocyte-stimulating hormone
ACTH	adrenocorticotropic hormone
ADAM	a desintegrin and metalloprotease
Adrb2	beta2-adrenergic receptor (gene)
AgRP	agouti-related peptide
AKT	protein kinase B
AP-1	activator protein 1
ARC	arcuate nucleus of the hypothalamus
BAT	brown adipose tissue
BBB	blood-brain barrier
BCDF	B-cell differentiation factor
BNST	bed nucleus of the stria terminalis
CART	cocaine- and amphetamine-regulated transcript
Casp3	caspase-3 (gene)
CeA	central nucleus of the amygdala
CKK	cholecystokinin
CNS	central nervous system
CNTF	ciliary neurotrophic factor
CRE	cyclic-AMP-response element
CRH	corticotropin-releasing hormone
CSF	cerebrospinal fluid
CT	cardiotrophin
C_t	threshold cycle (in qPCR)
DBH	dopamine beta-hydroxylase
DMH	dorsomedial hypothalamus
DRG	dorsal root ganglion
E	east
EDTA	ethylenediaminetetraacetic acid
ELISA	enzyme-linked immunosorbent assay
EPM	elevated plus maze
FS	forced swim
FSH	follicle-stimulating hormone
GABA	gamma aminobutyric acid
Gapdh	glyceraldehyde 3-phosphate dehydrogenase (gene)
GFAP	glial fibrillary acidic protein
GH	growth hormone
GLP-1	glucagon-like peptide-1
gp130	glycoprotein 130
sgp130	soluble gp130
GRE	glucocorticoid responsive element
GSK3B	glycogen synthase kinase-3β
HB	hole-board

HCRT	hypocretin/orexin
HFD	high-fat diet
HPA	hypothalamic-pituitary-adrenal (axis)
HSF	hepatocyte stimulating factor
ICV	intracerebroventricular
IFN	interferon
IGF	insulin-like growth factor
IGFBP	IGF binding protein
IKK	IκB kinase
IL-6Rα	IL-6 receptor alpha
mIL-6R	membrane IL-6 receptor
sIL-6R	soluble IL-6 receptor
IL	interleukin
IP	intraperitoneal
IR	insulin receptor
IRS	insulin receptor substrate
ISH	*in situ* hybridization
ITT	insulin tolerance test
IκB	NF-κB inhibitor
JAK/TYK	Janus kinase/Tyrosine kinase
JNK	c-Jun terminal kinase
LH	luteinizing hormone
LHA	lateral hypothalamic area
LIF	leukemia inhibitory factor
LPS	lipopolysaccharide
Mac1	macrophage-1 antigen (gene)
MAPK	mitogen-activated protein kinase
MC3/4R	melanocortin receptor 3 or 4
MCH	melanin-concentrating hormone
mTOR	mammalian target or rapamycin
MWM	Morris water maze
N	north
NAcc	nucleus accumbens
NE	norepinephrine
NF-IL6	nuclear factor for IL-6 expression
NF-κB	nuclear factor kappa B
NGF	nerve growth factor
NP	neuropoietin
NPY	neuropeptide Y
NSE	neuron-specific enolase
NTS	nucleus of the solitary tract
Ob-Rb	long form of the leptin receptor
OF	open field
OGTT	oral glucose tolerance test

OSM	oncostatin M
OVLT	organum vasculosum of the lamina terminalis
PBN	parabrachial nucleus
PGE_2	prostaglandin-E_2
PI3K	phosphatidyl-inositol-3-kinase
PIP_3	phosphatidyl-inositol-3,4,5-trisphosphate
POA	preoptic area
POMC	pro-opiomelanocortin
PRL	prolactin
PVN	paraventricular nucleus
qPCR	real time PCR (semiquantitative)
RANKL	receptor activator of NF-κB ligand
RIA	radioimmunoanalysis
RT-PCR	reverse transcription PCR
S	south
SHP2	SH2-domain-containing phosphatase 2
SNS	sympathetic nervous system
SOCS	suppressor of cytokine signaling
SON	supraoptic nucleus
SRE	serum-responsive enhancer
STAT	signal transducer and activator of transcription
Syn1	synapsin-1
TCR	T-cell receptor
TLR	Toll-like receptor
TNF	tumor necrosis factor
TS	tail suspension
VIP	vasoactive intestinal peptide
VMH	ventromedial hypothalamus
VTA	ventral tegmental area
W	west
WAT	white adipose tissue
Gn	gonadal
Sc	subcutaneous
WSxWS	tryptophan-serine-x-tryptophan-serine (motif)

1 INTRODUCTION

1.1 Interleukin-6

Cytokines are small secreted and soluble proteins, initially discovered in relation to the immune system, that allow cell-to-cell communication, either on the same cells that secrete them (**autocrine** action), on neighboring cells (**paracrine** action) or distant cells (**endocrine** action). Within the cytokine label there are classical naming conventions like lymphokine (cytokines made by lymphocytes), monokines (cytokines made by monocytes), chemokines (cytokines with chemotactic properties) or **interleukins** (cytokines made by and acting on leucocytes). A common trait of all of them is **pleiotropy** (*i.e*. being able to act on several target cells). In addition, many of them are **redundant** with each other, serving similar functions (Zhang and An 2007).

Interleukin-6 (IL-6) was first discovered (albeit not with that name) in the culture supernatants of mitogen or antigen-stimulated peripheral mononuclear cells and seen to be able to induce immunoglobin production in B-cells (Muraguchi et al. 1981). T-cells had been known to produce growth and differentiation factors to activate B-cells into antibody-secreting cells (Kishimoto et al. 1984) so it was only a matter of time until they were properly identified. Human B-cell differentiation factor (BCDF) was later purified as a molecule inducing the final differentiation of B-cells into high-rate immunoglobin (Ig)-secreting cells (BSFp-2) (Hirano et al. 1985). However, in parallel other groups were also working with the same molecule and giving it different names interferon-β2 (INF- β2), 26-kDa protein, hepatocyte stimulating factor (HSF) or hybridoma growth factor (HGF). When the cDNA of all of them was available, it was shown that they were in fact the same protein and the name IL-6 was proposed to unify all (Gauldie et al. 1987; Poupart et al. 1987; Sehgal et al. 1987; Van Damme et al. 1987).

INTRODUCTION

Human *Il6* is located in chromosome 7 (Sehgal et al. 1986), specifically in 7p15-p21 (Ferguson-Smith et al. 1988); and in the proximal region of chromosome 5 in mice (Mock et al. 1989). It was cloned early on in human (Yasukawa et al. 1987), mouse (Van Snick et al. 1988) and rat (Northemann et al. 1989) and all of them have 5 exons and 4 introns. The coding region of the human and murine genes is 60% homologous, while the 5'-flanking regions, implicated in transcriptional regulation, and 3'-untranslated regions, related to mRNA stability, are highly conserved (Tanabe et al. 1988). At the protein level, human IL-6 has 212 aminoacids (aa) and a molecular weight between 23 and 30 kDa, depending on post-translational modifications (e.g. *N*-glycosylation, *O*-glycosylation and serine phosphorylation) (May et al. 1988a; 1988b). Murine IL-6 has 211 aa and a molecular weight ranging from 22 to 29 kDa (Van Snick et al. 1986), due to *O*-glycosylation (Simpson et al. 1988). However, these modifications seem to lack any biological activity specificity since the recombinant molecule produced in bacteria is indistinguishable in function from natural IL-6 (Simpson and Moritz 1988). The homology between the human and the murine proteins is 41% (Figure 1), given that there is little homology in the N-terminal region, but a greater similarity in the middle and C-terminal regions (Simpson et al. 1988).

```
Human   1 MNSFSTSAFGPVAFSLGLLLVLPAAFPAPVPPGEDSKDVAAPHRQPLTSSERIDKQIRYI
Mouse   1 MKFLSARDFHPVAF-LGLMLVTTTAFPTSQVRRGDFTEDTTPNR-PVYTTSQVGGLITHV
            *   *   * **** *** **   ***       *      * * *          *

Human  61 LDGISALRKETCNKSNMCESSKEALAENNLNLPKMAEKDGCFQSGFNEETCLVKIITGLL
Mouse  59 LWEIVEMRKELCNGNSDCMNNDDALAENNLKLPEIQRNDGCYQTGYNQEICLLKISSGLL
          *  *   *** **    *     ******* **     *** * * * * ** **  ***

Human 121 EFEVYLEYLQNRF-ESSEEQARAVQMSTKVLIQFLQKKAKNLDAITTPDPTTNASLLTKL
Mouse 119 EYHSYLEYMKNNLKDNKKDKARVLQRDTETLIHIFNQEVKDLHKIVLPTPISNALLTDKL
          *   **** *          **  *  *  **       * *  *  * *  ** *  **

Human 180 QAQNQWLQDMTTHLILRSFKEFLQSSLRALRQ
Mouse 179 ESQKEWLRTKTIQFILKSLEEFLKVTLRSTRQ
            *  **   *   ** *  ***   **  **
```

Figure 1. Protein sequence alignment of human and mouse IL-6. Amino acid sequences were obtained from PubMed, accession numbers AAH15511.1 (human) and AAI38767.1 (mouse). Sequence alignment was carried out using ExPASy's SIM Alignment Tool for protein sequences (web.expasy.org/sim; Swiss Institute of Bioinformatics).

Structurally, IL-6 is a **four-helix bundle cytokine** (Somers et al. 1997) (Figure 2) and it is considered the founding member of the **neuropoietin** family, which includes other structurally-related cytokines such as IL-11 (Yin et al. 1993), IL-30 (Garbers et al. 2013), IL-31 (Diveu et al. 2004), leukemia inhibitory factor (LIF) (Gearing et al. 1991), ciliary neurotrophic factor (CNTF) (Davis et al. 1993), oncostatin M (OSM) (Gearing et al. 1992), cardiotrophin-1 (CT-1) (Pennica et al. 1995), neuropoietin/cardiotrophin-2 (NP/CT-2) (Derouet et al. 2004), and cardiotrophin-like cytokine factor 1 (CLC, also known as new neurotrophin-1 or B-cell stimulatory factor-3) (Senaldi et al. 1999).

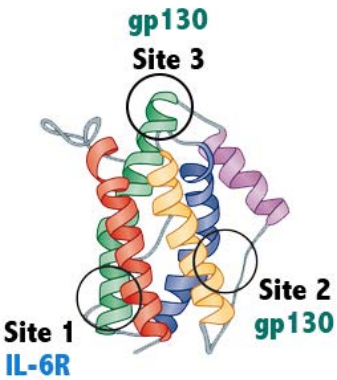

Figure 2. Structure of IL-6. The four helixes are colored in red, green, yellow and blue. Receptor binding sites for both IL-6R (1) and gp130 (2 and 3) are also indicated. Image modified from Hunter and Jones 2015.

1.2 Interleukin-6 receptor and signal transduction

IL-6 binds to the class I cytokine receptor **IL-6Rα** (also known as gp80 or CD126) (Yamasaki et al. 1988). Its N-terminal portion has an Ig-like domain, not required for IL-6 binding in humans but necessary for cell surface expression in mice (Wiesinger et al. 2009), and a cytokine receptor family domain, formed by two fibronectin type III modules and containing four conserved cysteine residues and a tryptophan-serine-x-tryptophan-serine (WSxWS) motif (Bazan 1990). Its intracellular portion is very short, and lacks intrinsic enzymatic activity or any signal transduction motifs (Yamasaki et al. 1988) (Figure 3, left).

Since this receptor cannot signal on its own, it forms a heterooligomer with the **transducing protein gp130** (Taga et al. 1989), a class I hematopoietin receptor, which consists of a N-terminal Ig-like module, a cytokine binding domain (such as the one described for IL-6R) and three membrane-proximal fibronectin type III modules. The intracellular portion of gp130 has tyrosine residues that become phosphorylated during signal transduction and also a di-leucine motif for endocytosis of the signaling complex (Dittrich et al. 1996; Schaper and Rose-John 2015) (Figure 3, right).

Gp130 is a glycoprotein which is ubiquitously expressed (Hibi et al. 1990) and that homodimerizes when interacting with the IL-6-IL6R complex (Taga et al. 1989; Murakami et al. 1993). Ligand binding elicits the internalization of the signaling complex, which could be a way of preventing overstimulation (Dittrich et al. 1994). The exact stoichiometry of the signaling complex is still debated. Initially, when the group of Kishimoto described the interaction with gp130, no specific model was discussed (Taga et al. 1989; Murakami et al. 1993). Later, through ultracentrifugation, co-precipitation or crystallization experiments with IL-6 or related cytokines, two models have been proposed for the interaction of IL-6, IL6-R and gp130 a **tetramer IL-6/IL-6R/(gp130)$_2$** (Grötzinger et al. 1997; Pflanz et al. 2000) or a **hexamer (IL-6) $_2$/(IL-6) $_2$/(gp130)$_2$** (Ward et al. 1994; Paonessa et al. 1995; Boulanger et al. 2003). An integrated model has been proposed by Grötzinger and colleagues (1999) in which the tetramer would be the active form and the hexamer an inactive one involved in inhibition of signaling in the presence of supraoptimal concentrations of the cytokine. The authors propose that this model explains the bell-shaped dose-response curve of IL-6 (van Dam et al. 1993), by which above an optimal concentration, the biological activity diminishes. Another possibility to explain the curve could be ligand-mediated endocytosis, which reduces binding sites and could be in place to prevent overstimulation (Dittrich et al. 1996).

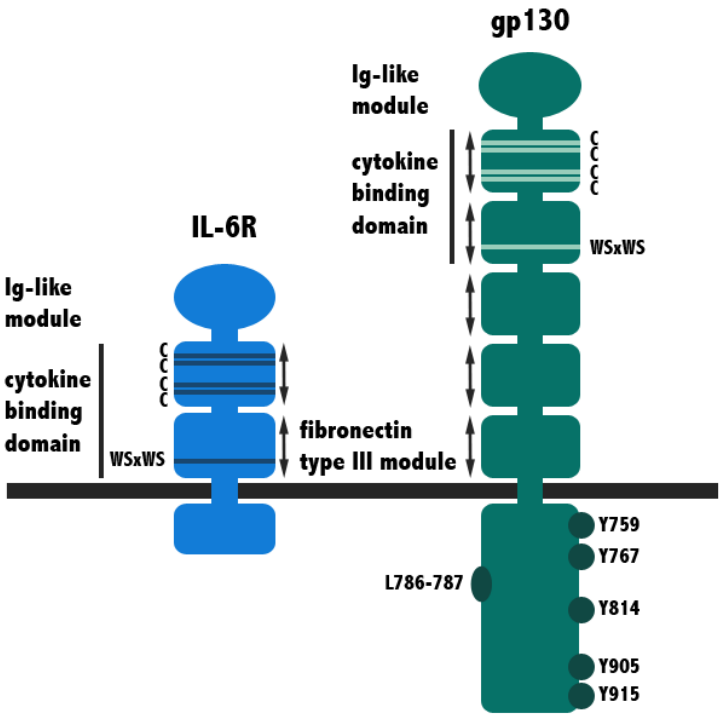

Figure 3. IL6-R and gp130. Both components of the IL-6 signaling complex have a similar extracellular structure composed of an N-terminal Ig-like module and a cytokine-binding domain. The IL6R has two fibronectin type III modules, one with 4 conserved cysteines, and the other (closer to the membrane) with a WSxWS motif. Gp130 has the same two, plus three additional fibronectin type III modules. The intracellular portion of IL-6R is very short and lacks signal transduction motifs, while that of gp130 has several tyrosines (Y) that participate in signaling and a di-leucine (L) motif implicated in endocytosis of the complex. Based on Kishimoto et al. 1995; Dittrich et al. 1996; Hammacher et al. 1998; Schaper and Rose-John 2015.

In any case, the homodimerization of gp130 causes the activation and cross-phosphorylation of the associated **JAK-TYK** kinases (JAK1, JAK2, TYK2) (Stahl et al. 1994), and the subsequent tyrosine-phosphorylation of gp130. This phosphorylation creates specific docking sites (Y767, Y814, Y905 and Y915; residue number pertains to human gp130, mice have an extra Y but the rest are analogous) (Stahl et al. 1995; Gerhartz et al. 1996) for signal transducers and activators of transcription (**STATs**) with SH2 domains (STAT1 and STAT3 –also named acute phase response factor (APRF)-), which then become phosphorylated, dimerize and translocate to the nucleus to regulate the transcription of target

genes (Lütticken et al. 1994; Zhong et al. 1994). It has also been described that SH2-domain-containing phosphatase 2 (**SHP2**) can bind to phosphorylated gp130 (at Y759) (Schaper et al. 1998), and lead to the activation of the mitogen-activated protein kinase (**MAPK**) (Fukada et al. 1996; Schiemann et al. 1997) and phosphatidyl-inositol-3-kinase (**PI3K**) pathways, through the adapter Gab1 (Takahashi-Tezuka et al. 1998). It associates with the plasma membrane through phosphatidyl-inositol-3,4,5-trisphosphate (PIP_3) in a MAPK-dependent process (Eulenfeld and Schaper 2009). It thus then recruits Grb2-SOS, which activates Ras and the rest of the MAPK cascade; or, through PI3K, elicits the activation of AKT (also known as protein kinase B, PKB). AKT acts on many downstream targets, e.g. inhibiting glycogen synthase kinase-3β (GSK3B), **stimulating NF-κB** through the activation of mTOR complex 1, and IKK, which promotes the degradation of the NF-κB inhibitor, IκB (Cross et al. 1995; Manning and Cantley 2007; Bai et al. 2009) (Figure 4).

There exists a **balance between JAK/STAT and SHP2 pathways**, orchestrated by the phosphorylation state of Y759. As mentioned, this is the docking site for SHP2 (when phosphorylated), but also, for suppressor of cytokine signaling 3 (**SOCS3**). This is an independent **inhibitor** of JAK/STAT signaling that is expressed after STAT-mediated transcription of target genes (Lehmann et al. 2003). So, when Y759 is phosphorylated, SOCS3 inhibits JAKs and therefore reduces this pathway, while SHP2 binds to the phosphorylated motif and initiates MAPK signaling. Conversely, when Y759 is not phosphorylated, SOCS3 cannot suppress STAT signaling and SHP2 cannot bind to gp130, favoring JAK/STAT signaling. In addition, SHP2 dephosphorylates gp130's tyrosine motifs, further reducing STAT-mediated signaling (Eulenfeld et al. 2012; Schaper and Rose-John 2015).

The mechanism described above is what is known as the **classical pathway** of IL-6, involving the membrane form of the IL-6R (**mIL-6R**) and **gp130**. However, at the same time as the interaction with gp130, Murakami and

colleagues described a phenomenon involving a soluble form of IL-6R (**sIL-6R**) which could also bind to gp130 in the presence of IL-6 and elicit signal transduction (Murakami et al. 1993). This is peculiar among cytokines since other soluble receptors, e.g. sIL-1-RII (Levine 2004), sTNF-R and sIL-4R (Fernandez-Botran 1991), act as antagonists of cytokine action by preventing binding to the membrane receptor.

Later on, this process has been named **trans-signaling** and the formation of sIL-6R studied further. In humans, it can be produced by limited proteolysis (**shedding**) of the membrane IL-6R (Müllberg et al. 1992; 1993b) or by **alternative splicing** of the mRNA (Lust et al. 1992; Horiuchi et al. 1994). In mice, only shedding has been confirmed. Two Zn^{2+} metalloproteases of the ADAM (a desintegrin and metalloprotease) family, **ADAM 10 and 17**, have been identified as the main responsible proteases for shedding (Marin et al. 2002; Matthews et al. 2003). (Figure 5). It seems that ADAM 10 carries out slow constitutive shedding, while ADAM17 is inducible by pro-inflammatory cytokines, cellular cholesterol depletion, bacterial toxins and apoptotic pathways, among others (Walev et al. 1996; Matthews et al. 2003; Franchimont et al. 2005; Chalaris et al. 2007).

Trans-signaling is **specifically inhibited** by the soluble form of gp130 (**sgp130**) (Jostock et al. 2001), which is produced primarily through alternative splicing (Müllberg et al. 1993a) and has been found in human serum in relatively high concentrations (~400 ng/ml) (Narazaki et al. 1993). Its specificity comes from sgp130 only being able to bind IL-6/sIL-6R and not mIL-6R.

Very recently, a third signaling mechanism has been proposed for dendritic cells. **Cluster signaling** consists in the presentation of an IL-6/IL-6Rα complex by a dendritic cell to a gp130-expressing T cell, in combination with the T-cell receptor (TCR) signal. This interaction elicits JAK/STAT signaling in the T lymphocyte and prompts T_H17 differentiation (Heink et al. 2016).

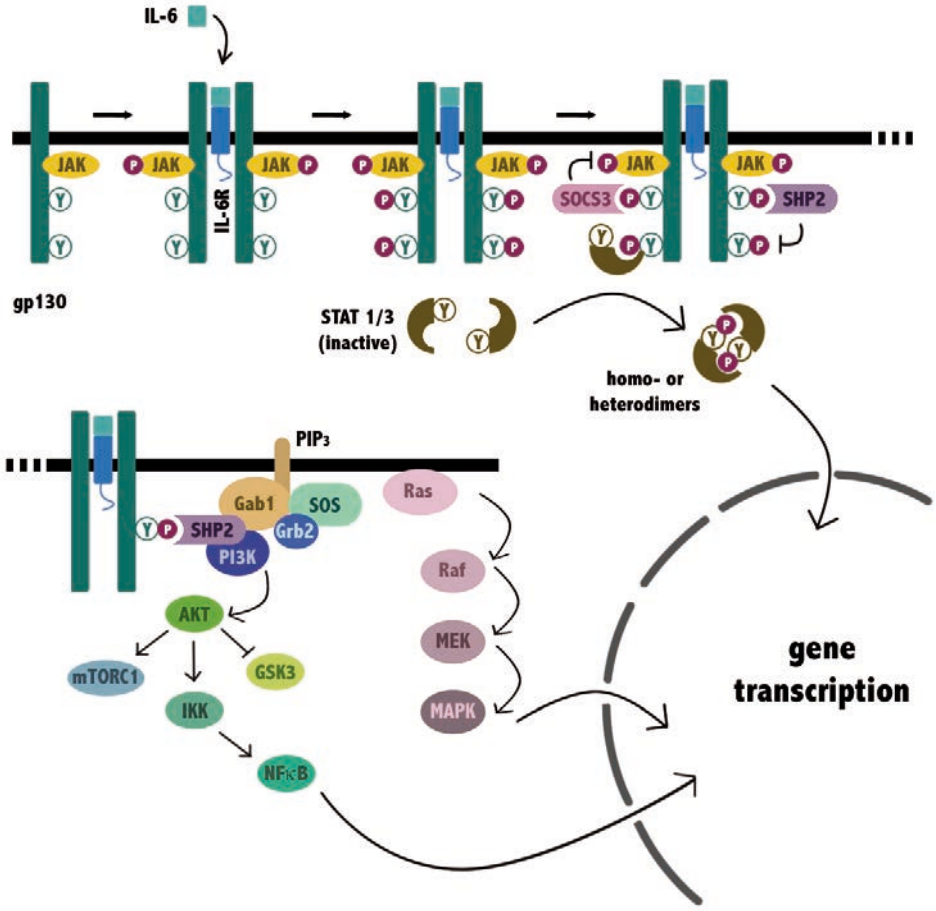

Figure 4. Intracellular signaling. Binding of IL-6 to IL-6R causes dimerization of gp130 and cross-phosphorylation of JAKS. Afterwards, they phosphorylate tyrosine (Y) residues in the intracellular domain of gp130 (top Y759, bottom simplification of the 4 distal motifs). JAKS can also phosphorylate STAT 1/3, which then form dimers and translocate to the nucleus to modify gene transcription. One of the genes they activate is the inhibitor of signaling SOCS3, which binds to Y759. To that same residue also binds SHP2, adaptor protein for MAPK and PI3K signaling. SHP2 also dephosphorylates the distal Y residues of gp130. JAK Janus kinase; STAT signal transducer and activator of transcription; SOCS3 suppressor of cytokine signaling 3; SHP2 SH2-domain containing phosphatase 2; Gab1 Grb2-associated-binding protein 1; PIP_3 phosphatidyl-inositol-3,4,5-trisphosphate; Grb2 growth factor receptor-bound protein 2; SOS son of sevenless; Ras rat sarcoma small GTPase; Raf rapidly accelerated fibrosarcoma kinase; MEK mitogen-activated kinase kinase; MAPK mitogen-activated kinase; PI3K phophatidyl-inositol-3-kinase; AKT protein kinase B; mTORC1 mammalian target of rapamycin complex 1; IKK IκB kinase; NF-κB nuclear factor kappa B; GSK3 glycogen synthase kinase-3β. Adapted from Heinrich et al. 1998; Heinrich et al. 2003; Eulenfeld et al. 2012; and Schaper and Rose-John 2015.

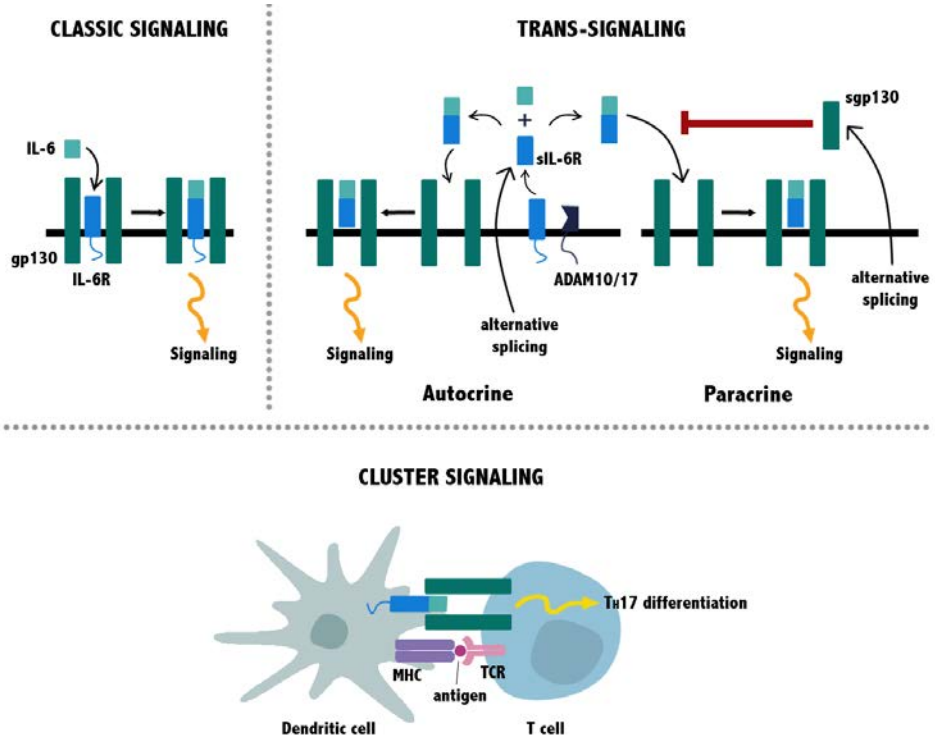

Figure 5. Classic-, trans-signaling and cluster signaling of IL-6. In classical signaling, mIL-6R binds to IL-6 and associates with a gp130 homodimer, eliciting intracellular signaling. In addition, trans-signaling occurs if mIL-6R is processed by ADAM proteases and generates sIL-6R, which can bind to IL-6 and also interact with gp130 in either the same cell (autocrine) or another one (paracrine), which may not express mIL-6R. The soluble form of gp130 (sgp130) is generated by alternative splicing and specifically inhibits trans-signaling by binding the IL-6/sIL-6R complex and preventing its interaction to membrane gp130. Cluster signaling occurs between dendritic cells and T-cells simultaneously with antigen presentation to the TCR. The dendritic cell presents IL-6 via the mIL6R to the gp130 of the T cell, initiating signaling in the latter cell to differentiate into a T_H17 phenotype. ADAM a desintegrin and metalloprotease; MHC major histocompatibility complex; TCR T-cell receptor. Based on Scheller et al. 2011; Erta et al. 2012 and Quintana 2016.

1.3 Expression of IL-6 and IL-6R

1.3.1 Peripheral and CNS cells express IL-6

As mentioned before, the first studies involving IL-6 (with any of its previous names) were done *in vitro* with various cell lines, including interleukin-1-stimulated fibroblasts (Poupart et al. 1987), several human liver cell lines (HepG2, Chang, HLF and HLE) (Lotz et al. 1989; Matsuguchi et al. 1990), a human T cell leukemia virus-1 transformed T cell line (TCL-Na1), a bladder cell carcinoma line (T24), an amnion-derived cell line (FL), an astrocytoma line (U373) and a glioblastoma line (SK-MG4) (Yasukawa et al. 1987). This already gave a hint of the numerous cell types, including CNS cells that can express IL-6 either constitutively or upon stimulation.

Primary cultures started revealing the same and other cell types as producers of the cytokine. For example, the earliest studies showed a clear immunological function of IL-6 when shown to be a monocyte-derived factor stimulating acute-phase response proteins in the liver (known then as hepatocyte-stimulating factor) (Ritchie and Fuller 1983), and produced by activated B- and T-cells (Horii et al. 1988). Isolated hepatocytes can also be made to express IL-6 (Lotz et al. 1989; Gauldie et al. 1990). And more recently, it has also been detected in dendritic cells (Pasare and Medzhitov 2003; Heink et al. 2016), highlighting its prominent role in immunity.

In vivo, IL-6 expression is detected in the endothelium of gonadotropin-primed hyper-stimulated ovaries and also in the one surrounding them in female mice (Motro et al. 1990). This cytokine is also produced by subcutaneous adipose tissue (Mohamed-Ali et al. 1997). However given that the tissue contains adipocytes, macrophages and blood vessels, it had to be later shown that isolated adipocytes directly secrete IL-6, even though they only account for a 10% of the total released by the tissue (Fried et al. 1998; Mohamed-Ali et al. 2001). Skeletal

muscle (Keller et al. 2001; Steensberg et al. 2002), osteoblasts (Ishimi et al. 1990), hepatocytes (Kitamura et al. 1997; Norris et al. 2014) and pancreatic β-cells (Campbell et al. 1989) also produce IL-6. In the human pituitary gland, IL-6 has been detected mainly in adrenocorticotropic hormone (ACTH)-, follicle-stimulating hormone (FSH)- and luteinizing hormone (LH)-producing cells, and in very few growth hormone (GH)- or prolactin (PRL)-producing cells (Kurotani et al. 2001).

Finally, IL-6 is produced in the nervous system, either in basal conditions or upon stimulation, by astrocytes, microglia, neurons, oligodendrocytes, Schwann cells, and in addition, by endothelial cells of the irrigating blood vessels (Frei et al. 1989; Rott et al. 1993; Schöbitz et al. 1993; Yamabe et al. 1994; Bolin et al. 1995; März et al. 1998).

The fact that IL-6 is produced in the periphery raises the question of whether there could be passive leakage or active transport into the CNS. The first mechanism is unlikely to be significant due to its molecular weight and its hydrophilic nature. However, there is a saturable transport system that can incorporate IL-6 into the cerebrospinal fluid (CSF) and the brain parenchyma, even though it is rapidly degraded (Banks et al. 1994), suggesting that blood-borne IL-6 does not contribute dramatically to central effects. Indeed, there seems to be a clear independence of serum and CSF levels, as seen in obese individuals where serum and CSF IL-6 are uncorrelated, while serum IL-6 is higher than in control patients. Transport to the CSF is unlikely since obese individuals have a lower CSFserum ratio (Stenlöf et al. 2003; Park et al. 2005).

1.3.2 Anatomical distribution of IL-6 in the brain

Not many extensive studies have been carried out to determine the spatial distribution of IL-6 in the brain, and they have the limitation of trying to detect a

very low level of the cytokine (in basal conditions), and most have been carried out in rats. An *in situ* hybridization (ISH) study (using oligonucleotide cDNA probes) performed in control rats showed that IL-6 was expressed in the lateral olfactory bulb, in pyramidal neurons of the piriform cortex, in the ependymal and subependymal cell layer of the olfactory ventricle, in the anterior part of the ependymal cells lining the lateral ventricle, in scattered neurons of the cortex, in the medial habenular nucleus, in certain neurons of the **ventromedial** (VMH) and **dorsomedial** (DMH) **hypothalamus**, as well as of the medial preoptic nucleus, in the CA1 to CA4 regions and dentate gyrus of the **hippocampal formation**, in the optic tract, fimbria, internal capsule, corpus callosum, and finally, in the granular layer of the cerebellum. Nevertheless, no signal was found in Purkinje cells of the cerebellum, in the brainstem or the spinal cord (Schöbitz et al. 1993). However, in another study using ISH with a longer cRNA probe, Purkinje cells were shown to express the cytokine and expression was confirmed in the hippocampus (Gadient and Otten 1994b). The same authors also used RT-PCR and Southern blot to detect IL-6 mRNA in the striatum, hippocampus, cerebellum and **pons/medulla oblongata** (Gadient and Otten 1994a). In mice, Campbell et al. failed to detect the mRNA with ISH or RPA (RNA protection assay) in control animals (Campbell et al. 1993; Campbell et al. 1994), another instance of the elusive character of this cytokine. However, the same group used a transgenic mouse with IL-6 under the control of the glial fibrillary acidic protein (GFAP) promoter (GFAP-IL6 mice) and detected a widespread expression of IL-6 in the brain, especially in the thalamus and cerebellum (Campbell et al. 1993). In contrast, a recent study characterized the expression of IL-6 by immunofluorescence and found that only in the border zone of the ventricles were astrocytes the main producers of IL-6 (95%), whereas in all other structures (olfactory bulb, hypothalamus, hippocampus, cerebral cortex, brainstem and cerebellum) most were neurons (90%) and a small proportion (8%) were microglia (the remaining 2% was unidentified) (Aniszewska et al. 2015). This seems to be in accordance with a previous report, where *Il6* mRNA and the protein had a distinct distribution from GFAP-positive

cells (Yan et al. 1992). Neuronal expression of IL-6 in the hypothalamus had also been reported in rats, particularly in vasopressin-expressing magnocellular neurons of the **paraventricular nucleus** (PVN) and their fibers in the internal zone of the median eminence (Jankord et al. 2010).

1.3.3 Regulation of expression of IL-6

Early characterization of the *Il6* gene showed that there were at least three initiation sites for transcription (Yasukawa et al. 1987). Further characterization of the human and mouse genes showed a great homology in the region upstream of the transcriptional start and several response elements were identified (Figure 6). It contains two glucocorticoid responsive elements (**GRE**); an activator protein 1 (**AP-1**) binding site, present in many phorbol-12-myristate-13-acetate (PMA)-inducible promoters. Furthermore, there are multiple regulatory elements to which the pathways of **IL-1**, **TNF**, **forskolin** (via protein kinase A) and **phorbol esters** (via protein kinase C) converge (Ray et al. 1989). In this region, there is also a c-*fos* serum-responsive enhancer (SRE) homology site, which in the c-*fos* gene is necessary for induction with serum, phorbol esters and ependymal growth factor (EGF), and which also includes a **cyclic-AMP-response element** (CRE). Finally, a **NF-κB binding site** is also present that participates in the induction after stimulation with PMA, LPS, TNF-α, poly(IC), and phytohemagglutinin (PHA) (Isshiki et al. 1990; Libermann and Baltimore 1990). The c-fos SRE homology site is responsible for binding the transcription factor **NF-IL6**, inducible by IL-1 (Isshiki et al. 1990; Natsuka et al. 1992). This factor associates with NF-κB to synergize in the activation of the gene (Matsusaka et al. 1993).

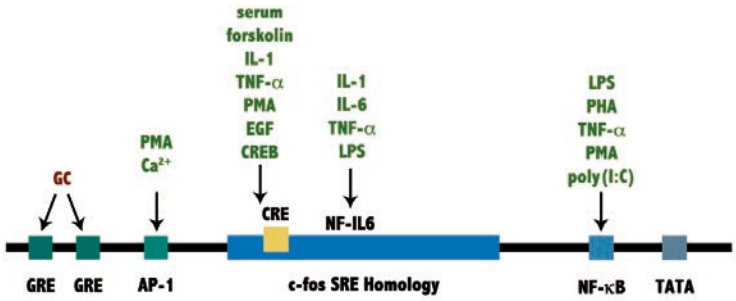

Figure 6. Regulatory elements in the Il6 gene. GC glucocorticoids; GRE glucocorticoid responsive element; PMA phorbol-12-myristate-13-acetate; AP-1 activator protein 1; c-fos SRE homology c-*fos* serum-responsive enhancer (SRE) homology site; TNF-α tumor necrosis factor alfa; EGF epithelial growth factor; CREB cyclic-AMP-response element binding protein; CRE cyclic-AMP-responsive element; LPS lipopolysaccharide; NF-IL6 nuclear factor for IL-6 expression; PHA phytohemagglutinin; poly(IC) polyinosinicpolycytidylic acid; NF-κB nuclear factor kappa B. Based on Akira et al. 1990.

1.3.3.1 Peripheral cells

Many *in vitro* studies have assessed the factors stimulating IL-6 production (mRNA and protein) and it seems that they are cell-specific. For example, human fibroblasts produce IL-6 after stimulation with IL-1α, TNF-α and platelet-derived growth factor (PDGF) (Zilberstein et al. 1986; Kohase et al. 1987); as do hepatoma cells after incubation with IL-1β or TNF-α (Lotz et al. 1989).

Human myeloma cells and murine monocytic cell lines (monocyte-macrophages) respond to LPS (Bazin and Lemieux 1987). In T-cells, IL-6 production has been seen after phorbol ester and phytohemagglutinin stimulation (Horii et al. 1988). And IL-6 itself stimulates its own mRNA expression in murine myeloid leukemia cells (Miyaura et al. 1989; Shabo et al. 1989).

Skeletal muscle responds to Ca^{2+} *in vitro* with *Il6* gene expression and protein release (Holmes et al. 2004). *In vivo*, this tissue releases IL-6 into the bloodstream in response to exercise and enhanced by low muscular glycogen

content (Keller et al. 2001), possibly by phosphorylation of c-Jun terminal kinase (JNK) and the AP-1 transcription factor (Whitham et al. 2012).

Regarding inhibitors, glucocorticoids are known suppressors of inflammation, and since *Il6* has a GRE, it is not surprising that they diminish IL-6 expression in several cell types, such as human monocytes, endothelial cells, the human fibroblast cell line FS4 and the murine macrophage cell line RAW 264.9 (Waage et al. 1990).

Post-transcriptional regulation seems to be another important point in cytokine regulation, consisting in altering mRNA stability. In the case of *Il6*, an RNA-binding protein called tristetrapolin (TTP) has been shown to accelerate *Il6* degradation upon binding to the mRNA's adenine and uridine-rich elements (AREs) in the 3'-untranslated region (UTR) in carcinoma cells (Van Tubergen et al. 2011).

1.3.3.2 Nervous system cells

Cultured cortical neurons increase both mRNA and protein after incubation with IL-1β and TNF-α (independently and synergistically) (Ringheim et al. 1995). Furthermore, in primary cortical and the PC-12 cell line, membrane depolarization increases intracellular Ca^{2+}, which ultimately results in the elevation of *Il6* mRNA (Sallmann et al. 2000). The exact mechanism has not been elucidated but could be the same as in skeletal muscle (Whitham et al. 2012), a likely possibility since in astrocytes the pathway Ca^{2+}/JNK/AP-1 has already been described (Gao et al. 2013).

In astrocytes, a Ca^{2+} ionophore, A23187, has been shown to increase IL-6 production (Benveniste et al. 1990). These cells also produce the cytokine after inhibition of the PI3K-mTOR pathway concomitant with an increase in cytosolic

Ca^{2+} through activation of p38 and NF-κB (Codeluppi et al. 2014), suggesting the possibility of a second pathway for Ca^{2+} action.

Bacterial lipopolysaccharide (LPS), a toll-like receptor (TLR)-4 inducer, is known to stimulate IL-6 production in rodent astrocytes and microglia, although the dynamics are faster in microglia (3 versus 5 hours) (Sawada et al. 1992). However, human and mouse astrocytes may respond differently to the same stimuli. For example, LPS fails to stimulate IL-6 production in human astrocytes, but IL-1β induces it; while in mouse, the reverse happens (Tarassishin et al. 2014). A previous report, however, found that both TNF-α and IL-1β stimulate IL-6 in astrocytes with a more delayed time course than LPS (Sawada et al. 1992).

Other inducers of IL-6 in cultured astrocytes are norepinephrine (NE), serotonin, histamine, bradykinin, vasoactive intestinal peptide (VIP), pituitary adenylate cyclase-activating polypeptide (PACAP38), adenosine, substance P (SP) and calcitonin (Maimone et al. 1993; Norris and Benveniste 1993; Cadman et al. 1994; Gitter et al. 1994; Gottschall et al. 1994; Kiriyama et al. 1997; Schwaninger et al. 1997; Schwaninger et al. 1999).

IL-6 itself has been demonstrated to stimulate its own mRNA expression in astrocytes in the presence of sIL6-R, an effect which is synergized by TNF-α or IL-1β (Van Wagoner et al. 1999).

There is much *in vivo* evidence of IL-6 expression in the CNS after an insult. In rats, neurotoxicity causes an increase in *Il6* in the hippocampus, corpus callosum, thalamus and hypothalamus (Minami et al. 1991; de Bock et al. 1996), and in humans with epileptic seizures IL-6 in the CSF is also elevated (Lehtimäki et al. 2004). In the case of cerebral trauma, IL-6 is also increased in the CSF (Hans et al. 1999; Maier et al. 2001).

1.3.4 IL6-R is also expressed in the periphery and the CNS

As seen in the early days of IL-6 research, B cells respond to IL-6 and indeed they express the IL-6R when activated (van der Meijden et al. 1998). Peripheral blood T-cells of the $CD4^+/CD8^-$ and $CD4^-/CD8^+$ phenotypes are also IL6-R+ (Hirata et al. 1989), and blood monocytes require the receptor in order to complete differentiation into macrophages (Chomarat et al. 2000). Apart from immune cells, other cellular types, such as hepatocytes (Bauer et al. 1989), adipocytes (Bastard et al. 2002), and α-cells of the endocrine pancreas (Ellingsgaard et al. 2008), all present IL-6R. The muscle, lung, kidney, spleen and adrenal gland of the mouse express it too, albeit in lower levels than in the pancreas (Ellingsgaard et al. 2008). The receptor's mRNA has also been detected in cultured murine osteoblasts (Udagawa et al. 1995) and osteoclasts of patients with renal osteodystrophy (Langub et al. 1996). And in the human pituitary gland, most GH- and PRL-, some FSH- and scarce LH-producing cells express IL-6R (Kurotani et al. 2001), showing an inverse pattern to IL-6.

In the brain, as assessed by RT-PCR and ISH, *Il6ra* is expressed and **essentially co-localizes with *Il6*** (Yan et al. 1992; Schöbitz et al. 1993; Gadient and Otten 1994a) (see *1.3.2 Anatomical distribution of IL-6 in the brain*). In addition, other authors have found expression of *Il6ra* (by ISH) in the bed nucleus of the stria terminalis (BNST), the central nucleus of the amygdala (CeA), in ependymal lining cells of the ventricular system and in the circumventricular organs, i.e. organum vasculosum of the lamina terminalis (OVLT), subfornical organ, median eminence and area postrema. The mRNA has also been detected in rat neurons of sympathetic and sensory ganglia, co-localizing with IL-6, and alone in cells surrounding axons of the dorsal root ganglion (DRG), which are possibly Schwann cells (Gadient and Otten 1996). The protein has also been detected by western blot in the hypothalamus of mice (Aniszewska et al. 2015).

1.3.5 Regulation of expression of IL-6R

There are not many extensive studies on the regulatory elements of the *Il6ra*. However, as for *Il6*, the *Il6ra* seems to be differentially controlled in the cells that express it. For example, it is down-regulated in peripheral $CD4^+$ and $CD8^+$ T-cells upon TCR engagement (Betz and Müller 1998), while remaining unaffected by phytohemagglutinin (Hirata et al. 1989). Dexamethasone, a synthetic corticosteroid, has been shown to increase *Il6ra* expression in osteoblasts (Udagawa et al. 1995) and in hepatocytes (Bauer et al. 1989; Rose-John et al. 1990; Snyers et al. 1990), while decreasing it in monocytes (Bauer et al. 1989). A similar opposed effect between hepatocytes and monocytes has also been described in response to IL-6 and IL-1β, where *Il6ra* expression increases in cultured hepatocytes while it decreases in monocytes (Bauer et al. 1989). These authors suggested that the opposite regulation of these two cell types could be related to a shift between non-inflammatory to inflammatory conditions (Bauer et al. 1989). Nevertheless, a posterior report found no down-regulation of the receptor after neither LPS nor IL-6 treatment on human blood monocytes, a difference they attribute to an incorrect purification (Schoester et al. 1994).

The up-regulation of the receptor by cortisol has also been proposed in the muscle. Acute exercise increases expression of the receptor in humans (Keller et al. 2005), and it could be due to the increased cortisol after moderate to intense exercise (Hill et al. 2008).

In the hypothalamus, where *Il6ra* could not be detected in basal conditions, intraperitoneal (IP) LPS induced its expression rapidly (2h) in the parvocellular neurons of the PVN (as opposed to IL-6 in magnocellular neurons, as mentioned before). Furthermore, this challenge also increases it in the cortex in the same time frame, and later (6h) in the hippocampus (Vallières and Rivest 1997; Utsuyama and Hirokawa 2002). These increases might be due, at least in

part, to the brain's microvasculature, which was negative for the receptor in basal conditions, even though it is not clear which cells are the producers (endothelial or glial) (Vallières and Rivest 1997). In this line of results, a mechanic injury to the striatum elicits an increase of the receptor's mRNA in the same areas with basal expression (Yan et al. 1992).

Recently, an example of post-transcriptional regulation has been described in the form of a micro-RNA (miR-125b). It attenuates IL-6/Stat3 signaling by interacting with the *Il6ra* mRNA, indirectly reducing the levels of pStat3 targets Mcl-1 and Bcl-xL, thereby promoting apoptosis and linking its increase with cancer development (Gong et al. 2012).

1.4 Functions of IL-6 in the periphery

1.4.1 Immunological

As mentioned before, one of the original functions described for IL-6 was the final differentiation of **B-cells into high-rate Ig-secreting** cells (Hirano et al. 1985). However, a couple of years prior, the cytokine (under the name HSF) had been shown to stimulate production, either directly or by synergizing with IL-1-type cytokines, of **acute phase response** proteins in the liver (Ritchie and Fuller 1983; Baumann and Gauldie 1994), e.g. C reactive protein, serum amyloid A, fibrinogen, haptoglobin and α_1-acid glycoprotein. These, together with its ability to co-stimulate thymocytes and T lymphocytes (Lotz et al. 1988), support its longstanding role as one of the major "pro-inflammatory" cytokines.

Nevertheless, IL-6 trans-signaling has been implicated in the **transition from innate to acquired immunity** and the resolution of the inflammatory response. In particular, switching the balance from neutrophils to mononuclear

leukocytes, by inhibiting neutrophil recruitment (Hurst et al. 2001), promoting neutrophil apoptosis (McLoughlin et al. 2003) and enhancing chemokine-dependent attraction of T-cells (McLoughlin et al. 2005). But it has also been shown to inhibit T-cell apoptosis in different milieus such as the eye and the intestine (Atreya et al. 2000; Curnow et al. 2004), and to participate in skewing the T_{reg}/T_H17 balance towards the latter, which are involved in the induction of auto-immune diseases (Dominitzki et al. 2007). Therefore, there seems not to be a clear-cut division of function between classic and trans-signaling, as some authors have suggested (Schaper and Rose-John 2015).

1.4.2 Growth factor

Other effects of IL-6 include growth factor-related properties. Firstly, it promotes **hepatic regeneration**, as its levels increase after a partial hepatectomy (Trautwein et al. 1996) and impaired proliferation can be rescued in IL-$6^{-/-}$ mice by treating them with the cytokine prior to the surgery (Cressman et al. 1996). This effect is likely mediated, or at least potentiated, by trans-signaling, since sIL-6R also increases after hepatectomy, and the trans-signaling blocker sgp130 reduces hepatocyte proliferation (Nechemia-Arbely et al. 2011). Furthermore, other authors have used transgenic mice and observed a synergy between IL-6/sIL-6 in basal conditions to increase liver proliferation (Schirmacher et al. 1998).

Regarding **hematopoiesis**, IL-6 promotes colony formation from multipotential blast cells, but not from more differentiated ones, acting synergistically with IL-3 and giving rise to neutrophil, macrophage and megakaryocyte lineages (Ikebuchi et al. 1987; Koike et al. 1988).

Moreover, IL-6 has been shown to stimulate **angiogenesis**, a critical step in inflammation and its resolution. Monocytes/macrophages and T-cells, among

other inflammatory cells, can secrete pro- and anti-inflammatory cytokines that orchestrate endothelial cell proliferation, migration, activation, survival, and apoptosis (Mihara et al. 2012). Its role in vascularization was first proposed by Motro et al. (1990) after their studies with developing ovarian follicles and embryonic implantation in mice. Furthermore, the already mentioned GFAP-IL-6 mice have increased vascularization specially in the areas with more prominent expression of IL-6 (Campbell et al. 1993). Its effect is most likely indirect, through the trans-signaling-mediated stimulation of vascular endothelial growth factor (VEGF) (Huang et al. 2004; Catar et al. 2016). However, the resulting angiogenesis appears to be more destabilized due to the down-regulation of angiopoietin (Ang)-1 and up-regulation of Ang-2 (an antagonist of Ang-1) (Kayakabe et al. 2012; Gopinathan et al. 2015).

Pancreatic islet α- and β-cells also proliferate in response to IL-6, via the mIL-6R, the MAPK pathway and the up-regulation of c-myc (mitogenic) and bcl-2 (anti-apoptotic), and down-regulation of p27 (cell cycle inhibitor). The cytokine also has differential effects on these cells regarding glucolipotoxicity-induced apoptosis; while the former are almost completely protected, the latter become more susceptible (Ellingsgaard et al. 2008).

IL-6 also stimulates osteoclast formation through trans-signaling (IL-6+sIL-6R), as shown in co-cultures of primary osteoblast-like cells and nucleated marrow cells, given that IL-6 alone failed to elicit differentiation (Tamura et al. 1993).

1.4.3 Other

Besides promoting the proliferation of the aforementioned cell types, IL-6 also has further effects on them.

In the pancreas, IL-6 increases pro-glucagon mRNA and glucagon secretion, without an effect on insulin (Ellingsgaard et al. 2008).

In the bone and in line with its relation to osteoclast progenitor differentiation, IL-6 has a prominent role in bone resorption, increasing mineral and matrix release. It increases receptor activator of NF-κB ligand (RANKL) expression in osteoblasts, which in turn acts on preosteoclasts to make them differentiate and fuse into multinucleated mature osteoclasts. Of note, it also increases osteoprotegerin (OPG), a decoy receptor of RANKL, so its resorptive effects are lower than other hormones which decrease OPG, while increasing RANKL, such as parathyroid hormone (Palmqvist et al. 2002). Transgenic mice overexpressing IL-6 in neurons show a generalized bone loss and stunted growth (Del Fattore et al. 2014) and, conversely, IL-6KO mice are protected from estrogen-dependent bone loss (Poli et al. 1994).

IL-6 is one of the links between the immune and the neuroendocrine system as evidenced by its *in vitro* induction of several anterior pituitary cells, such as GH-, PRL- and LH-producing cells (Spangelo et al. 1989). However, a subsequent *in vivo* analysis with third ventricle administration of IL-6 failed to determine any effects on GH or PRL secretion (Lyson and McCann 1991)

This myriad of functions is explained by the range of targets, which, as shown, is increased thanks to trans-signaling, allowing the enhancement and widening of the effects of IL-6, reaching cells that lack membrane IL-6R (either permanently or temporarily).

1.5 IL-6 in the CNS

As the aim of this thesis is to study the role of IL-6 produced in the CNS, this section will delve into more detail and, in the areas more pertinent to the main theme, a general introduction will be made prior to the specifics of IL-6. It

must be taken into consideration that some of these processes have inextricably linked peripheral events, and therefore a general picture will be presented.

1.5.1 Neurotrophic factor

Very early after the cloning of IL-6, several research groups discovered a role on neuronal development *in vitro*, which highlighted the pleiotropic and multifunctional character of IL-6. Many studies used PC12 cells, a cell line derived from a pheochromocytoma of the rat adrenal medulla and used for neuronal differentiation. One of the first, described a nerve growth factor (NGF)-like action on these cells, showing initiation of neuronal differentiation with neurite outgrowth, but lacking both long-term support of the culture and increase in acetylcholinesterase activity, unlike NGF (Satoh et al. 1988). This effect was proposed to be due to the presence of IL-6R in those cells, but further studies failed to replicate those findings. Even though the receptor's expression was corroborated by an independent group (März et al. 1996), Satoh's findings could not be replicated in normal PC12 cells (Sterneck et al. 1996; Wu and Bradshaw 1996). And even though IL-6 alone mildly induced GAP-43 (a protein related to neurite formation and neuronal development), sIL6R was needed to induce neurite outgrowth, together with GAP-43 and NSE expression. It also had additive effects with NGF, suggesting they acted through independent pathways (März et al. 1997). However, PC12 cells pretreated with NGF responded to IL-6 with neurite outgrowth (Ihara et al. 1996), suggesting that a certain internal milieu was necessary for IL-6 to exert its action. Indeed, a variant cell line called PC12-E2 demonstrated the ability for rapid neurite growth after just IL-6 treatment (Wu and Bradshaw 1996), which they later proposed was mediated by the Stat3 signaling pathway. Nevertheless, a previous study using NGF-primed PC12 cells, had proposed that neurite outgrowth occurred via MAPK upregulation and STAT3 suppression (Ihara et al. 1997). All these discrepancies could be due to differences

between PC12 lines and sublines, maybe involving the balance between the two pathways in each of them.

Other studies using cultured cholinergic neurons from the basal forebrain of postnatal rats demonstrated support of neuronal survival and a synergistic effect with NGF. However, no differentiation occurred, suggesting only a neurotrophic action on primary cultured CNS neurons (Hama et al. 1989). A similar effect was seen in mesencephalic catecholaminergic neurons of postnatal rats, which survived longer and maintained cell-type characteristics such as well-developed neurites, varicosities and dopamine release (Hama et al. 1991). In contrast, IL-6 failed to promote survival of embryonic mesencephalic neurons, and thus it is probably not related to their development; but it did attenuate the neurotoxicity caused by 1-methyl-4-phenylpyridinium (MPP^+). This effect is likely not mediated by glial proliferation since very few glial cells were present and they did not proliferate upon cytokine stimulation (Akaneya et al. 1995).

In the peripheral nervous system, IL-6 has been implicated in nerve regeneration after trauma. Cultured neurons from mouse embryonic DRG formed neurites after IL-6+IL-6R administration (but not IL-6 alone), pointing to a trans-signaling mechanism. Furthermore, hypoglossal nerve injury caused up-regulation of IL-6 in Schwann cells and marginally IL-6R in the nerve proper, but of both in the nerve cell bodies in the hypoglossal nucleus (brain stem). The role of the cytokine is highlighted by the retardation of regeneration caused by an anti-IL-6R antibody, and also by the fact that transgenic mice over-expressing both IL-6 and IL-6R regenerated the nerve faster (Hirota et al. 1996).

Astrocytes in culture have also been proven to respond to IL-6 (in conjunction with sIL-6R) by producing NGF, neurotrophin (NT)-3 and NT-4/5, in a brain region-dependent manner, maybe as part of a network of trophic support for neurons (Frei et al. 1989; März et al. 1999). Furthermore, primary culture astrocytes proliferate in serum-free medium in response to IL-6 (Selmaj et al.

1990), something that has also been observed *in vivo*, since GFAP-IL6 mice have prominent astrocytosis correlating with IL-6 expression (Campbell et al. 1993).

1.5.2 Behavior

Being produced by several cells in the CNS, albeit in small quantities, it was only a matter of time before numerous studies uncovered roles of IL-6 in normal and pathological behaviors.

Many studies carried out to elucidate the role of IL-6 in normal behavior have been carried out with IL-6 knock out mice (IL-6KO). Nevertheless, there are several models mutating the gene at different points and generated in various genetic backgrounds. This is a critical issue in any experiment, but even more so when attempting to analyze behavior. In the case of IL-6KO mice generated by Kopf and colleagues (1994) (now called B6.129S2-*Il6*^{tm1Kopf}/J, and the one that has persisted in the literature), they were generated in a 129S2/SvPas background and then crossed to a C57BL/6 background (unspecified strains). Others have used the 129S9/SvEvH background and apparently not backcrossed them into another strain (Poli et al. 1994; Braida et al. 2004); and a third model has also been utilized, BALB.B/Ai-[KO]IL6N9 (Swiergiel and Dunn 2006). Thus, conflicting results have been published by the different groups. Our laboratory found that IL-6KO mice presented less ambulation, head-dippings and rearings in the hole-board (HB), and less entries in the open arms of the elevated plus maze (EPM), suggesting more emotional reactivity in novel environments. (Armario et al. 1998). Butterweck and colleagues (2003) reported the same mice to have increased activity in the open field (OF) test, seemingly in contrast with the previous study, while having less rearings and entries into the open arms of the EPM, which does agree with those results, supporting at least an anxiolytic role of IL-6. However, the same model was recently reported to have increased travelled distance and time spent in the central part of an OF, while maintaining equal total

activity, which could point to decreased anxiety of the knock-out (Aniszewska et al. 2015). The second model also showed no differences in spontaneous activity, but suggested a facilitative role of IL-6 deficiency in both reference and working memory (Braida et al. 2004), which was confirmed with the IL-6KO in the C57BL/6 background, which is resistant to LPS-induced impairment of working memory, possibly by avoiding hippocampal production of inflammatory cytokines such as IL-1β and TNFα (Sparkman et al. 2006). Finally, with the third model, no differences were found in the OF, the EPM, even after physiological (IL-1) or emotional (restraint) stressors, nor in despair models such as tail suspension (TS) and forced-swim (FS) tests (Swiergiel and Dunn 2006).

It is evident from the previous paragraph that drawing clear-cut conclusions from the systemic IL-6KO is quite difficult, due both to the heterogeneity of genetic backgrounds and the fact that many cells in the CNS produce the cytokine. Therefore, pinpointing the role of each source is certainly interesting. Our group has focused on this very issue for the past years and has used a conditional astrocyte-specific IL-6KO mouse to ascertain the role of astrocyte-produced IL-6 and the response of those cells to the cytokine by means of its membrane receptor. This model was shown to have decreased ambulation in the HB and increased anxiety in the EPM evidenced by less time in the open arms (Quintana et al. 2013; Erta et al. 2015), which is consistent with our previous findings with the systemic IL-6KO (Armario et al. 1998) and would suggest a prominent role of astrocytic IL-6 in the regulation of novel environment exploration.

Behavioral studies to elucidate the role of IL-6 have also used GFAP-IL6 mice, primarily to assess alterations related to inflammatory neurodegeneration. For example, conditioned avoidance was hindered in mice with chronic expression of IL-6 and it worsened with age (Heyser et al. 1997). It could be argued that these results mirror the facilitated memory in IL-6KO mice described before, but it is important to account for the extensive microgliosis and neuronal

alterations in this model, which might be the reason for the deficit instead of a direct action of IL-6.

Nevertheless, it must be considered that the role of IL-6 in behavior may arise from permanent changes in the embryonic stage, as evidenced by the observation that IL-6 administration to pregnant rats causes latent inhibition and pre-pulse inhibition deficits in their adult offspring. The deleterious role of IL-6 is further evidenced by the fact that IL-6KO mice show no effects on the adult offspring when treated with double-stranded poly(IC), an innate immune system inductor (Smith et al. 2007). Since schizophrenia and autism present these traits (Wynn et al. 2004; Perry et al. 2007), maternal infection could be a significant environmental risk factor for the development of these diseases in the offspring.

1.5.2.1 Sickness behavior

Sickness behavior refers to the unspecific, yet highly orchestrated, behavioral changes that occur in animals suffering from an infection, which include reduced general activity, grooming and social interactions, hunched posture, anorexia, adipsia, and hypersomnia. It is an adaptive response aimed at conserving energy while the organism fights the infection (Dantzer and Kelley 2007).

This response is mediated by cytokines in two phases. First, peripherally released cytokines (produced by inflammatory cells in the context of the infection) activate afferent nerve fibers, such as the vagal nerve, ultimately entering the brain at the nucleus of the solitary tract (NTS). Then, certain brain areas, *e.g.* the parabrachial nucleus (PBN), the hypothalamic PVN and supraoptic nuclei (SON), the CeA and the BNST, may become sensitized to locally released cytokines, widening the scope of peripheral cytokines (Dantzer 2001).

Several pro-inflammatory cytokines have been linked to the induction of sickness behavior, such as TNFα, IL-1β and IL-6 (Johnson 2002). Indeed, peripherally administered IL-6 antiserum alleviates LPS-induced sickness behavior in rats (manifested through voluntary running and feeding), suggesting that this cytokine is relevant to the response (Harden et al. 2006). However, intracerebroventricular (ICV) administration of IL-6 fails to elicit sickness behavior in rats (up to 6 hours), and needs co-administration of IL-1β to significantly reduce activity and social interactions (Lenczowski et al. 1999). This could mean that a synergy of cytokines is needed to initiate the response rapidly, since at a later time point (9 hours after injection) IL-6 alone seems to be sufficient (Schöbitz et al. 1995). A possible mechanism in physiological conditions could be related to the afore-mentioned sensitization of the brain before local release, since prior ICV administration of sIL-6R significantly enhances and lengthens the effects of IL-6 (Schöbitz et al. 1995).

Infection can be considered a systemic stressor (as opposed to an emotional one) and does indeed activate the hypothalamic-pituitary-adrenal (HPA) axis (Tilders et al. 1994). The relationship between IL-6 and the HPA axis and its consequences will be discussed in the next section.

1.5.2.2 The HPA axis, stress and depression

A role of IL-6 in stress has been suggested above with the studies with IL-6KO and conditional astrocyte IL-6KO mice in anxiety-related tests, such as the EPM; and the activation of the HPA axis after a systemic infection. The relationship between IL-6 and the HPA axis is bidirectional, each affecting the other.

1.5.2.2.1 IL-6 affects the HPA axis

ICV administration of IL-6 in the rat increases plasma ACTH and corticosterone (Lenczowski et al. 1999), possibly by stimulating corticotropin-releasing hormone (**CRH**) production on IL-6R-positive parvocellular neurons of the paraventricular nucleus of the hypothalamus that increase the receptor after LPS injection (Vallières and Rivest 1997). *In vitro* studies also support this possibility, as IL-6 increases CRH in rat hypothalamic explants (Navarra et al. 1991). However, peripheral administration of IL-6 in humans also induces **ACTH** and **cortisol** secretion, possibly pointing to a direct action on the pituitary and/or the adrenal gland (Späth-Schwalbe et al. 1994). Indeed, primary cultures of rat adrenal glands stimulated with IL-6 produce corticosterone in a dose-dependent way; and, in addition, at low doses it acts synergistically with ACTH suggesting a regulation of the long-term response to stress (Salas et al. 1990; Päth et al. 2000). Nevertheless, in rats with jugular vein administration, the increase in ACTH could be blocked by anti-CRH antiserum (Naitoh et al. 1988), suggesting rather a central effect. In summary, it seems that IL-6 can act on all three levels of the HPA axis, but maybe the preferential one depends on the level of IL-6 and where it is produced (CNS or periphery).

1.5.2.2.2 Stress affects IL-6

Stress can also in turn influence IL-6. Mild stress caused by a novel environment (OF) increases *Il6* mRNA in the hypothalamus, pituitary and adrenal gland (Butterweck et al. 2003) as well as plasma IL-6 (LeMay et al. 1990b). Restraint (a psychogenic stressor) also increases *Il6* mRNA in the hypothalamus, specifically in vasopressin magnocellular neurons of the PVN and supraotic nucleus (SON) of the hypothalamus, and IL-6 in the plasma (Jankord et al. 2010). In humans, **psychological stress** also increases plasma IL-6, along with other cytokines such as TNFα and interferon γ (IFNγ) (Maes et al. 1998).

The main source for plasma IL-6 after stress seems to be the liver (Kitamura et al. 1997) and not the adrenal gland (Takaki et al. 1994) as suggested by Zhou and colleagues (1993). The increase in IL-6 seems to be mediated by catecholamines acting on β–adrenergic receptors in the CNS, since it can be reduced by ICV 6-hydroxidopamine (6-OHDA), a neurotoxin that kills catecholaminergic neurons (Takaki et al. 1994) and by β–adrenergic receptor antagonists (Soszynski et al. 1996); even though conflicting results exist with a different stress paradigm and antagonist dosage (Zhou et al. 1993). In support of the former view, several types of cancer cells produce IL-6 in response to NE through the β-adrenergic receptor and cAMP-protein kinase A and/or Src tyrosine kinase (Nilsson et al. 2007; Yang et al. 2014). However, it should be remembered that glucocorticoids have an inhibitory effect on *Il6* transcription (see *1.3.3 Regulation of expression of IL-6*), and could also contribute to this process. Certainly, blockade of corticosterone with an antagonist is able to further increase open field-induced IL-6 (Morrow et al. 1993), which would suggest that the increase is at least partially due to lack of glucocorticoid inhibition.

1.5.2.2.3 Depression

The fact whether IL-6 itself can induce or is a risk factor for depression in humans has been cause of speculation (Dantzer et al. 1999; Leonard 2001; Wichers et al. 2006). This causality is supported by studies in mice with central administration of recombinant mouse IL-6, where it produces depressive-like phenotypes and increases the expression of the cytokine in the hippocampus, hypothalamus and frontal cortex, with participation of trans-signaling (Sukoff Rizzo et al. 2012).

Major depression in humans has been associated both with increased **inflammatory factors**, *e.g.* TNFα, IL-6, sIL-6R, IL-1β, IFN and C-reactive protein (CRP), and with **immunosuppressive** mediators, *e.g.* prostaglandin E_2 (PGE_2),

sIL-2R, IL-1 receptor antagonist secretion and hyperactivity of the HPA axis, the latter proposed to be a compensatory mechanism (Maes et al. 1995a; Maes et al. 1995b; Howren et al. 2009; Valkanova et al. 2013), even though some controversy exists (Basterzi et al. 2005; Sasayama et al. 2013).

Nevertheless, these observed changes are in circulating markers and, as mentioned before, CSF and plasma IL-6 levels are independent. Data regarding the CNS in humans is controversial since decreased (Levine et al. 1999; Stübner et al. 1999), equal (Carpenter et al. 2004) and increased (Lindqvist et al. 2009; Sasayama et al. 2013) CSF levels of IL-6 have been reported in depressive individuals compared to healthy controls. Again, differences in specific diagnostic, sex, age and concomitant pharmacological treatment or other conditions might explain the divergence.

Animal models provide additional information on the relationship between depressive-like behavior and IL-6. In IL-6KO mice, a prior learned helplessness procedure (inescapable footshocks) does not result in the expected increase in immobility in the FST or TS. In addition, *Il6* mRNA increases in the hippocampus of wild-type animals with the inescapable shocks (Chourbaji et al. 2006). Moreover, the paradigm of constant darkness also increases IL-6 both in plasma and the hippocampus, by means of NF-κB, and IL-6KO mice show again resistance to the induced depression-like behavior (Monje et al. 2011). However, some authors failed to demonstrate a significant increase in IL-6 (or *Il6* mRNA*)* in the rat cortex and hippocampus after a chronic stress paradigm (inescapable footshocks) or a prolonged restraint stress (Sukoff Rizzo et al. 2012; Voorhees et al. 2013).

1.5.3 Neuroimmunology

In the 20th century, the discovery that skin allografts survived better in the brain (Medawar 1948) prompted the thought that the CNS was completely independent from the peripheral immune system, lacked lymphatic drainage, and that it was also immunologically inert (Carson et al. 2006). However, the finding that microglial cells were the resident macrophages of the brain exerting a continuous vigilance of the parenchyma, responding when necessary (Ling and Wong 1993; Nimmerjahn et al. 2005), started to change the picture on "immune privilege." More recently, the presence of immune cells in the meninges, their trafficking into the CSF along with macromolecules via classic lymphatic vessels, and the existence of a glymphatic system allowing the drainage of fluid from the brain parenchyma into the CSF have all helped modify the old perception of an enclosed CNS (Louveau et al. 2015). Also, other components of the classical immune response, the major histocompatibility complex (MHC) I and the complement system, have been identified in the CNS in relation to neural plasticity and synaptic pruning (Shatz 2009; Stephan et al. 2012).

It is therefore clear that, even if **the inflammatory response of the brain is different from that of peripheral tissues**, it certainly exists and its main purpose is to limit secondary degeneration. It is characterized by a fast glial activation and synthesis of cytokines, free radicals and prostaglandins, edema, MHC expression, a systemic acute phase response, complement activation, expression of adhesion molecules and a delayed invasion of immune cells (Lucas et al. 2006). However, given the physical restrictions of the cranium and the importance of the CNS in coordinating the whole organism, it is critical the inflammation be resolved appropriately to avoid permanent damage or a chronic disease.

1.5.3.1 Neuroinflammation

Neuroinflammation can be either acute or chronic. **Acute** injuries include traumatic brain injury (TBI), stroke and ischemia; and **chronic** CNS conditions are neurodegenerative diseases such as multiple sclerosis (MS), Alzheimer's disease (AD), Parkinson's disease (PD), amyotrophic lateral sclerosis (ALS) and Creutzfeldt–Jakob disease (CJD).

A major breakthrough in the role of IL-6 in neuroinflammation was obtained using transgenic mouse models with chronic expression of the cytokine under different promoters. **GFAP-IL6 mice** display a marked astrogliosis, neuronal degeneration and increased vascularization in the hippocampus and cerebellum. All these morphological changes result in runting, tremor, ataxia and seizures (Campbell et al. 1993). The expression of the cytokine under the neuron-specific enolase promoter (**NSE-IL6 mice**) results also in reactive astrogliosis in the brain and cerebellum, ramified microglia but no neuronal damage, no neovascularization and no evident neurological or behavioral deficits (Fattori et al. 1995). The authors on the latter model attribute the differences to the anatomical localization of astrocytic feet in close proximity to the endothelium and to the lower affinity of human IL-6 (the one used in their construct) for the murine receptor. Taken together these results emphasize the role of IL-6 in astrogliosis and microgliosis, which were later found to be mediated by the JAK2/STAT3 and MAPK/ERK pathways (Sriram et al. 2004; Krady et al. 2008), mostly after IL-6 binds to the sIL-6R and then binds to gp130 (trans-signaling) (Campbell et al. 2014).

More evidence on the harmful action of IL-6 came from systemic **IL-6KO mice**, which are resistant to the induction of experimental autoimmune encephalomyelitis (EAE), a common model of MS (Samoilova et al. 1998). Our group aimed at describing the role of astrocytic IL-6 in the development of the disease by using conditional astrocytic IL-6KO mice but little effect was seen (Erta

et al. 2016). Rather, the resistance of IL-6KO animals appears to be a process mediated by a lack of trans-presentation of IL-6 by dendritic cells to T cells (the novel cluster signaling) to differentiate into pathogenic T_h17 cells (Heink et al. 2016).

Nevertheless, the role of **IL-6 is not always detrimental**. Evidence from the IL-6KO mouse and models of TBI shows that lack of IL-6 increases oxidative stress and results in more neurodegeneration, as well as reduced sensory perception, activity and balance (Penkowa et al. 2000; Swartz et al. 2001; Ley et al. 2011). This neuroprotection is mediated, at least in some cases, by astrocytes producing IL-6 in response to ATP (Fujita et al. 2009). In addition, chronic expression of IL-6 in the CNS (GFAP-IL6 mice) accelerates the recovery after a TBI due to the extensive re-vascularization, adding to the neuroprotective role of the cytokine.

Apart from the aforementioned neurological insults, inflammation in the CNS, specifically in the hypothalamus, occurs in models of diet-induced obesity (Thaler and Schwartz 2010). As this is a main point of this thesis, it will be covered in the corresponding specific section (see *1.5.4 Regulation of body weight and linear growth*).

1.5.3.2 Fever and body temperature

One of the key features of inflammation is fever, an elevation of body temperature due to alteration of the hypothalamic set point, thought to aid in fighting the pathogen, but acting through different mechanisms as a hyperthermia induced by low temperatures.

Body temperature is normally regulated from the **preoptic area** (POA) by integration of peripheral information coming from thermoreceptors on the skin

(outside temperature), in the splanchnic and vagal nerve afferent fibers distributed in the abdomen (internal core temperature) through relay on the PBN, and in POA neurons themselves. The mechanisms for temperature adjustment depend on efferent pathways to the DMH and the rostral medullary raphe region (rMR), and they include activation or inhibition of brown adipose tissue (**BAT**) thermogenesis (**non-shivering**), skeletal muscle thermogenesis (**shivering**), regulation of **heart rate** and **cutaneous vasomotion** (dilation or constriction) (Boulant 2000; Nakamura 2011).

Fever can be accomplished in an experimental setting through the administration of LPS to mimic an infection, and occurs through a IL-1β-mediated increase of IL-6 (LeMay et al. 1990a), even though plasma levels of IL-1 remain low (Bristow et al. 1991; Klir et al. 1993). The rise of IL-6 levels occurs both in plasma and in the anterior hypothalamus (Klir et al. 1994) and as demonstrated using IL-6 deficient mice, it is critical for the development of LPS-induced fever (Chai et al. 1996). Ultimately, the rise in temperature occurs partially by the action of PGE_2 on anterior hypothalamus (AH)/POA neurons (Fernández-Alonso et al. 1996). The source of brain PGE_2 are endothelial cells (Yamagata et al. 2001) and astrocytes (at least in culture) (Chikuma et al. 2009). The former are an obvious connection with circulating cytokines that could act on the brain's endothelium to secrete IL-6 into the parenchyma.

1.5.4 Regulation of body weight and linear growth

1.5.4.1 Energy balance

Maintenance of body weight is dependent on energy balance, which is determined by energy intake and energy expenditure being equivalent. This process depends on the central integration of **satiation** (phasic, related to meals) and **adiposity** (tonic) peripheral signals (Chambers et al. 2013) (Figure 7).

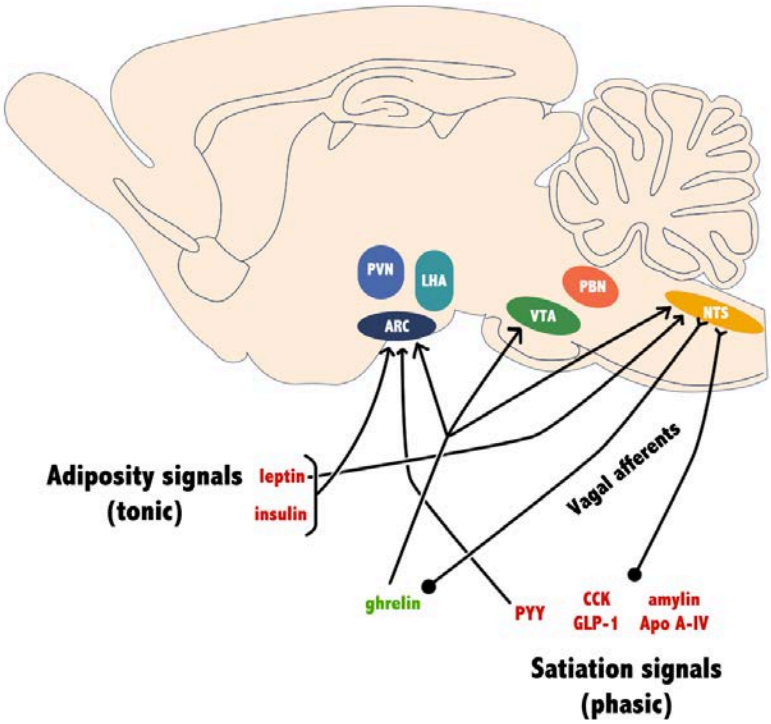

Figure 7. Central integration of satiation and adiposity signals. Peripheral signals get access to the CNS either through the median eminence and then to the ARC or in the NTS. Signaling to the NTS can be humoral or through vagal afferents. Hypothalamus and brainstem, are connected to each other and to the PBN to integrate all the inputs and elicit the appropriate response. The VTA mediates the reward value of food. In red anorexigenic signals; in green orexigenic signals. Apo A-IV apolipoprotein A-IV; ARC arcuate nucleus of the hypothalamus; CCK cholecystokinin; GLP-1 glucagon-like peptide 1; LHA: lateral hypothalamic area; NTS nucleus of the solitary tract; PBN parabrachial nucleus; PVN paraventricular nucleus of the hypothalamus; PYY peptide YY; VTA ventral tegmental area. Based on Cone 2005; Morton et al. 2006; Chambers et al. 2013; Tokita et al. 2014; and Roman et al. 2016.

Phasic signals include **cholecystokinin** (CKK), **glucagon-like peptide-1** (GLP-1) and other derivatives of the proglucagon gene, **peptide YY** (PYY), **amylin**, **apolipoprotein A-IV** (Apo A-IV), and **nutrients** themselves, among others. All of them decrease meal size and most can act either in the periphery or the brain. For example, CKK and GLP-1 have specific receptors in the sensory branches of the vagal nerve that then innervate the NTS and ultimately the

hypothalamus (Smith et al. 1981; Nakagawa et al. 2004; Sullivan et al. 2007), some at least through a relay on the PBN (Roman et al. 2016). GLP-1 can also act directly in the brain (Turton et al. 1996) and bind to its receptors in brain areas related to food intake such as the arcuate nucleus of the hypothalamus (ARC), lateral hypothalamic area (LHA), VMH and the NTS (Göke et al. 1995). It is also possible that they enter the brain through the circumventricular organs and act on neighboring nuclei (Ørskov et al. 1996; Lutz et al. 1998).

In addition, **ghrelin** production in the stomach when fasted has an orexigenic and growth hormone-releasing effect. This hormone does not only increase appetite, but it also reduces the utilization of fat depots (Kojima et al. 1999; Tschöp et al. 2000). It can act either peripherally, through vagal afferents in the stomach, or centrally, in the hypothalamus and brainstem (Guan et al. 1997; Bailey et al. 2000; Date et al. 2002).

Tonic signals are secreted proportionally to body fat mass. Pancreatic β-cells secrete **insulin** and white adipocytes produce **leptin**. These hormones can cross the blood-brain barrier (BBB) by independent saturable transporter systems and then act on brain areas where their receptors are expressed (Banks et al. 1996; Banks et al. 1997). The insulin receptor (IR) is expressed in the olfactory bulb, the cortex, the lateral septum, the nucleus accumbens (NAcc), the dentate gyrus (DG) and the *Cornu Ammonis* (CA) fields of the hippocampus, the mammillary bodies, the PVN, the SON, the ARC, DMH, the granule cell layer of the cerebellum and the dorsal tegmental nucleus in the brainstem (Werther et al. 1987; Marks et al. 1990). The leptin receptor (Ob-Rb splice variant in the mouse) is much more restricted, and is expressed in the ARC, VMH, LHA, DMH, and also in the NTS and other nuclei of the caudal brainstem (Fei et al. 1997; Grill 2006). Of all these, the **ARC** is critical regarding regulation of energy balance since it is a circumventricular organ (Cone et al. 2001), so adiposity signals have increased access, it contains neurons expressing energy balance-related neuropeptides, and it also receives information from satiation and reward signals.

1.5.4.1.1 Hypothalamic neuropeptides and circuitry

There are two major insulin- and leptin-sensing cell populations in the ARC, pro-opiomelanocortin (**POMC**)/ cocaine- and amphetamine-regulated transcript (**CART**) neurons and neuropeptide Y (**NPY**)/agouti-related peptide (**AgRP**) neurons (Figure 8).

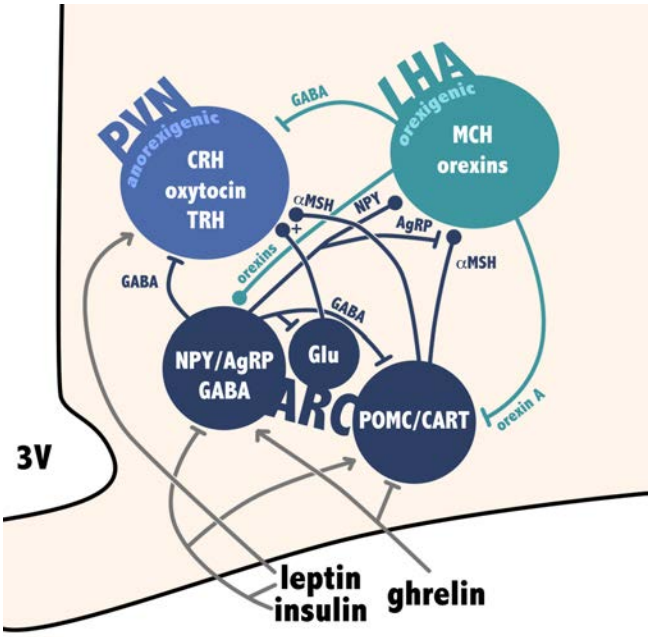

Figure 8. Hypothalamic circuits regulating food intake and energy expenditure. ARC NPY/AgRP, POMC/CART and glutamatergic neurons innervate the PVN and the LHA. GABA from NPY/AgRP neurons inhibits PVN neurons and neighboring ARC glutamatergic neurons (Orxt, see text). α-MSH potentiates glutamate action in the PVN and also stimulates LHA neurons, the latter being antagonized by AgRP. Leptin and insulin have opposing effects to ghrelin in ARC subpopulations. Leptin also stimulates TRH neurons in the PVN. Based on Morton et al. 2006; and Morello et al. 2016.

POMC (the same precursor that in the adenohypophysis originates ACTH) is cleaved in the ARC to produce α-melanocyte-stimulating hormone (**α-MSH**), a neuropeptide that binds melanocortin receptor 3 and 4 (MC3R and MC4R) (Gantz et al. 1993; Roselli-Rehfuss et al. 1993) and has an **anorectic** effect (Huszar et al. 1997; Kim et al. 2000). Leptin and insulin stimulate POMC mRNA expression (Schwartz et al. 1997; Benoit et al. 2002), and their action depends on α-MSH signaling (Seeley et al. 1997; Benoit et al. 2002); while ghrelin inhibits them (Cowley et al. 2003). The other peptide expressed by these neurons, **CART**,

potently inhibits food intake, even in starved rats, and can counteract the effects of NPY. Its expression depends on leptin signaling, and it is therefore suppressed in genetic models of obesity such as the ob/ob mouse (leptin deficient) (Kristensen et al. 1998). However, its deficiency has no major consequences on food intake in basal conditions, but leads to increased body weight gain when *Cart*$^{-/-}$ mice are fed a high-fat diet (Asnicar et al. 2001).

On the other hand, **NPY** binds to Y receptors to ultimately **stimulate food intake** (Clark et al. 1984; Levine and Morley 1984), while **AgRP** has the same net effect by antagonizing MC3R and MC4R (Ollmann et al. 1997). It has also been proposed that AgRP might act as an inverse agonist of MC3R and MC4R (to block constitutive activity), independently of α-MSH (Haskell-Luevano and Monck 2001; Nijenhuis et al. 2001). Both neuropeptides are suppressed by insulin and leptin (Morrison et al. 2005), and stimulated by ghrelin (Goto et al. 2006), therefore integrating adiposity and satiation signals. In addition, AgRP/NPY neurons also coexpress γ-aminobutyric acid (**GABA**) that allows inhibition of POMC/CART neurons both directly at the soma and post-synaptically in targets like the PBN to promote eating (Cowley et al. 2001; Wu and Palmiter 2011).

Very recently, a novel population of glutamatergic ARC neurons expressing the oxytocin receptor (**Oxtr neurons**) has been described and involved in **rapid meal termination**. They are inhibited by GABA from Agrp/NPY neurons and their target synapses potentiated by α-MSH (Fenselau et al. 2017). They have been proposed to be the actual counter-point to AgRP/NPY neurons, since POMC/CART neurons are much slower acting.

These neuropeptides also affect **energy expenditure**, through sympathetic activity and thermogenesis, in an inverse way to food intake (Bray 2000). Orexigenic neuropeptides (those stimulating food intake) also decrease energy expenditure and that is why they are considered to have an anabolic profile (Egawa et al. 1990; Joly-Amado et al. 2012). Conversely, anorexigenic ones

(those inhibiting food intake) increase energy expenditure and therefore have a catabolic profile (Egawa et al. 1990).

Both of the described neuron populations project to other areas to affect behavior or autonomic circuits in order to obtain the anabolic or catabolic effect. One of those targets, the **PVN**, contains glutamatergic neurons that express MC4R and that project to the PBN (an integration point with visceral information) (Shah et al. 2014), and synthesizes other anorexigenic neuropeptides such as **CRH**, **oxytocin** and thyrotropin-releasing hormone (**TRH**) (Krahn et al. 1988; Arletti et al. 1990). The latter acts both through stimulation of thyroid hormones (via thyroid-stimulating hormone, TSH) and at the central level, reducing food intake and increasing thermogenesis. TRH-expressing neurons are located in the parvocellular division of the PVN and receive stimulatory input from POMC/CART neurons (Lechan and Segerson 1989; Fekete et al. 2000). Furthermore, these projections are inhibited by NPY/AgRP projections, creating a crosstalk between ARC subpopulations and the PVN (Toni et al. 1990). In addition, MC4R expression in TRH neurons is stimulated by leptin, increasing energy expenditure to compensate for more adiposity (Harris et al. 2001; Ghamari-Langroudi et al. 2010; Ghamari-Langroudi et al. 2011). However, The PVN can also respond to NPY to increase food intake and decrease BAT thermogenesis (Stanley and Leibowitz 1984; Billington et al. 1994), pointing that its role in energy homeostasis is not one-sided.

The other main target of ARC projections is the **LHA**, which harbors neurons expressing melanin-concentrating hormone (**MCH**) or hypocretin 1, 2/orexins A, B (**HCRT**) (Broberger et al. 1998). The general profile of this nucleus is **anabolic**. Orexins increase food intake upon ICV administration and they are also up-regulated in response to fasting (Sakurai et al. 1998). Likewise, MCH administered ICV also increases food intake (Della-Zuana et al. 2002) and its deficiency results in hypophagic and lean mice, with increased metabolic rate

(Shimada et al. 1998). This nucleus also receives input from the PBN, therefore integrating ARC input with visceral information (Tokita et al. 2014).

1.5.4.1.2 Reward circuits

It is important to also take into consideration the motivational aspects of food intake to paint the big picture of energy balance.

A **tonic inhibition by adiposity signals** of the reward value of food was proposed after observing that food-deprivation increased drug relapse and the rewarding effects of drugs in a leptin-dependent way (Cabeza de Vaca and Carr 1998; Shalev et al. 2001). Furthermore, leptin or a dopamine antagonist revert the place preference conditioned by sucrose pellets in food deprived rats (Figlewicz et al. 2001). Similarly, ICV administration of insulin or leptin interferes with place preference conditioned by a high-fat diet in rats fed *ad libitum* (Figlewicz et al. 2004). The co-expression of dopaminergic markers with IR and Ob-R receptors in the ventral tegmental area (VTA) and *substantia nigra* (SN) supports that these areas, relevant in reward pathways, are responsive to these adiposity signals to modulate the seeking of palatable food (Figlewicz et al. 2003).

Conversely, **ghrelin** can act on the VTA to **promote feeding**. This mesolimbic area expresses ghrelin receptors and its neurons increase action potentials after infusion. Also, *in vivo* peripheral administration of ghrelin after intra-VTA ghrelin blocker infusion prevents increase of food intake (Abizaid et al. 2006).

Opioids play also a significant role interacting with other signals in the energy balance circuitry to modulate the rewarding aspects of feeding. The PVN, NTS, central and basolateral amygdala, and NAcc are important sites for integration of hypothalamic neuropeptides, adiposity signals and opioid signaling (Kotz et al. 1995; Will et al. 2004; Woolley et al. 2006).

1.5.4.1.3 Obesity and central inflammation

The World Health Organization (WHO) defines overweight and obesity "as abnormal or excessive fat accumulation that presents a risk to health." A body mass index (BMI, a person's weight in kilograms divided by his or her height in meters squared) of 25 is considered overweight, and above 30 is generally considered as obese. It is a major concern in today's society since in 2014 (last data available) 1.9 x 10^9 adults were overweight or obese, and more worrisome, 41 million children under the age of 5 were too (WHO 2017). Even though some diseases can lead to obesity as a by-product, the most common cause for excess weight nowadays is excessive eating of caloric foods and sedentarism.

Obesity is associated with an initial **macrophage infiltration** and expression of inflammatory markers in the white adipose tissue (**WAT**) (Xu et al. 2003), followed by development of **insulin and leptin resistance**. Because of its many peripheral functions in glucose and lipid metabolism, peripheral insulin resistance is quite critical in the context of obesity. Hepatic insulin resistance originates in the adipose tissue, where IL-6 secretion mediated by c-Jun NH_2-terminal kinase 1 (Jnk1), increases hepatic SOCS3 (Sabio et al. 2008), which in turn decreases tyrosine phosphorylation of insulin receptor substrate (IRS)-1 and also reduces the association of the p85 subunit of PI3K with IRS-1 and insulin-dependent activation of AKT, all elements of the insulin signaling cascade (Senn et al. 2002; Ueki et al. 2004). Leptin resistance occurs in the adipose tissue in a SOCS-dependent process too, with a concomitant reduction in Ob-R (Wang et al. 2000; Wang et al. 2005). However, central resistance to both insulin and leptin is even more important since it can have a whole-system effect.

Saturation of the transport system of leptin and insulin may be the first point of decreased responsiveness in the CNS, since the amount to reach the parenchyma would not be representative of the peripheral situation (Israel et al. 1993; Caro et al. 1996). But the reduced responsiveness of hypothalamic circuits,

or **central resistance**, to insulin and leptin is what ultimately leads to a defective regulation of energy balance.

The current view on the cause for this resistance is **hypothalamic chronic inflammation**. Saturated fatty acid-rich diets induce the hypothalamic (in the ARC and LHA) production of pro-inflammatory cytokines by microglia such as IL-1β, TNF-α and IL-6 through a TLR-4-mediated process involving endoplasmic reticulum (ER) stress (Milanski et al. 2009). This cytokine secretion has also been shown in cultured astrocytes independently of microglia (Gupta et al. 2012), even though this point is contended (Holm et al. 2012). In addition, increased serine phosphorylation of the IR and IRS-2, which is associated to insulin resistance, occurs in hypothalamic neurons, which also express TNF-α (Hotamisligil et al. 1996; De Souza et al. 2005). Blocking signal transduction of TLR-4 lessens high-fat diet-induced weight gain, improves leptin sensitivity and peripheral glucose metabolism (Kleinridders et al. 2009). The effects on insulin and leptin signaling and body weight appear to be mediated by **NF-κB** activation (due to IKKβ-mediated degradation of its inhibitor IκBα) in, at least, AgRP neurons, due to increased SOCS3 expression (Zhang et al. 2008; Benzler et al. 2015).

Moreover, the resulting inflammation also contributes to worsen the situation. Mimicking of this inflammation with a low dose of TNF-α results in reduced leptin signaling in the hypothalamus and expression of *Pomc* and *Crh*. This translates into reduced expression of thermogenesis markers in the BAT (e.g. uncoupling protein-1 UCP1) and mitochondrial respiration in the skeletal muscle; as well as in increased insulin secretion but impaired insulin signal transduction in the liver and skeletal muscle (Arruda et al. 2011).

This inflammation occurs very **early after initiation of high-fat diet** (in an experimental setting), and before peripheral inflammation occurs; suggesting that it is independent from it. Inflammation markers in the whole hypothalamus

can be detected after only 1 day of high-fat diet (Waise et al. 2015). Thaler and colleagues (2012) observed microgliosis and astrogliosis in the ARC by day 3, and suggest that this gliosis is the result of neuronal injury caused by the fatty acids and that it eventually causes a reduction in POMC neurons in the ARC. Human data corroborates these findings, since there is evidence from obese subjects for similar injury in the mediobasal hypothalamus by magnetic resonance imaging (MRI) studies, and they also present increased microgliosis (Thaler et al. 2012; Baufeld et al. 2016). This microglial activation may have a dual role depending on the moment. The initial acute response is of a pro-inflammatory nature but a shift occurs at later time-points that could mean they adopt a more neuroprotective state (Baufeld et al. 2016). Also in the long term, astrogliosis persists (Buckman et al. 2013); but, whether peripheral monocyte infiltration occurs is still debated, even though the most recent evidence suggests that this is not the case (Buckman et al. 2014; Baufeld et al. 2016).

1.5.4.1.4 IL-6: evidence from animal and pharmacological models

The data from studies on sickness behavior were the first to point at a role of IL-6 in the regulation of energy balance, and suggested a negative effect of IL-6 on food intake, which was potentiated by sIL-6R (Schöbitz et al. 1995; Plata-Salamán 1996). The first milestone in the elucidation of the cytokine's role in this process came from systemic **IL-6KO** mice, and their **mature-onset obesity**. From 6 months of age on, these mice displayed a higher body weight due to higher fat depots, increased leptin levels, leptin intolerance, decreased glucose tolerance and increased food intake, which, notably, was uncorrelated with body weight (Wallenius et al. 2002b). However, in another group, the same model failed to develop any of the previous phenotypes, except for the glucose intolerance (Di Gregorio et al. 2004). Of note, in our group the same IL-6KO mice did develop obesity, more prominently in males (Navia et al. 2014). Nevertheless, ICV

administration of IL-6 increases colonic temperature and resting O_2 consumption (Rothwell et al. 1991), while it decreases body fat of high-fat diet-fed rats, with an average food intake lower than controls (Wallenius et al. 2002a), supporting the notion that **IL-6 suppresses body fat**.

More evidence on the catabolic profile of IL-6 comes from the transgenic **GFAP-IL6** mouse, with chronic expression of IL-6 in astrocytes. This model is somewhat (males) or completely (females) **resistant to high-fat diet-induced obesity**, has reduced visceral adipose tissue, and, surprisingly, has impaired glucose tolerance when fed the high-fat diet (Hidalgo et al. 2010).

One of the proposed mechanisms for the systemic changes elicited by IL-6 is an increased sympathetic tone. Indeed, IL-6KO mice have deficient upregulation of energy expenditure during new-cage stress and cold-exposure, as well as lower plasma NE (Wernstedt et al. 2006), but the results with GFAP-IL6 and impaired thermogenesis after cold-exposure suggest a complicated picture (Hidalgo et al. 2010).

The **source of IL-6** is also a relevant issue, given all the cells that produce it in the CNS. Our group has begun to tackle the question with a conditional astrocytic IL-6KO mouse. This model displays a higher body weight (in males) than wild-type mice as seen in the IL-6KO model, but from an earlier age (Quintana et al. 2013).

1.5.4.2 Neural regulation of bone

Bone remodeling results from a balance between bone **resorption** (break down by **osteoclasts**) and **formation** (by **osteoblasts**). The first evidence from a central regulation of bone mass came from the anti-osteogenic effects of **leptin**. Genetic models of obesity, ob/ob and db/db mice (leptin receptor deficient), show

increased bone mass in the vertebrae, linked to higher osteoblast function compensating the increased resorption caused by their hypercortisolism and hypogonadism. This process is hypothalamus-mediated, as shown by the bone loss resulting from third ventricle administration of leptin in both ob/ob and wild-type mice. However, the fact that NPY also causes bone loss, suggests that this process follows different mechanisms than the energy balance circuitry (Ducy et al. 2000). Of note, femora of ob/ob mice have been found to be shorter and less dense, but this process is probably related to reduced muscle (Hamrick et al. 2004).

The **VMH**, which expresses Ob-Rb (Fei et al. 1997), is critical for responding to leptin and exerting its anti-osteogenic effect, independently of its ARC-mediated anorectic effects. Ablation of this nucleus results in a high bone mass phenotype such as in ob/ob mice, with an increased bone formation rate, that cannot be rescued by leptin ICV infusion (Takeda et al. 2002). In addition, mice deficient in the catecholamine-synthesizing enzyme dopamine β–hydroxylase (DBH) present high bone mass that is unaffected by adrenal medulla removal or leptin ICV administration, supporting a **sympathetic nervous system** (SNS) mechanism (Takeda et al. 2002). Further evidence for the sympathetic action on osteoblasts came from β_2-adrenergic receptor (β2AR) deficient mice (*Adrb2*$^{-/-}$) that also have a high bone mass, linked to high bone formation and low bone resorption. In this model, lack of β2-adrenergic signaling in osteoblasts results in increased activity of those cells, plus deficient secretion of the osteoclast differentiation factor RANKL. Based on the similar phenotype to leptin deficient mice (high bone mass), but ob/ob mice being hypogonadic and *Adrb2*$^{-/-}$ not responding to ovariectomy with bone loss, the authors propose an additional pathway of leptin action to sympathetic signaling via β2AR inhibition of osteoclast differentiation by CART (Elefteriou et al. 2005). The only apparent difference between those models is the blunted expression of CART in ob/ob mice (Kristensen et al. 1998). Certainly, *Cart*$^{-/-}$ mice have decreased bone mass and an

exacerbated response to the anti-osteogenic effect of leptin due to increased resorption (Elefteriou et al. 2005); while the increase in its expression (due to MC4R deficiency) is associated with high bone mass in both mice and humans, and can be reversed by just deleting *Cart* (Farooqi et al. 2000; Ahn et al. 2006).

1.5.4.2.1 Central IL-6 may participate in bone remodeling

The similarities with leptin regarding energy balance, and the fact that they share STAT3-dependent signaling pathways, could suggest a role for IL-6 in bone remodeling, given that sympathetic neurons produce it (März et al. 1998). However, no studies have specifically addressed this possibility. Available evidence comes from systemic alterations of IL-6 production, such as the observation that mice with constituent expression of human IL-6/s-IL-6R are smaller and weigh less (Peters et al. 1997). However, in line with this observation and supporting a central action of IL-6, GFAP-IL6 were noted to be considerably smaller than controls and with a hunched position (Campbell et al. 1993), but no explanation was proposed or explored.

1.5.5 Final considerations

It has been mentioned before that a saturable system exists that allows IL-6 to **cross the BBB**, although it is rapidly degraded (see *1.3.1 Peripheral and CNS cells express IL-6*). In addition, it should be noted that the reverse is also possible. Radioactively-labelled IL-6 injected into the lateral ventricle of the brain (of both rats and mice) can be detected in the blood after 4 hours and is thought to do so by venous drainage through the superior sagittal sinus (Banks et al. 1994; Chen et al. 1997). However, our group previously used GFAP-IL6 mice and found no increase in serum levels, either in basal conditions (where it was barely detectable by ELISA) or after an LPS injection or EAE, relative to wild-type

animals. This could be due to the fact that in this model IL-6 expression is chronic and clearance could prevent detection of small changes, or rather, that the amount that reaches the ventricle is insufficient to make a difference in peripheral blood. Nevertheless, in the case of the double transgenic mouse GFAP-IL6-IL-6KO, a total IL-6 knock-out with GFAP-guided expression of IL-6, a modest but detectable amount of IL-6 (compared to the undetectable levels in IL-6KO) was measured in serum after LPS injection (Giralt et al. 2013), suggesting indeed a **certain clearance into the blood** but that is **unlikely to be very relevant**.

2 HYPOTHESIS

Given that IL-6 acts in the CNS to regulate body weight and behavior, the local production of this cytokine is likely very relevant in these processes. In addition, due to the multiple sources of IL-6 within the CNS, their relative contribution is probably different. **Astrocytes**, being the most abundant cell in the CNS, are in a unique position to be modulators by secreting IL-6; and given that **neurons** regulate energy balance and multiple behavioral processes, both their production of IL-6 and their response to it will probably be significant as well.

3 OBJECTIVES

1. To obtain mice with astrocytic deficit of IL-6 and characterize their phenotype with regard to weight and metabolism, in basal conditions or in response to several challenges such as a high-fat diet and fasting.

2. To obtain mice with neuronal deficit of IL-6 and characterize their phenotype with regard to behavior, weight and metabolism, in basal conditions or in response to several challenges such as a high-fat diet and fasting.

3. To obtain mice with neuronal deficit of IL-6Rα and start their phenotyping, both behaviorally and regarding food intake.

4. To obtain mice with chronic expression of IL-6 in astrocytes and characterize their response to two energy challenges such as fasting and a short-term high-fat diet.

4 MATERIALS AND METHODS

4.1 Cre-lox technology

Cre-lox technology is a technique used for activating or inactivating genes in the mouse, among other species. It profits from the capacity of the P1 bacteriophage *cre* recombinase to recombine two specific sequences called *lox* (Sternberg and Hamilton 1981). These sequences are incorporated into the DNA of a mouse, flanking a section of the gene of interest (critical for its function). The resulting mouse is called a *floxed* mouse. Depending on the orientation of the lox sites (*cis*, same orientation; or *trans*, opposite), which surround the genetic area of interest, the result of the recombination will be the excision of the fragment (Figure 9, top) or its inversion (Figure 9, bottom).

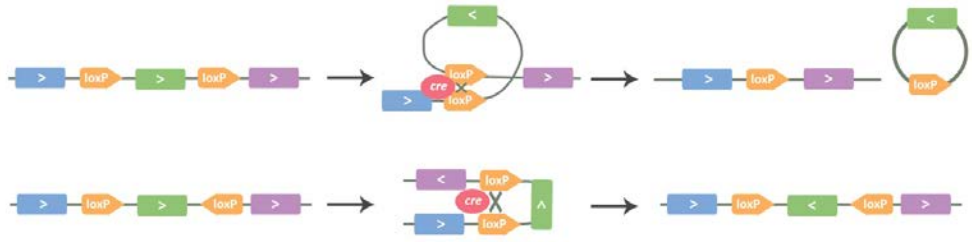

Figure 9. Cre-mediated recombination. *Top* loxP sequences in *cis* result in the excision of the region of interest. *Bottom* loxP sequences in *trans* result in the inversion of the sequence.

Cell-specific or time-controlled expression of *cre* can be achieved by putting it under the control of different promoters and combining it with response elements to different drugs, such as tamoxifen, tetracycline or doxycycline (Zhang et al. 1996; Shimizu et al. 2000; Zeng et al. 2008).

4.2 Mice

4.2.1 Il6 floxed mice

Il6 floxed (flanking exon 2) mice were produced as previously described (Quintana et al. 2013) and backcrossed at least 10 times with C57BL/6OlaHsd mice (from Envigo) before further crossing.

4.2.2 IL6ra floxed mice

IL6ra floxed mice were a kind gift of Dr. Angela Drew, and were created as stated elsewhere (McFarland-Mancini et al. 2010). In these transgenic mice exons 4–6 of the interleukin 6 receptor alpha chain gene (*Il6ra*, encoding the cytokine receptor biding module) are flanked by two loxP sites, originally in a C57BL/6N genetic background.

4.2.3 Glial Fibrillary Acidic Protein cre mice (GFAP-Cre)

GFAP-Cre mice (01XN3, C57BL/6-Tg(GFAP-Cre)8Gtm) were produced by Dr. David H. Gutmann and obtained from the National Cancer Institute Mouse Models of Human Cancers Consortium (MMHCC) at Frederick, MD 21702, USA. This mouse line expresses *Cre* recombinase by E13.5 under the human glial fibrillary acidic protein promoter, showing robust expression in astrocytes but not in MAP-positive neurons or APC-positive oligodendrocytes (Bajenaru et al. 2002).

4.2.4 Synapsin-1 cre mice (Syn1-Cre mice)

Syn1-Cre mice (B6.Cg-Tg(Syn1-cre)671Jxm/J), were produced by Dr. Jamey Marth and we obtained them from The Jackson Laboratory. These mice express *Cre* recombinase under the control of the rat synapsin I promoter. Cre recombinase activity can be detected in neuronal cells, including brain, spinal cord and dorsal root ganglion, as early as E12.5, as well as in neurons in adult (Zhu et al. 2001).

4.2.5 Conditional Il6 knockouts

4.2.5.1 In astrocytes

In order to obtain ast-IL6KO mice, we carried out the following breeding strategy. First, we crossed *GFAP-Cre*$^{+/-}$ with homozygous floxed *Il6* mice, and selected the progeny positive for *GFAP-Cre*. We then crossed these animals again to homozygous floxed *Il6* mice and obtained four genotypes, which we called wild-type (*Il6*$^{lox/wt}$, wt), floxed (*Il6*$^{lox/lox}$), heterozygous (*GFAP-Cre*$^{+/-}$ *Il6*$^{lox/wt}$, from now on *Il6*$^{\Delta Gfap/wt}$) and conditional knockout (*GFAP-Cre*$^{+/-}$ *Il6*$^{lox/lox}$, from now on *Il6*$^{\Delta Gfap}$) (Figure 10). All these animals have at least one floxed allele of *Il6* (exon 2) in all their cells, which will only be excised in those cells expressing *Cre* under the *GFAP* promoter. Initially, we used both wt and floxed as controls in order to determine the putative phenotype of the floxed gene. Later, we chose floxed mice as the more suitable control for our conditional knockouts, which have the floxed gene in all cells.

4.2.5.2 In neurons

The same breeding strategy as for conditional astrocytic knockouts was followed in this case. *Syn1-Cre* mice were crossed with homozygous floxed *Il6* mice, and then the progeny positive for *Syn1-Cre* was crossed again to floxed *Il6* mice. The four genotypes obtained were wild-type ($Il6^{lox/wt}$, wt), floxed ($Il6^{lox/lox}$), heterozygous ($Syn1\text{-}Cre^{+/-}$ $Il6^{lox/wt}$, from now on $Il6^{\Delta Syn1/wt}$) and conditional knockout ($Syn1\text{-}Cre^{+/-}$ $Il6^{lox/lox}$, from now on $Il6^{\Delta Syn1}$) (Figure 10).

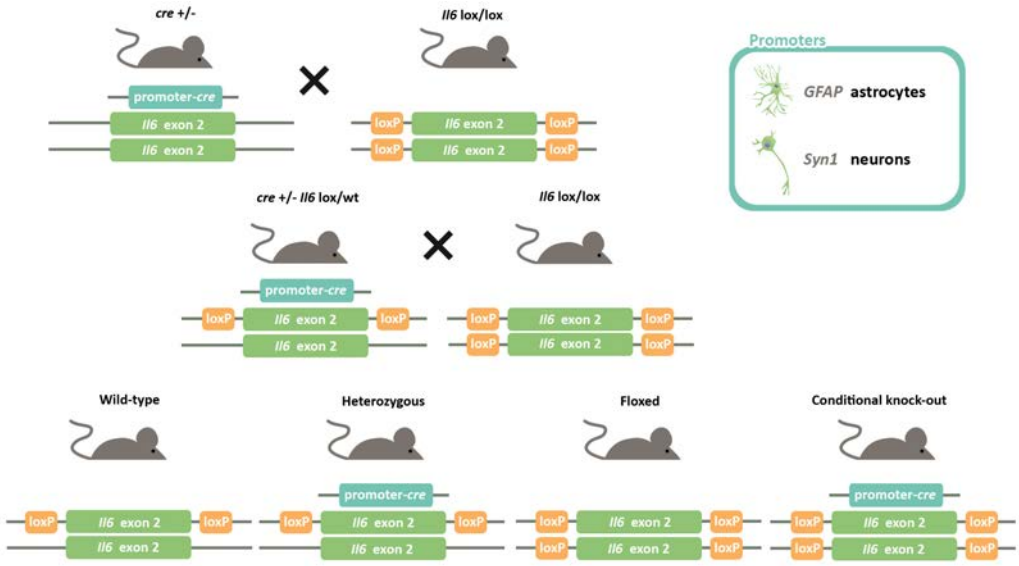

Figure 10. Breeding strategy for obtaining conditional Il6 knockout mice in astrocytes or neurons. Cell-specific promoters drive *Cre*-expression in the target cell; in astrocytes, glial fibrillary acidic protein (GFAP), and in neurons, synapsin-1 (Syn1). *Cre* expression causes excision of exon 2 of the floxed *Il6* gene.

4.2.6 Conditional Il6ra knockout in neurons

Neuronal IL-6Rα deficient mice and their littermate floxed controls were produced following the same method as stated above for the conditional neuronal knockout model, but using *Il6ra* floxed mice. The four genotypes obtained after the second crossing were wild-type ($Il6ra^{lox/wt}$, wt), floxed ($Il6ra^{lox/lox}$),

heterozygous (*Syn1-Cre*$^{+/-}$ *Il6ra*$^{lox/wt}$, from now on *Il6ra*$^{\Delta Syn1/wt}$) and conditional knockout (*Syn1-Cre*$^{+/-}$ *Il6ra*$^{lox/lox}$, from now on *Il6ra*$^{\Delta Syn1}$) (Figure 11).

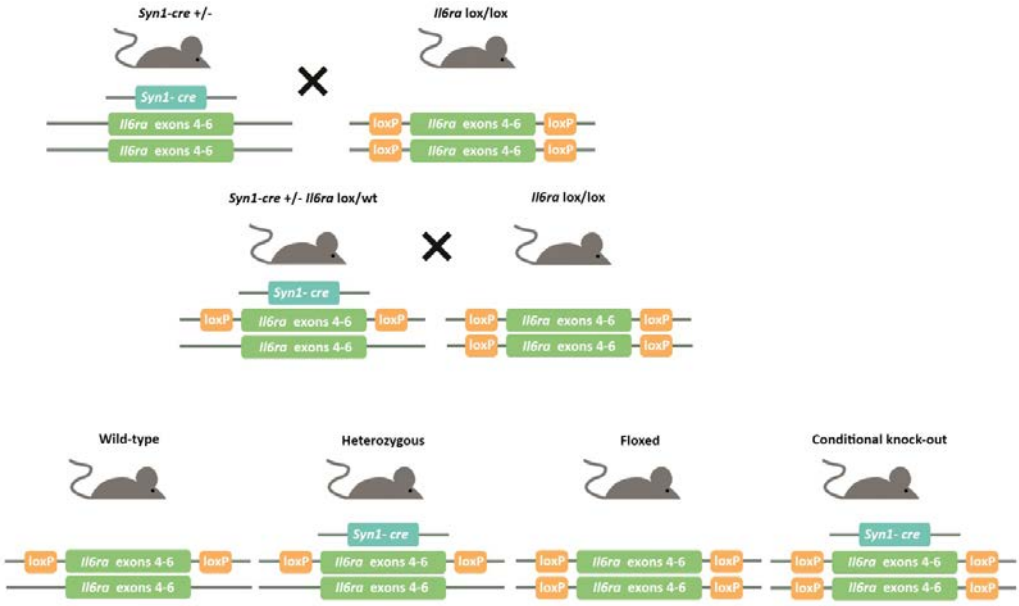

Figure 11. Breeding strategy for obtaining conditional Il6ra knockout mice in neurons. *Cre* recombinase expression is driven by the synapsin-1 (*Syn1*) promoter. Expression of *Cre* prompts de excision of exons 4-6 of the floxed *Il6ra* gene.

4.2.7 GFAP-IL6 mice

Hemizygous mice with chronic expression of IL-6 under the GFAP promoter (Campbell et al. 1993) were kindly given by Dr. Iain Campbell and bred with C57BL/6OlaHsd (from Envigo) to obtain the experimental animals wt and GFAP-IL6. The animals were 4-5 moths-old when used for the experiment.

4.2.8 Genotyping of animals

DNA was extracted by boiling a ~1 mm piece of tail in 100 µl of 50 mM NaOH for 7 minutes, and then used immediately for PCR or stored at -20°C.

Afterwards, the appropriate PCR was set up (see Tables 1-4 for reactions, thermal cycler conditions and primer sequences) with 1 µl of the DNA extraction. DNA polymerase and buffers were purchased from Biotools (*taq* DNA polymerase, ref. 10.013) or Thermo Fisher (Dream *taq* DNA polymerase, ref. EP0703) and primers and oligonucleotides from Sigma-Aldrich.

Table 1. Reagents and conditions for the *Il6* floxed, *Cre* recombinase, *Il6* recombination and *Il6ra* recombination PCRs.

	Volume (µl)	Final concentration
H_2O	11.62	-
Buffer 10x (includes $MgCl_2$)	1.5	1x (2 mM)
dNTPs	0.3	200 µM each
Forward	0.75	0.5 µM
Reverse	0.75	0.5 µM
Dream *taq* polymerase	0.08	26.7 mU/µl
Final volume	15	

Il6			*Cre*			*Il6* recombination			*Il6ra* recombination		
Temperature	Time (s)	Cycles	Temperature	Time (s)	Cycles	Temperature	Time (s)	Cycles	Temperature	Time (s)	Cycles
94°C	180	1	94°C	120	1	94°C	180	1	94°C	180	1
94°C	30		94°C	10		94°C	45		94°C	10	
56°C	30	30	63°C	10	25	55°C	45	33	60°C	10	30
72°C	30		72°C	40		72°C	70		72°C	120	
72°C	300	1	72°C	300	1	72°C	300	1	72°C	300	1

Table 2. Reagents and conditions for the *Il6ra* PCR.

	Volume (µl)	Final concentration
H_2O	9.15	-
Buffer 10x ($MgCl_2$ free)	1.5	1x
$MgCl_2$	0.75	2.5 mM
dNTPs	0.3	200 µM each
Primer *Il6ra* F	1.5	1 µM
Primer *Il6ra* R	1.5	1 µM
Taq polymerase	0.3	20 mU/µl
Final volume	15	

Temperature	Time (s)	Cycles
94°C	180	1
94°C	30	
58°C	30	33
72°C	30	
72°C	300	1

Table 3. Reagents and conditions for the *GFAP-Il6* PCR

.

	Volume (µl)	Final concentration	Temperature	Time (s)	Cycles
H_2O	4	-			
Buffer 10x ($MgCl_2$ free)	1.5	1x	94°C	180	1
$MgCl_2$	1	3.3 mM			
dNTPs	1.5	1 mM	94°C	30	
Primer *Il6ra* F	1.5	1 µM	53°C	40	33
Primer *Il6ra* R	1.5	1 µM	72°C	30	
Primer *GFAP-Il6* F	1.5	1 µM	72°C	300	1
Primer *GFAP-Il6* R	1.5	1 µM			
Taq polymerase	1	66.7 mU/µl			
Final volume	15				

4.2.8.1 *Il6* recombination PCR

DNA was extracted from tail, brain and/or liver samples. Using primers *Il6* rec forward (F) and *Il6* rec reverse (R) the bands to be obtained were approximately 900, 1000, and 260 base pairs (bp) for the wild-type, floxed and recombined (delta) alleles, respectively (Figure 12).

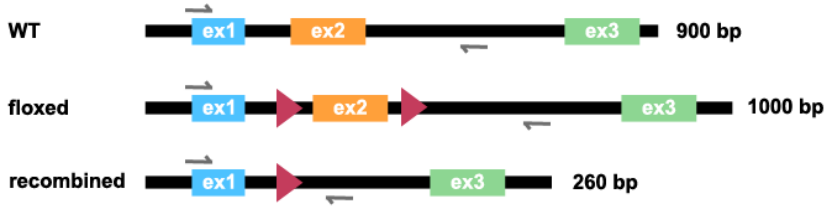

Figure 12. Schematic representation of the bands obtained in the Il6 recombination PCR. Homologous recombination in the floxed gene by *Cre* excises exon 2 (orange) and gives a 260 bp product when amplified. Grey arrows indicate F and R primer placement; red triangles represent loxP sequences. Ex exon; bp base pairs; WT wild-type.

4.2.8.2 *Il6* floxed PCR

This PCR distinguishes the floxed and wild-type alleles of *Il6*. The F primer is located in exon 1 and the R primer in exon 2. Since the floxed sequences surround exon 2, the amplified product will have a length of 373 bp in the wild-type allele and 476 bp in the floxed one.

4.2.8.3 *Cre* recombinase PCR

Cre-specific primer sequences were the same as used by Sanz et al. (2009). The amplified product yields a band of 375 bp in the case of a *Cre*-positive animal and no-band in the case of *Cre*-negative ones. Positive and negative controls were always included in each run.

4.2.8.4 *Il6ra* recombination PCR

DNA was extracted from tail, brain and/or liver samples. Using primers *Il6ra* rec F and *Il6ra* rec R the bands to be obtained were approximately 1900, 2000, and 230 bp for the wild-type, floxed and recombined (delta) alleles, respectively (Figure 13).

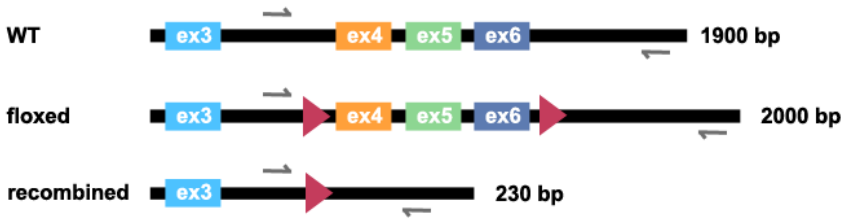

Figure 13. Schematic representation of the bands obtained in the Il6ra recombination PCR. Homologous recombination in the floxed gene by *Cre* excises exons 4-6 and gives a 230 bp product when amplified. Grey arrows indicate primer placement; red triangles represent loxP sequences. Ex exon; bp base pairs; WT wild-type.

Table 4. Primer sequences for genotyping and validation of recombination.

	Sequence (5' → 3')
***Il6* F**	CAA TTC CAG AAA CCG CTA TGA
***Il6* R**	TCC ACG ATT TCC CAG AGA AC
***Il6ra* F**	GAA GGA GGA GCT TGA CCT TGG
***Il6ra* R**	AAC CAT GCC TAT CAT CCT TTG G
***Cre* F**	GCA TTA CCG GTC GAT GCA ACG AGT G
***Cre* R**	GAA CGC TAG AGC CTG TTT TGC ACG TTC
***Il6* rec F**	CCC ACC AAG AAC GAT AGT CA
***Il6* rec R**	ATG CCC AGC CTA ATC TAG GT
***Il6ra* rec F**	CTG GGA CAG GGA AGG GCT TTT
***Il6ra* rec R**	CCC AGT GAG CTC CAC CAT CAA A
GFAP-IL6 F	GAT CCA GAC ATG ATA AGA TA
GFAP-IL6 R	CCG AAA AAA CCT CCC ACA CC
Mt1 F	TCA CCA GAT CTC GGA ATG G
Mt1 R	AAG AAC CGG AAT GAA TCG C

4.2.8.5 *Il6ra* floxed PCR

This PCR distinguishes the floxed and wild-type alleles of *Il6ra*. The F primer is located after exon 3 and the R primer in exon 4. The amplified product will have a length of 527 bp in the wild-type allele and 671 bp in the floxed one.

4.2.8.6 GFAP-*Il6* PCR

This PCR detects the presence of the GFAP-IL6 transgene. In positive mice, the amplified product will show at 196 bp. A control band at 178 bp (for the *Mt1* gene) should appear in all samples.

4.2.9 Animal husbandry

All mice were kept under constant temperature (23 ± 2°C) and under a standard 12-h light/12-h dark cycle and with free access to food and water unless otherwise stated. Mice from the same sex were housed together from weaning (usually 2-4 mice per cage) to limit fights between males (a few males had to be isolated because of aggressiveness).

All procedures were approved by the "Comisión de Ética en la Experimentación Animal y Humana" (Universitat Autònoma de Barcelona, Spain) and Generalitat de Catalunya.

4.3 Diet-induced obesity

Several experiments have been carried out using a diet-induced obesity model in *Il6*$^{\Delta Gfap}$ and *Il6*$^{\Delta Syn1}$mice. Below there is a general explanation of all the procedures, however, not all were done in all experiments.

4.3.1 Diets

Both the high-fat diet (HFD) TD 03584 and the control diet 2018 were obtained from Envigo (Table 5).

The experiment started at age 5-11 weeks and mice were maintained on their respective diets for 12-17 weeks. In the case of GFAP-IL6 mice the diet was short term and lasted only 5 days.

Table 5. Percentage of calories from different macronutrients in the experimental diets.

	Control diet	HFD
% calories from protein	24	15
% calories from fat	18	58.4
% calories from carbohydrate	58	26.6
Energy density (kcal/g)	3.1	5.4

4.3.2 Energy intake and fast-refeeding

Body weight and energy intake per cage were recorded weekly for the duration of the experiment or at the end after individualization of the animals.

When measured in group-housed animals, energy intake was estimated as the total intake divided by the number of animals in the cage, with sample size being the number of cages.

Feed efficiency in group-housed animals was calculated across the whole experiment by dividing the average of their weight increase on week 17 by the sum of the cage's weekly per animal energy intake.

For individual food intake, mice were acclimated to isolation for a week before recording energy intake (average of three consecutive days at 900 h). Afterwards, they were fasted for 24 hours (at 1430 h) and energy intake was measured for 4 hours (hourly) upon refeeding. Weight was recorded at the beginning of fasting, at the end, and 4 hours after that.

4.3.3 Body temperature

Body temperature was measured after 12 weeks on the experimental diet with a lubricated rectal probe (Cibertec) for 4 consecutive days at 900 h and the values averaged for each animal.

4.3.4 Activity

On week 9, activity was assessed with the open field test (see *4.7.1 Open field*).

4.3.5 Insulin tolerance test (ITT)

This test was carried out on week 10 or 14 of the diet to test insulin responsiveness. The animals were injected IP with a dosage of 1 U/kg of insulin after a 4-hour fast and blood glucose was measured from the tail at 0, 15, 60 and 120 minutes after the injection with an ACCU-CHECK glucometer (Roche).

4.3.6 Oral glucose tolerance test (OGTT)

This test was performed a week after the ITT to assess insulin production. Animals were fasted overnight (16 hours approximately), and administered 2 g/kg of a glucose solution (diluted in tap water) by oral gavage. Glucose was also measured from tail blood at 0, 15, 60 and 120 minutes after administration with an ACCU-CHECK glucometer.

4.3.7 Euthanasia

Mice were killed by decapitation; the blood was collected from the trunk and allowed to clot and centrifuged at 10,000 g for 10 minutes at 4°C to obtain the serum for analysis of hormones and metabolites. If blood glucose was to be measured, mice were fasted for 3 hours (starting at 7 am, with lights on) before decapitation and, immediately after collection, blood glucose was measured with an ACCU-CHECK glucometer. Visceral (gonadal) and subcutaneous (dorsal area) WAT depots, BAT and liver were removed and weighed immediately. For *in situ*

hybridization, the brain was extracted as a whole and frozen on dry ice. For microarray or real-time PCR (qPCR), the hypothalamus was dissected and snap-frozen in liquid nitrogen.

4.4 Fasting

Group-housed animals fed the control diet where deprived from food for either 16 (overnight), 24 or 48 hours, depending on the group. After fasting (16 and 48 hours) mice were killed by decapitation, as previously described, and the hypothalamus was dissected for qPCR. In the case of the 24-hour fast, mice were refed and monitored as described in *4.3.2 Energy intake and fast-refeeding.*

4.5 Blood metabolites and hormones

4.5.1 Triglycerides and cholesterol

Serum triglyceride and total cholesterol levels were analyzed using Cromatest kits (Linear Chemicals S.L.). The triglyceride one (ref. 1118010) is based on the enzymatic hydrolysis of serum triglycerides to glycerol and free fatty acids through action of lipoprotein lipase. The cholesterol kit (ref. 1155010) involves three enzymes cholesterol esterase, cholesterol oxidase and peroxidase.

4.5.2 Leptin and insulin

Serum insulin and leptin levels were measured using radioimmunoanalysis (RIA) kits (Millipore, sensitive rat insulin SRI-13K, mouse leptin ML-82K) following manufacturer's instructions. Assayed volume was 100 µl in both cases. The stated sensitivity of the assays for the volume used was 0.0329

ng/ml for insulin and 0.377 ng/ml for leptin. Both kits had 100% specificity to the respective mouse protein, and cross-reactivity to rat, human, pork, sheep and hamster (insulin, 100% specificity each) or rat and human (leptin, 50% and <0.2%, respectively).

4.5.3 IGF-1

Serum or plasma IGF-1 was measured using a DuoSet ELISA Development System (R&D, DY791 and DY009) introducing an acid extraction in the manufacturer's protocol to allow for separation of IGF-1 from its binding proteins (IGFBPs). Specifically, samples were diluted 18 in extraction solution (87.5% ethanol, 12.5% 2N HCl), centrifuged and neutralized with 0.5 volumes of a NaOH solution equivalent for equivalent. Finally, they were diluted in the manufacturer's reagent diluent to a final 1/250. The standard curve was prepared with reagent diluent containing 2.8% ethanol to mimic the samples, even though no effect of ethanol was detected during optimization.

4.5.4 IGFBP-1 and 3

IGFBP-1 and -3 were measured in plasma or serum using a mouse IGF Binding Protein Magnetic Bead Panel (Millipore, MIGFBPMAG-43K) following manufacturer's instructions and using a 1/25 dilution.

4.6 Linear growth

Nose-rump distance was measured with a ruler on isofluorane-anesthesized animals.

Tibia length was measured using a Vernier caliper from the proximal epiphysis to the medial malleolus. The bone was removed at the moment of euthanasia and left in water for 3 months. At the moment of measurement, the remaining muscle tissue was removed with forceps and scissors.

4.7 Behavioral tests

Mice were transferred to the testing animal facility and left to habituate for at least one week. The mice were handled for five days in the behavioral testing room before being tested in the different apparatuses. The protocol was as follows on day 1 (following handling), mice performed the open field test and then returned to the animal room; on day 3, the mice were subjected to the hole-board apparatus; on day 5, they were tested in the elevated plus-maze; and finally, on day 7 the Morris water-maze procedure was initiated. All tests were carried out in a blind manner.

4.7.1 Open field

The OF was introduced by Calvin Hall back in 1934 and has been widely used for measuring general locomotor activity in rodents, and faces the animal with a conflicting situation due to the brightly lit and open (and therefore aversive) but novel environment.

The OF apparatus consists of a rectangular white plastic box (56 x 36.5 x 31 cm) (Belda et al. 2012). The floor is subdivided in 12 areas, conforming 10 external and 2 internal areas (Figure 14). A video camera was used for recording the sessions. Prior to placing each animal in the OF, the box was wiped with a 5% alcohol solution and dried. Mice were placed in a corner facing the wall of the apparatus and left in the apparatus for 5 min. The measurements taken were

latency to leave the start section, number of total, internal and external sections crossed, rearings and defecations. The animal was considered to have crossed a section when the 4 paws were in it at the same time. A rearing was counted when the animal stands erect on its hind legs. All measures were carried out from the recorded video by the same experimenter using a slightly modified version of a previously developed Visual Basic macro in Excel (Quintana et al. 2013).

4.7.2 Hole-board

The HB test was first introduced by Boissier and Simon (1962) and it is used to separately evaluate locomotion and exploration (File and Wardill 1975; Arenas et al. 2014; Erta et al. 2015), although there exists some controversy as to the validity of this distinction (Brown and Nemes 2008). In principle, the holes present a choice to the animal to really explore (neophilia), as opposed to an empty open space where the animal has nothing else to do.

The HB apparatus is a square white box subdivided in 16 square areas and with four holes, one on each outside vertex of the four inner squares (Figure 14). Before placing the animals in the HB, the apparatus was wiped with a 5% alcohol solution and dried. They were placed in a corner section facing the wall and left to explore for 5 minutes. Head-dipping behavior in the HB was recorded *in situ* (number and time), while all other variables were analyzed from the recorded videos using a slightly modified version of a previously developed Visual Basic macro in Excel (Quintana et al. 2013). A head-dipping is recorded when the mouse introduces its head up to the base of the ears (at least) in one of the holes; and area crossings used the same criterion as in the OF test.

4.7.3 Elevated plus maze

The EPM is the most widespread test in the study of anxiety-like behaviors in rodents. It is based on the conflict generated in the animal when faced with a new environment (eagerness to explore) with unprotected areas (avoidance of open spaces) (Nadal et al. 2006).

The EPM apparatus consists of a cross section of four white arms (each 18 cm long and 5 cm wide, divided in 3 rectangles of 6 x 5 cm) connected by a central square of 5 x 5 cm (Figure 14). The apparatus is elevated 50 cm from the floor by two metallic legs. Two opposite arms have 15 cm high walls, whereas the other two only have a small ridge to prevent the mice from falling. Prior to placing the animal in the EPM, it was wiped with a 5% alcohol solution and dried. Mice were placed in the central square facing a closed arm (Nadal et al. 2006) and left in the apparatus for 5 minutes. The test was recorded and all measures were carried out afterwards using a slightly modified version of a previously developed Visual Basic macro in Excel (Quintana et al. 2013). Total areas crossed, closed or open arm entries, time in closed or open arms, head dippings (the mouse lowers its head over the ridge) and rearings were measured. For analysis, the percentage time in closed or open arms (over total time in arms) was calculated to exclude time spent in the center, which is difficult to interpret.

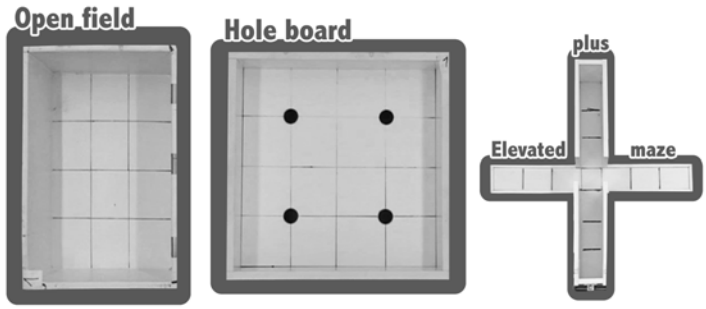

Figure 14. Behavioral apparatuses. *Open field:* the arena is divided in 12 areas 2 internal and 10 external ones. *Hole board:* the arena is divided in 16 areas 4 internal and 12 external ones, with 4 holes to measure exploration (through head dippings). *Elevated plus maze:* the maze has two closed and two open arms, divided in 3 areas each, with a central square in between. The arms are located 50 cm above the floor.

4.7.4 Morris Water Maze

The Morris water maze (MWM) was originally developed by Richard Morris to evaluate spatial learning, which is hippocampus-dependent (Morris 1981; Morris 1984). It is based in the use of distal cues (separate from the goal) to locate a hidden platform (goal) by the animal. It assesses spatial learning when the platform is hidden underwater; reference memory when the platform is removed, and the ability to extinguish the initial learning and acquire a new one when the platform is moved to a new location.

This test is widely used in neuroscience, though with certain changes in the protocol from one laboratory to the other. In this case, the basis was the method previously used in our group (Manso et al. 2012) with minor changes as suggested by Vorhees and Williams (Vorhees and Williams 2006).

The MWM test is carried out in a round pool (120 cm in diameter, 60 cm deep) which has a removable round platform (8 cm in diameter) with adjustable height. The water is made opaque by the addition of white latex, and kept at 22±1°C. The walls of the pool have two-dimensional black cues (different shapes) in 4 virtual cardinal points (north, south, east and west). In the intermediate cardinal points (northeast, northwest, southeast and southwest) there were 4 high-contrast three-dimensional cues. The pool was surrounded by a black curtain to block all further cues and a video camera was placed zenithal to the pool (Figure 15).

In the next section there is a detailed explanation of each day of testing (see Figure 16 for an outline).

Figure 15. Pool set-up for the Morris water maze test. Two- and three-dimensional cues were placed around the pool as distal cues. A black curtain surrounded the pool to block all other visual information during testing (including the experimenter).

Figure 16. Experimental outline of the Morris Water Maze test. The procedure lasted 11 days with an initial probe trial and cued learning. Then, spatial learning took place for four days, followed by an immediate probe trial and another one 24 hours later. Afterwards, four days of spatial reversal were performed with an immediate probe trial and a 24-hours later one.

4.7.4.1 Stages

4.7.4.1.1 Day 1 Probe trial and cued learning.

At this point no cues were placed in the pool or around it.

The protocol started with a probe trial (no platform) in which the mouse was left in the center of the pool and allowed to swim freely for 60 seconds. This was done to rule out quadrant preference.

Afterwards (60-80 minutes later), the platform was placed at water level and 30 cm away from the wall with a "flag" attached to it (in this case, a black 10 cm-high pole). The animal was released facing the wall and allowed to swim to the

platform in a maximum of 60 seconds and left there for an extra 15 seconds. If the animal did not reach the platform in the allotted time, it was guided to it. A total of four trials were carried out, each one starting in and with the flagged platform at different cardinal points (Table 6), with an inter-trial interval of 60-80 minutes. This procedure was done to establish that there was an escape point, as well as to ensure that all mice could swim and climb to the platform properly.

Table 6. Start and platform locations for the cued learning phase. These combinations guarantee short and long paths to the platform as well as right and left turns from the initial location, as suggested by Vorhees and Williams (2006).

	Trial 1	Trial 2	Trial 3	Trial 4
Start	N	E	S	W
Platform	SE	NE	SW	SE

4.7.4.1.2 Day 2-5 Spatial acquisition.

All distal cues were placed before starting this phase.

The platform was submerged 1 cm in the southwest quadrant (midway to the center of the pool).

The animal was released facing the wall and allowed to swim to the platform in a maximum of 60 seconds and left there for an extra 15 seconds. If the animal did not reach the platform in the allotted time, it was guided to it. A total of four trials were carried out, each one starting from a different cardinal point (Table 7), with an inter-trial interval of 60-80 minutes. The latency to reach the platform (just before climbing) was measured *in situ*.

Table 7. Start locations for the spatial learning phase. The fact that the starting location changes in each trial guarantees that the animal is guided by distal cues and not by always following the same path, as suggested by Vorhees and Williams (2006).

	Trial 1	Trial 2	Trial 3	Trial 4
Day 7	N	E	SE	NW
Day 8	SE	N	NW	E
Day 9	NW	SE	E	N
Day 10	E	NW	N	SE

4.7.4.1.3 Day 5 Immediate probe trial.

The platform was removed and the mice were placed in the pool facing the wall in the northeast point (opposite of where the platform used to be). They were left to swim freely for 30 seconds and then removed from the pool.

4.7.4.1.4 Day 6 24 hours later probe trial.

The same was done as in the immediate probe trial.

4.7.4.1.5 Day 7-10 Spatial reversal.

The platform was changed to the southwest quadrant (30 cm from the wall, as before) and everything proceeded as in the spatial learning phase but with a change in starting positions (Table 8).

Table 8. Start locations for the spatial reversal phase. The fact that the starting location changes in each trial guarantees that the animal is guided by distal cues and not by always following the same path, as suggested by Vorhees and Williams (2006).

	Trial 1	Trial 2	Trial 3	Trial 4
Day 7	S	W	NW	SE
Day 8	NW	S	SE	W
Day 9	SE	NW	W	S
Day 10	W	SE	S	W

4.7.4.1.6 Day 10 Immediate probe trial.

The platform was removed and the mice were placed in the pool facing the wall in the southwest point (opposite of where the platform used to be in the reversal phase). They were left to swim freely for 30 seconds and then removed from the pool.

4.7.4.1.7 Day 11 24 hours later probe trial.

The procedure was the same as in the immediate probe trial.

4.7.4.2 Analysis

As mentioned before, latency to reach the platform was measured at the moment of testing. For probe trials, an automated analysis with ImageJ was used. A macro was developed to measure time spent in each quadrant by adapting the ImageJ wrMTrck plug-in (Nussbaum-Krammer et al. 2015) to the Morris water maze (Fernandez-Gayol 2015). Essentially, the plug-in allowed for the creation of a mask representing the mouse and tracked its movement in a region of interest (the target quadrant or the opposite one).

4.8 LPS injection

Mice were injected IP with 400 µg/kg LPS (from *Escherichia coli* O55B5, Sigma-Aldrich L2880) or saline at 9 am. Six hours post-injection, the animals were anesthetized with 0.3 ml/mouse of a mixture of ketamine 10 mg/ml (Imalgene, Merial Laboratorios S.A.) and xylazine 12.5 mg/ml (Rompun, Bayer), a sample of plasma was obtained by cardiac puncture and then they were transcardially perfused with ice-cold PBS EDTA 2 mM. The hypothalamus was dissected and snap-frozen in liquid nitrogen for qPCR analysis.

All mice had been handled for five days prior to the experiment (saline injection).

4.9 RT-qPCR

4.9.1 RNA extraction

RNA was extracted either with TRI Reagent (T9424, Sigma-Aldrich), which contains phenol and guanidine thiocyanate, based on the method developed by Chomczynski and Sacchi (1987); or with the Maxwell RSC SimplyRNA Tissue Kit (AS1380, Promega), with a semi-automated procedure that used paramagnetic particles.

Briefly, ~10 mg tissue samples were homogenized in either 1 ml of TRI Reagent (1st method) or 200 µl of 1-thioglycerol/homogenization solution (containing guanidine thiocyanate; 2nd method) with a MM-400 mixer mill (Retsch) using zirconium oxide 3 mm beads (22455.0007, Biometa S.A.) and two 2-minute cycles at 30 Hz.

For the first method, RNA was suspended with 0.2 volumes of chloroform (C2432, Sigma-Aldrich) and then precipitated with 0.25 volumes of isopropanol

(34863, Sigma-Aldrich), cleaned with 75% ethanol and then resuspended in diethylpyrocarbonate (DEPC)-treated water.

For the second method, homogenized samples were lysed using the provided buffer and loaded into the cartridges. The DNase treatment in the kit was increased to 10 µl following manufacturer's instructions. Finally, samples were resuspended in nuclease-free water.

All samples were quantified using a NanoDrop 2000 device (Thermo Fisher).

4.9.2 cDNA synthesis

Afterwards, 2 µg of RNA (from both methods) were treated with DNase I (final concentration 0.027 Kunitz/µl) (79254, QIAGEN) and cDNA was synthesized with the iScript cDNA synthesis kit (170-8891BioRad) from 1 µg of DNase-treated RNA.

4.9.3 qPCR

qPCR reactions were set up using a iTaq Universal SYBR Green Supermix (1725124, Bio-Rad Laboratories) and custom primers from Sigma-Aldrich. A 2-step protocol was used, followed by a melting curve (Table 9). All samples were loaded in duplicate to the plate and a 3-point 10-fold dilution curve was included for every gene to assess efficiency. Non-template (water) and non-retrotranscriptase (pool of DNase-treated RNA) controls were also always added. Initial cDNA quantity depended on the primers used (Table 10).

Table 9. qPCR reaction and program conditions. All reactions contained 7.5 µl of mix and 2.5 µl of cDNA at the appropriate concentration. The program was also the same in all cases, with a hot-start followed by 40 cycles and a melt curve. The latter consists in a 0.5°C increment every 5 seconds from 65 to 95°C to determine the temperature at which the product(s) denaturalizes and therefore causes a decrease in fluorescence (SYBR binds to double-stranded DNA only). F forward; R reverse.

	Volume (µl)	Final concentration
H_2O	1.9	-
SYBR Green supermix (2x)	5	1x
primer F	0.3	0.3 µM
primer R	0.3	0.3 µM
Mix volume	7.5	
cDNA	2.5	Variable
qPCR reaction	10	

Temperature	Time (s)	Cycles
95°C	180	1
94°C	10	40
60°C	30	
Melt curve		
95°C	10	1
65-95°C (Δ0.5°C)	5 (each)	

Table 10. qPCR primers and initial cDNA concentrations.

	Sequence (5' → 3')	Initial cDNA (ng/µl)
***Il6* F**	GCT TAA TTA CAC ATG TTC TCT GGG AAA	10
***Il6* R**	CAA GTG CAT CAT CGT TGT TCA TAC	
***Il6ra* F**	CCT GAG ACT CAA GCA GAA ATG G	10
***Il6ra* R**	AGA AGG AAG GTC GGC TTC AGT	
***Npy* F**	ATG CTA GGT AAC AAG CGA ATG G	0.625
***Npy* R**	TGT CGC AGA GCG GAG TAG TAT	
***Agrp* F**	AGA GTT CCC AGG TCT AAG TCT G	0.625
***Agrp* R**	GCG GTT CTG TGG ATC TAG C	
***Pomc* F**	CGC AGA GGC GTG CGG AGG AAG A	0.625
***Pomc* R**	TCC CTC TTG AAC TCT AGG GGA AA	
***Pmch* F**	GTC TGG CTG TAA AAC CTT ACC TC	0. 625
***Pmch* R**	CCT GAG CAT GTC AAA ATC TCT CC	

***Hcrt* F**	GCC GTC TCT ACG AAC TGT TGC	0. 625
***Hcrt* R**	CGC TTT CCC AGA GTC AGG ATA	
***Crh* F**	CTT GAA TTT CTT GCA GCC GGA G	0.625
***Crh* R**	GAC TTC TGT TGA GGT TCC CCA G	
***Gfap* F**	GGG GCA AAA GCA CCA AAG AAG	0.5
***Gfap* R**	GGG ACA ACT TGT ATT GTG AGC C	
Casp3 F	ATG GAG AAC AAC AAA ACC TCA GT	10
***Casp3* R**	TTG CTC CCA TGT ATG GTC TTT AC	
Socs3 F	ATG GTC ACC CAC AGC AAG TTT	10
Socs3 R	TCC AGT AGA ATC CGC TCT CCT	
Mac1 F	GGG AGG ACA AAA ACT GCC TCA	10
Mac1 R	ACA ACT AGG ATC TTC GCA GCA T	
***Gapdh* F**	GGC AAA TTC AAC GGC ACA	Same as target (Reference gene)
***Gapdh* R**	CGG AGA TGA TGA CCC TTT	

4.9.4 Analysis

Fold change expression was calculated using an adaptation of the delta-delta-Ct method with different efficiencies (Equation 1) (Pfaffl 2001) and glyceraldehyde 3-phosphate dehydrogenase (*Gapdh*) as the reference gene. The modification consisted in using the whole control group as calibrator so that its fold change average is always 1. Efficiencies were calculated using Equation 2 from the slope of the standard curve for each gene.

Equation 1. Fold change calculation for qPCR experiments. The left ratio (numerator) is calculated for all samples. The average of those ratios for the control group is calculated and called the calibrator (denominator). Every sample is divided by the calibrator to obtain its fold change (target *vs* reference) and averages for each group are calculated. Ct threshold cycle.

$$fold\ change = \frac{(E_{ref})^{C_t Sample}}{(E_{target})^{C_t Sample}} \div \sum_{i=0}^{n} \frac{\frac{(E_{ref})^{C_t CalSample_i}}{(E_{target})^{C_t CalSample_i}}}{n}$$

Equation 2. Efficiency calculation. The efficiency of amplification was calculated using the slope (m) of the standard curve. A perfect efficiency has a value of 2 (m=-3.33), meaning that every cycle DNA duplicates. Deviations from that value denote problems in amplification, but efficiencies from 1.9 to 2.1 were accepted.

$$E = 10^{-\frac{1}{m}}$$

4.10 *In situ* hybridization

Snap-frozen brains were embedded with Tissue-Tek optimal cutting temperature (OCT) compound (4583, Sakura Finetek), cut at 30 μm with a cryotome (Leica CM 3050 S) and mounted on SuperFrost Plus slides (4951PLUS4, Thermo Fisher). The plasmid containing the probe for *Crh* (1.2kb fragment from rat cDNA) was kindly provided by Dr. K. Mayo (Northwestern University, Evanston, IL, USA) and those for *Agrp* and *Pomc* (PCR-amplified from mouse cDNA) by Dr. Richard Palmiter and Dr. Stephanie Padilla (University of Washington, Seattle, WA, USA) (Table 12). Probes were labeled with [α-^{35}S]UTP using SP6 (for *Crh*) or T7 (for *Agrp* and *Pomc*) polymerases. In the case of *Crh*, the plasmid was digested using HindIII. For *Agrp* and *Pomc*, a PCR using M13 primers (Table 11) was carried out to obtain the linear probe.

Relevant slides where identified by relative position to the PVN following a mouse brain atlas (Franklin and Paxinos 2007), which was located by hematoxylin staining of a reference slide.

Before the protocol, slides were brought to room temperature. For pre-hybridization, slides were fixed in 4% paraformaldehyde for 30 minutes, then rinsed in KPBS, treated with HCl 0.1N in PBS for 5 minutes, rinsed with trietanolamine (TEA) 0.1M, treated with acetic anhydride 0.25% in TEA 0.1M and washed with 2x SSC. Finally, slides were dehydrated in an ethanol battery and air-dried. Afterwards, they were hybridized overnight at 60°C. Hybridization solution contained 10% dextran sulphate, 50% deionized formamide, 2x SSC, 10mM Tris pH8, 1mM EDTA, 1x Denhardt's solution, 1mg/ml tRNA, 10mM dithiothreitol (DTT), and the labeled probe at 10^7dpm/ml. Then, slides were rinsed in decreasing concentrations of SSC and 1mM DTT, including a step with RNAse treatment to digest the probe. Finally, slides were dehydrated in a battery of increasing concentrations of ethanol. The slides for each probe and sex were exposed to the same Carestream Kodak BioMax MR film (Z358479-50EA, Sigma-Aldrich) for 25 hours (*Crh*), 23 hours (*Agrp*, females), 47 hours (*Agrp*, males) or 8.5 hours (*Pomc*), and then photographed on an Eclipse E400 microscope (Nikon, Japan) with a DXM1200 digital camera (Nikon, Japan). Densitometry analysis was carried out with ImageJ (Schneider et al. 2012) on 3-6 slices per animal by measuring their integrated density (sum of all pixel intensities above threshold) and subtracting the background (average integrated density of 10 areas without specific signal) from each one, before averaging them.

Table 11. M13 primer sequences. M13 primers were used for obtaining the *Agrp* and *Pomc* probes from the PCRII-TOPO plasmid.

	Sequence (5' → 3')
M13 F	GTAAAACGACGGCCAG
M13 R	CAGGAAACAGCTATGAC

Table 12. cDNA sequences of probes for in situ hybridization. The *Crh* probe was included in a pGEM-4Z vector and those for *Agrp* and *Pomc* in PCRII-TOPO vectors. For labeling, probes were transcribed using SP6 or T7 polymerases and [α-^{35}S]UTP.

	Sequence (5' → 3')	Length (bases)
Crh	AGAAACTCAGAGCCCAAGTACGTTGAGAAACTGAAGAGAAAGGGGA AAGGCAAAGAAAAGGAGAAGAGAAAGGAGAAGAGGAAGAAAACCT GCAGGAGGCATCCTGAGAGAGGTACCTCGCAGAACAACAGTGCGGG CTCACCTGCCAAGGGAGGAGAAGAGAGCGCCCCTAACATGCGGCTG CGGCTGCTGGTGTCCGCGGGCATGCTGCTGGTGGCTCTGTCGCCCTG TCTGCCTTGCAGGGCCCTGCTGAGCAGGGGATCCGTCTCTGGAGCGC CGCGGGCCCCGCAGCCGTTGAATTTCTTGCAACCGGAGCAGCCCCAG CAACCTCAGCCGATTCTGATCCGCATGGGTGAAGAATACTTCCTCCG CCTGGGGAACCTCAACAGAAGTCCCGCTGCTCGGCTGTCCCCCAACT CCACGCCCCTCACCGCGGGTCGCGGCAGCCGCCCCTCGCACGACCAG GCTGCGGCTAACTTTTTCCGCGTGTTGCTGCAGCAGCTGCAGATGCC TCAGCGCCCGCTCGACAGCAGCACGGAGCTGGCGGAACGCGGCGCCG AGGATGCCCTCGGTGGCCACCAGGGGGCGCTGGAGAGGGAGAGGCG GTCCGAGGAGCCGCCCATCTCTCTGGATCTCACCTTCCACCTTCTGA GGGAAGTCTTGGAAATGGCCAGGGCAGAGCAGTTAGCTCAGCAAGC TCACAGCAACAGGAAACTGATGGAGATTATCGGGAAATGAAATGTT GCGCTTGGCCAAAACGATTCTGCATTTAGCACACAAGTAAAAATAA AAAATTTAAAACACAGTATTCTGTACCATACTGCAGCTCTGATATC ATTTGTTTATTTTTATATAGCTTGAAGCATAGAAGATGTACAGGGA GAGAGCCTATATACCCCTTAATTAGCATGCACAAAGTGTGTTTCTT TGTAGTAACAAAACAGCGTTATTTGTATTGCCCACGCTTAGTTTCT ATGTGCAAATAAGTGTCTTTATAGCGATATCTTAAAGAAAATGTGG ATCCAAGGAGGAAACCTTTAAAAAAGCAGATGGAAGTCACCCAGTT GTTTTTATTTGGAGACACAGTGTAAGAGAATTCATTCTTGAGGGGT GGCTAGGACAAAATGTGTAAGCTCTTTGAATCAACTTTTTCTTGTA AATGTTTCAATAATAAAACATCTTTCTGATCCTTGGTC	1196
Agrp	ACCTTAGGGAGGCACCTCATGCCCTGGCTACAGGAAGCAGTCACGT GTGGACCCTTTATTAGGCACTGCCATATAAGCTCAGGGCACAAGAG ACCAGGACATCCCTAGGCAAAGATCAGCAAGCAAAGGCCATGCTGA CTGCAATGTTGCTGAGTTGTGTTCTGCTGTTGGCACTGCCTCCCACA CTGGGGGTCCAGATGGGCGTGGCTCCACTGAAGGGCATCAGAAGGC CTGACCAGGCTCTGTTCCCAGAGTTCCCAGGTCTAAGTCTGAATGGC CTCAAGAAGACAACTGCAGACCGAGCAGAAGAAGT	313
Pomc	CATCTTTGTCCCCAGAGAGCTGCCTTTCCGCGACAGGGGTCCCTCCA ATCTTGTTTGCCTCTGCAGAGACTAGGCCTGACACGTGGAAGATGC CGAGATTCTGCTACAGTCGCTCAGGGGCCCTGTTGCTGGCCCTCCTG CTTCAGACCTCCATAGATGTGTGGAGCTGGTGCCTGGAGAGCAGCC AGTGCCAGGACCTCACCACGGAGAGCAACCTGCTGGCTTGCATCCGG GCTTGCAAACTCGACCTCTCGCTGGAGACGCCCGTGTTTCCTGGCAA CGGAGATGAACAGCCCCTGACTGAAAACCCCCGGAAGTACGTCATG GGTCACTTCCGCTGGGACCGCTTCGGCCCCAGGAACAGCAGCAGTGC TGGCAGCGCGGCGCAGAGGCGTGCGGAGGAAGAGGCGGTGTGGGGA GATGGCAGTCCAGAGCCGAGTCCACGCGAGGGCAAGCGCTCCTACTC CATGGAGCACTTCCGCTGGGGCAAGCCGGTGGGCAAGAAACGGCGC CCGGTGAAGGTGTACCCCAACGTTGCTGAGAACGAGTCGGCGGAGG CCTTTCCCCTAGAGTTCAAGAGGGAGCTGGAAGGCGAGCGGCCATT AGGCTTGGAGCAGGTCCTGGAGTCCGACGCGGAGAAGGACGACGGG CCCTACCGGGTGGAGCACTTCCGCTGGAGCAACCCGCCCAAGGACAA GCGTTACGGTGGCTTCATGACCTCCGAGAAGAGCCAGACGCCCCTGG TGACGCTCTTCAAGAACGCCATCATCAAGAACGCGCACAAGAAGGG CCAGTGAGGGTGCAGGGGTCTTCTCATTC	819

4.11 Statistics

All data are presented as mean ± SEM. For the sake of simplicity, sample sizes are expressed as the range between the group with the least subjects to that with the most.

Statistical calculations were performed using the Statistical Package for Social Sciences (SPSS) software. Most data were analyzed with the generalized linear model (GzLM) with genotype and treatment (where applicable) as main factors, in each of the sexes separately. The maximum likelihood as a method of estimation, normality distribution and identity as a link function were always used.

Generalized estimating equations (GEE) were used for repeated measures such as diets, refeeding, and the MWM learning phases. In general, the independent working matrix was used but for spatial and reversal learning of the MWM, the AR(1) working correlation matrix structure was used instead, as suggested by (Vorhees and Williams 2006).

The post-hoc sequential Bonferroni test was carried out in all relevant comparisons when significant interactions between factors were obtained. The correction for multiple comparisons in this test consists in ordering the relevant comparisons (Table 13) from least to most significant and comparing their p-value to 0.05/(comparison position); e.g. for the fourth least significant pair-wise comparison the target p-value for significance would be 0.0125 (0.05/4) (Holm 1979). In the text, the specific significance will not be stated, every comparison mentioned as significant passed its correspondent p-value.

In the case of comparisons between two groups, the t-Student test was used. The Levene test for homogeneity of variances was checked beforehand, and if it was significant, the t-Student not assuming equal variances was chosen, which adjusts the degrees of freedom to be more restrictive.

Table 13. Pair-wise comparisons. Relevant comparisons depending on the number of factors and levels of each one (in parenthesis). Treatment may refer to fast, LPS or HFD.

Pair-wise comparisons genotype (3), diet (2)	
wt control	wt HFD
floxed control	floxed HFD
Il6$^{\Delta Gfap}$ control	*Il6*$^{\Delta Gfap}$ HFD
wt control	floxed control
wt control	*Il6*$^{\Delta Gfap}$ control
floxed control	*Il6*$^{\Delta Gfap}$ control
wt HFD	floxed HFD
wt HFD	*Il6*$^{\Delta Gfap}$ HFD
floxed HFD	*Il6*$^{\Delta Gfap}$ HFD

Pair-wise comparisons genotype (2), treatment (2)	
floxed control	floxed treated
Il6$^{\Delta Gfap}$ control	*Il6*$^{\Delta Gfap}$ treated
floxed control	*Il6*$^{\Delta Gfap}$ control
floxed treated	*Il6*$^{\Delta Gfap}$ treated

Pair-wise comparisons genotype (3)	
wt	floxed
wt	*Il6*$^{\Delta Gfap}$
floxed	*Il6*$^{\Delta Gfap}$

For genotype frequency analysis, a Chi-Square (χ^2) was performed.

Significance was set at $p<0.05$. Wald Chi-Square (χ^2-Wald), t-Student(degrees of freedom) or Chi-Square (χ^2) and p-values for significant effects of the main factors or the interactions between factors will be shown.

In graphs, statistical significant will be indicated by ★ for genotype and • for treatment. Main effect significance will be marked with black color, and significant pair-wise comparisons will have the color of the genotype against which that group is significant.

GzLM and GEE were chosen because they are more flexible statistical tools than the standard general lineal model. They allow the use of different distributions and covariance structures for repeated measures data. Moreover, they tolerate heteroscedasticity and admit missing values.

5 RESULTS

5.1 *Il6* and *Il6ra* recombination

An unforeseen excessive recombination of the floxed genes due to Cre recombinase activity in tissues other than the CNS (Figure 17 and 18) was detected late in the development of this thesis. As a consequence, some of the experiments suffered from a reduction in sample size of real conditional knock-out and floxed mice that in some cases could not be increased later on. When possible, an extensive check of recombination status in peripheral tissues (tail and liver) was carried out, and compared to recombination in brain homogenates. In this case, the results will be presented for the whole initial sample and for just the mice with no peripheral recombination.

During this process, we detected that not only $Cre^{+/-}$ mice had peripheral recombination, but also floxed animals that were $Cre^{-/-}$. The explanation for this is recombination in the germline of the $Cre^{+/-}$ parent, which generated hemizygote mice (for exon 2 of *Il6* or exons 4-6 of *Il6ra*). Wild-type mice never showed any recombination because it is impossible, since their floxed allele can only come from the floxed homozygous parent (a separate line that never had contact with *Cre* and is free of recombination issues) (see *4.2 Mice*). In general, approximately 23% of floxed mice from a *GFAP-Cre* line had recombination in peripheral tissues, while 56% of $Il6^{\Delta Gfap}$ mice did. Regarding *Syn1-Cre*, the numbers were higher, with 51% of floxed and 60% of $Il6^{\Delta Syn1}$ mice having peripheral recombination.

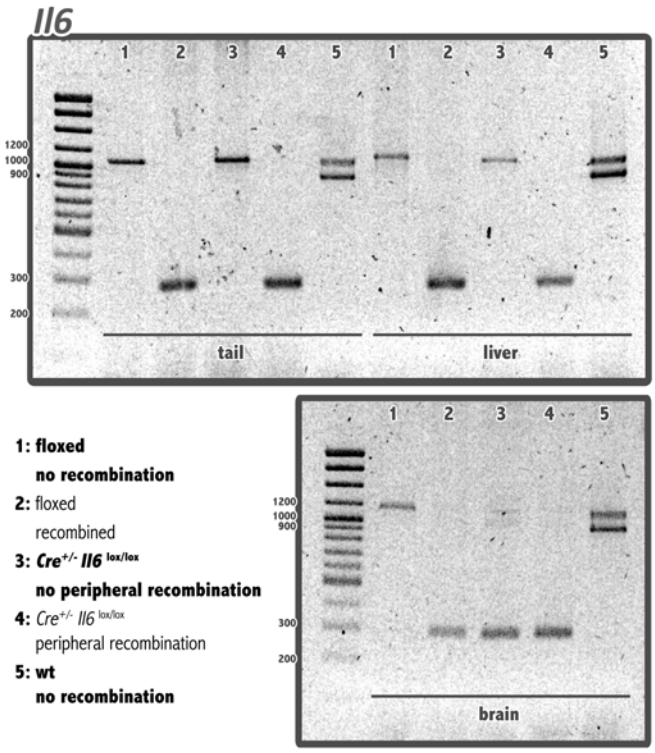

Figure 17. *Il6* recombination PCR from tail, liver and brain DNA. Five representative samples of the different possibilities encountered while genotyping mice from either the astrocytic or neuronal *Il6* conditional knock-out lines. The valid ones are 1, 3 and 5 a floxed (1) or wt (5) mouse should have no recombination of *Il6* at all, and a Cre$^{+/-}$ *Il6*$^{lox/lox}$ (3) mouse should only recombine *Il6* in the brain. The recombination band can be seen at 260 base pairs (bp), the floxed gene at ~1000 bp and the wt allele at ~900 bp. Remember that wt mice are actually *Il6*$^{lox/wt}$.

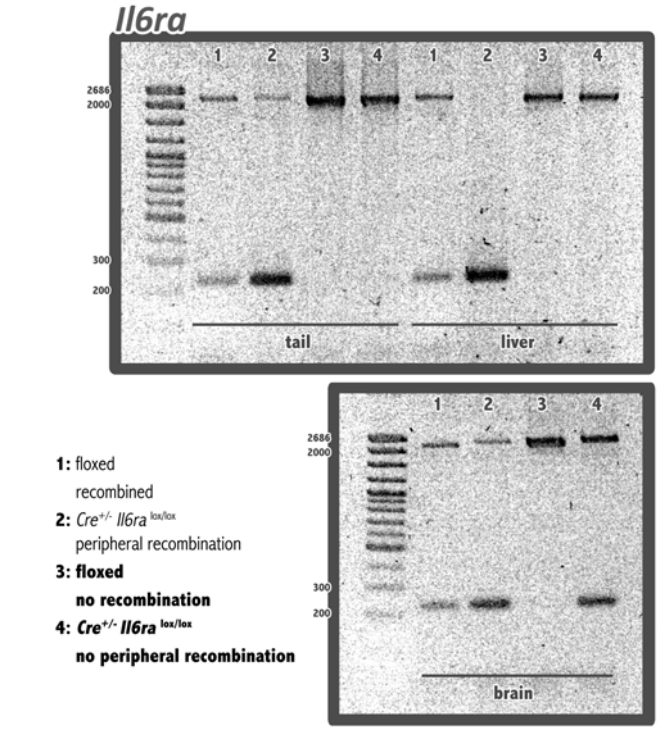

Figure 18. *Il6ra* recombination PCR from tail, liver and brain DNA. Four representative samples of the different possibilities encountered while genotyping mice from the neuronal *Il6ra* conditional knock-out line. The valid ones are 3 and 4 a floxed (3) mouse should have no recombination of *Il6ra* at all, and a Cre$^{+/-}$ *Il6ra*$^{lox/lox}$ (4) mouse should only recombine *Il6ra* in the brain. The recombination band can be seen at 230 base pairs (bp), and the floxed gene at ~2000 bp.

5.2 Regulation of body weight

5.2.1 Astrocytic IL-6 conditional knock-out

5.2.1.1 Frequencies at weaning

Analysis of frequencies at weaning was performed in all the available data from our line since its creation (some of those animals have therefore not been used in this thesis), comparing the four genotypes obtained in the crossing described in material and methods (see *4.2.5.1 Conditional Il6 knockout in astrocytes*). No differences in the number of males and females were detected ($\chi 2$ 0.357, $p>0.05$). However, $Il6^{\Delta Gfap}$ and $Il6^{\Delta Gfap/wt}$ mice were clearly underrepresented ($\chi 2$ 21.348, $p<0.05$) (Table 14).

Table 14. Observed and expected frequencies at weaning of each genotype and sex. No significant differences between sexes were detected but there was a reduced number of $Il6^{\Delta Gfap}$ and $Il6^{\Delta Gfap/wt}$ mice.

	Observed N	Expected N	Residual
Genotype			
wt	262	227	35
floxed	261	227	34
***Il6*$^{\Delta Gfap}$**	186	227	-41
***Il6*$^{\Delta Gfap/wt}$**	199	227	-28
Sex			
males	445	454	-9
females	463	454	9
Total	**908**		

5.2.1.2 Weaning weight

The animals were weighed at three weeks of age to determine pre-existing differences in body weight. Both male and female mice showed differences due to genotype (χ^2-Wald 9.27 and 12.63, $p<0.05$, respectively), particularly between wild-type and *Il6*$^{\Delta Gfap}$ (in both sexes, as per sequential Bonferroni) and wt and floxed (in females, as per sequential Bonferroni). When animals with peripheral recombination were removed, very similar results were obtained (genotype χ^2-Wald 11.38, $p<0.05$, in males; genotype χ^2-Wald 10.283, $p<0.05$, in females), with the addition that *Il6*$^{\Delta Gfap}$ males differed from both floxed and wt littermates (Figure 19).

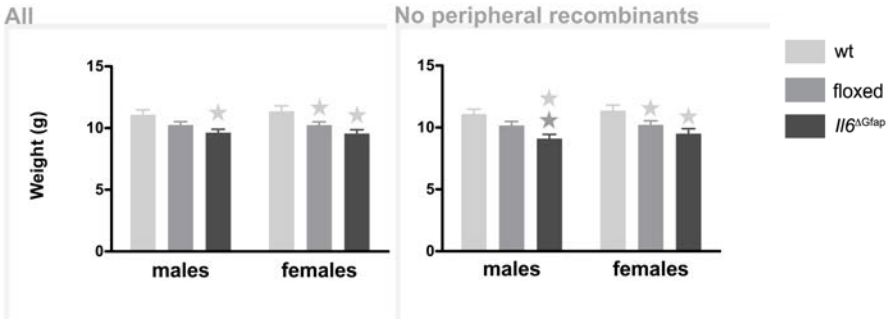

Figure 19. Weaning weight. Both male and female *Il6*$^{\Delta Gfap}$ mice weighed less than wt littermates, and only in the group where peripheral recombinants were excluded, did male *Il6*$^{\Delta Gfap}$also weigh less than floxed mice. Significant sequential Bonferroni pair-wise comparisons ★ vs wt, ★ vs floxed. N=22-58 (all), n=22-46 (no peripheral recombinants).

5.2.1.3 Linear growth

Data concerning tibial length and serum IGF-1 were obtained from the 48-hour fast experiment, and IGFBPs were measured in sera from the first diet experiment in control diet-fed mice. The first two measures were analyzed accounting for treatment (fed/fasted) as well, and in each sex separately (Figure 20).

Both *Il6*$^{\Delta Gfap}$ males and females presented longer tibiae than floxed littermates, regardless of feeding state (genotype χ^2-Wald 13.58 and 13.436, $p<0.05$, for males and females, respectively).

Food deprivation increased IGF-1 in males, which otherwise had no genotype differences (fast χ^2-Wald 6.442, $p<0.05$). In females, on the other hand, IGF-1 remained unaffected by fasting but had an inherent increased level in the *Il6*$^{\Delta Gfap}$ genotype (genotype χ^2-Wald 4.312, $p<0.05$).

No genotype differences were apparent in either of the two measured IGFBPs.

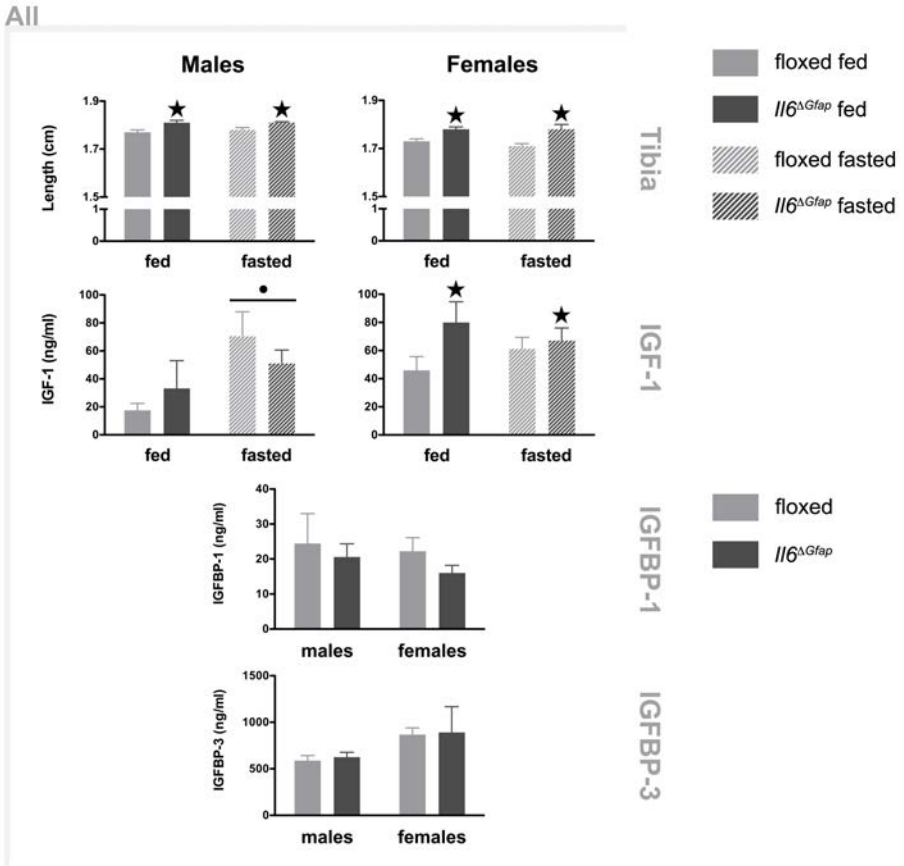

Figure 20. Linear growth. Tibiae were longer in *Il6*$^{\Delta Gfap}$ compared to floxed mice of both sexes. In females, this also translated to higher IGF-1 serum levels. IGFBP-1 and -3 showed no differences between genotypes. • $p<0.05$ (fast), ★ $p<0.05$ (genotype). For tibiae n=6-8; for IGF-1 n=4-8; for IGFBP-1 and -3 n=5-10.

5.2.1.4 High-fat diet

5.2.1.4.1 Body weight and weight gain

Two separate experiments were carried out to assess the effects of a HFD on weight and weight gain in this model (Figure 21). Only the first included wt mice due to the nature of the second experiment, which required individualization and would have supposed an unmanageable number of cages. The values have been pooled for the first 12 weeks of the diet, which is the common part of the two experiments.

In the complete group, there was a significant interaction of diet and genotype for absolute weight (χ^2-Wald 7.469 and 18.590, $p<0.05$, in males and females respectively). Upon decomposition, a clear effect of diet was found for all genotypes, and in females fed a HFD, *Il6*$^{\Delta Gfap}$ mice were significantly heavier than both floxed and wt littermates.

When mice with peripheral recombination were removed, the same differences were observed (diet*genotype χ^2-Wald 15.342 and 17.168, $p<0.05$, in males and females respectively).

Regarding weight gain in the whole group, there was also a significant interaction of diet and genotype (χ^2-Wald, 7.276 and 12.086, $p<0.05$, in males and females respectively). After decomposing it, both males and females displayed a prominent effect of diet. But again, only in females did *Il6*$^{\Delta Gfap}$ show more weight gain than wt and floxed mice. Finally, floxed males fed the control diet gained significantly less weight than wt littermates.

In mice without peripheral recombination, the same differences were observed (diet*genotype χ^2-Wald 12.462 and 17.210, $p<0.05$, in males and females respectively). And in addition, the difference between HFD-fed *Il6*$^{\Delta Gfap}$ and wt or floxed mice was apparent in males as well.

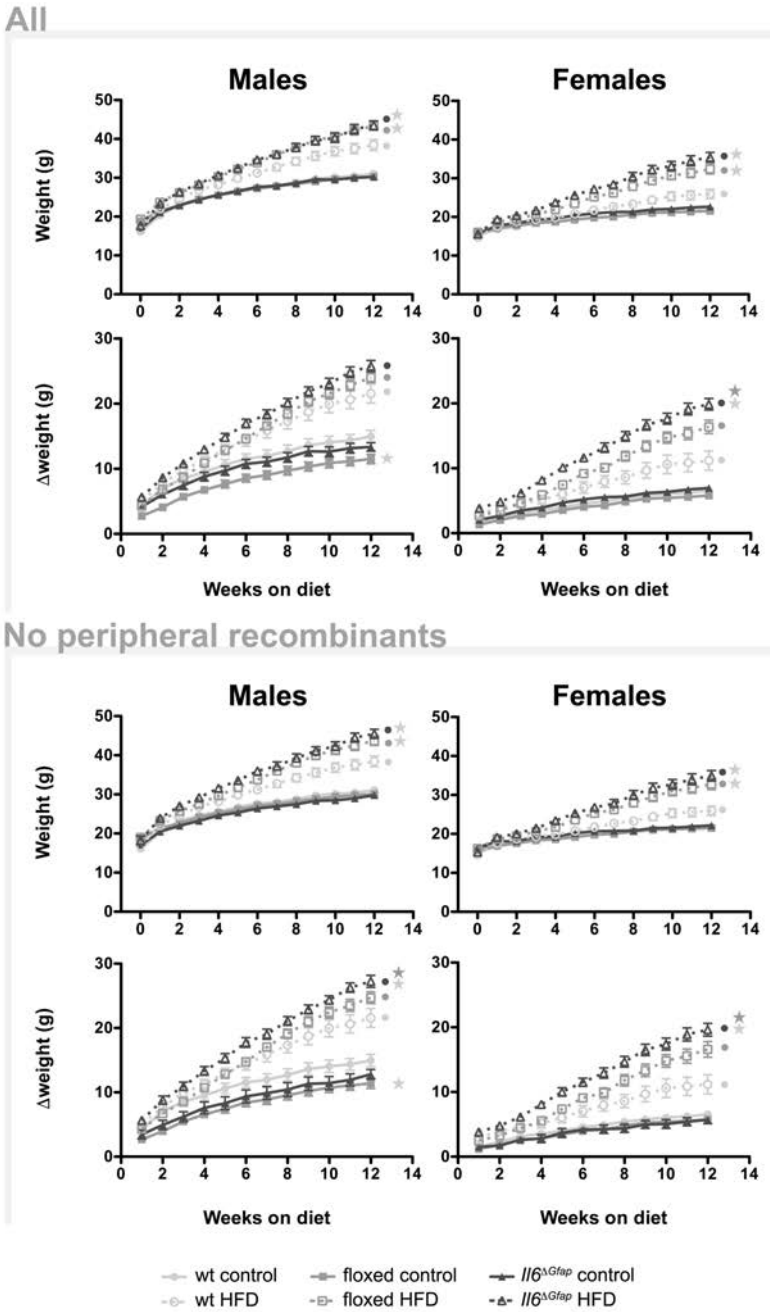

Figure 21. Body weight and weight gain after 12 weeks of control or HFD. Both male and female mice increased their weight with a HFD. Female *Il6*$^{\Delta Gfap}$ mice gained significantly more weight than floxed and wt littermates on the same diet. Similar results are seen in either the mixed group or just in mice without peripheral recombination. Significant sequential Bonferroni pair-wise comparisons ★ vs wt (same diet), ★ vs floxed (same diet), • vs wt control diet, • vs floxed control diet, • vs *Il6*$^{\Delta Gfap}$ control diet. N=12-29 (all), n=10-25 (no peripheral recombinants).

5.2.1.4.2 Energy intake and feed efficiency

In the first experiment, animals were group-housed while energy intake was being monitored and weekly measurements had a great variability, especially in the HFD, likely because the mice "played" with the food and the texture is much less firm than the control diet. Therefore, in order to get potentially meaningful data, the average of all weeks was taken to carry out the statistical analysis (Figure 22, top). Still, a peak in energy intake was significant in floxed males fed a HFD compared to wt and *Il6*$^{\Delta Gfap}$ (diet*genotype χ^2-Wald 9.827, $p<0.05$; sequential Bonferroni pair-wise comparisons wt HFD vs floxed HFD, floxed HFD vs *Il6*$^{\Delta Gfap}$ HFD). Diet had a clear effect in females (diet χ^2-Wald 50.313, $p<0.05$), while only floxed males fed a HFD showed an increased energy intake compared to floxed controls (diet*genotype χ^2-Wald 9.827, $p<0.05$; sequential Bonferroni pair-wise comparison floxed control vs floxed HFD).

Feed efficiency, or weight gain relative to kcal ingested (Figure 23), is increased in mice fed a HFD (diet χ^2-Wald 8.676 and 24.801, for males and females, respectively; $p<0.05$). The slight reduction in feed efficiency in floxed males fed a HFD, albeit not significant, might back the explanation given before for the excessive intake in this group, since they do not gain as much weight as would be expected from that amount of kcal.

In the second experiment, animals were individualized after 12-13 weeks on their respective diet and the average of three consecutive days was taken in an attempt to correct the problems in the previous group (Figure 22, middle and bottom).

In this case, a clear increase of energy intake was seen due to the HFD in both sexes in the complete group (diet χ^2-Wald 67.838 and 38.577, $p<0.05$, in males and females respectively), and also when peripheral recombinants were excluded (diet χ^2-Wald 51.360 and 26.954, $p<0.05$, in males and females respectively).

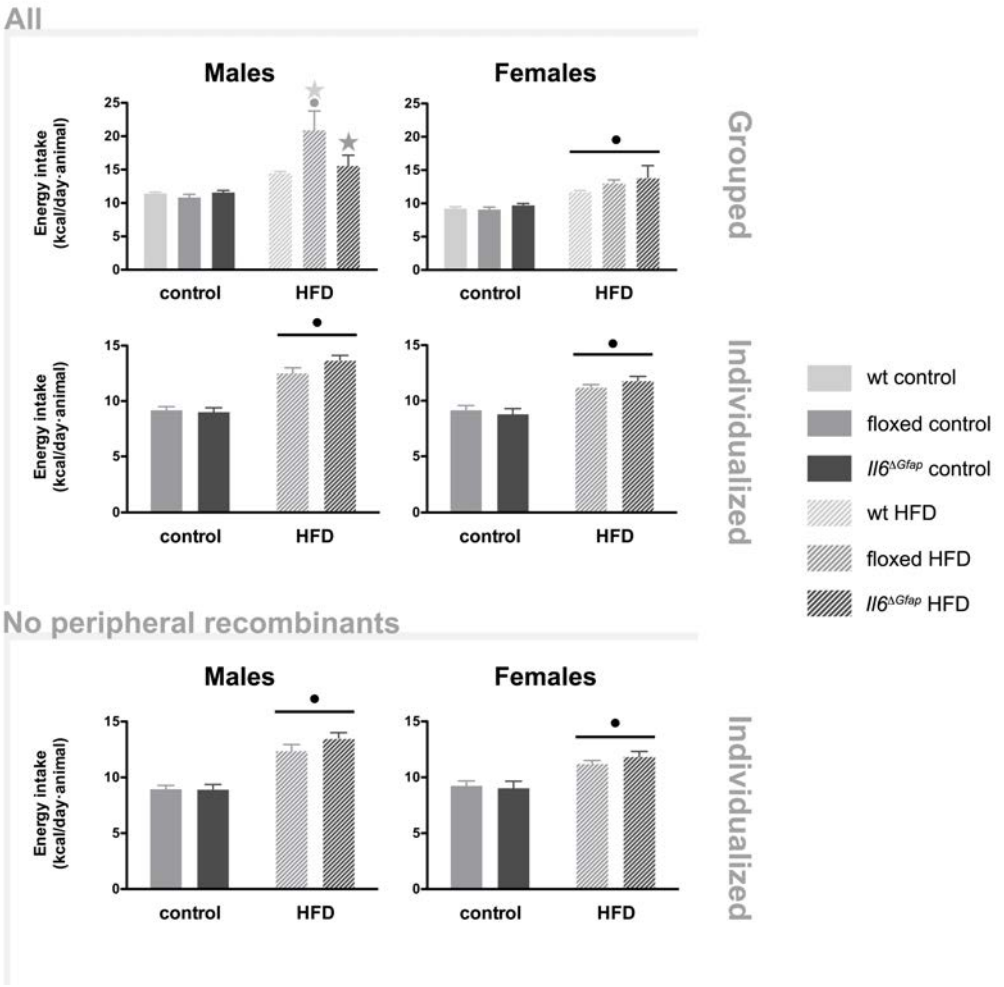

Figure 22. Energy intake with control and HFD. In general, HFD increases energy intake in all genotypes, both in group and individual measures. In group-housed males, however, no effect of diet is seen but in floxed mice, which also have a higher intake than their littermates on the same diet. • $p<0.05$ (diet). Significant sequential Bonferroni pair-wise comparisons ★ vs wt (same diet), ★ vs floxed (same diet), • vs floxed control diet. N=3-7 (grouped, cages), n=7-18 (individualized, all), n=6-15 (individualized, no peripheral recombinants).

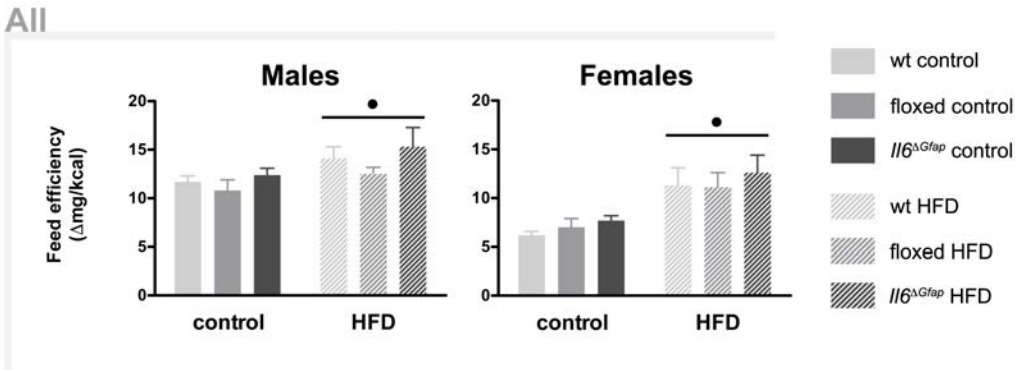

Figure 23. Feed efficiency with control and HFD. The HFD has a higher feed efficiency than the control one independently of genotype, the same amount of kcal has a higher impact in body weight gain. • p<0.05 (diet). N=3-7 (cages).

5.2.1.4.3 ITT and OGTT

These tests were only performed in the first experiment.

In the complete group, administration of insulin (ITT, Figure 24) resulted in the expected time-dependent decrease in glucose levels (time χ^2-Wald 417.347 and 865.192, p<0.05, for males and females, respectively). The HFD curve was significantly higher, starting already at a higher fasting glucose level (diet χ^2-Wald 27.695 and 19.860, p<0.05, for males and females, respectively). Genotype, however, had only a minor effect on males (genotype χ^2-Wald 6.058, p<0.05), which upon decomposition showed no significant pair-wise differences. When peripheral recombinants were removed, the same patterns were observed (time χ^2-Wald 290.273 and 827.500, p<0.05; diet χ^2-Wald 16.29 and 47.928, p<0.05, for males and females, respectively). But in this case, male wt mice were significantly different from floxed littermates (genotype χ^2-Wald 7.389, p<0.05; sequential Bonferroni pair-wise comparison wt vs floxed).

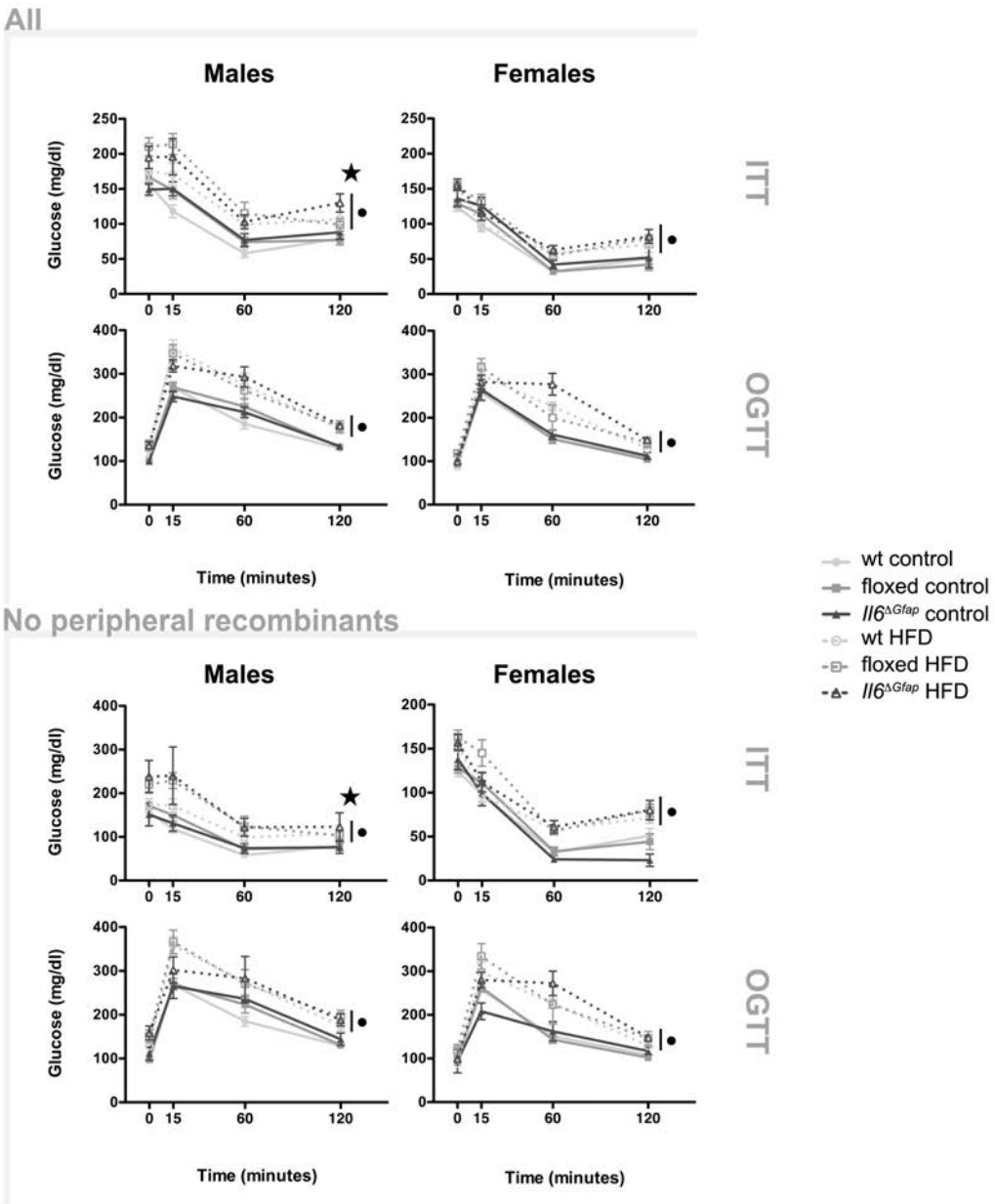

Figure 24. ITT and OGTT after 14-15 weeks of diet. In the first experiment, both male and female mice on a HFD showed impaired insulin and glucose tolerance. In the ITT of males, there was a significant effect of genotype, but pair-wise comparisons were not significant. The same results are seen in either the mixed group or just in mice without peripheral recombination. Note the different axis on the ITT of males (no peripheral recombinants). ★ $p<0.05$ (genotype), • $p<0.05$ (diet). N=8-14 (all), n=2-13 (no peripheral recombinants).

In the whole group, oral administration of glucose (OGTT, Figure 24) caused the predicted change in glucose levels (time χ^2-Wald 1011.519 and 697.955, $p<0.05$, for males and females, respectively). HFD-fed mice had a significant impairment in dropping blood glucose (diet χ^2-Wald 48.674 and 29.472, $p<0.05$, for males and females, respectively). No differences due to genotype were observed.

Removal of mice with peripheral recombination drew the same results (time χ^2-Wald 685.703 and 466.189, $p<0.05$; diet χ^2-Wald 24.976 and 40.298, $p<0.05$, for males and females, respectively).

5.2.1.4.4 Twenty-four hour fast and 4-hour refeeding

This procedure was carried out in the second experiment on single-housed animals.

Table 15 summarizes the weight lost by each group expressed as percentage of the weight prior to the fast. Male *Il6*$^{\Delta Gfap}$ mice on the control diet lost proportionally less weight than floxed littermates, while in females the reverse was true. Furthermore, HFD-fed mice were, relatively, less affected by fast-induced weight loss given their higher body weight, and the genotype differences were lost. The almost exact results were replicated once peripheral recombinants were removed.

For energy intake after the fast, a great variability was seen with the HFD as mentioned before, again probably due to mice crumbling the pellets. Therefore, an exclusion criterion was implemented, consisting in removing animals that at the 4th time point had an intake of over 2 standard deviations over the mean. For the group without peripheral recombinants, this was done after removal of animals with recombination.

Table 15. Percentage weight loss and statistical significances after a 24-hour fast. Percentage weight loss was calculated as Δweight*100/(pre-fast weight). Significant pair-wise comparisons ★ p<0.05 vs floxed (same diet), ● p<0.05 vs floxed control diet, ● p<0.05 vs *Il6*$^{\Delta Gfap}$ control diet.

		ALL				NO PERIPHERAL RECOMBINANTS			
		Males		Females		Males		Females	
		floxed	*Il6*$^{\Delta Gfap}$	floxed	*Il6*$^{\Delta Gfap}$	floxed	*Il6*$^{\Delta Gfap}$	floxed	*Il6*$^{\Delta Gfap}$
% lost	control	9.5 ± 0.3	8.1 ± 0.1 ★	10.8 ± 0.5	12.5 ± 0.9 ★	9.5 ± 0.4	8.2 ± 0.1 ★	10.8 ± 0.5	13.0 ± 1.1 ★
	HFD	5.6 ± 0.2 ●	6.00 ± 0.3 ●	5.2 ± 0.2 ●	5.1 ± 0.2 ●	5.6 ± 0.2 ●	5.8 ± 0.1 ●	5.3 ± 0.2 ●	5.2 ± 0.2 ●
χ^2-Wald		genotype*diet χ^2-Wald 10.59 p<0.05		genotype*diet χ^2-Wald 4.062 p<0.05		genotype*diet χ^2-Wald 5.722 p<0.05		genotype*diet χ^2-Wald 5.426 p<0.05	

When all animals were analyzed, there was a clear effect of time in the cumulative kcal intake (time χ^2-Wald 190.511 and 130.521, for males and females, respectively; p<0.05) (Figure 25). In addition, males showed an interaction between diet and genotype, with HFD-fed *Il6*$^{\Delta Gfap}$ having a greater energy intake than control-fed *Il6*$^{\Delta Gfap}$, while on the control diet this genotype had a significantly lower intake than floxed males (diet*genotype χ^2-Wald 6.403, p<0.05; sequential Bonferroni pairwise comparisons control *Il6*$^{\Delta Gfap}$ vs HFD *Il6*$^{\Delta Gfap}$, control floxed vs control *Il6*$^{\Delta Gfap}$).

With the exclusion of peripheral recombinants, the same results were maintained (time χ^2-Wald 218.581 and 208.628, p<0.05, for males and females, respectively; diet*genotype χ^2-Wald 6.003, in males, p<0.05; sequential Bonferroni pairwise comparisons control *Il6*$^{\Delta Gfap}$ vs HFD *Il6*$^{\Delta Gfap}$, control floxed vs control *Il6*$^{\Delta Gfap}$).

Figure 25. Cumulative energy intake during refeeding (4 hours) after a 24-hour fast. Male *Il6*$^{\Delta Gfap}$ mice on the control ate significantly less upon refeeding, but with the HFD, they reached the same kcal as both floxed control and HFD. • p<0.05 (diet), ★ vs floxed (same diet). N=7-17 (all), n=6-14 (no peripheral recombinants).

5.2.1.4.5 Temperature

Rectal temperature was measured too in the second experiment on single-housed animals (Figure 26).

If all animals were considered, no significant effects were observed; even though genotype was marginally significant in males (genotype χ^2-Wald 3.822, p=0.051).

When peripheral recombinants were removed, genotype became clearly significant in males (genotype χ^2-Wald 5.256, p<0.05).

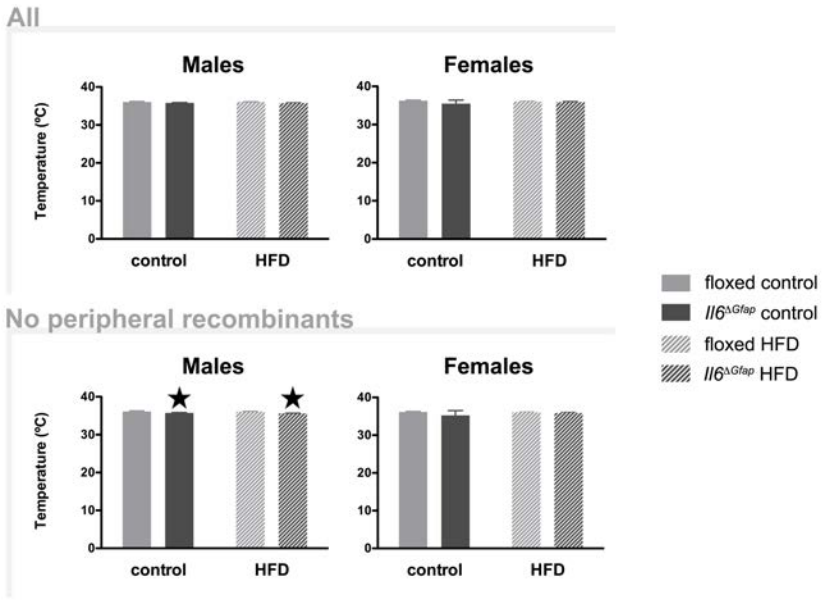

Figure 26. Rectal temperature. In males with no peripheral recombination, *Il6$^{\Delta Gfap}$* had a lower rectal temperature than floxed mice, regardless of diet. This same effect was a non-significant tendency in the complete male group. No significant differences were seen in females. ★ p<0.05 (genotype). N=7-18 (individualized, all), n=6-15 (individualized, no peripheral recombinants).

5.2.1.4.6 Tissue weight

5.2.1.4.6.1 Absolute weight

Figure 27 shows the results from all these variables in both the complete group and the group without peripheral recombination.

All mentioned tissues were weighed in both experiments, with the exception of BAT, which was added in the second one.

Liver weight showed a significant interaction between the factors diet and genotype in male mice (diet*genotype χ^2-Wald 13.65 p<0.05). Pair-wise comparisons showed that HFD increased liver weight in floxed and *Il6$^{\Delta Gfap}$* mice, compared to control animals of the same genotype (p<0.006); and also, that in animals fed a HFD, wt males differed from both floxed and *Il6$^{\Delta Gfap}$* littermates (p<0.006). In female mice, there were clear effects of diet and genotype (diet χ^2-

Wald 18.978, p<0.05; genotype χ^2-Wald 8.057, p<0.05), due to wt being significantly different from *Il6*$^{\Delta Gfap}$ mice (p=0.006).

Analysis only of animals without peripheral recombination had the same results. In males, the interaction between diet and genotype (diet*genotype χ^2-Wald 30.35, p<0.05) had to be decomposed, and HFD was found to increase liver weight in both floxed and *Il6*$^{\Delta Gfap}$ mice (p<0.006); furthermore, in HFD-fed animals, wt were different from both floxed and *Il6*$^{\Delta Gfap}$ mice (p<0.006). In females, however, genotype and diet were significant, with no interaction between them (diet χ^2-Wald 11.023, p<0.05; genotype χ^2-Wald 8.066, p<0.05). As described before, only wt differed from *Il6*$^{\Delta Gfap}$ mice (p<0.017). Of note, the comparison floxed vs *Il6*$^{\Delta Gfap}$ was significant on its own (p=0.045) but failed the correction for multiple comparisons.

Weight of the subcutaneous WAT pad showed a significant interaction between diet and genotype (diet*genotype χ^2-Wald 7.389 and 6.002, p<0.05, for males and females, respectively) when accounting for all animals. Pair-wise comparisons manifested a clear effect of the HFD in all genotypes (wt/floxed/ *Il6*$^{\Delta Gfap}$ control vs HFD, p<0.006); and when comparing genotypes within the HFD, wt differed from both floxed and *Il6*$^{\Delta Gfap}$ (p<0.006), in both males and females.

In males, the exclusion of peripheral recombinants left the results unaltered (diet*genotype χ^2-Wald 8.597, p<0.05), with the same significant pair-wise comparisons as mentioned above. In females, however, genotype and diet were significant without interaction (diet χ^2-Wald 132.218, p<0.05; genotype χ^2-Wald 9.966, p<0.05); and pair-wise comparisons between genotypes showed a difference between wt and floxed and wt and *Il6*$^{\Delta Gfap}$ mice (p<0.017).

The gonadal WAT pad weight was affected by both genotype and diet in males (diet χ^2-Wald 253.47, p<0.05; genotype χ^2-Wald 7.055, p<0.05); but pair-wise comparisons were not significant due to the correction applied (wt vs floxed

and floxed vs *Il6*$^{\Delta Gfap}$). In females, only an effect of diet was seen (diet χ^2-Wald 111.74, $p<0.05$).

When peripheral recombinants were removed, both sexes showed an effect of diet (diet χ^2-Wald 182.394 and 84.798, $p<0.05$, for males and females, respectively).

The interescapular BAT pad was weighed in the second experiment, per suggestion of reviewers of one of our submitted papers. Only an effect of HFD was seen, both in the complete group (diet χ^2-Wald 88.059 and 102.727, $p<0.05$, for males and females, respectively) and the one without peripheral recombinants (diet χ^2-Wald 93.523 and 73.514, $p<0.05$, for males and females, respectively).

5.2.1.4.6.2 Relative weight

Relativization of tissue weights for body weight was done in order to evaluate which compartment was more implicated in the body weight change. Figure 28 shows the different tissues for the whole group and the one without peripheral recombinants, and Table 16 summarizes statistical results.

The effect of the HFD was maintained in all fat pads. Regarding genotype effects, the only difference between absolute and relative weight is found in the subcutaneous WAT (in the "no peripheral recombinants" group), where Il6ΔGfap males have a higher relative weight of said fat pad than both wt and floxed littermates.

Of note, the liver actually represents a lower percentage of total body weight in the HFD-fed females and wt males, while in floxed and *Il6*$^{\Delta Gfap}$ males it remains unaltered.

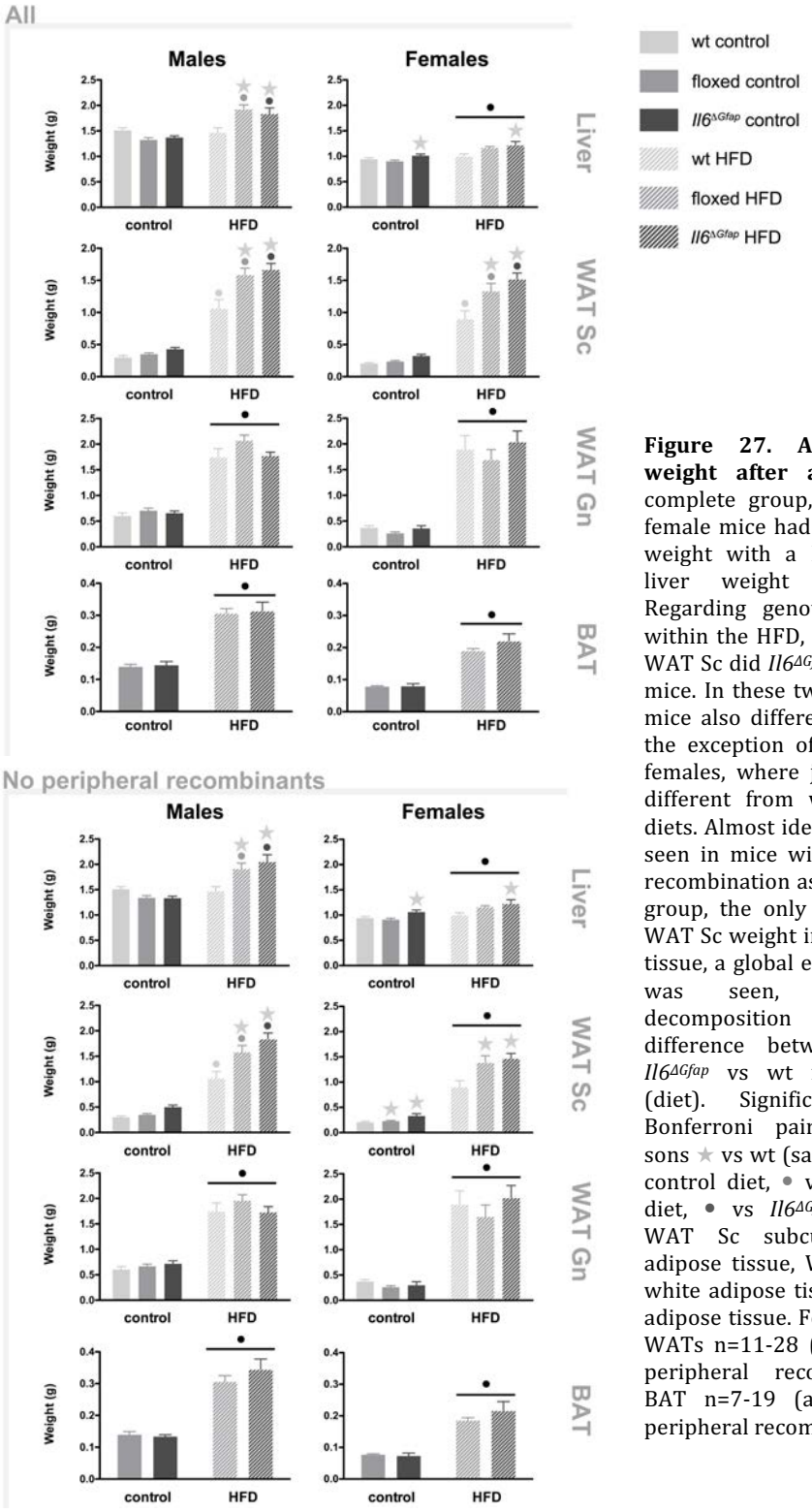

Figure 27. Absolute tissue weight after a HFD. In the complete group, both male and female mice had increased tissue weight with a HFD, except for liver weight in wt mice. Regarding genotype differences within the HFD, only in liver and WAT Sc did *Il6*$^{\Delta Gfap}$ differ from wt mice. In these two tissues, floxed mice also differed from wt, with the exception of liver weight in females, where just *Il6*$^{\Delta Gfap}$ were different from wt, but in both diets. Almost identical results are seen in mice without peripheral recombination as in the complete group, the only exception being WAT Sc weight in females. In this tissue, a global effect of genotype was seen, which upon decomposition showed a difference between floxed or *Il6*$^{\Delta Gfap}$ vs wt mice. • $p<0.05$ (diet). Significant sequential Bonferroni pair-wise comparisons ★ vs wt (same diet), • vs wt control diet, • vs floxed control diet, • vs *Il6*$^{\Delta Gfap}$ control diet. WAT Sc subcutaneous white adipose tissue, WAT Gn gonadal white adipose tissue, BAT brown adipose tissue. For liver and both WATs n=11-28 (all), n=8-22 (no peripheral recombinants); for BAT n=7-19 (all), n=6-14 (no peripheral recombinants).

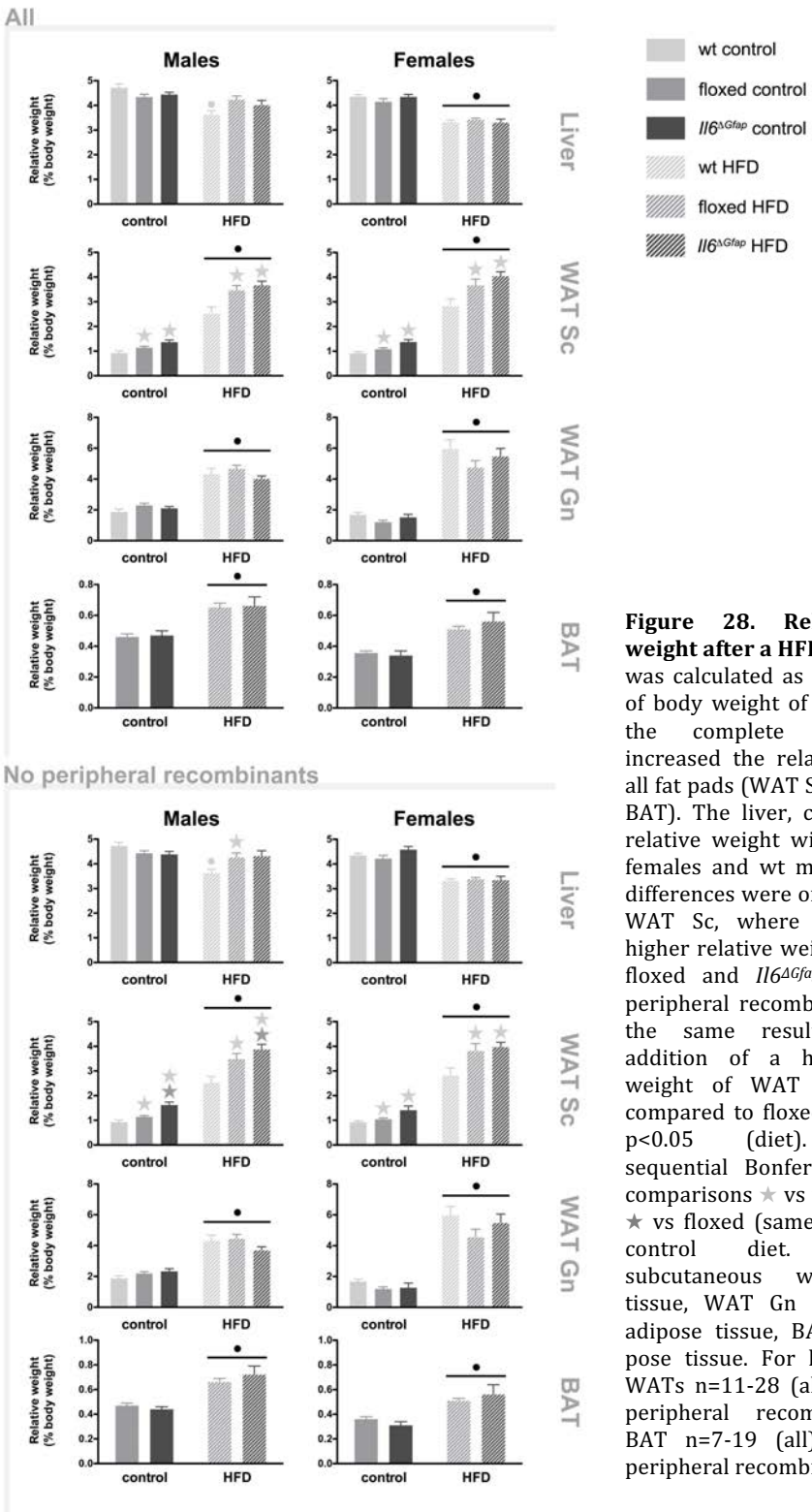

Figure 28. Relative tissue weight after a HFD. This variable was calculated as the percentage of body weight of each tissue. In the complete group, HFD increased the relative weight of all fat pads (WAT Sc, WAT Gn and BAT). The liver, conversely, lost relative weight with the HFD in females and wt males. Genotype differences were only apparent in WAT Sc, where wt mice had higher relative weights than both floxed and *Il6*$^{\Delta Gfap}$. Removal of peripheral recombinants showed the same results, with the addition of a higher relative weight of WAT Sc in *Il6*$^{\Delta Gfap}$ compared to floxed male mice. • $p<0.05$ (diet). Significant sequential Bonferroni pair-wise comparisons ★ vs wt (same diet), ★ vs floxed (same diet), • vs wt control diet. WAT Sc subcutaneous white adipose tissue, WAT Gn gonadal white adipose tissue, BAT brown adipose tissue. For liver and both WATs n=11-28 (all), n=8-22 (no peripheral recombinants); for BAT n=7-19 (all), n=6-14 (no peripheral recombinants).

Table 16. Statistical significances of relative tissue weights. Only significant main effects or interactions are shown. In parenthesis significant sequential Bonferroni pair-wise comparisons.

	ALL		NO PERIPHERAL RECOMBINANTS	
	Males	**Females**	**Males**	**Females**
Liver	**genotype*diet** χ^2-Wald 9.54, p<0.05 *(wt control vs wt HFD)*	**diet** χ^2-Wald 101.137, p<0.05	**genotype*diet** χ^2-Wald 10.864, p<0.05 *(wt control vs wt HFD, wt HFD vs Il6$^{\Delta Gfap}$ HFD)*	**diet** χ^2-Wald 102.346, p<0.05
WAT Sc	**genotype** χ^2-Wald 21.028, p<0.05 *(wt vs floxed, wt vs Il6$^{\Delta Gfap}$)* **diet** χ^2-Wald 254.614, p<0.05	**genotype** χ^2-Wald 14.488, p<0.05 *(wt vs floxed, wt vs Il6$^{\Delta Gfap}$)* **diet** χ^2-Wald 211.551, p<0.05	**genotype** χ^2-Wald 26.446, p<0.05 *(wt vs floxed, wt vs Il6$^{\Delta Gfap}$, floxed vs Il6$^{\Delta Gfap}$)* **diet** χ^2-Wald 188.777, p<0.05	**genotype** χ^2-Wald 11.721, p<0.05 *(wt vs floxed, wt vs Il6$^{\Delta Gfap}$)* **diet** χ^2-Wald 174.2, p<0.05
WAT Gn	**diet** χ^2-Wald 158.244, p<0.05	**diet** χ^2-Wald 130.426, p<0.05	**diet** χ^2-Wald 100.914, p<0.05	**diet** χ^2-Wald 104.644, p<0.05
BAT	**diet** χ^2-Wald 28.2, p<0.05	**diet** χ^2-Wald 31.208, p<0.05	**diet** χ^2-Wald 37.242, p<0.05	**diet** χ^2-Wald 26.846, p<0.05

5.2.1.4.7 Circulating metabolites

Due to serum limitation and the peripheral recombination issue, sample size of non-peripheral recombinant mice was greatly reduced (in some cases down to just one). Thus, no results for just the animals without peripheral recombination will be presented in this section (Figure 29).

5.2.1.4.7.1 Glucose

Tail blood glucose was measured only in the first experiment after a 3-hour fast.

Fasting glucose levels were clearly raised with the HFD, regardless of genotype (diet χ^2-Wald 37.616 and 14.254, p<0.05, for males and females, respectively).

5.2.1.4.7.2 Triglycerides

Only males displayed any significant effects in triglyceride levels, with a significant interaction between diet and genotype, which when decomposed, evidenced a lowering effect of the diet only in wt males, as well as a basal difference between wt and both floxed and *Il6*$^{\Delta Gfap}$ (diet*genotype χ^2-Wald 15.503, $p<0.05$; sequential Bonferroni pair-wise comparisons wt control vs wt HFD, wt control vs floxed control, wt control vs *Il6*$^{\Delta Gfap}$ control).

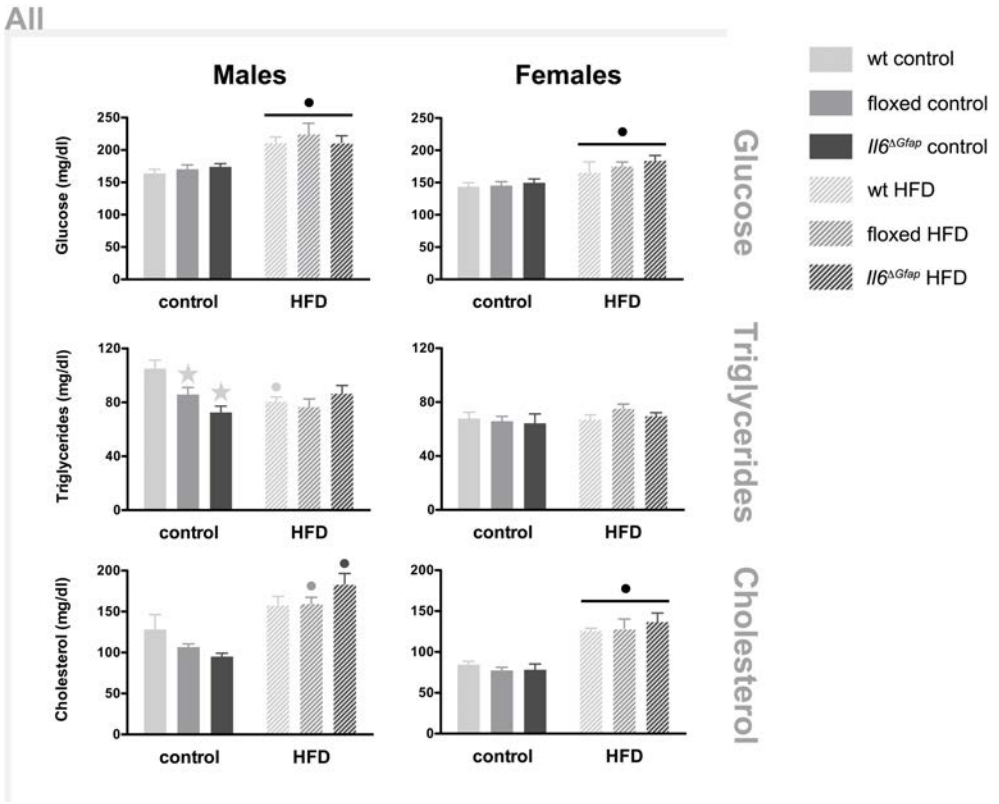

Figure 29. Circulating metabolites after 17 weeks of diet. In general, both male and female mice had increased fasting blood glucose with the HFD. Triglycerides decreased in wt males fed the HFD compared to controls, and in the control diet the other two genotypes had significantly lower levels than wt males. Cholesterol levels increased with HFD in floxed and *Il6*$^{\Delta Gfap}$ males, and across all genotypes in females. • $p<0.05$ (diet). Significant sequential Bonferroni pair-wise comparisons ★ vs wt (same diet), • vs wt control diet, • vs floxed control diet, • vs *Il6*$^{\Delta Gfap}$ control diet. For glucose n=8-14; for triglycerides n=8-13; for cholesterol n=6-13.

5.2.1.4.7.3 Cholesterol

Males showed an interaction between diet and genotype in cholesterol levels, with significant pair-wise differences between diets in the floxed and *Il6*$^{\Delta Gfap}$ genotypes (diet*genotype χ^2-Wald 7.702, $p<0.05$; sequential Bonferroni pair-wise comparisons floxed control vs floxed HFD, *Il6*$^{\Delta Gfap}$ control vs *Il6*$^{\Delta Gfap}$ HFD).

In females, diet had a significant effect on its own in raising cholesterol levels (diet χ^2-Wald 63.547, $p<0.05$).

5.2.1.4.8 Hormones

As was the case with metabolites, serum limitation and peripheral recombination, downsized the group of non-peripheral recombinant mice. Given the inherent variability of hormone measures, only results for the complete group will be presented here (Figure 30).

5.2.1.4.8.1 Leptin

HFD caused a significant increase in circulating serum levels of leptin in both sexes, with no effect of genotype or interaction between the two factors (diet χ^2-Wald 19.684 and 54.815, $p<0.05$, for males and females, respectively).

5.2.1.4.8.2 Insulin

Similarly, HFD significantly raised circulating serum levels of insulin in both males and females, regardless of genotype and without an interaction between the two factors (diet χ^2-Wald 40.655 and 14.887, $p<0.05$, for males and females, respectively).

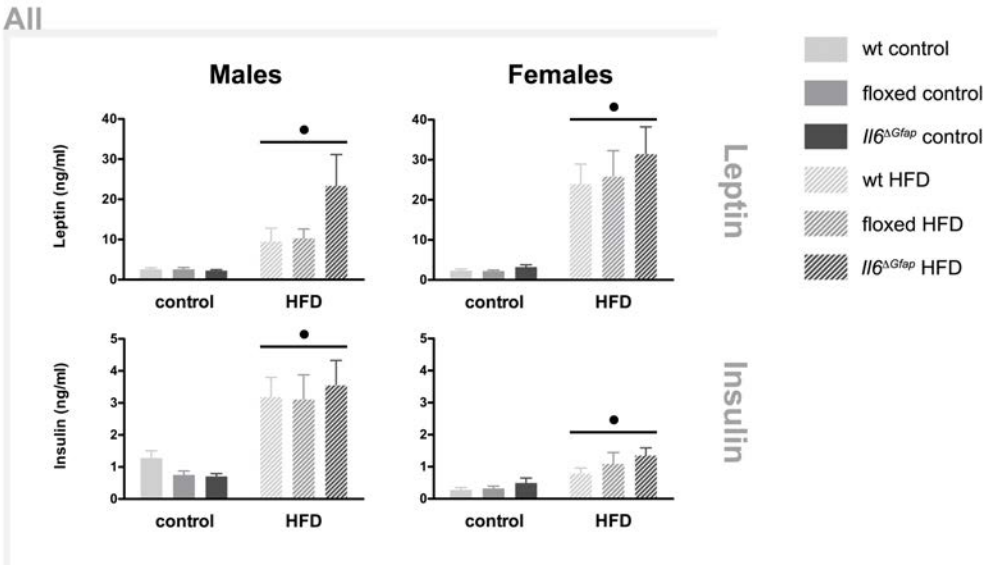

Figure 30. Circulating hormones after 17 weeks of diet. Both male and female mice had increased serum leptin and insulin with the HFD, with no effect of genotype. • $p<0.05$ (diet). For leptin n=6-14; for insulin n=5-14.

5.2.1.4.9 In situ hybridization

Some slides for the probes *Agrp* and *Pomc* had to be removed because the location was incorrect, a consequence of the method for selecting them being based on relative position to the PVN. Therefore, only the complete group will be analyzed, since removal of peripheral recombinants yielded very reduced sample sizes (Figure 31).

Agrp expression showed no significant changes in males, but females displayed genotype and diet effects (genotype χ^2-Wald 4.892, $p<0.05$; diet χ^2-Wald 8.359, $p<0.05$), both of them lowering the expression of the neuropeptide.

Crh remained unchanged in males and females, in both genotypes and diets.

Pomc showed a significant interaction between genotype and diet in males (diet*genotype χ^2-Wald 4.548, $p<0.05$), but no significant pair-wise comparisons.

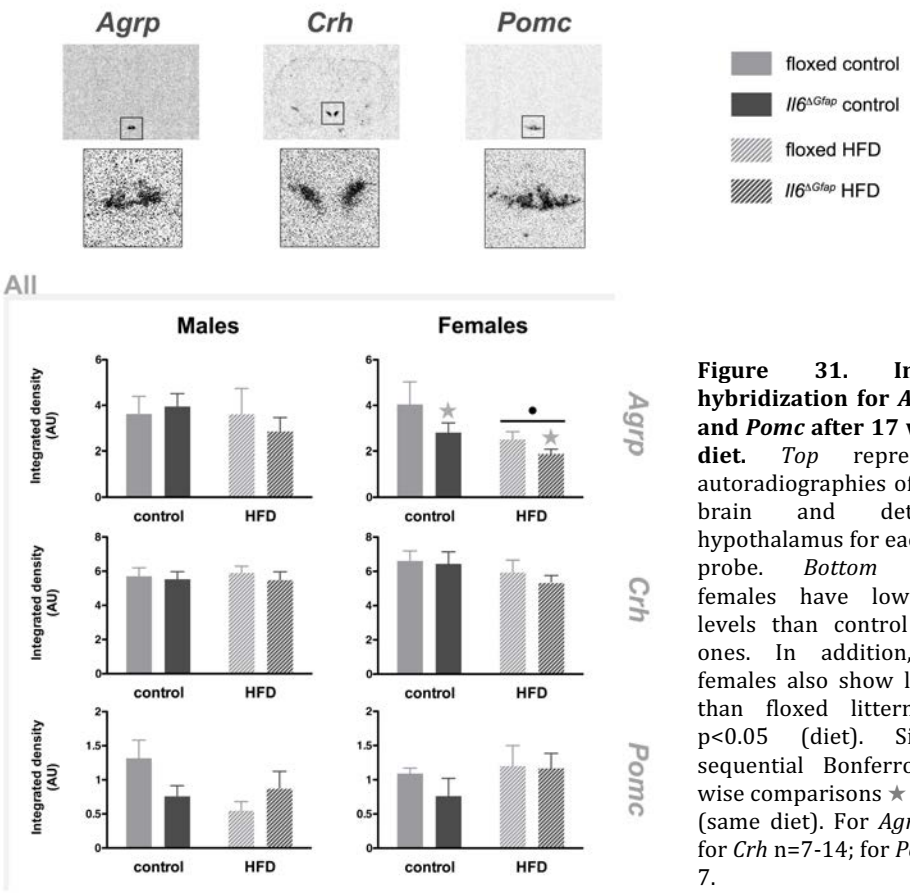

Figure 31. In situ hybridization for *Agrp*, *Crh* and *Pomc* after 17 weeks of diet. *Top* representative autoradiographies of a whole brain and detail of hypothalamus for each mRNA probe. *Bottom* HFD-fed females have lower *Agrp* levels than control diet-fed ones. In addition, *Il6$^{\Delta Gfap}$* females also show less Agrp than floxed littermates. • $p<0.05$ (diet). Significant sequential Bonferroni pair-wise comparisons ★ vs floxed (same diet). For *Agrp* n=4-9, for *Crh* n=7-14; for *Pomc* n=4-7.

5.2.1.5 Fasting

Preliminary experiments with an overnight (ON) fast elicited faint responses from the classical orexigenic neuropeptides, *Npy* and *Agrp*.

In an initial study with floxed and *Il6$^{\Delta Gfap}$* males, *Npy* expression, as measured by qPCR, increased 2.4-fold in the fasted floxed group compared to the fed floxed one (2.42±0.32 vs 1.00±0.10; genotype*fast χ^2-Wald 7.828, $p<0.05$;

pair-wise comparison floxed fed vs floxed fasted p<0.006) and *Agrp* increased 2.7-fold between the same groups (2.68±0.27 vs 1.00±0.26; genotype*fast χ^2-Wald 10.725, p<0.05; sequential Bonferroni pair-wise comparison floxed fed vs floxed fasted). A later study incorporating both sexes, showed similar increases in *Npy* and *Agrp* expression in floxed mice (Table 17); but in males, the *Agrp* increase failed to reach significance.

Table 17. Fold-change of orexigenic neuropeptides after an ON fast in floxed animals. Note that males and females were analyzed separately and therefore the expression level of the control group is not necessarily the same in both sexes (or genes).

	Males		Females	
	Floxed fed	**Floxed fasted**	**Floxed fed**	**Floxed fasted**
Npy	1.00 ± 0.13	2.57 ± 0.74	1.00 ± 0.26	2.41 ± 0.53
Agrp	1.00 ± 0.07	3.13 ± 0.82	1.00 ± 0.28	2.69 ± 0.69

Furthermore, in an unrelated experiment to this thesis (carried out during my stay in Dr. Palmiter's group), but relevant since its aim was to make a preliminary comparison of 24- and 48-hour fast, we observed a 3.6-fold increase in C57BL/6 male mice fasted for 24 hours compared to *ad libitum*-fed controls (3.63±1.53 vs 1.00±0.09, n=2), and a 12.7-fold change after 48 hours (12.66 ± 3.9, n=2).

Therefore, we changed the ON protocol to a 48-hour fast when needing to assess mRNA of hypothalamic neuropeptides. In the case of refeeding after a fast, we maintained the 24-hour interval to avoid excessive stress.

5.2.1.5.1 Twenty-four-hour fast and 4-hour refeeding

Since this experiment was carried out in group-housed animals, only data for the complete group will be analyzed.

Animals fed a control diet were fasted for 24 hours. The weight lost, as percentage of their initial body weight, was essentially the same in both genotypes of males and females (Table 18).

Table 18. Percentage weight loss after a 24-hour fast. Percentage weight loss was calculated as Δweight*100/(pre-fast weight). No significant differences were observed between genotypes in either sex.

	ALL			
	Males		Females	
	floxed	*Il6*$^{\Delta Gfap}$	floxed	*Il6*$^{\Delta Gfap}$
% lost	10.3±1.1	10.7±0.6	11.0±0.5	10.9±0.4

Energy intake after reintroduction of the control diet was monitored for the following 4 hours and showed a more or less steady increase after the first hour (when most of the eating occurs), with no differences between genotypes (time χ^2-Wald 244.501, $p<0.05$) (Figure 32).

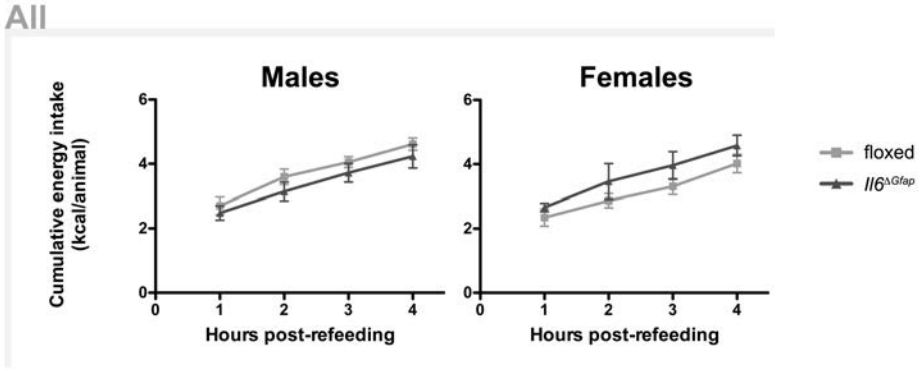

Figure 32. Cumulative energy intake during the 4 hours after reintroduction of the control diet after a 24-hour fast. Animals were group-housed and total intake was divided by the number of animals per cage (n=5-8, cages). Both genotypes present the same compensatory energy intake after the fast.

5.2.1.5.2 Forty-eight-hour fast

For this experiment, there was no chance of assessing peripheral recombination, so the data presented regard the complete group.

5.2.1.5.2.1 Relative body weight loss

Forty-eight-hour fasted animals lost more weight (relative to pre-fast levels) than *ad libitum*-fed controls (Figure 33). In males, only the fast had a significant effect (fast χ^2-Wald 1078.996, $p<0.05$), but in females, there was a significant interaction of fast and genotype, which upon decomposition, showed a higher weight loss not only in food-deprived, but also in fasted *Il6*$^{\Delta Gfap}$ compared to fasted floxed females, and a lower increase in fed *Il6*$^{\Delta Gfap}$ compared to fed floxed females (fast*genotype χ^2-Wald 12.046, $p<0.05$; sequential Bonferroni pair-wise comparisons fed floxed vs fasted floxed, fed *Il6*$^{\Delta Gfap}$ vs fasted *Il6*$^{\Delta Gfap}$, fed floxed vs fed *Il6*$^{\Delta Gfap}$, fasted floxed vs fasted *Il6*$^{\Delta Gfap}$).

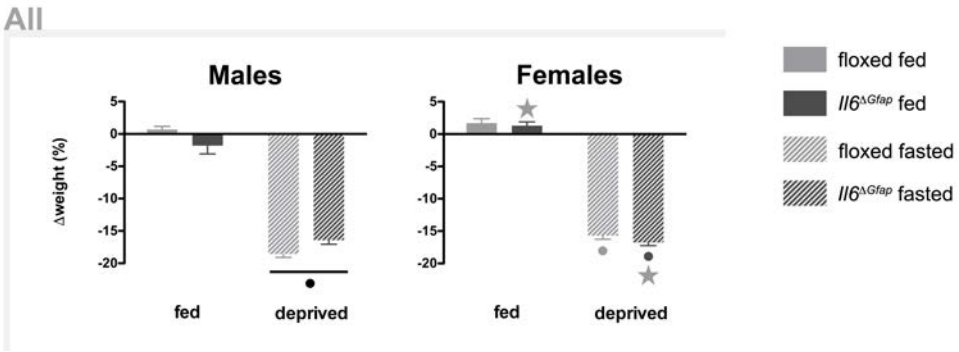

Figure 33. Percentage weight loss after a 48-hour fast. Fasted animals lost significantly more weight. *Il6*$^{\Delta Gfap}$ females were more affected by the fast and even in the fed state, they did not gain as much weight during that period. • $p<0.05$ (diet). Significant sequential Bonferroni pair-wise comparisons ★ vs floxed (same treatment), • vs fed floxed, • vs fed *Il6*$^{\Delta Gfap}$. N=5-8.

5.2.1.5.2.2 Hypothalamic neuropeptides and Il6

Regarding the expression of hypothalamic neuropeptides (Figure 34), the prototypical orexigenic ones (*Npy* and *Agrp*) behave very similarly within each sex, but IL-6 deficiency has opposite effects with fasting in males and females. In males, the decomposition of the interaction between the two factors showed that fasting increases expression of both *Npy* and *Agrp* in fasted $Il6^{\Delta Gfap}$ compared to the same genotype in the fed group (fast*genotype χ^2-Wald 10.017 and 21.828, $p<0.05$, for *Npy* and *Agrp*, respectively; sequential Bonferroni pair-wise comparisons fasted $Il6^{\Delta Gfap}$ vs fed $Il6^{\Delta Gfap}$; fasted $Il6^{\Delta Gfap}$ vs fasted floxed), while not changing in floxed mice. In females, conversely, the decomposition of the interaction between fast and genotype revealed a block in $Il6^{\Delta Gfap}$ mice in the fast-induced increase of *Npy* and *Agrp* (fast*genotype χ^2-Wald 3.848 and 6.86, $p<0.05$, for *Npy* and *Agrp*, respectively; sequential Bonferroni pair-wise comparisons fasted floxed vs fed floxed, fasted $Il6^{\Delta Gfap}$ vs fed $Il6^{\Delta Gfap}$ -only *Agrp*-; fasted $Il6^{\Delta Gfap}$ vs fasted floxed).

The anorectic *Crh* displayed an interaction of fasting and genotype in males, but pair-wise comparisons were not significant enough to withstand the correction for multiple comparisons (fast*genotype χ^2-Wald 7.82, $p<0.05$). Females, however, showed no significant effects.

The rest of the hypothalamic neuropeptides failed to reveal any significant changes due to either genotype or the 48-hour fast. In the case of *Pomc*, probably due to the great variability, especially in the control group (fed floxed).

In this experiment, we also measured *Il6* in order to try and detect the effect of the astrocytic knock-out. Unfortunately, no decrease was detected in either sex and fasting also elicited no significant changes, even though in females, there was an interaction of the two factors (fast*genotype χ^2-Wald 5.274, $p<0.05$).

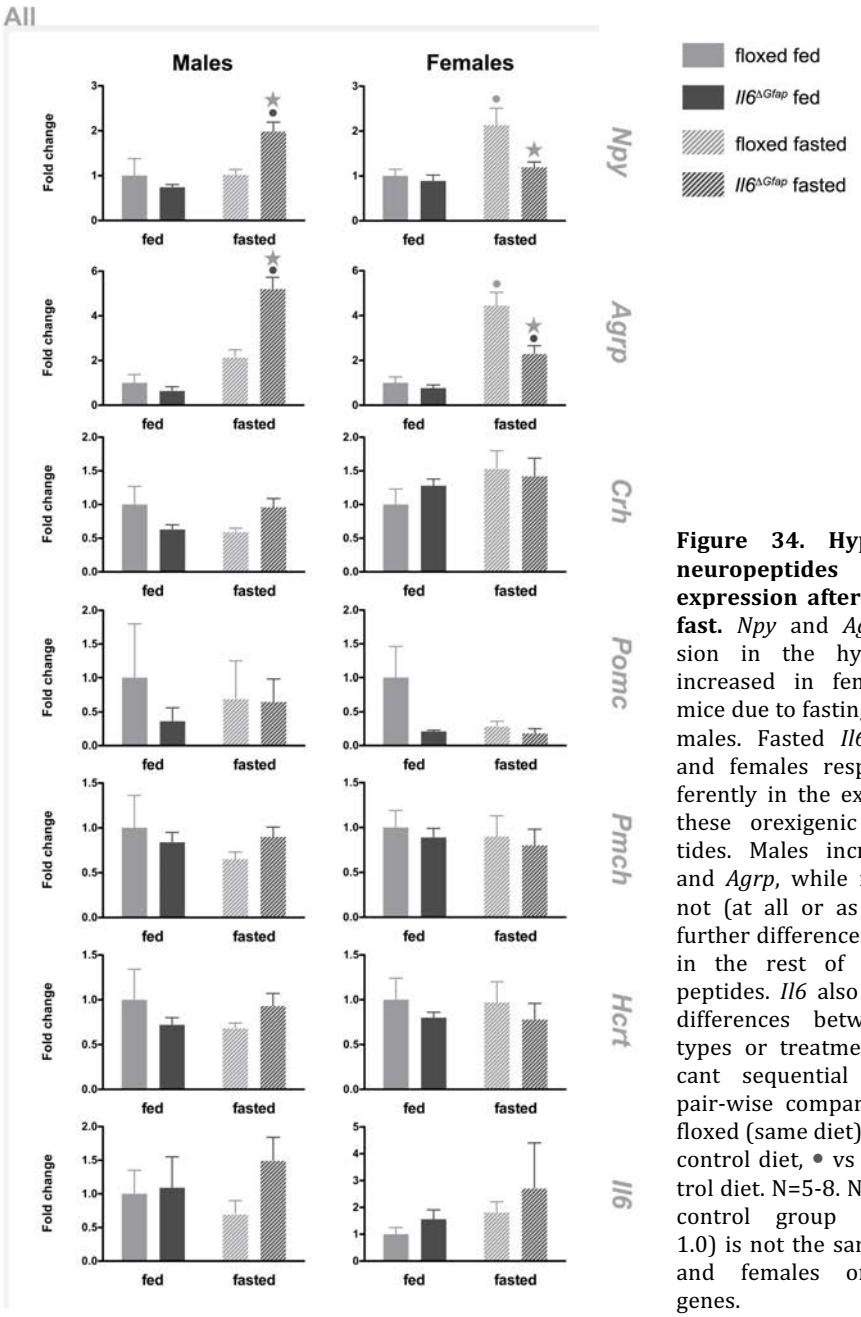

Figure 34. Hypothalamic neuropeptides and *Il6* expression after a 48-hour fast. *Npy* and *Agrp* expression in the hypothalamus increased in female floxed mice due to fasting, but not in males. Fasted *Il6*$^{\Delta Gfap}$ males and females responded differently in the expression of these orexigenic neuropeptides. Males increased *Npy* and *Agrp*, while females did not (at all or as much). No further differences were seen in the rest of the neuropeptides. *Il6* also lacked any differences between genotypes or treatments. Significant sequential Bonferroni pair-wise comparisons ★ vs floxed (same diet), • vs floxed control diet, • vs *Il6*$^{\Delta Gfap}$ control diet. N=5-8. Note that the control group (expression 1.0) is not the same in males and females or between genes.

5.2.2 Neuronal IL-6 conditional knock-out

5.2.2.1 Frequencies at weaning

The first analysis of frequencies at weaning was done considering the four genotypes obtained in the crossing described in material and methods (see *4.2.5.2 Conditional Il6 knockout in neurons*). This showed no significant differences between the four genotypes (χ^2 5.959, p=0.114) (Table 19), but the more reduced numbers in *Il6*$^{\Delta Syn1}$ and *Il6*$^{\Delta Syn1/wt}$ pointed to a possible effect of *cre*. Indeed, when taking into account the two separate genes that give rise to the four genotypes (*Cre* and *Il6*), a significant effect of the presence of *Cre* was evident (χ^2 4.446, p=0.035), while the floxing of two versus one allele of *Il6* seemed to have no effect (χ^2 1.643, p=0.2). Incidentally, females were underrepresented (χ^2 5.95, p=0.015).

Table 19. Observed and expected frequencies at weaning of each genotype and sex. No significant differences between genotypes were detected. However, the underrepresentation of *Il6*$^{\Delta Syn1}$ and *Il6*$^{\Delta Syn1/wt}$ suggested otherwise.

	Observed N	Expected N	Residual
Genotype			
wt	148	146	2
floxed	169	146	23
***Il6*$^{\Delta Syn1}$**	137	146	-9
***Il6*$^{\Delta Syn1/wt}$**	130	146	-16
Sex			
males	322	292.5	29.5
females	263	292.5	-29.5
Total	**585**		

5.2.2.2 Basal weight

Possible weight differences were assessed at weaning, when the mice were 3 weeks-old. No significant effect of genotype was found at that point. However, further assessment of body weight for the following weeks (up to week 11), evidenced a lower body weight in *Il6*$^{\Delta Syn1}$ mice of both sexes, compared to floxed mice (genotype Wald-χ^2 6.692 and 6.986, $p<0.05$, for males and females, respectively; sequential Bonferroni pair-wise comparisons floxed vs *Il6*$^{\Delta Syn1}$) (Figure 35).

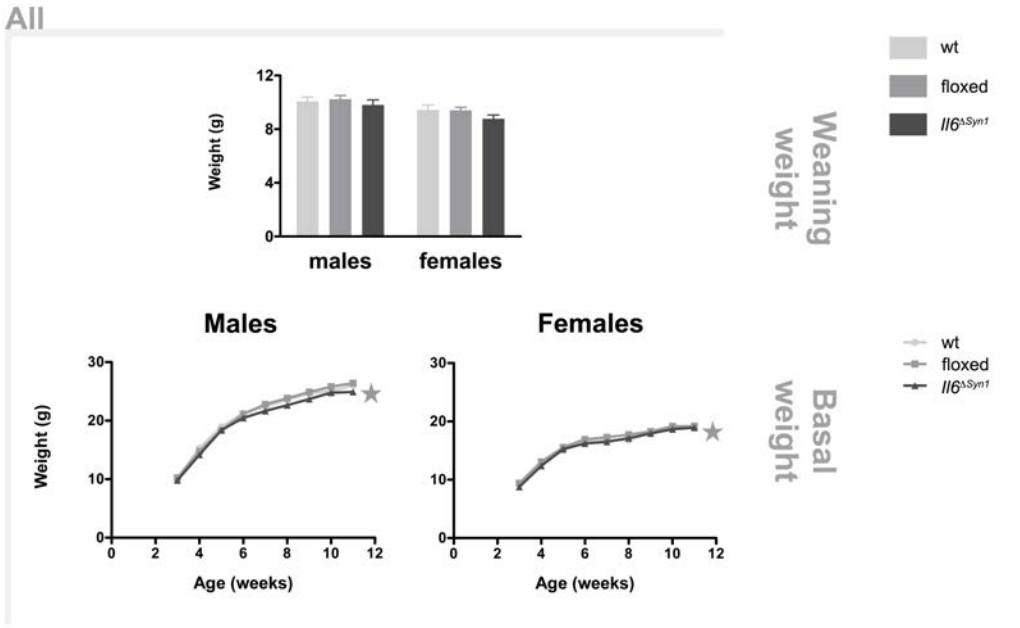

Figure 35. Weaning weight and basal weight from week 3 (weaning) to week 11. No significant differences where observed in either sex at weaning regarding genotype. However, during the following weeks, *Il6*$^{\Delta Syn1}$ exhibited a lower body weight than floxed mice, in both sexes. Significant sequential Bonferroni pair-wise comparisons ★ vs floxed. N=21-71 (the great range is due to a lesser number of wt and the fact that not all mice were weighed every week).

5.2.2.3 Temperature

Rectal temperature was recorded as an indirect measure of metabolism (Figure 36). *Il6*$^{\Delta Syn1}$ females had a lower rectal temperature than floxed littermates, while males presented no such difference (t-Student(26) -0.187 and 2.474, for males and females, respectively, $p<0.05$).

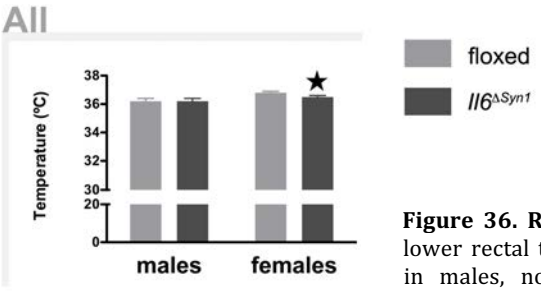

Figure 36. Rectal temperature. *Il6*$^{\Delta Syn1}$ females had a lower rectal temperature than floxed littermates; while in males, no differences were observed. ★ $p<0.05$. N=13-15.

5.2.2.4 Linear growth

Body length-related measures (Figure 37) were taken in an unrelated experiment to this thesis (induction of experimental autoimmune encephalomyelitis, EAE) and after ruling out a possible treatment effect the two conditions were pooled. In addition to that experiment, tibial length was measured after the 48-hour fast experiment detailed further on (see *5.2.2.6.2 48-hour fast*).

IGF-1 and IGFBP-1 and -3 (Figure 37) were measured in the sera of the controls of the EAE and an LPS injection experiment (IGF-1 was measured in LPS-treated samples too, as a control) (Fan et al. 1994).

Nose-rump distance and tibial length were consistent in that *Il6*$^{\Delta Syn1}$ mice of both sexes were found to be smaller (nose-rump t-Student(26) 4.362 and 2.894, $p<0.05$, for males and females, respectively; tibial length t-Student(56) 5.433 and 4.34, $p<0.05$, for males and females, respectively).

However, analysis of mice without peripheral recombination was affected by a very important reduction in sample size, which meant that despite having almost identical means as in the complete group, the reduction in tibial length previously seen in *Il6*$^{\Delta Syn1}$ mice was not detected (t-Student(15) 2.076 and t-Student(7) 1.036, for males and females, respectively).

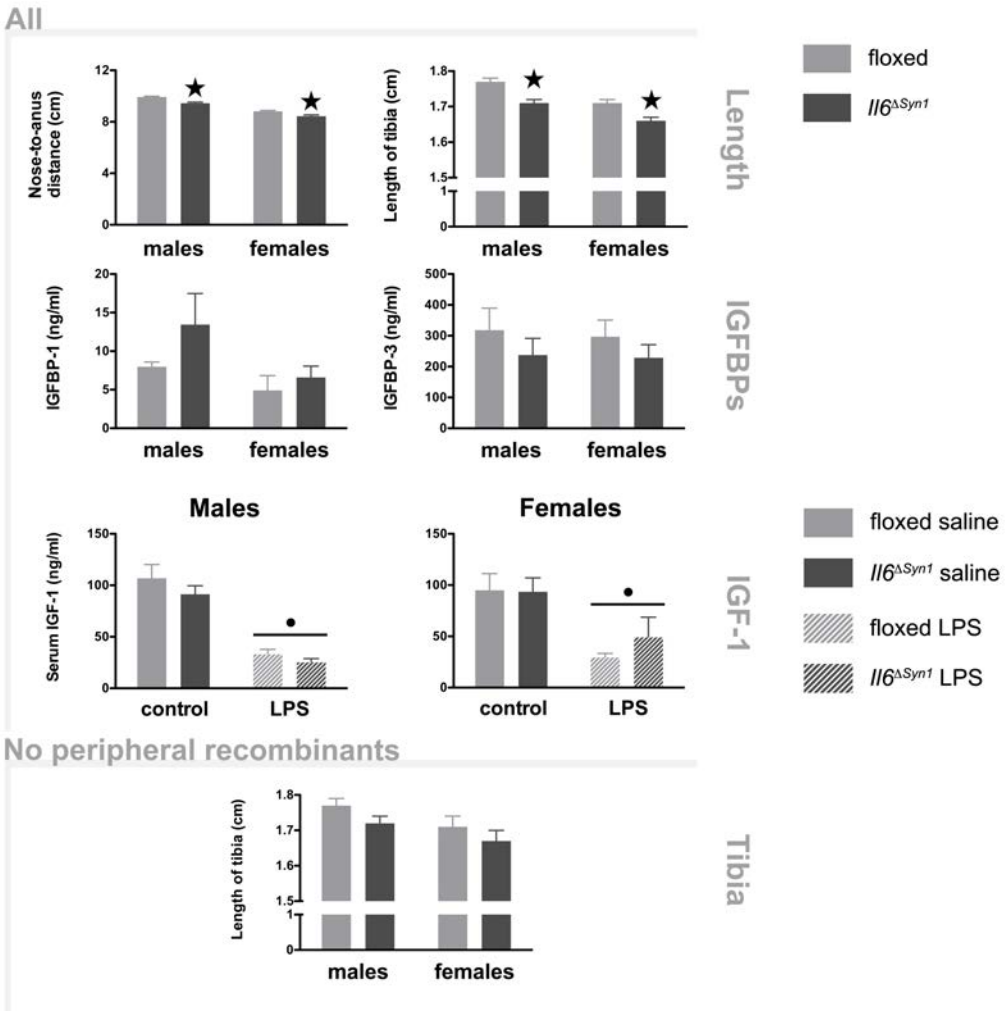

Figure 37. Linear growth-related measures. Both nose-rump distance (measured in anesthetized animals) and length of the tibia were significantly shorter in the *Il6*$^{\Delta Syn1}$ genotype, in both males and females, but only in the complete group despite the trends being the same without peripheral recombinants. No significant genotype differences where observed in either sex regarding IGFBPs or IGF-1, but a marked descent of the latter was seen after LPS administration. • $p<0.05$ (treatment), ★ $p<0.05$ (genotype). For nose-rump distance n=12-15, for tibial length n=24-30 (all), n=3-10 (no peripheral recombinants); for IGFBPs n=6-8; for IGF-1 n=3-6.

No effect of genotype was observed in serum IGF-1 levels, but LPS treatment lowered them significantly (χ^2-Wald 90.336 and 19.856, $p<0.05$, for males and females, respectively).

Regarding IGFBPs, they were not affected by genotype either (IGFBP-1 t-Student(7.32) -1.339 and t-Student(12) -0.71, in males and females, respectively; IGFBP-3 t-Student(14) 0.906 and t-Student(14) 0.998, in males and females, respectively).

5.2.2.5 High-fat diet

One experiment was carried out with wt, floxed and *Il6*$^{\Delta Syn1}$ mice but, due to the later detected recombination, two further *Il6*$^{\Delta Syn1}$ female mice were added afterwards (with a different batch of HFD). These extra animals are only included in the analysis of absolute body weight, weight gain and tissue weights.

5.2.2.5.1 Body weight and weight gain

In the complete group, both males and females weighed more with the HFD (diet χ^2-Wald 292.082 and 44.294, $p<0.05$, for males and females respectively). In addition, males showed a significant effect of genotype on body weight, which upon decomposition evidenced that *Il6*$^{\Delta Syn1}$ mice were lighter than both wt and floxed littermates (regardless of diet) (genotype χ^2-Wald 11.987, $p<0.05$, sequential Bonferroni pair-wise comparisons wt vs *Il6*$^{\Delta Syn1}$ and floxed vs *Il6*$^{\Delta Syn1}$) (Figure 38).

Removal of mice with peripheral recombination, yielded similar results. Female mice continued to only have a significant effect of diet (diet χ^2-Wald 19.952, $p<0.05$). However, males showed an interaction between genotype and diet, which manifested a diet effect for each genotype, and also a genotype

difference on the HFD between *Il6*$^{\Delta Syn1}$ and wt or floxed mice (diet*genotype χ^2-Wald 8.934, $p<0.05$, sequential Bonferroni pair-wise comparisons wt control vs wt HFD, floxed control vs floxed HFD, *Il6*$^{\Delta Syn1}$ control vs *Il6*$^{\Delta Syn1}$ HFD, wt HFD vs *Il6*$^{\Delta Syn1}$ HFD, floxed HFD vs *Il6*$^{\Delta Syn1}$ HFD).

Taken all animals into consideration, males gained more weight on the HFD (diet χ^2-Wald 501.27, $p<0.05$). In females, an interaction between diet and genotype appeared, showing and effect of HFD for each genotype, as well as differences between floxed and *Il6*$^{\Delta Syn1}$ on both diets (diet*genotype χ^2-Wald 18.851, $p<0.05$, sequential Bonferroni pair-wise comparisons wt control vs wt HFD, floxed control vs floxed HFD, *Il6*$^{\Delta Syn1}$ control vs *Il6*$^{\Delta Syn1}$ HFD, floxed control vs *Il6*$^{\Delta Syn1}$ control, floxed HFD vs *Il6*$^{\Delta Syn1}$ HFD).

When only mice without peripheral recombination were considered, males again showed a significant diet effect (diet χ^2-Wald 296.216, $p<0.05$), and females an interaction between the two main factors. In this case, however, the decomposition left only a significant effect of HFD on wt and floxed mice, with genotype effects being lost due to multiple comparisons correction (diet*genotype χ^2-Wald 8.79, $p<0.05$, sequential Bonferroni pair-wise comparisons wt control vs wt HFD, floxed control vs floxed HFD).

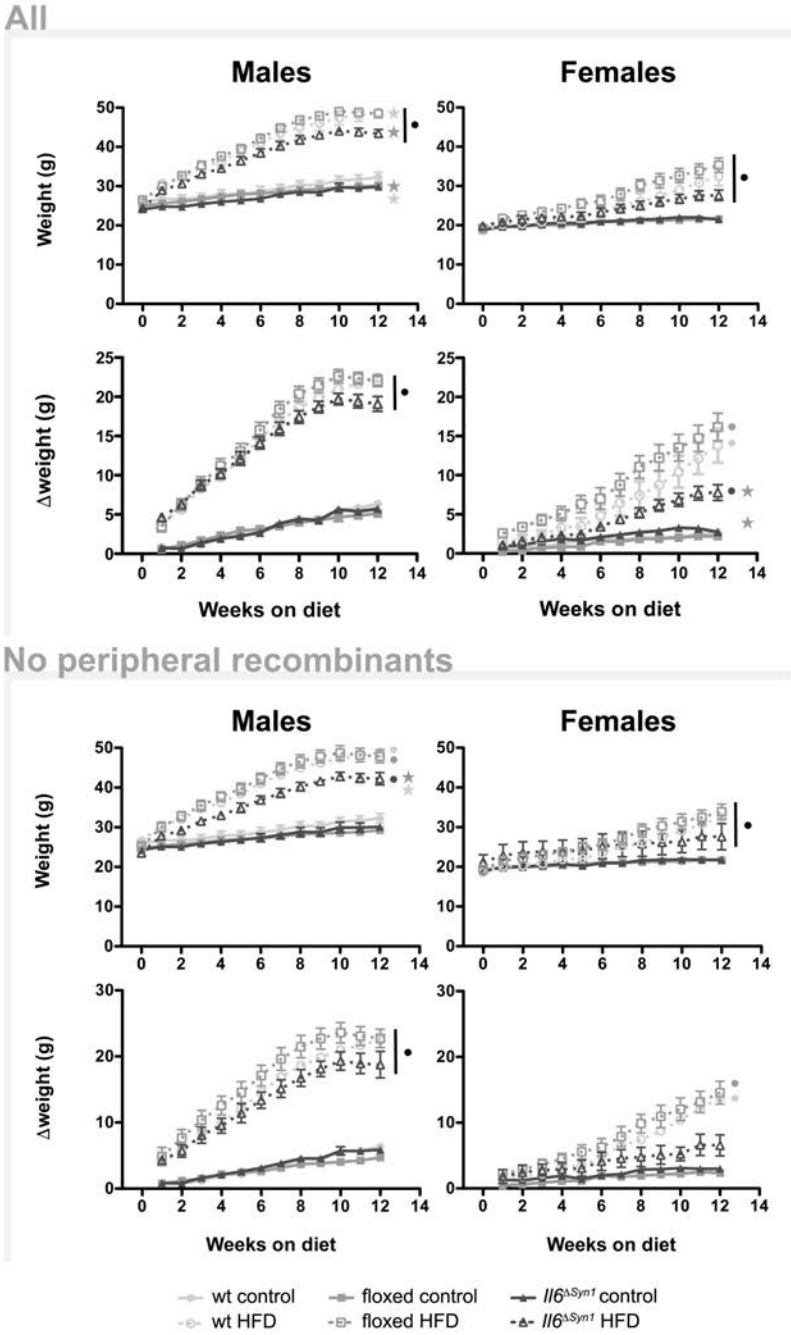

Figure 38. Body weight and weight gain after 12 weeks of control or HFD. Both male and female mice increased their weight with a HFD. The genotype effect of *Il6*$^{\Delta Syn1}$ was seen in the absolute weight of males, and more clearly in the weight gain of females. Similar results are seen in mice without peripheral recombination. • p<0.05 (diet). Significant sequential Bonferroni pair-wise comparisons ★ vs wt (same diet), ★ vs floxed (same diet), • vs wt control diet, • vs floxed control diet, • vs *Il6*$^{\Delta Syn1}$ control diet. N=6-12 (all), n=4-8 (no peripheral recombinants).

5.2.2.5.2 Energy intake and feed efficiency

Animals were group-housed when energy intake was measured, so no separation of recombinants could be performed. Figure 39 shows the average daily intake over the complete experiment.

Both male and female mice on a HFD have a higher energy intake than littermates on the control diet (diet χ^2-Wald 226.636 and 95.864, $p<0.05$, for males and females, respectively) (Figure 39).

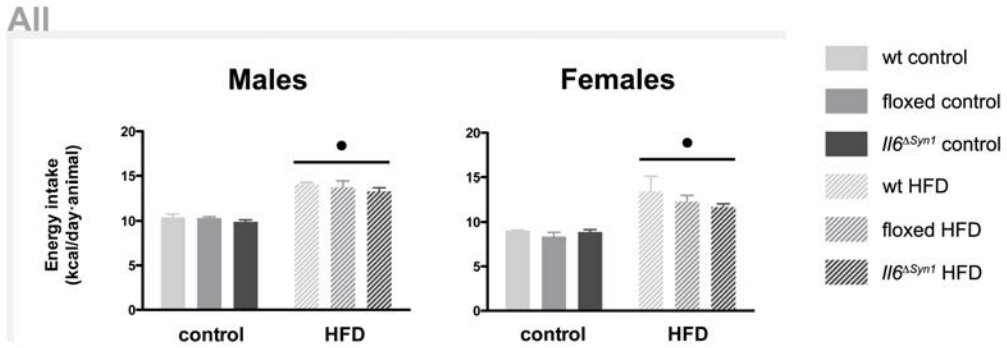

Figure 39. Energy intake with control or HFD. Average of all weeks with the diet. The total intake of the cage was divided by the number of mice in it. Mice on a HFD ingest more calories than mice on the control diet, with no genotype differences. • $p<0.05$ (diet). N= 3-8 (cages).

Feed efficiency was also calculated (Figure 40), and it clearly reflected the differences observed in body weight in *Il6$^{\Delta Syn1}$* females. While HFD had an increased efficiency in males regardless of genotype (diet χ^2-Wald 276.608, $p<0.05$), and in wt and floxed females, lack of neuronal IL-6 prevented the excess body weight gain per kcal on the HFD (diet*genotype χ^2-Wald 22.027, $p<0.05$; sequential Bonferroni pair-wise comparisons control wt vs HFD wt, control floxed vs HFD floxed, HFD wt vs HFD *Il6$^{\Delta Syn1}$*, HFD floxed vs HFD *Il6$^{\Delta Syn1}$*).

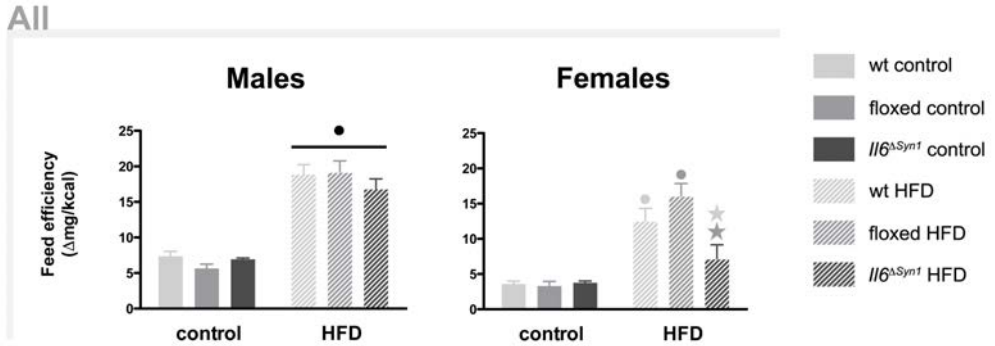

Figure 40. Feed efficiency with control or HFD. HFD had an increased efficiency (weight gain per kcal ingested) in all genotypes in males, and in wt and floxed females. *Il6*$^{\Delta Syn1}$ females on the HFD were resistant to that increased efficiency, in line with their lower body weight. • p<0.05 (diet). Significant sequential Bonferroni pair-wise comparisons ★ vs wt (same diet), ★ vs floxed (same diet), • vs wt control diet, • vs floxed control diet. N= 3-8 (cages).

5.2.2.5.3 Activity

Activity on an open field was assessed after 9 weeks of diet to assess a measure of energy expenditure. Due to time constraints, only floxed and *Il6*$^{\Delta Syn1}$ were evaluated (Figure 41).

In males of the complete group, rearings were reduced with the HFD (diet χ^2-Wald 6.195, p<0.05). While in females, diet had no effect, but genotype did, with a higher number in *Il6*$^{\Delta Syn1}$ (genotype χ^2-Wald 8.582, p<0.05).

Total activity was increased in *Il6*$^{\Delta Syn1}$ females, regardless of diet (genotype χ^2-Wald 9.158, p<0.05). In males, there was a significant interaction between diet and genotype, which when decomposed showed that floxed mice on a HFD were less active than their controls, and different from *Il6*$^{\Delta Syn1}$ on the HFD (diet*genotype χ^2-Wald 7.835, p<0.05, sequential Bonferroni pair-wise comparisons floxed control vs floxed HFD, floxed HFD vs *Il6*$^{\Delta Syn1}$ HFD).

These differences were mostly due to activity in the external areas of the open field (close to the walls), since the results in that zone mimic the ones above. In females, only genotype contributed to the differences (genotype χ^2-Wald 6.343, p<0.05). And in males, the decomposition of the interaction of both

factors showed again that floxed mice on the HFD were indeed moving less than controls of the same genotype and *Il6*$^{\Delta Syn1}$ on the same diet (diet*genotype χ^2-Wald 8.285, $p<0.05$, sequential Bonferroni pair-wise comparisons floxed control vs floxed HFD, floxed HFD vs *Il6*$^{\Delta Syn1}$ HFD).

Activity in the internal areas was only affected by diet in males, which visited them less (diet χ^2-Wald 4.432, $p<0.05$).

Removal of peripheral recombinants resulted in a very limited sample size, which for behavior is certainly insufficient. Most significances were lost.

Rearings did show a similar pattern, with males being affected by diet (diet χ^2-Wald 5.201, $p<0.05$) and females by genotype (genotype χ^2-Wald 8.378, $p<0.05$) in the same way as in the complete group. There was also a significant effect of diet in the internal activity of females (diet χ^2-Wald 7.557, $p<0.05$).

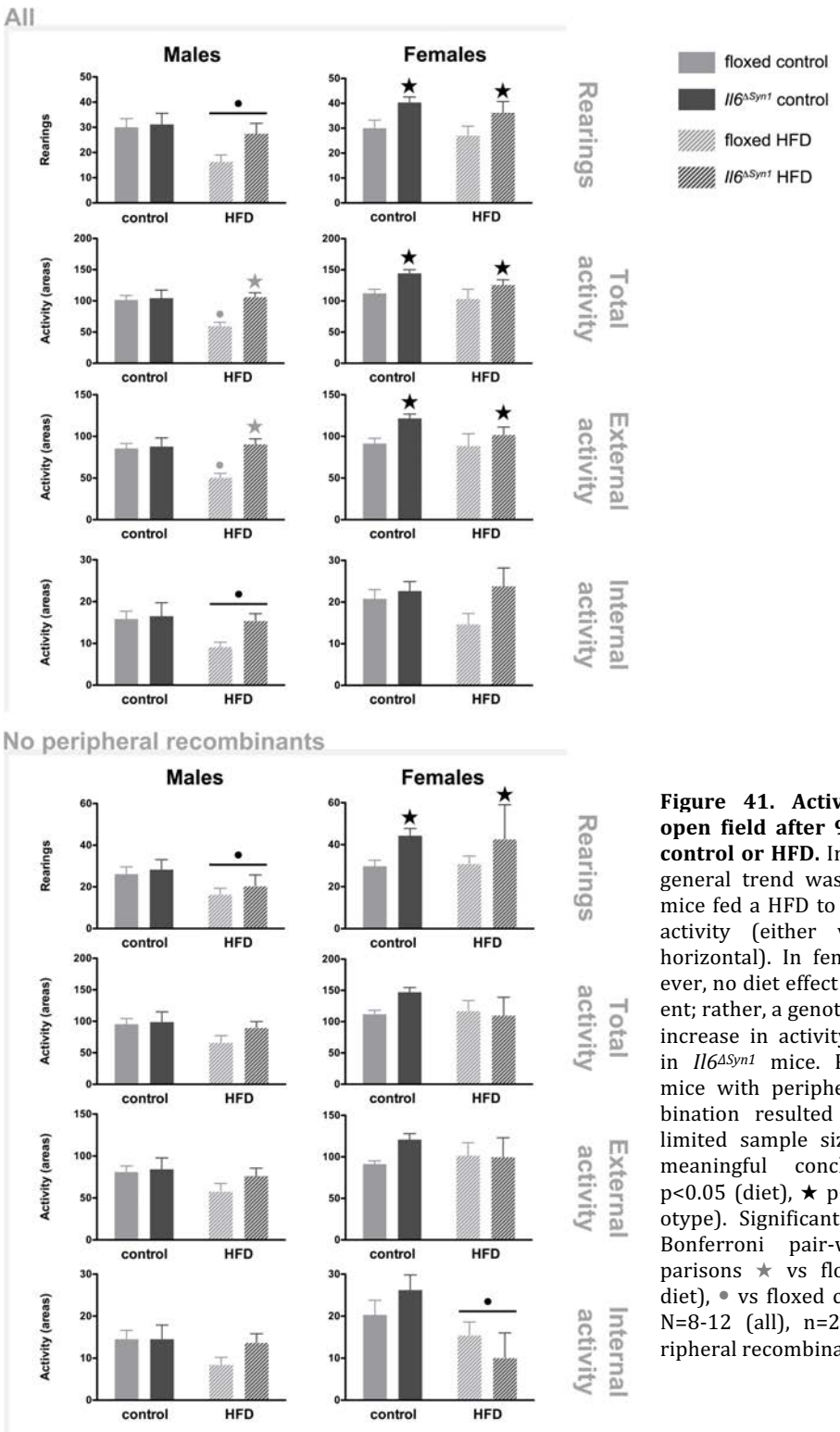

Figure 41. Activity in an open field after 9 weeks of control or HFD. In males, the general trend was for floxed mice fed a HFD to have lower activity (either vertical or horizontal). In females, however, no diet effect was apparent; rather, a genotype-related increase in activity was seen in *Il6*$^{\Delta Syn1}$ mice. Removal of mice with peripheral recombination resulted in a very limited sample size to draw meaningful conclusions. • $p<0.05$ (diet), ★ $p<0.05$ (genotype). Significant sequential Bonferroni pair-wise comparisons ★ vs floxed (same diet), • vs floxed control diet. N=8-12 (all), n=2-8 (no peripheral recombinants).

5.2.2.5.4 ITT and OGTT

In the ITT of complete group (Figure 42, top), insulin administration resulted in the expected time-dependent decrease in blood glucose (time χ^2-Wald 549.333 and 660.619, $p<0.05$, in males and females, respectively). In males, there was also a clear effect of HFD, causing insulin resistance (diet χ^2-Wald 82.837, $p<0.05$); which also became apparent in females after decomposing the interaction between diet and genotype (diet*genotype χ^2-Wald 4.82, $p<0.05$, sequential Bonferroni pair-wise comparisons floxed control vs floxed HFD, *Il6*$^{\Delta Syn1}$ control vs *Il6*$^{\Delta Syn1}$ HFD).

Removal of peripheral recombinants (Figure 42, bottom) made apparent the genotype difference within the HFD. Males fed a HFD had higher glucose levels, but among those, *Il6*$^{\Delta Syn1}$ had lower glucose (diet*genotype χ^2-Wald 12.278, $p<0.05$, sequential Bonferroni pair-wise comparisons floxed control vs floxed HFD, *Il6*$^{\Delta Syn1}$ control vs *Il6*$^{\Delta Syn1}$ HFD, floxed HFD vs *Il6*$^{\Delta Syn1}$ HFD). In females, decomposition of the interaction manifested that HFD only raised glucose levels in floxed mice, which were significantly higher than HFD-fed *Il6*$^{\Delta Syn1}$ (diet*genotype χ^2-Wald 12.278, $p<0.05$, sequential Bonferroni pair-wise comparisons floxed control vs floxed HFD, floxed HFD vs *Il6*$^{\Delta Syn1}$ HFD).

In the OGTT of the whole group, glucose resulted in the anticipated initial increase and subsequent decrease in blood glucose (time χ^2-Wald 1683.377 and 695.324, $p<0.05$, for males and females, respectively). In males, the HFD resulted in more elevated glucose in both genotypes (diet χ^2-Wald 89.286, $p<0.05$). In females, the same was true, but was found after decomposing the interaction of both factors (diet*genotype χ^2-Wald 4.966, $p<0.05$, sequential Bonferroni pair-wise comparisons floxed control vs floxed HFD, *Il6*$^{\Delta Syn1}$ control vs *Il6*$^{\Delta Syn1}$ HFD).

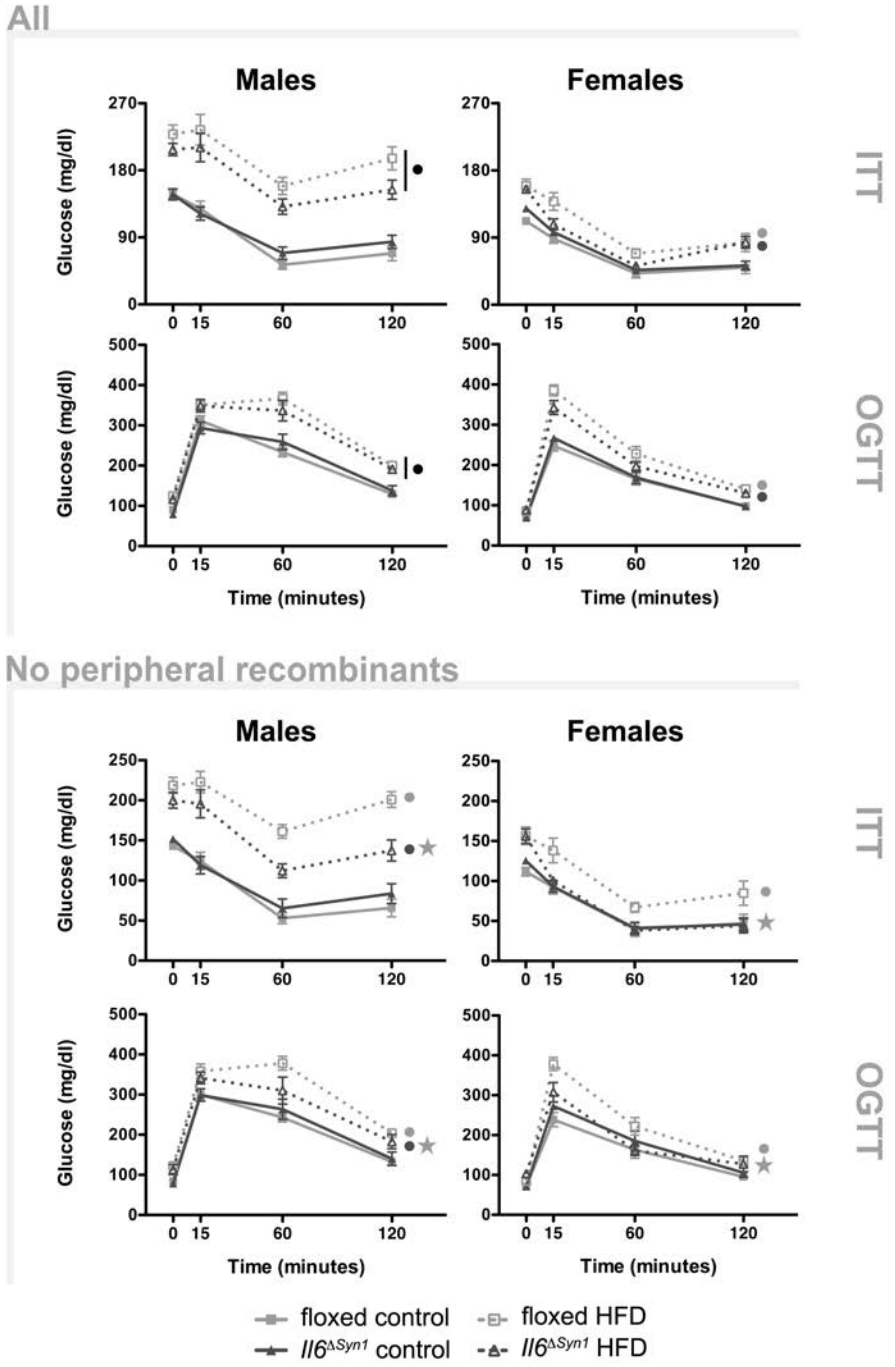

Figure 42. ITT and OGTT after 10-11 weeks of diet. When all animals are considered, just HFD has an effect on blood glucose levels after administration of either insulin or glucose itself. However, removal of peripheral recombinants results in an apparent difference between floxed and *Il6*$^{\Delta Syn1}$ mice, the latter being more resistant to the effects of the HFD. • $p<0.05$ (diet). Significant sequential Bonferroni pair-wise comparisons ★ vs floxed (same diet), • vs floxed control diet, • vs *Il6*$^{\Delta Syn1}$ control diet. N=8-12 (all), n=2-7 (no peripheral recombinants).

When mice with peripheral recombination were removed, both males and females showed an interaction between diet and genotype. In males, HFD increased glucose in each genotype, and HFD-fed floxed and *Il6*$^{\Delta Syn1}$ were significantly different from each other (diet*genotype χ^2-Wald 4.284, $p<0.05$, sequential Bonferroni pair-wise comparisons floxed control vs floxed HFD, *Il6*$^{\Delta Syn1}$ control vs *Il6*$^{\Delta Syn1}$ HFD, floxed HFD vs *Il6*$^{\Delta Syn1}$ HFD). In females, however, only floxed mice had increased glucose with the HFD, which was significantly higher than that of HFD *Il6*$^{\Delta Syn1}$ (diet*genotype χ^2-Wald 8.736, $p<0.05$, sequential Bonferroni pair-wise comparisons floxed control vs floxed HFD, floxed HFD vs *Il6*$^{\Delta Syn1}$ HFD).

5.2.2.5.5 Tissue weight

5.2.2.5.5.1 Absolute weight

Taking all animals into account, liver weight presented an interaction between genotype and diet in both sexes (Figure 43). In general, the differences lay in HFD-fed wt and floxed mice compared to the respective control diet group, as well as between floxed and *Il6*$^{\Delta Syn1}$ with the HFD. In addition, male *Il6*$^{\Delta Syn1}$ on a HFD also had a greater liver weight than controls, and were also significantly different from wt on the HFD (diet*genotype χ^2-Wald 8.118 and 16.472, $p<0.05$, for males and females, respectively; sequential Bonferroni pair-wise comparisons wt control vs wt HFD, floxed control vs floxed HFD, *Il6*$^{\Delta Syn1}$ control vs *Il6*$^{\Delta Syn1}$ HFD (only males), wt HFD vs *Il6*$^{\Delta Syn1}$ HFD (only males), floxed HFD vs *Il6*$^{\Delta Syn1}$ HFD).

The subcutaneous WAT depot showed the same patterns in males and females, with an interaction of diet and genotype. HFD increased the depots in all three genotypes, and within the HFD, *Il6*$^{\Delta Syn1}$ differed from both wt and floxed mice (diet*genotype χ^2-Wald 16.511 and 15.283, $p<0.05$, for males and females, respectively; sequential Bonferroni pair-wise comparisons wt control vs wt HFD,

floxed control vs floxed HFD, *Il6*$^{\Delta Syn1}$ control vs *Il6*$^{\Delta Syn1}$ HFD, wt HFD vs *Il6*$^{\Delta Syn1}$ HFD, floxed HFD vs *Il6*$^{\Delta Syn1}$ HFD).

The gonadal WAT depot showed similar differences in females to the subcutaneous one. The interaction between diet and genotype manifested in differences due to diet in the three genotypes. But with the HFD, *Il6*$^{\Delta Syn1}$ were only significantly different to floxed mice (diet*genotype χ^2-Wald 12.003, $p<0.05$; sequential Bonferroni pair-wise comparisons wt control vs wt HFD, floxed control vs floxed HFD, *Il6*$^{\Delta Syn1}$ control vs *Il6*$^{\Delta Syn1}$ HFD, floxed HFD vs *Il6*$^{\Delta Syn1}$ HFD). In males, only an effect of diet was detected (diet χ^2-Wald 189.414, $p<0.05$).

Removing peripheral recombinants resulted in results with some notable differences. Liver weight in males had an interaction of both factors again, even though this time HFD only increased tissue weight in wt and floxed mice, and *Il6*$^{\Delta Syn1}$ on the HFD only had significantly lower weight than wt (diet*genotype χ^2-Wald 6.752, $p<0.05$; sequential Bonferroni pair-wise comparisons wt control vs wt HFD, floxed control vs floxed HFD, wt HFD vs *Il6*$^{\Delta Syn1}$ HFD). Females had a general increase of liver weight due to the diet (diet χ^2-Wald 4.945, $p<0.05$).

Subcutaneous WAT tissue showed an interaction of diet and genotype in both males and females. In both sexes, HFD increased its weight in wt and floxed mice, but failed to do as much in HFD-fed *Il6*$^{\Delta Syn1}$ when compared to floxed mice. In males, HFD also increased the weight of the depot in the *Il6*$^{\Delta Syn1}$ group. And in females, HFD-fed *Il6*$^{\Delta Syn1}$ were also significantly different from HFD-fed floxed subjects (diet*genotype χ^2-Wald 10.656 and 10.72, $p<0.05$, for males and females, respectively; sequential Bonferroni pair-wise comparisons wt control vs wt HFD, floxed control vs floxed HFD, *Il6*$^{\Delta Syn1}$ control vs *Il6*$^{\Delta Syn1}$ HFD (only males), wt HFD vs *Il6*$^{\Delta Syn1}$ HFD (only females), floxed HFD vs *Il6*$^{\Delta Syn1}$ HFD).

Finally, the gonadal WAT depot increased only because of diet in males (diet χ^2-Wald 159.255, $p<0.05$), while in females, the interaction of the two factors showed an effect of diet only in wt and floxed, both of them being

different from *Il6*$^{\Delta Syn1}$ when fed a HFD (diet*genotype χ^2-Wald 14.789, $p<0.05$; sequential Bonferroni pair-wise comparisons wt control vs wt HFD, floxed control vs floxed HFD, wt HFD vs *Il6*$^{\Delta Syn1}$ HFD, floxed HFD vs *Il6*$^{\Delta Syn1}$ HFD).

5.2.2.5.5.2 Relative weight

Correction of tissue weights for body weight was carried out to account for the variations in body weight of the different experimental groups. Figure 44 shows the different tissues for the whole group and the one without peripheral recombinants, and Table 20 summarizes statistical results.

Relativization of liver weight meant the HFD had no effect in males but that its percentage decreased in females.

Regarding fat pads, HFD increased their relative weight. Female *Il6*$^{\Delta Syn1}$ fed the HFD had smaller WAT Sc and Gn fat pads than floxed littermates, while in males this was only true for the WAT Sc.

Removal of peripheral recombinants showed very similar effects, with the notable differences of a higher relative weight of WAT Gn in male *Il6*$^{\Delta Syn1}$ mice and a lack of HFD-related increase in WAT Gn in *Il6*$^{\Delta Syn1}$ females.

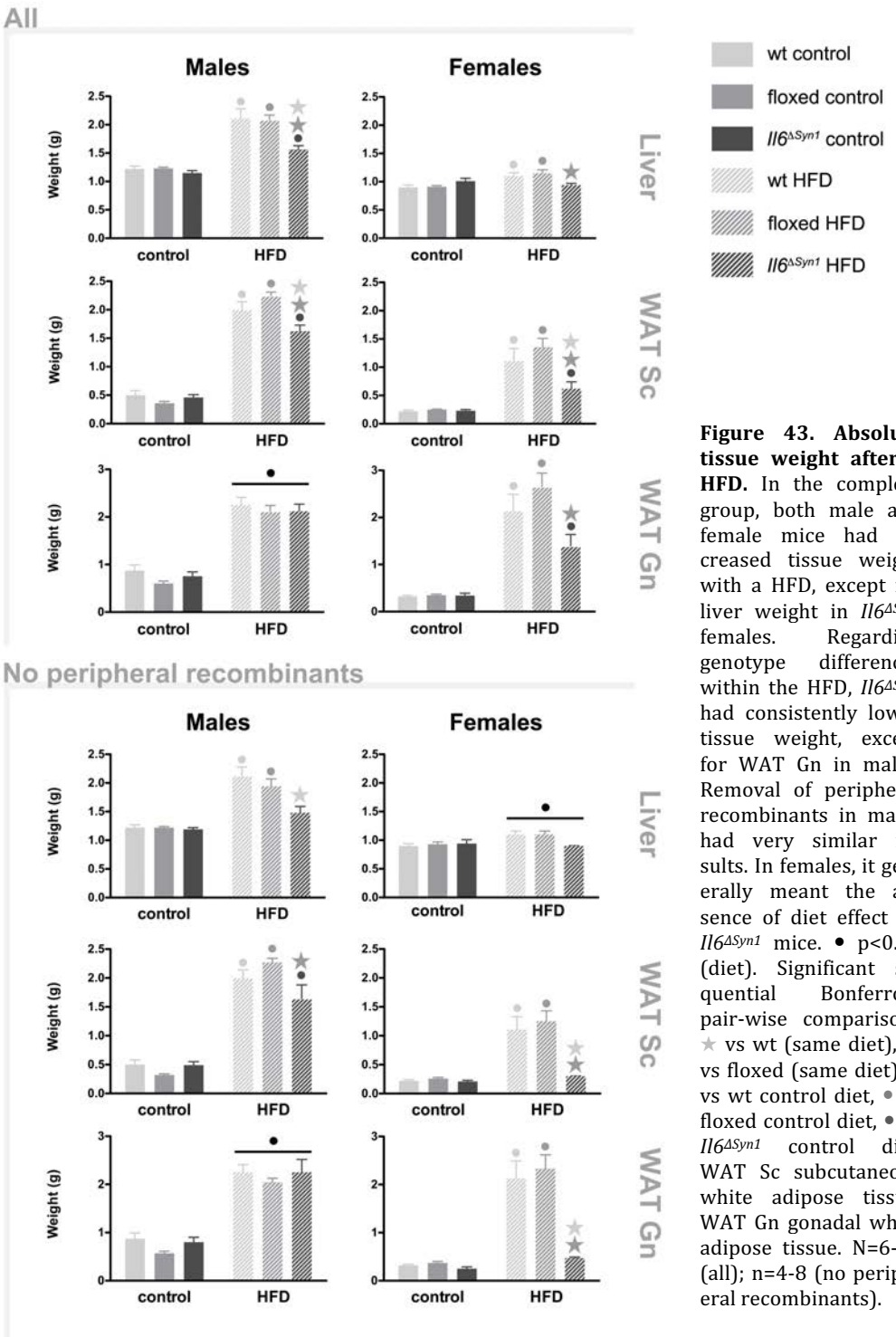

Figure 43. Absolute tissue weight after a HFD. In the complete group, both male and female mice had increased tissue weight with a HFD, except for liver weight in *Il6*$^{\Delta Syn1}$ females. Regarding genotype differences within the HFD, *Il6*$^{\Delta Syn1}$ had consistently lower tissue weight, except for WAT Gn in males. Removal of peripheral recombinants in males had very similar results. In females, it generally meant the absence of diet effect on *Il6*$^{\Delta Syn1}$ mice. • p<0.05 (diet). Significant sequential Bonferroni pair-wise comparisons ★ vs wt (same diet), ★ vs floxed (same diet), • vs wt control diet, • vs floxed control diet, • vs *Il6*$^{\Delta Syn1}$ control diet. WAT Sc subcutaneous white adipose tissue, WAT Gn gonadal white adipose tissue. N=6-12 (all); n=4-8 (no peripheral recombinants).

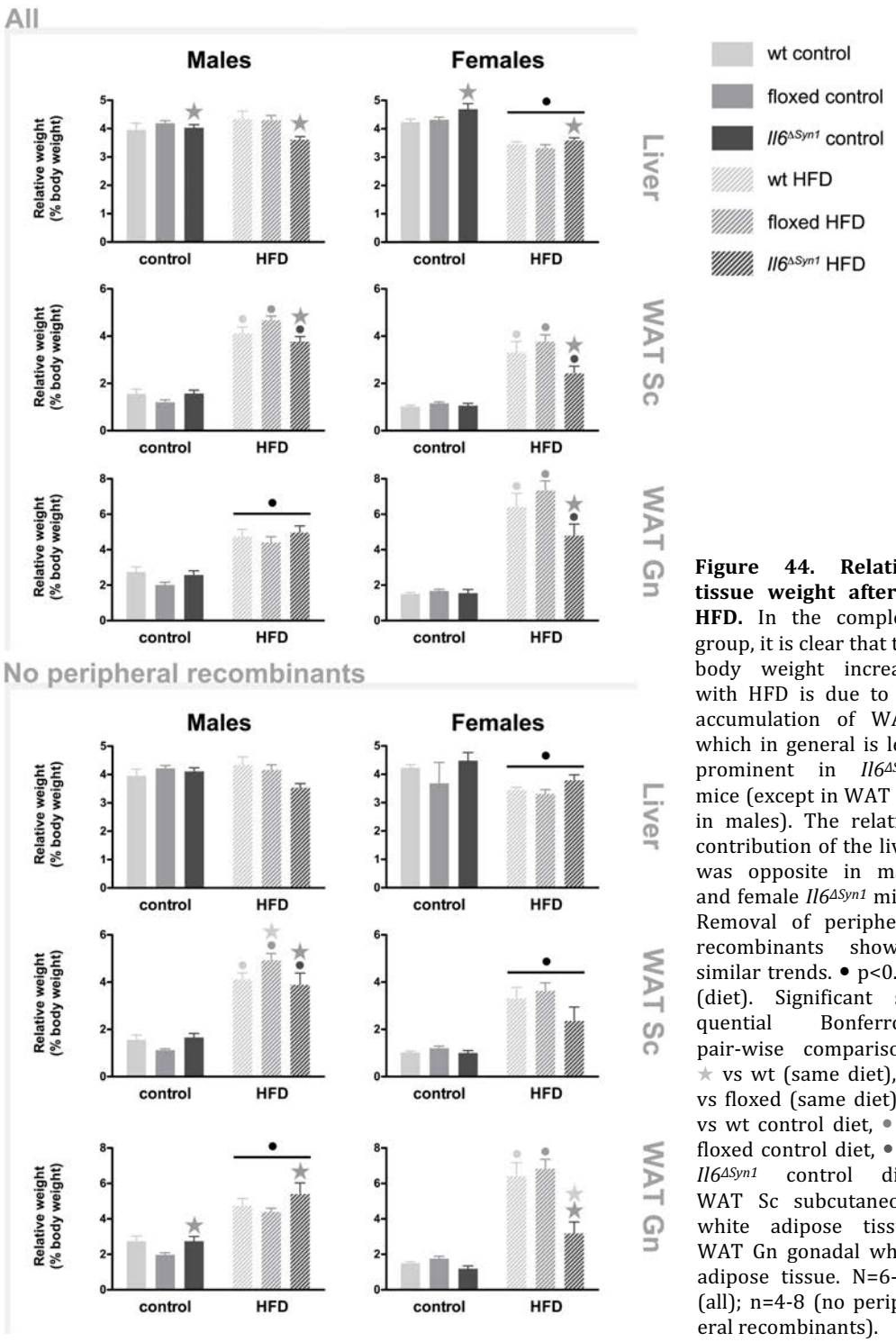

Figure 44. Relative tissue weight after a HFD. In the complete group, it is clear that the body weight increase with HFD is due to an accumulation of WAT, which in general is less prominent in *Il6*$^{\Delta Syn1}$ mice (except in WAT Gn in males). The relative contribution of the liver was opposite in male and female *Il6*$^{\Delta Syn1}$ mice. Removal of peripheral recombinants showed similar trends. • $p<0.05$ (diet). Significant sequential Bonferroni pair-wise comparisons ★ vs wt (same diet), ★ vs floxed (same diet), • vs wt control diet, • vs floxed control diet, • vs *Il6*$^{\Delta Syn1}$ control diet. WAT Sc subcutaneous white adipose tissue, WAT Gn gonadal white adipose tissue. N=6-12 (all); n=4-8 (no peripheral recombinants).

Table 20. Statistical significances of relative tissue weights. Only significant main effects or interactions are shown. In parenthesis: significant sequential Bonferroni pair-wise comparisons.

	ALL		NO PERIPHERAL RECOMBINANTS	
	Males	**Females**	**Males**	**Females**
Liver	**genotype** χ^2-Wald 7.788, p<0.05 *(floxed vs Il6$^{\Delta Syn1}$)*	**genotype** χ^2-Wald 7.956, p<0.05 *(floxed vs Il6$^{\Delta Syn1}$)* **diet** χ^2-Wald 72.316, p<0.05	—	**diet** χ^2-Wald 39.62, p<0.05
WAT Sc	**genotype*diet** χ^2-Wald 13.961, p<0.05 *(wt control vs wt HFD, floxed control vs floxed HFD, Il6$^{\Delta Syn1}$ control vs Il6$^{\Delta Syn1}$ HFD, floxed HFD vs Il6$^{\Delta Syn1}$ HFD)*	**genotype*diet** χ^2-Wald 9.079, p<0.05 *(wt control vs wt HFD, floxed control vs floxed HFD, Il6$^{\Delta Syn1}$ control vs Il6$^{\Delta Syn1}$ HFD, floxed HFD vs Il6$^{\Delta Syn1}$ HFD)*	**genotype*diet** χ^2-Wald 14.666, p<0.05 *(wt control vs wt HFD, floxed control vs floxed HFD, Il6$^{\Delta Syn1}$ control vs Il6$^{\Delta Syn1}$ HFD, wt HFD vs floxed HFD, floxed HFD vs Il6$^{\Delta Syn1}$ HFD)*	**diet** χ^2-Wald 73.666, p<0.05
WAT Gn	**diet** χ^2-Wald 79.605, p<0.05	**genotype*diet** χ^2-Wald 8.882, p<0.05 *(wt control vs wt HFD, floxed control vs floxed HFD, Il6$^{\Delta Syn1}$ control vs Il6$^{\Delta Syn1}$ HFD, floxed HFD vs Il6$^{\Delta Syn1}$ HFD)*	**genotype** χ^2-Wald 7.25, p<0.05 *(floxed vs Il6$^{\Delta Syn1}$)* **diet** χ^2-Wald 63.754, p<0.05	**genotype*diet** χ^2-Wald 15.667, p<0.05 *(wt control vs wt HFD, floxed control vs floxed HFD, wt HFD vs Il6$^{\Delta Syn1}$ HFD, floxed HFD vs Il6$^{\Delta Syn1}$ HFD)*

5.2.2.5.6 qPCR

5.2.2.5.6.1 Hypothalamic neuropeptides

Figure 45 shows the expression, assessed by qPCR, of several hypothalamic neuropeptides.

Agrp decreased significantly with the HFD in females (diet χ^2-Wald 8.092, p<0.05) and was increased in *Il6$^{\Delta Syn1}$* compared to wt (genotype χ^2-Wald 8.826, p<0.05; sequential Bonferroni pair-wise comparisons wt vs *Il6$^{\Delta Syn1}$*). In males, the decomposition of the interaction detected between diet and genotype drew no significant pair-wise comparisons (diet*genotype χ^2-Wald 8.546, p<0.05).

Crh, *Pmch* and *Pomc* all increased with HFD in males (diet χ^2-Wald 5.87, 13.649 and 19.731, respectively, p<0.05), the latter being also increased in females (diet χ^2-Wald 33.822, p<0.05).

Hcrt was unaffected by either diet or genotype.

When removing peripheral recombinants, the same differences were observed, with the addition of a higher *Agrp* expression in female *Il6*$^{\Delta Syn1}$ compared to floxed (genotype χ^2-Wald 11.838, $p<0.05$; sequential Bonferroni pair-wise comparisons wt vs *Il6*$^{\Delta Syn1}$, floxed vs *Il6*$^{\Delta Syn1}$).

5.2.2.5.6.2 Inflammatory markers

Some inflammatory markers were evaluated in the hypothalamus of these animals *Gfap* for astrogliosis, *Casp3* for apoptosis, *Socs3* for IL-6 negative feedback, and *Mac1* as a microglia/macrophage marker (Figure 46).

In the complete group, HFD increased *Gfap*, *Casp3*, *Socs3* and *Mac1* expression in males (diet χ^2-Wald 8.036, 10.646, 69.442 and 5.35, $p<0.05$).

In females, *Socs3* showed an interaction between diet and genotype, which manifested in an effect of HFD in wt and floxed mice.

Il6 remained unaltered by diet, but had a genotype effect in both sexes, particularly between wt and floxed or *Il6*$^{\Delta Syn1}$ (diet*genotype χ^2-Wald 20.057 and 19.437, for males and females, respectively, $p<0.05$; sequential Bonferroni pair-wise comparisons wt vs floxed, wt vs *Il6*$^{\Delta Syn1}$).

In the group without peripheral recombinants, males still showed an increase of *Gfap* and *Socs3* with HFD (diet χ^2-Wald 9.46 and 44.513, respectively, $p<0.05$). *Socs3* was also significantly lower in floxed and *Il6*$^{\Delta Syn1}$ males (genotype χ^2-Wald 16.572, $p<0.05$; sequential Bonferroni pair-wise comparisons wt vs floxed, wt vs *Il6*$^{\Delta Syn1}$). In females, the decomposition of the interaction found in *Casp3* showed that *Il6*$^{\Delta Syn1}$ had higher expression than wt in the control diet (diet*genotype χ^2-Wald 7.097, $p<0.05$; sequential Bonferroni pair-wise comparisons wt control vs *Il6*$^{\Delta Syn1}$ control).

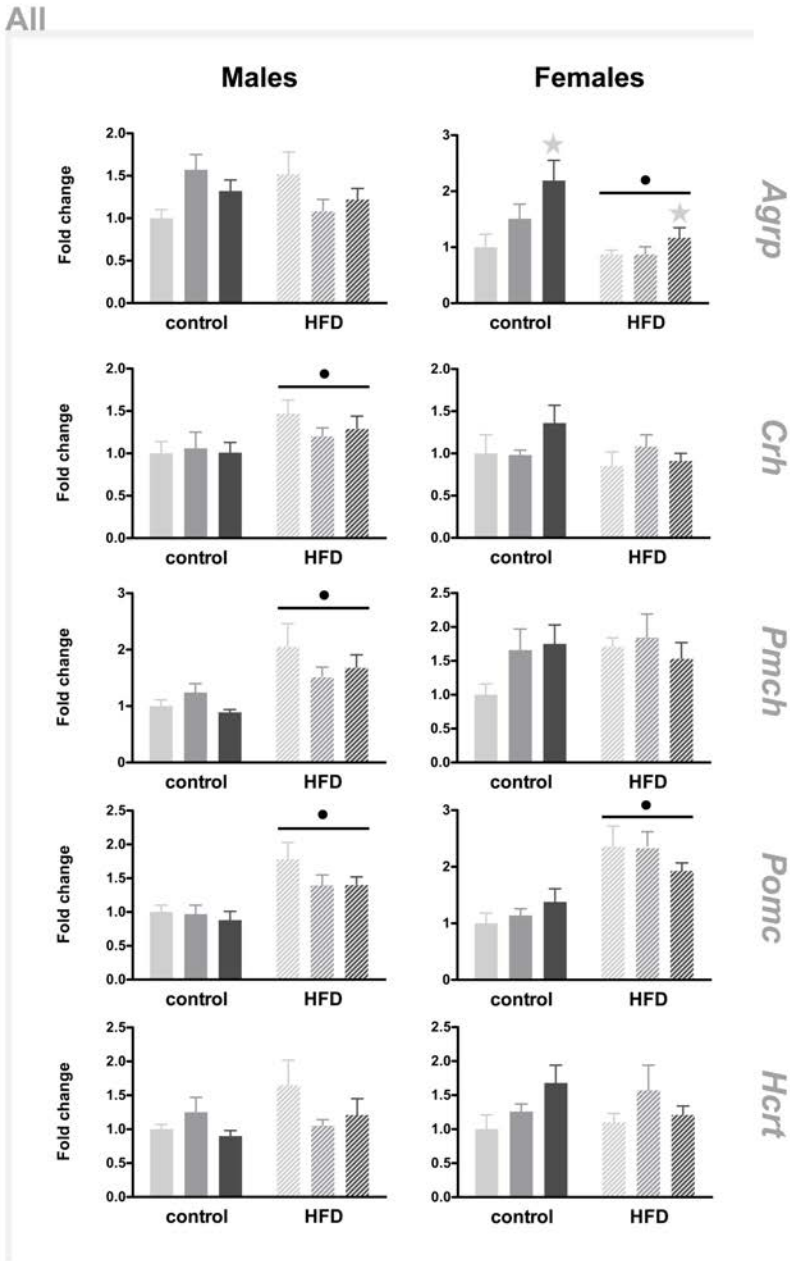

Figure 45. Expression of hypothalamic neuropeptides (qPCR) after 12 weeks of diet. HFD lowered *Agrp* and increased *Pomc* in females, while it increased *Crh*, *Pmch* and *Pomc* expression in males. • $p<0.05$ (diet). Significant sequential Bonferroni pair-wise comparisons ★ vs wt (same diet). N=6-12 (all) *(continues on the next page).*

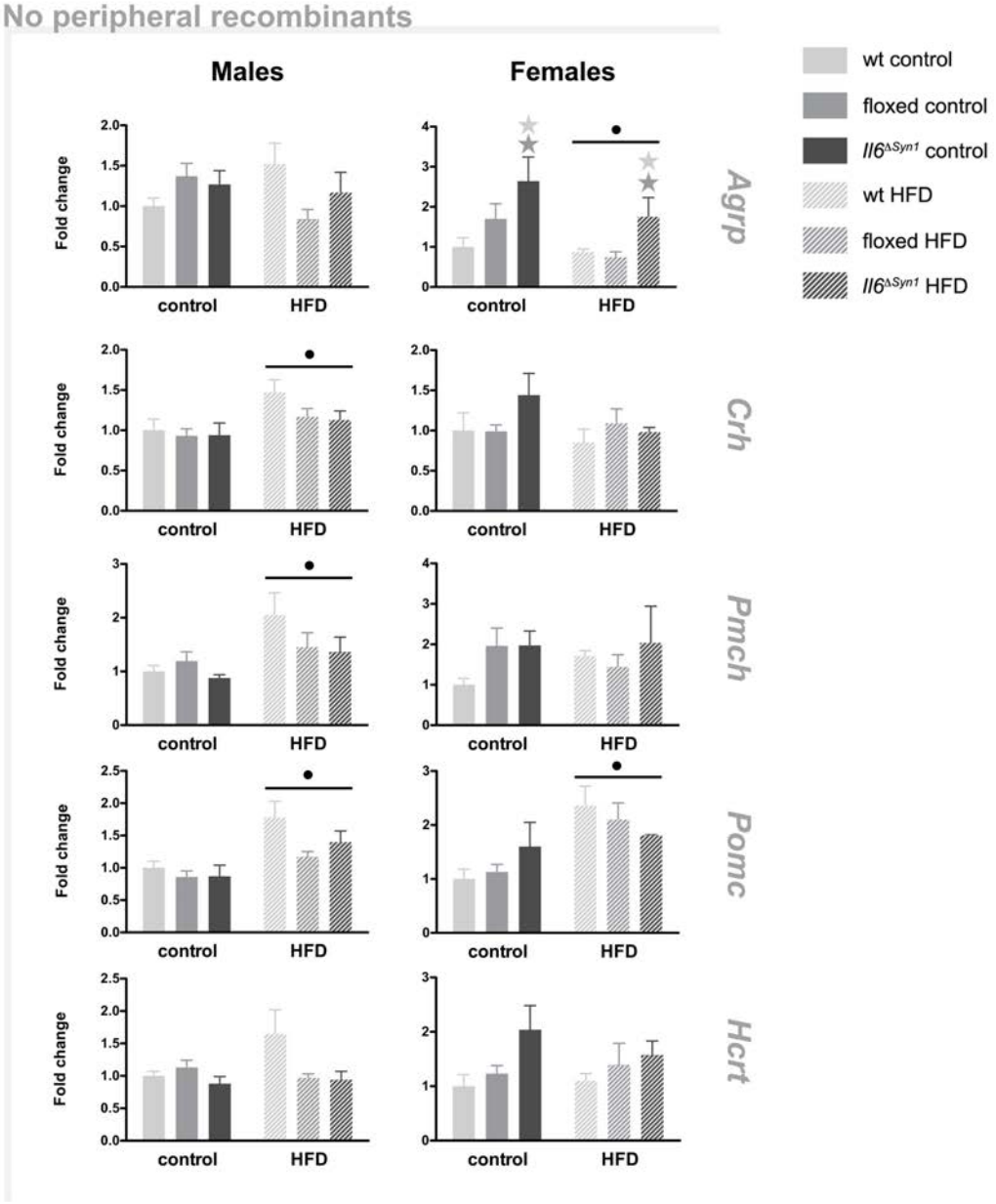

Figure 45 (continued). Expression of hypothalamic neuropeptides (qPCR) after 12 weeks of diet. Differences between *Il6*$^{\Delta Syn1}$ and wt and floxed were only seen in *Agrp* in females, where that genotype had higher expression than the other two, in both diets. • $p<0.05$ (diet). Significant sequential Bonferroni pair-wise comparisons ★ vs wt (same diet), ★ vs floxed (same diet). N=2-10 (no peripheral recombinants).

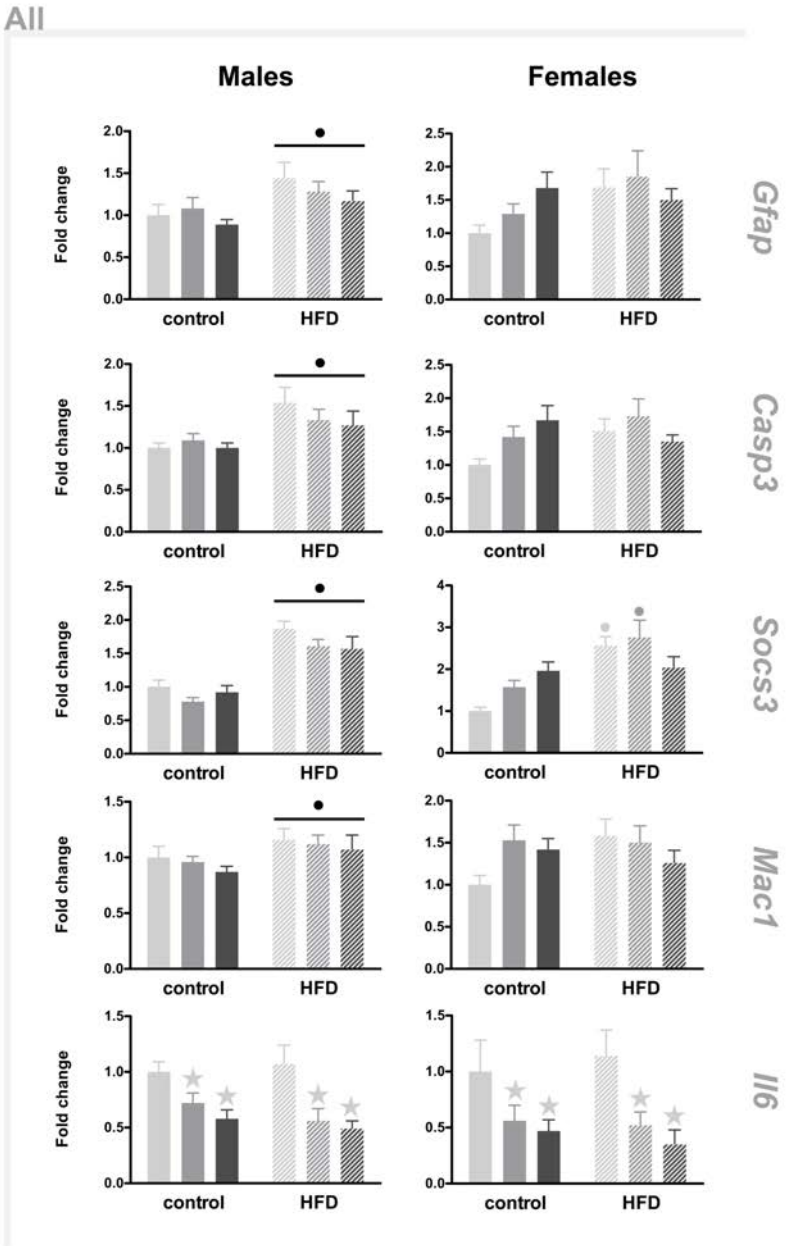

Figure 46. Expression of inflammatory markers in the hypothalamus (qPCR) after 12 weeks of diet. In the complete group HFD increased the expression of *Gfap*, *Casp3*, *Socs3* and *Mac1* in males. In females, *Socs3* was only increased in wt and floxed mice due to diet. Il6 was decreased in floxed and *Il6*$^{\Delta Syn1}$. • p<0.05 (diet). Sequential Bonferroni pair-wise comparisons ★ p<0.05 vs wt (same diet). N=6-12 (all) *(continues on the next page)*.

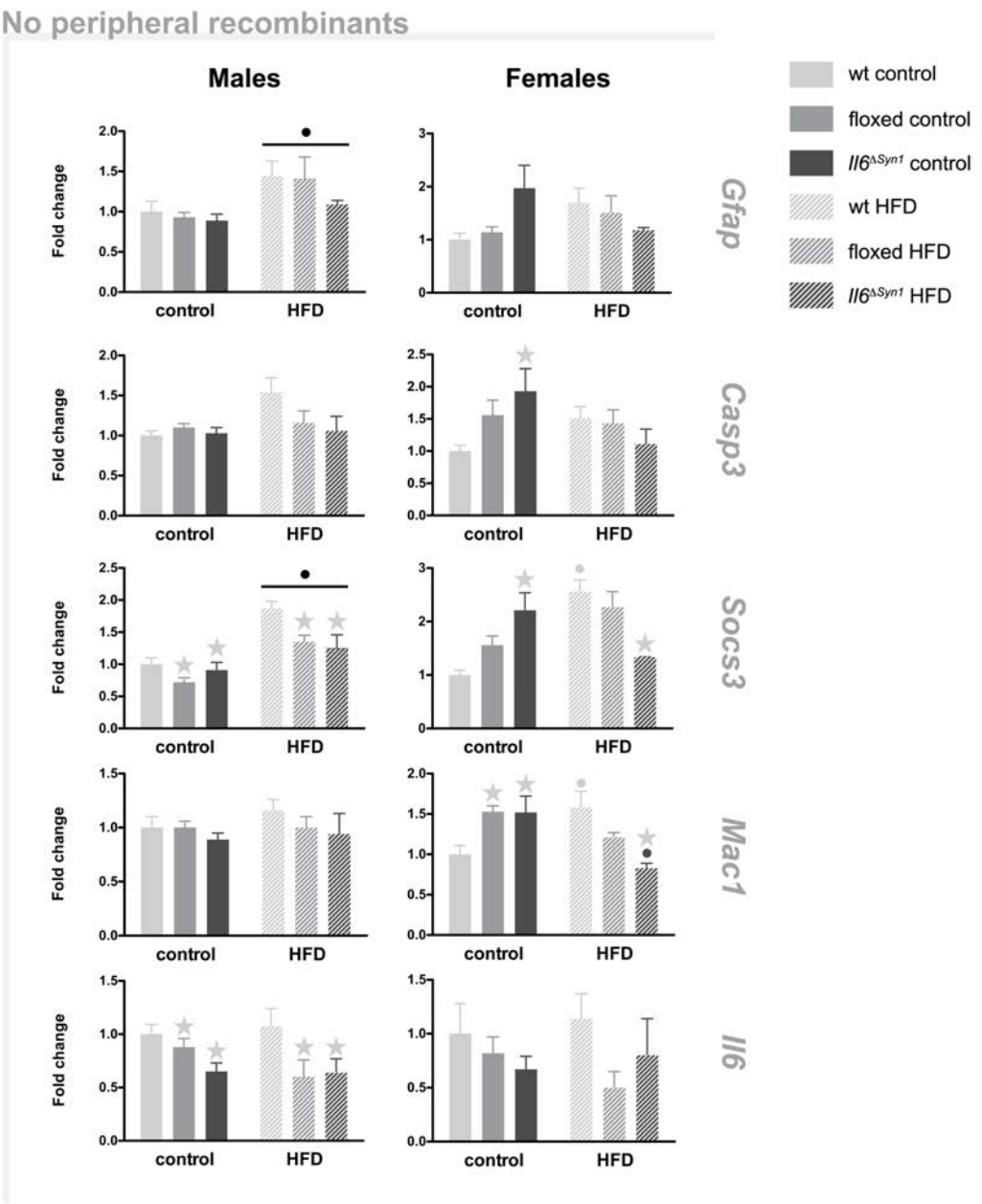

Figure 46 (continued). Expression of inflammatory markers in the hypothalamus (qPCR) after 12 weeks of diet. Exclusion of peripheral recombinants maintained the diet effect in *Gfap* and *Socs3* for males. The latter was decreased in floxed and *Il6*$^{\Delta Syn1}$, as was *Il6*. Female *Il6*$^{\Delta Syn1}$ had increased *Casp3*, *Socs3* and *Mac1* compared to wt on the control diet, but when fed a HFD, they had reduced *Socs3* and *Mac1* expression. • $p<0.05$ (diet). Sequential Bonferroni pair-wise comparisons ◦ vs wt control diet, ★ vs wt (same diet). N=2-10 (no peripheral recombinants).

Another interaction was seen for *Socs3*, which was increased with diet in wt females, in *Il6*$^{\Delta Syn1}$ compared to wt on the control diet, but decreased in the HFD in tha same genotype (diet*genotype χ^2-Wald 20.607, $p<0.05$; sequential Bonferroni pair-wise comparisons wt control vs wt HFD, wt control vs *Il6*$^{\Delta Syn1}$ control, wt HFD vs *Il6*$^{\Delta Syn1}$ HFD).

A similar pattern was seen for *Mac1*, with a significant interaction of diet and genotype, which in this case meant an increase in wt and decrease in *Il6*$^{\Delta Syn1}$ with HFD, an increase in floxed and *Il6*$^{\Delta Syn1}$ controls compared to wt, and significantly lower expression in HFD-fed *Il6*$^{\Delta Syn1}$ compared to wt on the same diet (diet*genotype χ^2-Wald 22.061, $p<0.05$; sequential Bonferroni pair-wise comparisons wt control vs wt HFD, *Il6*$^{\Delta Syn1}$ control vs *Il6*$^{\Delta Syn1}$ HFD, wt control vs floxed control, wt control vs *Il6*$^{\Delta Syn1}$ control, wt HFD vs *Il6*$^{\Delta Syn1}$ HFD).

Il6 only presented an effect of genotype in males, where wt had higher expression than both floxed and *Il6*$^{\Delta Syn1}$ (genotype χ^2-Wald 10.094, $p<0.05$; sequential Bonferroni pair-wise comparisons wt vs floxed, wt vs *Il6*$^{\Delta Syn1}$).

5.2.2.6 Fasting

5.2.2.6.1 Twenty-four hour fast and 4-hour refeeding

Since animals were group-housed no separation concerning peripheral recombination was performed and the data pertains to all animals.

Male *Il6*$^{\Delta Syn1}$ had a cumulative energy intake below floxed mice (genotype χ^2-Wald 4.0, $p<0.05$) (Figure 47), despite having lost a comparable percentage of body weight (Table 21). In females, there was an interaction between genotype and hour post-refeeding, which resulted in a difference between genotypes after 2 hours (hour*genotype χ^2-Wald 9.179, $p<0.05$; sequential Bonferroni pair-wise comparisons 2 hours floxed vs 2 hours *Il6*$^{\Delta Syn1}$). In this case, however, *Il6*$^{\Delta Syn1}$ had

lost significantly more weight than floxed females (t-Student(22) -2-214, p<0.05) (Table 21).

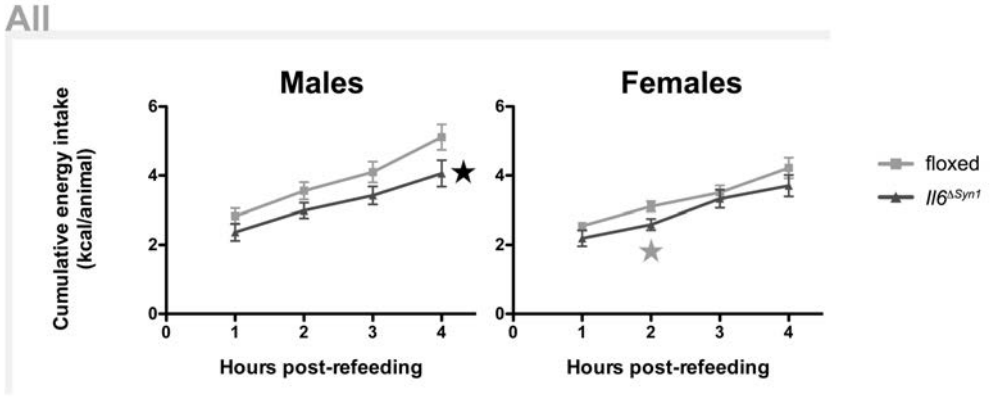

Figure 47. Cumulative energy intake during the 4 hours after reintroduction of the control diet after a 24-hour fast. Animals were group-housed and total intake was divided by the number of animals per cage (n=5-7, cages). In males, *Il6$^{\Delta Syn1}$* ate significantly less than floxed mice during the 4-hours. In females, the difference was less clear. ★ p<0.05 (genotype). Significant sequential Bonferroni pair-wise comparison ★ vs floxed (same time-point).

Table 21. Percentage weight loss and statistical significances after a 24-hour fast. Percentage weight loss was calculated as Δweight*100/(pre-fast weight). Female *Il6$^{\Delta Syn1}$* lost proportionally more weight than floxed littermates. N=10-15.

	ALL			
	Males		Females	
	floxed	*Il6$^{\Delta Syn1}$*	floxed	*Il6$^{\Delta Syn1}$*
% lost	11.9±0.5	12.3±0.7	12.0±0.4	13.6±0.7

5.2.2.6.2 Forty-eight hour fast

In this experiment, peripheral recombination could not be assessed, so the data presented regard the complete group.

5.2.2.6.2.1 Relative body weight loss

The fast caused a significant weight loss (as % of initial weight) in both genotypes (fast*genotype χ^2-Wald 924.341 and 256.506, for males and females, respectively, $p<0.05$) (Figure 48). There was a slight trend for *Il6*$^{\Delta Syn1}$ males to lose more weight when fasted, but it was not significant (genotype χ^2-Wald 3.447, $p=0.063$).

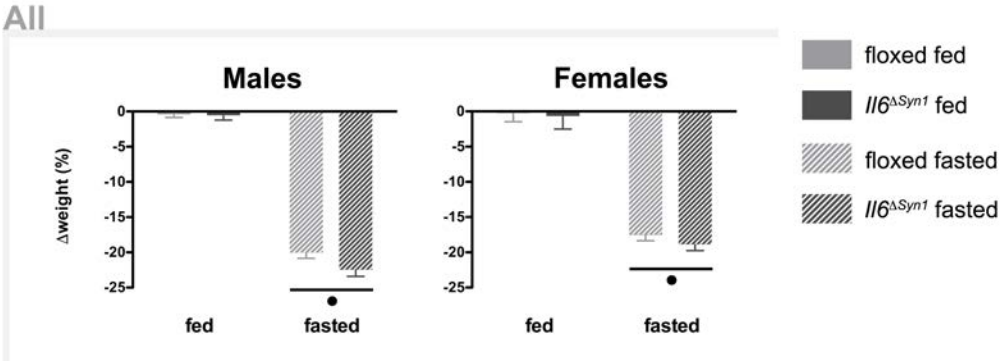

Figure 48. Percentage weight loss after a 48-hour fast. Fasted animals lost significantly more weight, but there were no significant differences between genotypes, just a trend of *Il6*$^{\Delta Syn1}$ males to lose proportionally more weight. • $p<0.05$ (diet). N=5-8.

5.2.2.6.2.2 Hypothalamic neuropeptides

Expression (by qPCR) of *Agrp*, *Crh*, *Pomc*, *Pmch* and *Hcrt* is shown in Figure 49.

Agrp increased significantly in both fasted males and females (fast χ^2-Wald 55.581 and 17.317, for males and females, respectively, $p<0.05$).

Crh expression was raised with fast only in *Il6*$^{\Delta Syn1}$ males (fast*genotype χ^2-Wald 6.923, $p<0.05$; sequential Bonferroni pair-wise comparisons *Il6*$^{\Delta Syn1}$ fed vs *Il6*$^{\Delta Syn1}$ fasted).

There was a significant interaction of fast and genotype in *Pomc* in males (fast*genotype χ^2-Wald 4.77, $p<0.05$), but without any significant pair-wise comparisons. No differences were seen in *Pmch* or *Hcrt*.

5.2.2.6.2.3 Inflammatory markers

Expression (by qPCR) of *Gfap*, *Casp3*, *Socs3*, *Mac1* and *Il6* is shown in Figure 50.

Casp3, *Mac1* and *Il6* expression increased with the 48-hour fast (fast χ^2 Wald 5.794, 12.119 and 8.341, respectively, $p<0.05$). However, no genotype effect was detected in any of the markers.

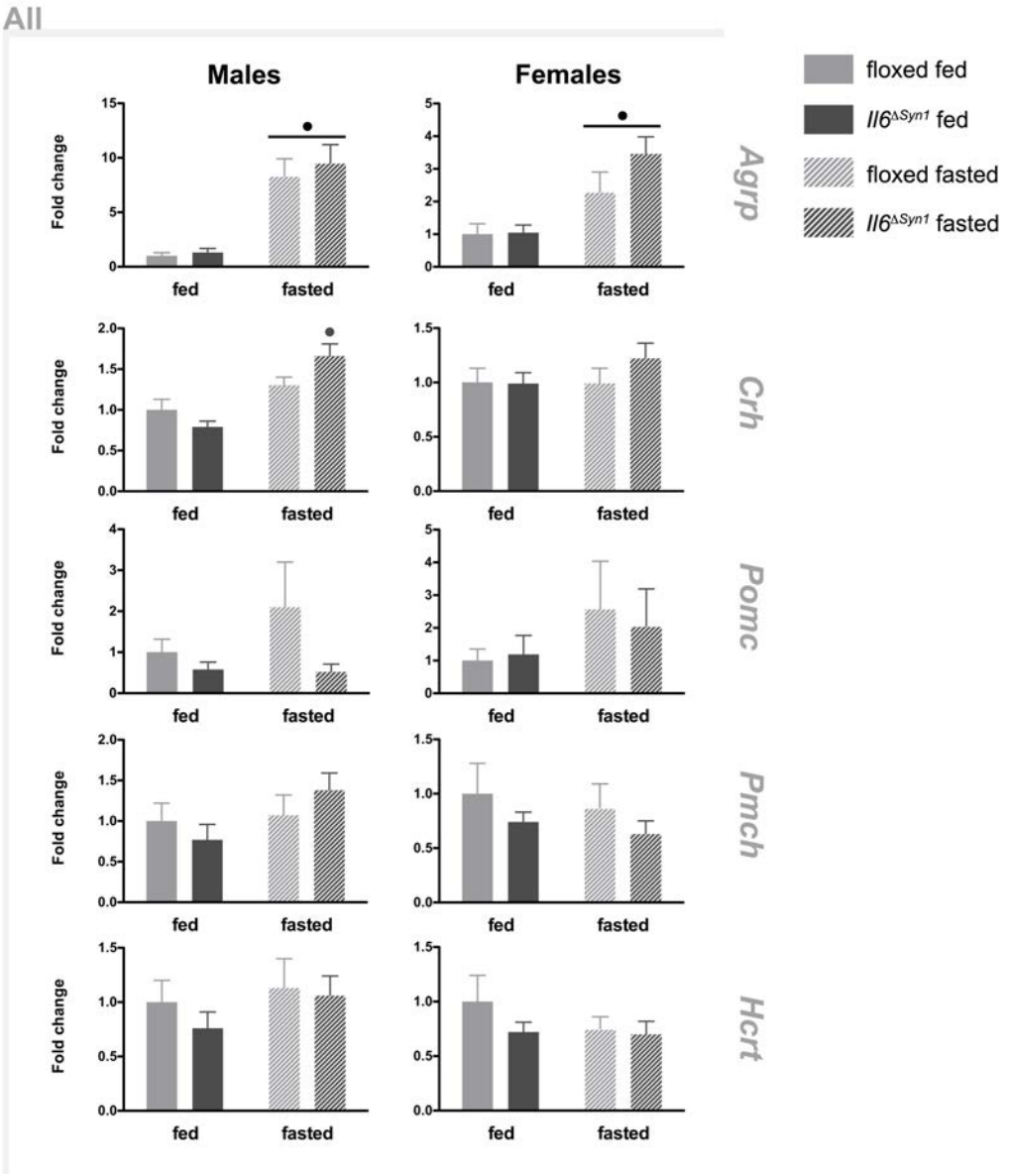

Figure 49. Expression of hypothalamic neuropeptides after a 48-hour fast. *Agrp* increased with fast, and *Crh* was also raised but only in *Il6*$^{\Delta Syn1}$ males. • p<0.05 (diet). N=5-8.

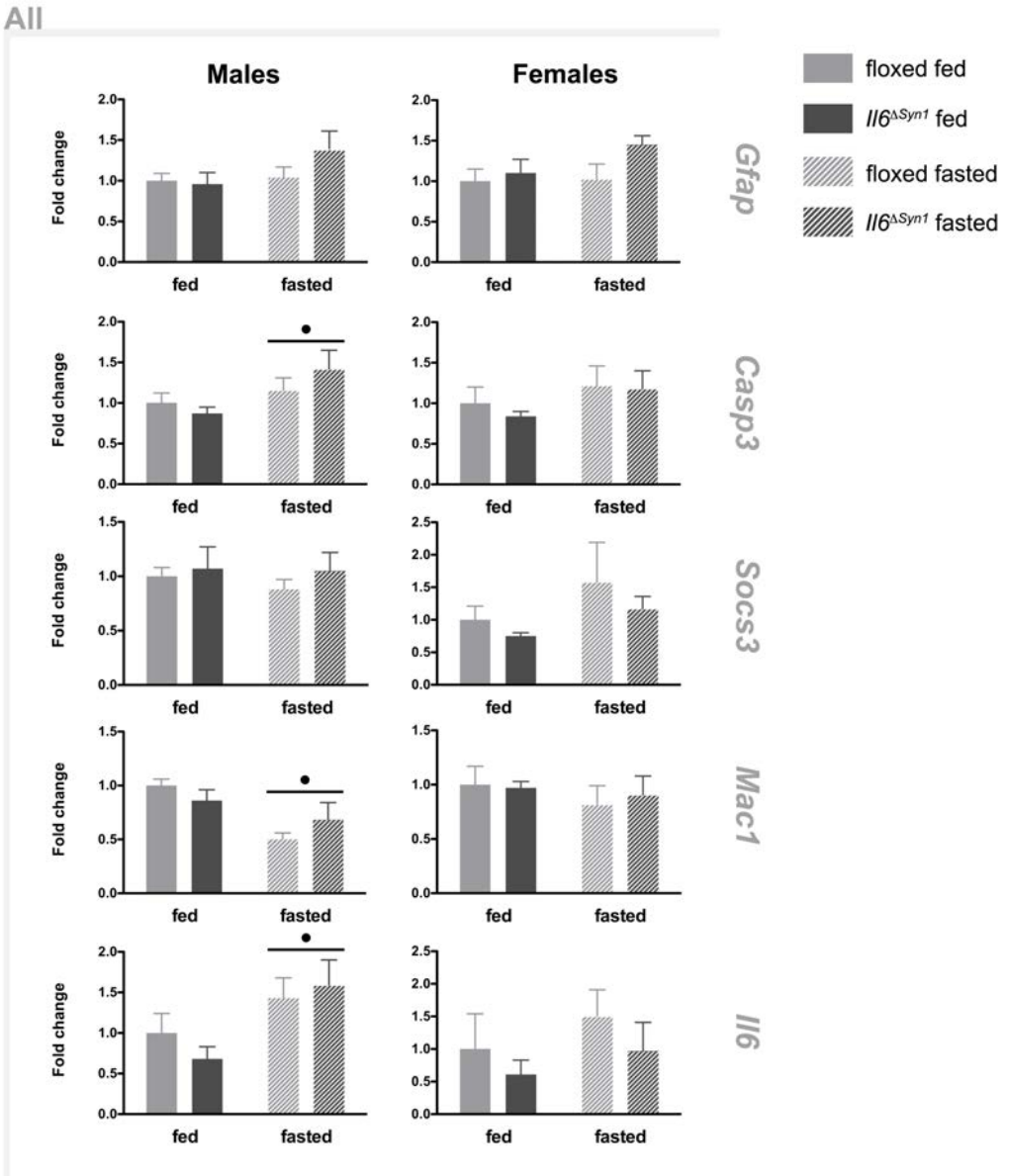

Figure 50. Expression of inflammatory markers in the hypothalamus after a 48-hour fast. *Casp3* and *Il6* were increased, and *Mac1* decreased, in fasted males, regardless of genotype. In females, no significant differences were detected. • $p<0.05$ (diet). N=5-8.

5.2.3 Neuronal IL-6R conditional knock-out

5.2.3.1 Frequencies at weaning

Analysis of frequencies at weaning was done considering the four genotypes obtained in the crossing described in material and methods (see *4.2.6 Conditional Il6ra knockout in neurons*). It must be noted that less animals were generated in this model, because of the preliminary nature of the results. However, no apparent differences between the four genotypes (χ^2 2.315, p>0.05) or the two sexes (χ^2 0.175, p>0.05) were detected (Table 22).

Table 22. Observed and expected frequencies at weaning of each genotype and sex. No significant differences between genotypes or sexes were detected.

	Observed N	Expected N	Residual
Genotype			
wt	36	35.8	0.3
floxed	33	35.8	-2.8
***Il6ra*$^{\Delta Syn1}$**	43	35.8	7.3
***Il6ra*$^{\Delta Syn1/wt}$**	31	35.8	-4.8
Sex			
males	74	71.5	2.5
females	69	71.5	-2.5
Total	**143**		

5.2.3.2 Linear growth

Length of tibia and serum IGF-1 and IGFBP-1 and -3 were evaluated as indicators of linear growth (Figure 51). IGF-1 was measured in saline- and LPS-administered mice.

Measurement of tibial length showed a shorter bone in both male and female *Il6ra*$^{\Delta Syn1}$ mice (t-Student(25) 2.098 and 2.236, for males and females respectively, $p<0.05$). Removing mice with peripheral recombination yielded similar results, but due to the limited sample size the difference was only significant in males (t-Student(5) 2.72, $p<0.05$).

IGFBP-1 and -3 did not vary with genotype in this model.

IGF-1 was decreased by LPS treatment (LPS χ^2 Wald 14.176 and 20.46, for males and females respectively, $p<0.05$). In addition, *Il6ra*$^{\Delta Syn1}$ males had lower levels of IGF-1, regardless of treatment (genotype χ^2 Wald 9.144, $p<0.05$).

5.2.3.3 Energy intake

Basal energy intake was averaged over 4 consecutive days while mice were single-housed and on a control diet (Figure 52).

Male *Il6ra*$^{\Delta Syn1}$ mice had a significantly lower energy intake than floxed littermates (t-Student(26) 2.956, $p<0.05$), while females had comparable values, both before and after removal of peripheral recombinants.

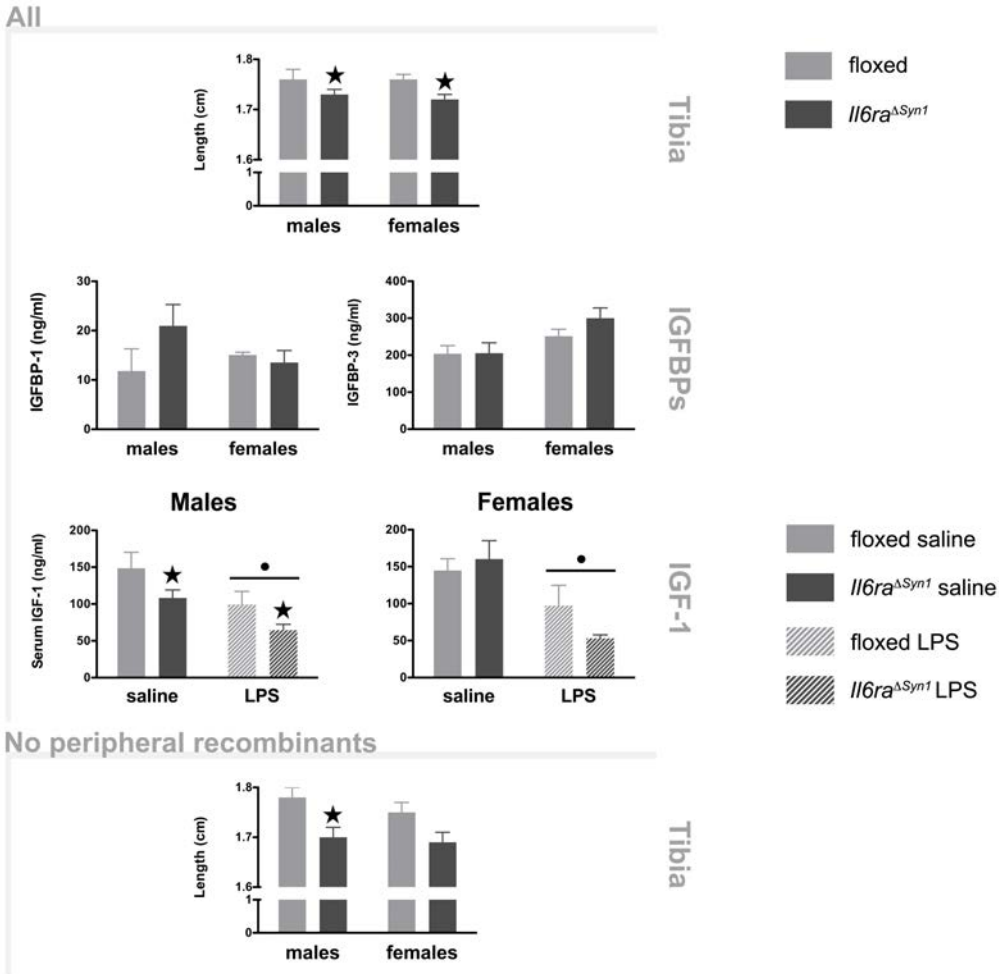

Figure 51. Linear growth-related measures. Tibiae were shorter in *Il6ra*$^{\Delta Syn1}$ compared to floxed mice of both sexes. In males, this also translated to lower IGF-1 serum levels. IGFBP-1 and -3 showed no differences between genotypes. Removal of peripheral recombinants, greatly reduced sample size and only tibiae could be analyzed. In this case, male *Il6ra*$^{\Delta Syn1}$ still show a shorter bone. • p<0.05 (LPS), ★ p<0.05 (genotype). N= 8-20 (all); n=3-5 (no peripheral recombinants).

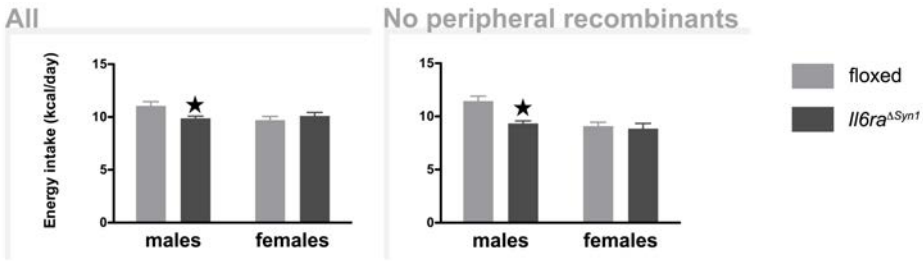

Figure 52. Energy intake with a control diet. Average of 4 consecutive days. Mice were single-housed and measures were performed after acclimation to isolation. *Il6ra*$^{\Delta Syn1}$ male mice have a significantly lower energy intake than floxed littermates. ★ p<0.05. N= 8-20 (all); n=3-6 (no peripheral recombinants).

5.2.3.4 Twenty-four-hour fast and 4-hour refeeding

Single-housed mice on a control diet were fasted for 24-hours and then refed, and their intake monitored every hour for 4 hours (Figure 53).

Relative weight loss was calculated for the fasting period (Table 23). All animals considered, female *Il6ra*$^{\Delta Syn1}$ lost more weight relative to their initial one, than floxed controls (t-Student(29) -2.227, $p<0.05$), while males lost similar percentages. Removal of peripheral recombinants increased variability in females and the significance disappeared.

Table 23. Percentage weight loss and statistical significances after a 24-hour fast. Percentage weight loss was calculated as Δweight*100/(pre-fast weight). Female *Il6ra*$^{\Delta Syn1}$ lost proportionally more weight than floxed littermates. N=8-20 (all); n=3-6 (no peripheral recombinants).

		ALL				NO PERIPHERAL RECOMBINANTS			
		Males		Females		Males		Females	
		floxed	*Il6ra*$^{\Delta Syn1}$	floxed	*Il6ra*$^{\Delta Syn1}$	floxed	*Il6ra*$^{\Delta Syn1}$	floxed	*Il6ra*$^{\Delta Syn1}$
% lost	control	10.4±0.9	12.0±0.5	13.3±0.7	15.5±0.7★	9.6±0.7	9.7±0.7	11.1±0.6	15.3±1.9

In males, no effect of genotype was detected during the 4 hours of refeeding. Conversely, female *Il6ra*$^{\Delta Syn1}$ mice had a lower compensatory energy intake after the fast, which was evident after the third hour (hour*genotype χ^2-Wald 12.381, $p<0.05$; sequential Bonferroni pair-wise comparisons 3 hours floxed vs 3 hours *Il6ra*$^{\Delta Syn1}$, 4 hours floxed vs 4 hours *Il6ra*$^{\Delta Syn1}$).

Analysis of only animals without peripheral recombination yielded similar yet more limited results in females (hour*genotype χ^2-Wald 11.361, $p<0.05$; sequential Bonferroni pair-wise comparisons 3 hours floxed vs 3 hours *Il6ra*$^{\Delta Syn1}$).

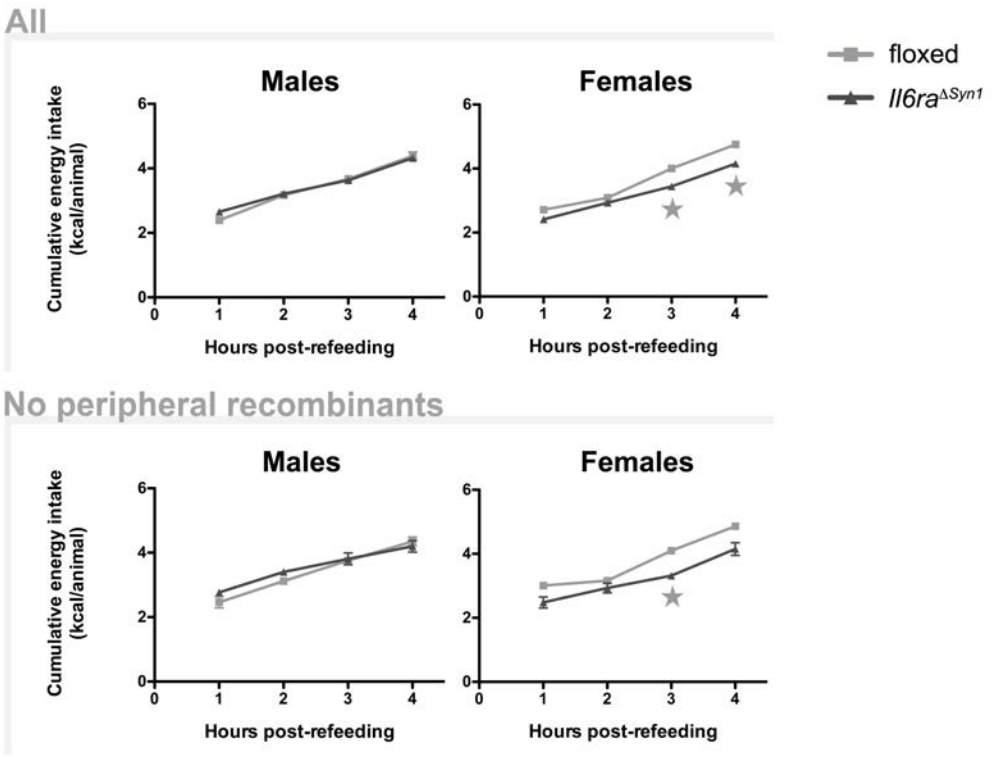

Figure 53. Cumulative energy intake during the 4 hours after reintroduction of the control diet after a 24-hour fast. Animals were single-housed. In females, *Il6ra*$^{\Delta Syn1}$ ate significantly less than floxed mice, evidenced at the latter time points. ★ p<0.05 vs floxed (same time-point). N=8-20 (all); n=3-6 (no peripheral recombinants).

5.2.3.5 LPS administration

LPS was administered intraperitoneally to carry out a qPCR of *Il6ra* and *Il6* in the hypothalamus, to potentially detect differences in expression (Figure 54).

Even though LPS increased the expression of both *Il6ra* (LPS χ^2 Wald 16.156 and 25.68, for males and females respectively, p<0.05) and *Il6* (LPS χ^2 Wald 6.233 and 10.54, for males and females respectively, p<0.05), no reduction due to genotype was observed.

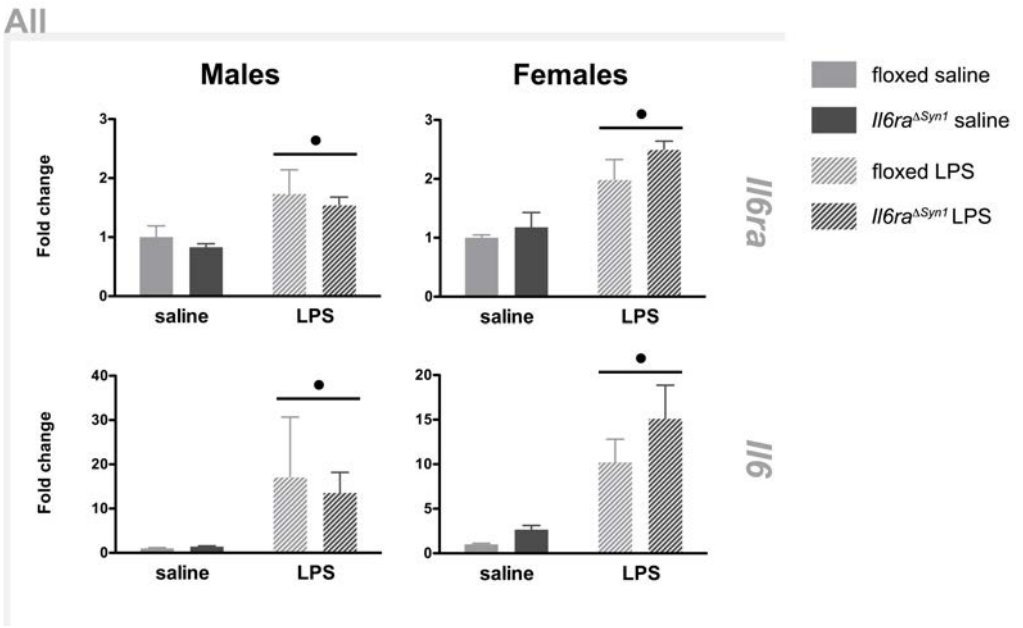

Figure 54. Expression of *Il6ra* and *Il6* in the hypothalamus after LPS administration (qPCR). Intraperitoneal LPS administration increased expression of *Il6ra* and *Il6* regardless of genotype in both sexes. • p<0.05 (LPS). N=8-20.

5.2.4 GFAP-IL6

5.2.4.1 Twenty-four-hour fast and 4-hour refeeding

Individualized mice fed a control diet were fasted for 24-hours and then refed, and their intake monitored every hour for 4 hours (Figure 55).

No differences were seen in either males or females in energy intake during the four hours, even though a slight tendency to a lower intake was present in females (genotype χ^2 Wald 3.42, p=0.064), despite having lost a significantly greater weight (relative to their initial one) than wt (Table 24).

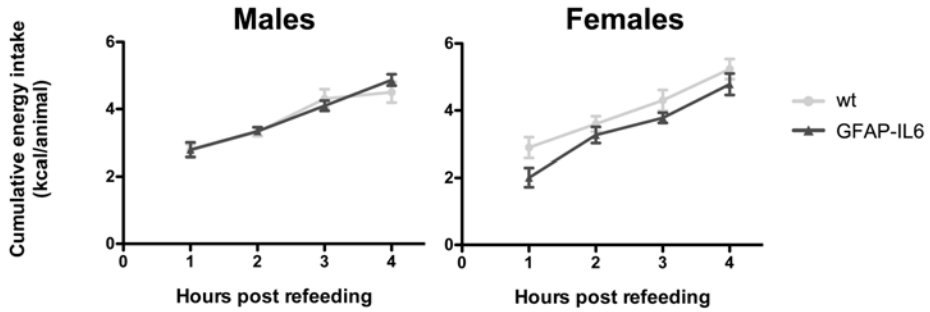

Figure 55. Cumulative energy intake during the 4 hours after reintroduction of the control diet after a 24-hour fast. Animals were single-housed. No differences were observed on either sex in the compensatory intake after the fast. N=8.

Table 24. Percentage weight loss and statistical significances after a 24-hour fast. Percentage weight loss was calculated as Δweight*100/(pre-fast weight). Female GFAP-IL6 mice lost proportionally more weight than wt littermates. N=8.

	Males		Females	
	wt	*GFAP-IL6*	wt	*GFAP-IL6*
% lost	7.1±0.2	7.6±0.4	8.4±0.5	10.0±0.3*

5.2.4.2 High-fat diet

A short-term diet experiment was carried out in this model. Single-housed mice were fed a control or HFD for five days.

5.2.4.2.1 Energy intake and weight gain

Energy intake was higher in mice fed the HFD, but both wt and GFAP-IL6 ingested comparable values (diet χ^2 Wald 119.834 and 121.609, for males and females, respectively, $p<0.05$) (Figure 56, top).

As expected, HFD-fed mice gained more weight than controls (Figure 56, bottom), but no differences due to genotype were observed (diet χ^2 Wald 45.187 and 17.755, for males and females, respectively, $p<0.05$).

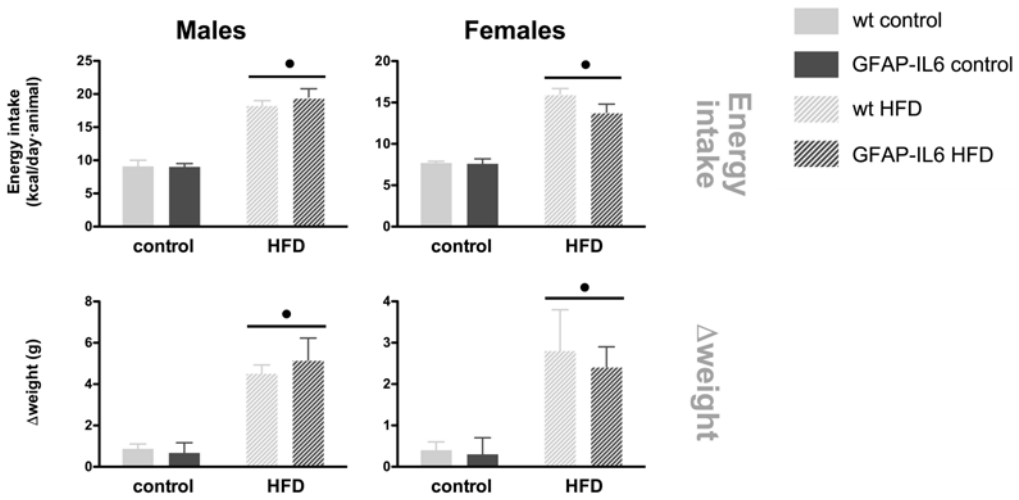

Figure 56. Energy intake and weight gain after 5 days of control or HFD. Animals were single-housed. HFD increased both energy intake and weight gain in males and females, but no differences were observed between wt and GFAP-IL6 mice. • $p<0.05$ (diet). N=8.

5.2.4.2.2 qPCR

Evaluation of expression of several hypothalamic neuropeptides (only performed in males) related to energy balance (Figure 57, left) yielded no significant differences except for a decrease in *Npy* with the HFD (diet χ^2 Wald 5.108, $p<0.05$).

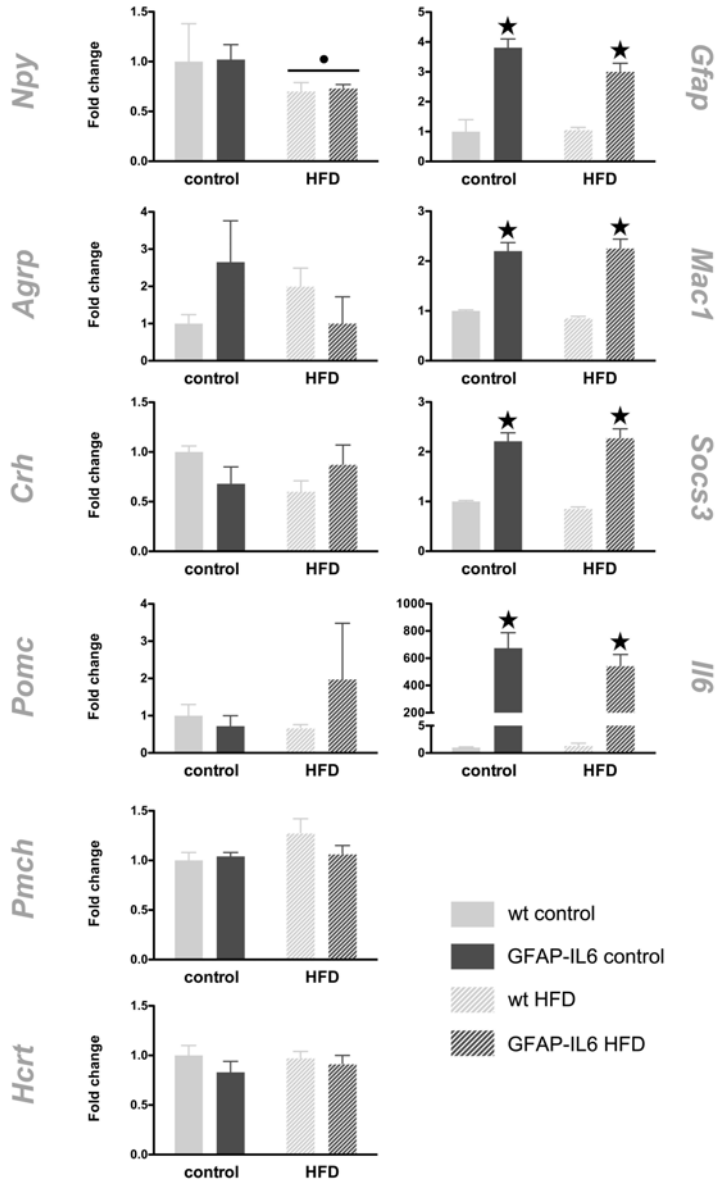

Figure 57. Hypothalamic expression of neuropeptides and inflammatory markers (qPCR). Only males were analyzed because female hypothalami were used for a microarray. *Npy* expression decreased with HFD. All inflammatory markers were elevated in GFAP-IL6 compared to wt mice, but remained unaffected by diet. • $p<0.05$ (diet), ★ $p<0.05$ (genotype). N=8.

Expression of inflammatory markers was also assessed in the hypothalamus (Figure 57, right) and was found to have a clear genotype effect, with all *Gfap*, *Mac1*, *Socs3* and *Il6* being increased in GFAP-IL6 mice (genotype χ^2 Wald 90.854, 84.044, 83.605 and 53.091, respectively, $p<0.05$), but unaltered by HFD.

5.3 Behavior

5.3.1 Neuronal IL-6 conditional knock-out

5.3.1.1 Open field

The analysis of all animals showed a consistent increase in activity, both vertical (rearings) and horizontal (areas crossed), in male *Il6*$^{\Delta Syn1}$ mice. Females exhibited a similar difference regarding rearings and total activity (Figure 58 and Table 25).

Removal of animals with peripheral recombination left the results essentially the same, but the significance of the difference in females and in external and internal activity in males was lost.

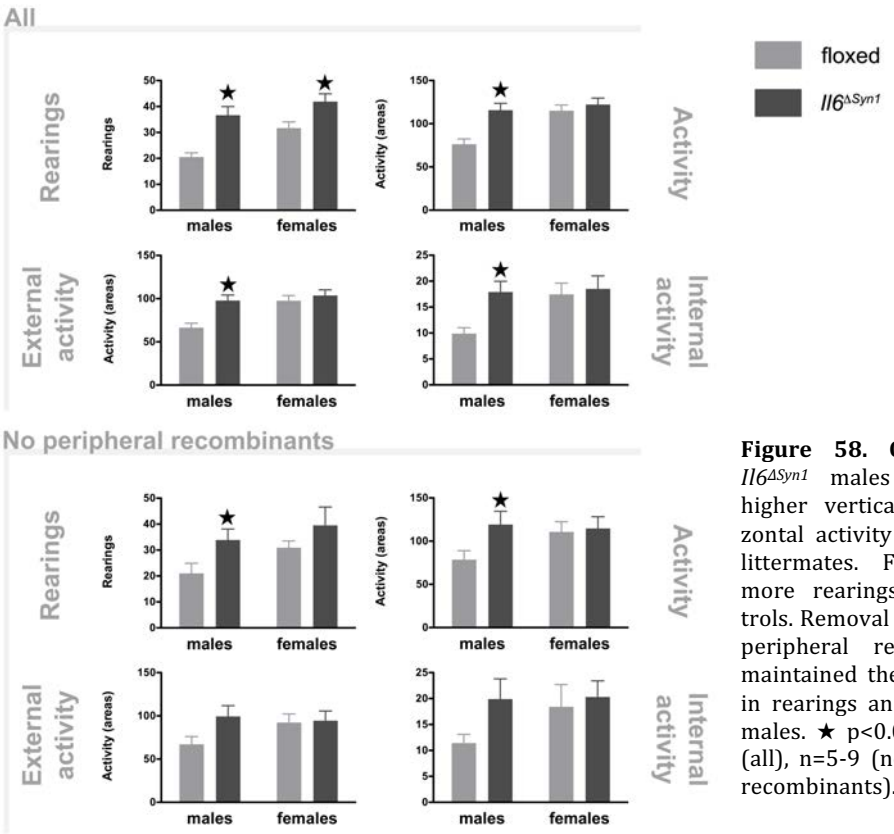

Figure 58. Open field. *Il6*$^{\Delta Syn1}$ males showed a higher vertical and horizontal activity than floxed littermates. Females did more rearings than controls. Removal of mice with peripheral recombination maintained the differences in rearings and activity in males. ★ $p<0.05$. N=20-24 (all), n=5-9 (no peripheral recombinants).

Table 25. Statistical results for the open field. Significant t-Student tests. N=20-24 (all), n=5-9 (no peripheral recombinants).

	ALL		NO PERIPHERAL RECOMBINANTS	
	Males	**Females**	**Males**	**Females**
Rearings	*t(32.4) -4.341*	*t(39) -2.66*	*t(15) -2.23*	—
Activity	*t(45) -4.014*	—	*t(15) -2.14*	—
External activity	*t(45) -3.831*	—	—	—
Internal activity	*t(34.7) -3.402*	—	—	—

5.3.1.2 Hole-board

In the complete group, males recapitulated the results of the open field regarding rearings, and activity (Figure 59 and Table 26). In addition, *Il6*$^{\Delta Syn1}$ mice carried out more head dippings and spent more time doing them. *Il6*$^{\Delta Syn1}$ females, again did more rearings than floxed controls.

However, removal of peripheral recombinants failed to yield any significant differences between the genotypes.

5.3.1.3 Elevated plus maze

In this test (Figure 60 and Table 27), male *Il6*$^{\Delta Syn1}$ had a very similar behavior to the previous two tests in the comparable measures (complete group). Here they also had increased rearings and head dippings. In addition, regarding anxiety-like-related measures, they entered and spent more time in the open arms. Females, however, only had increased head dipping number and time, compared to floxed controls.

Upon removal of peripheral recombinants, all significances were lost, but the general trends were maintained.

Table 26. Statistical results for the hole-board. Significant t-Student tests. N=31-37 (for HD, all), n=23-24 (for the rest, all); n=13-15 (for HD, no peripheral recombinants), n=5-9 (for the rest, no peripheral recombinants). HD head dippings.

	ALL		NO PERIPHERAL RECOMBINANTS	
	Males	Females	Males	Females
HD (number)	*t(48.3) -2.343*	—	—	—
HD (time)	*t(44.3) -2.203*	—	—	—
Rearings	*t(44.8) -3.975*	*t(39) -3.255*	—	—
Activity	*t(45) -3.689*	—	—	—
External activity	*t(45) -3.579*	—	—	—
Internal activity	*t(45) -2.401*	—	—	—

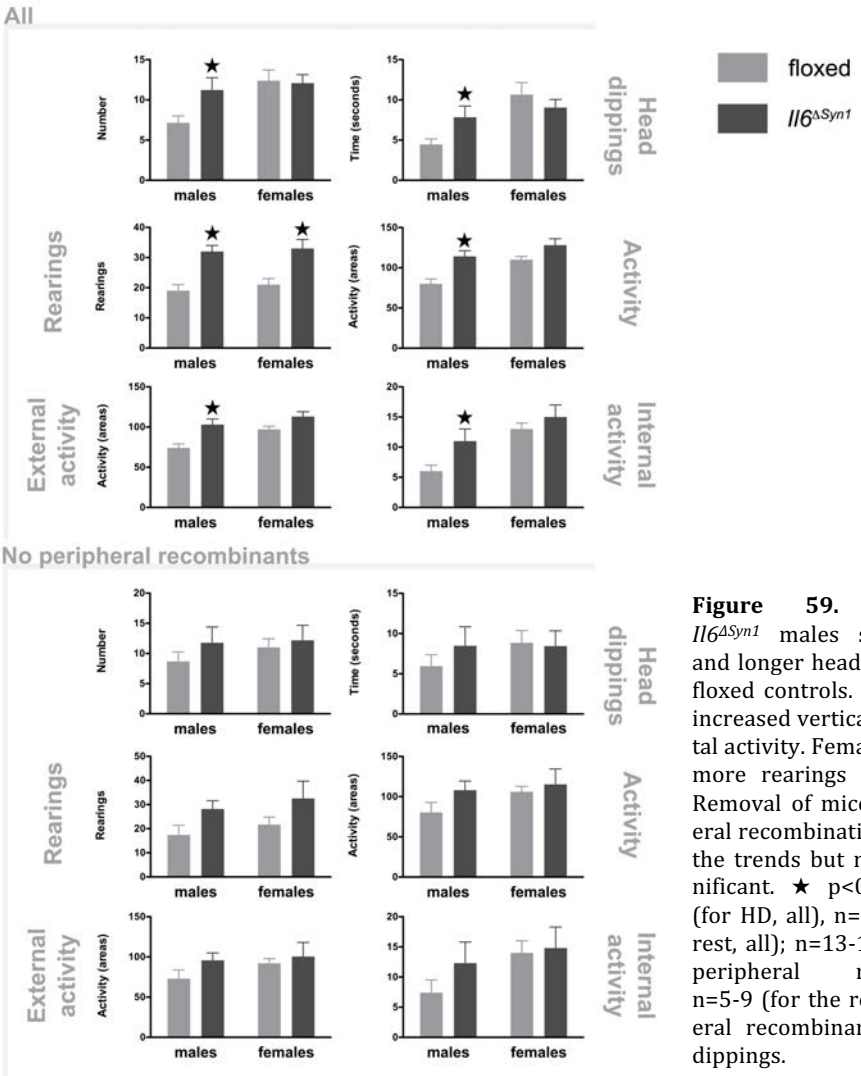

Figure 59. Hole-board. *Il6$^{\Delta Syn1}$* males showed more and longer head dippings than floxed controls. Also, they had increased vertical and horizontal activity. Females performed more rearings than controls. Removal of mice with peripheral recombination maintained the trends but none were significant. ★ p<0.05. N=31-37 (for HD, all), n=23-24 (for the rest, all); n=13-15 (for HD, no peripheral recombinants), n=5-9 (for the rest, no peripheral recombinants). HD head dippings.

Table 27. Statistical results for the elevated plus maze. Significant t-Student tests. N=20-24 (all), n=5-9 (no peripheral recombinants). HD head dippings.

	ALL		NO PERIPHERAL RECOMBINANTS	
	Males	Females	Males	Females
HD (number)	*t(45) -2.869*	*t(39) -3.466*	—	—
HD (time)	—	*t(39) -2.784*	—	—
Rearings	*t(45) -2.724*	—	—	—
% time in open arms	*t(45) -3.183*	—	—	—
% entries in open arms	*t(45) -3.116*	—	—	—

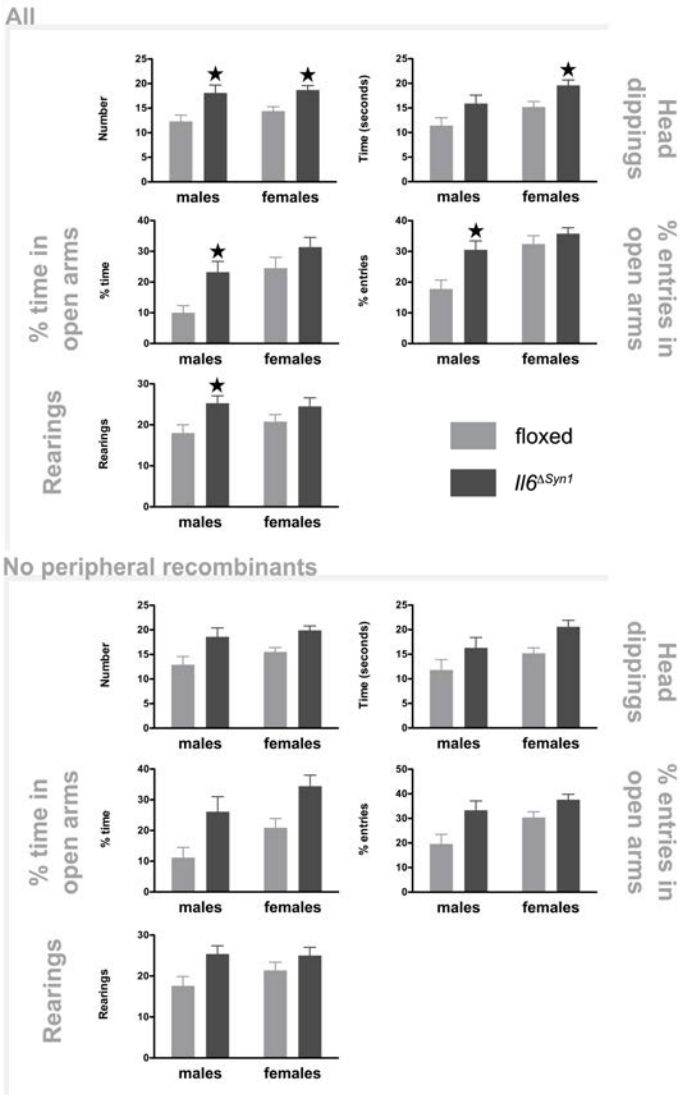

Figure 60. Elevated plus maze. *Il6*$^{\Delta Syn1}$ males showed more head dippings than floxed controls. Also, they entered open arms more and spent more time in them. Females performed more and longer head dippings than controls. Removal of mice with peripheral recombination yielded similar trends but without significant differences. ★ $p<0.05$. N=20-24 (all), n=5-9 (no peripheral recombinants).

5.3.1.4 Morris water maze

An initial trial without any cues or platform was performed to detect possible confounding factors due to *a priori* quadrant preference. Analyzing all animals (grouped by genotype and sex) showed quadrant differences in floxed males, floxed females and *Il6*$^{\Delta Syn1}$ females (quadrant χ^2 Wald 12.312, 12.767 and 11.739, respectively, $p<0.05$). Pair-wise comparisons yielded several significant comparisons, always against the south-east quadrant (floxed males north-east, north-west; floxed females north-west; *Il6*$^{\Delta Syn1}$ females north-west), which was the highest in all cases. Taking out peripheral recombinants maintained the quadrant effect in floxed males and females (quadrant χ^2 Wald 11.316 and 10.948, respectively, $p<0.05$), where again the south-east quadrant was significantly higher than some of the others (north-east and north-west in males, and north-west in females). Even though it is not optimal, given that the "preferred" quadrant is not one where the platform was located, the results are probably still valid.

In the complete group, there were no differences between genotypes in performance in the cued learning task (Figure 61), so it was supposed that all mice had the ability to swim and recognize the platform as the escape point.

There were also no genotype differences in learning during the spatial acquisition phase, and all mice learnt to locate the platform faster each day (day χ^2 Wald 97.953 and 82.573, for males and females, respectively, $p<0.05$).

During the probe trials, all animals stayed in the target quadrant above chance (25% of the time), but no differences were found between the two genotypes. Females, however, performed worse after 24 hours, when they stopped looking for the platform as much in the target quadrant (trial χ^2 Wald 3.966, $p<0.05$).

When the platform was changed to the opposite quadrant (spatial reversal), again both floxed and *Il6*$^{\Delta Syn1}$ mice learnt to locate it equally (day χ^2

Wald 52.197 and 102.053, for males and females, respectively, $p<0.05$). But during the probe trials, no genotype differences were observed. However, an interaction between trial and quadrant was detected in both sexes. Particularly, males look more for the platform on its old location in the 24-hours trial, and less in the target quadrant as they initially did; while females initially swim more in the target quadrant but then the difference dissipates (probe*quadrant χ^2 Wald 5.488 and 4.482, for males and females, respectively, $p<0.05$; sequential Bonferroni pair-wise comparisons 24-hours target vs 24-hours old, 1-hour target vs 24-hours target (males); 1-hour target vs 1-hour old (females)).

Removal of peripheral recombinants also yielded no differences in learning between genotypes, but reversal probe trials had similar differences in males, which looked for the platform less in the target quadrant and more in the old one after 24 hours (probe*quadrant χ^2 Wald 8.172, $p<0.05$; sequential Bonferroni pair-wise comparisons 1-hour target vs 24-hours target, 1-hour old vs 24-hours old).

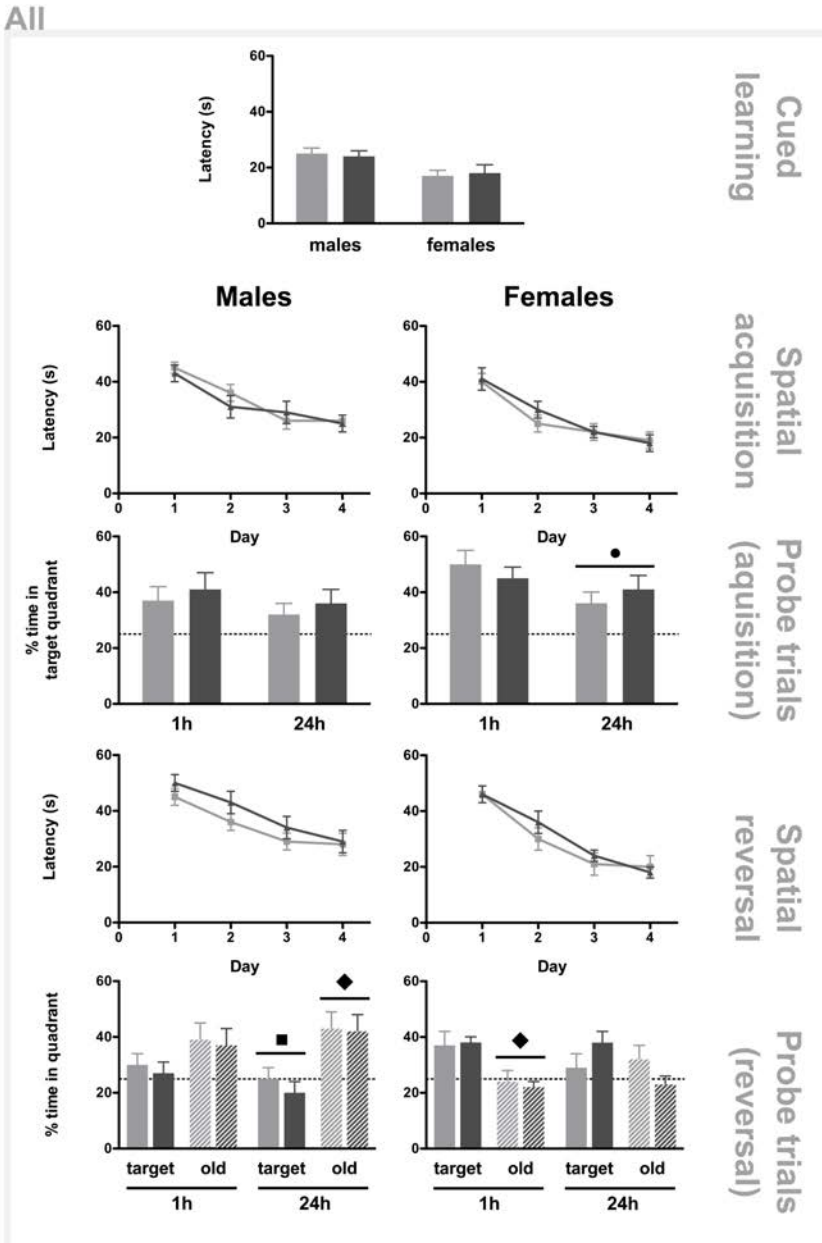

Figure 61. Morris water maze. No differences in learning were observed during the acquisition or reversal phases. Sexes behaved differently upon removal of the platform, with males persisting more in the old location as time passed, and females initially looking for the platform in the correct location but later on diluting the difference between quadrants. • $p<0.05$ (trial). Significant sequential Bonferroni pair-wise comparisons ■ vs probe 1h (same quadrant); ◆ vs target quadrant (same probe trial). N= 15-23 (all) *(continues on the next page).*

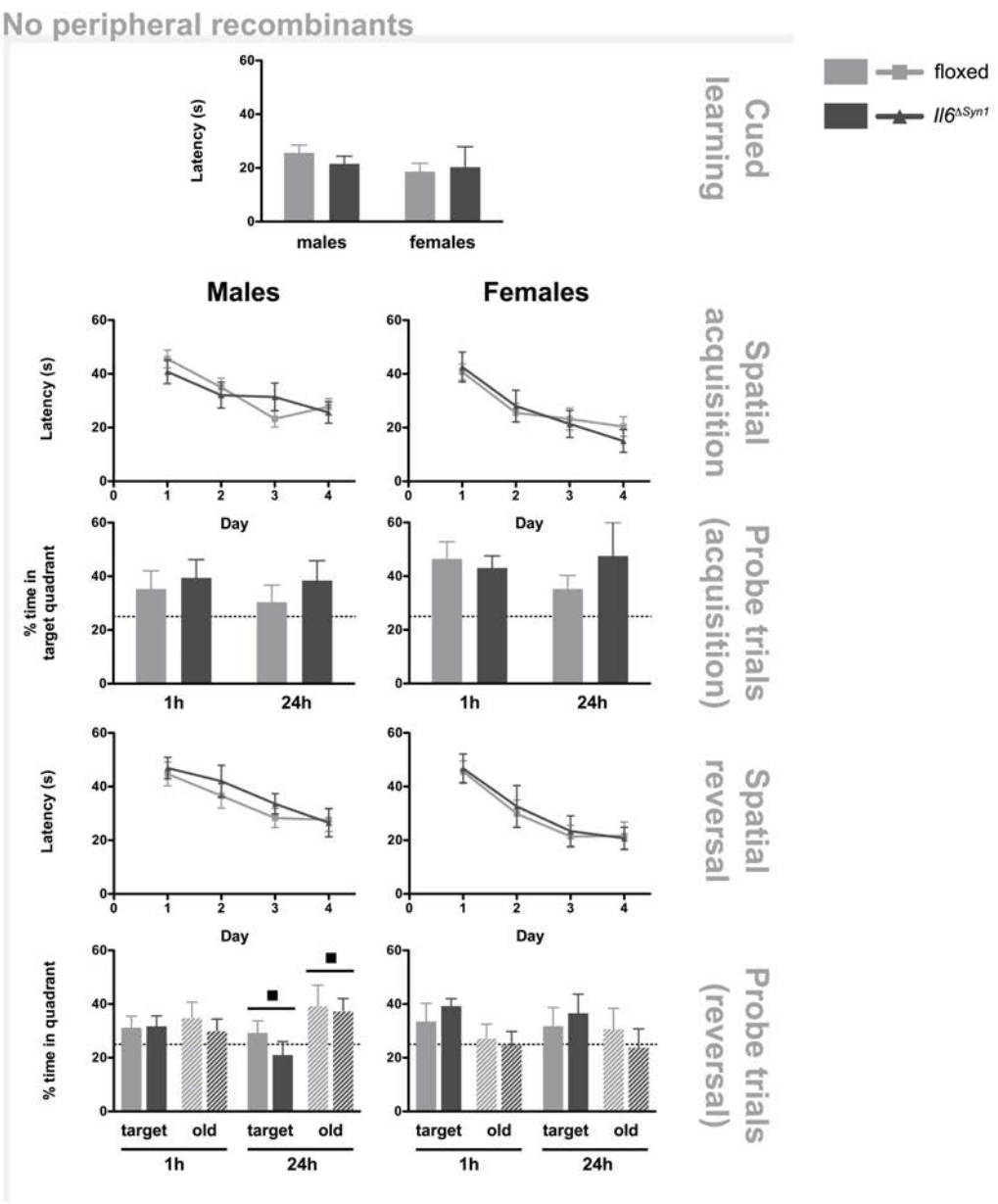

Figure 61 (continued) Morris water maze. In the group without peripheral recombinants, no differences in learning were observed during the acquisition or reversal phases either. Males' performance deteriorates after 24 hours, when they look for the platform more in the old quadrant and less in the target than the previous day. Significant sequential Bonferroni pair-wise comparisons ■ vs probe 1h (same quadrant). N= 5-13 (no peripheral recombinants).

5.3.2 Neuronal IL-6R conditional knock-out

5.3.2.1 Open field

The analysis of all animals showed only a minor effect of genotype, with *Il6ra*$^{\Delta Syn1}$ females performing more rearings than floxed controls (t-Student (29) -2.63, $p<0.05$). The other activity-related variables showed no differences (Figure 62).

Removal of peripheral recombinants, did not uncover any further differences.

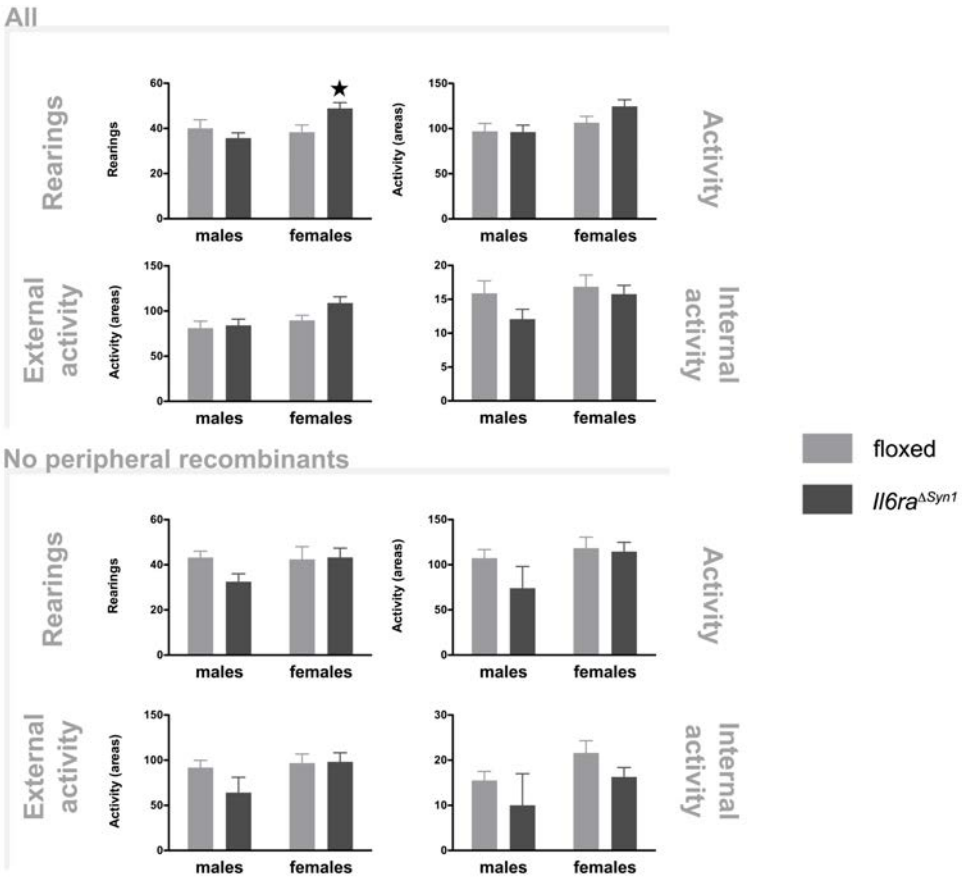

Figure 62. Open field. *Il6ra*$^{\Delta Syn1}$ females showed increased rearings compared to controls. Removal of mice with peripheral recombination made these differences disappear. ★ $p<0.05$. N= 9-18 (all); n=2-6 (no peripheral recombinants).

5.3.2.2 Hole-board

In this test, female *Il6ra*$^{\Delta Syn1}$ also had an increased number of rearings (t-Student (19.4) -3.798, $p<0.05$), as well as more activity in the external areas of the arena (t-Student (29) -2.306, $p<0.05$) (Figure 63).

Without peripheral recombinants, these differences disappeared and none other were detected.

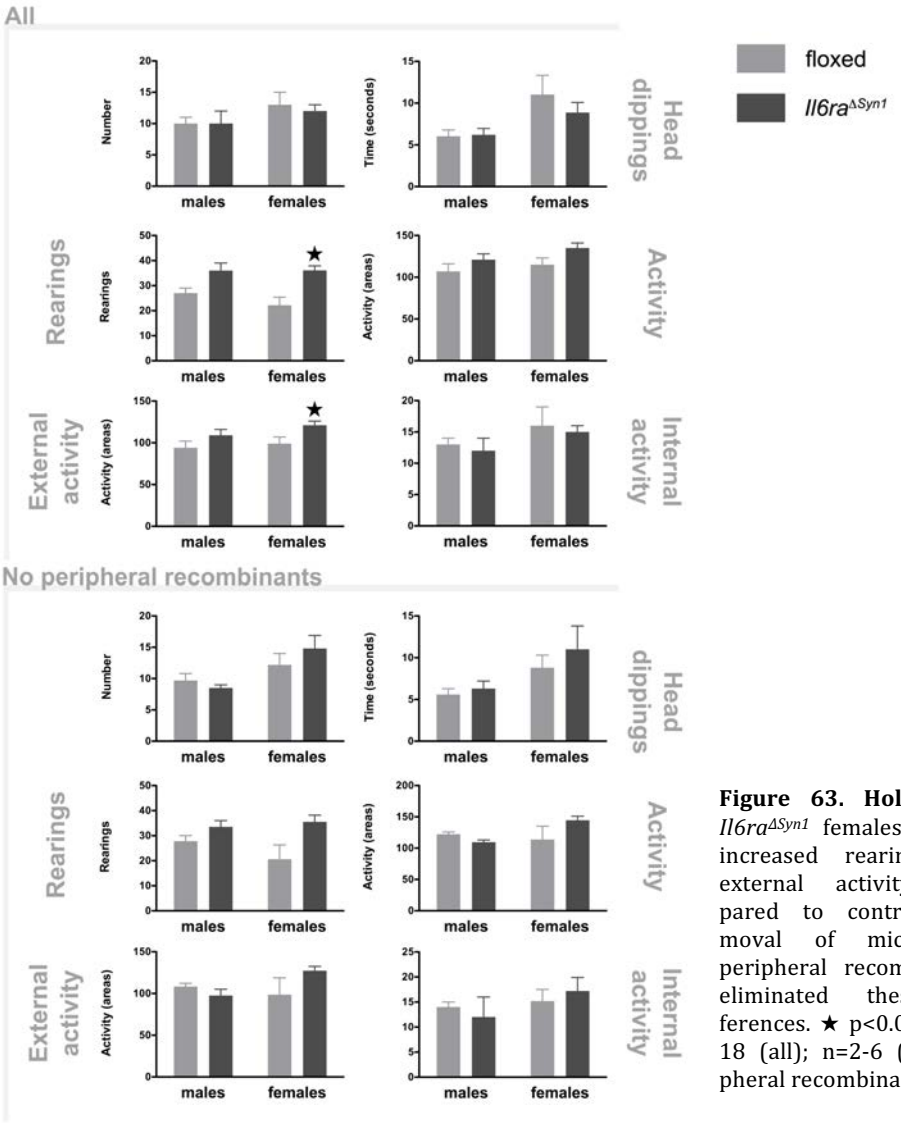

Figure 63. Hole-board. *Il6ra*$^{\Delta Syn1}$ females showed increased rearings and external activity compared to controls. Removal of mice with peripheral recombination eliminated these differences. ★ $p<0.05$. N= 9-18 (all); n=2-6 (no peripheral recombinants).

5.3.2.3 Elevated plus maze

No significant effects of genotype were seen in any variable of the test (Figure 64), either in the complete group or after elimination of peripheral recombinants.

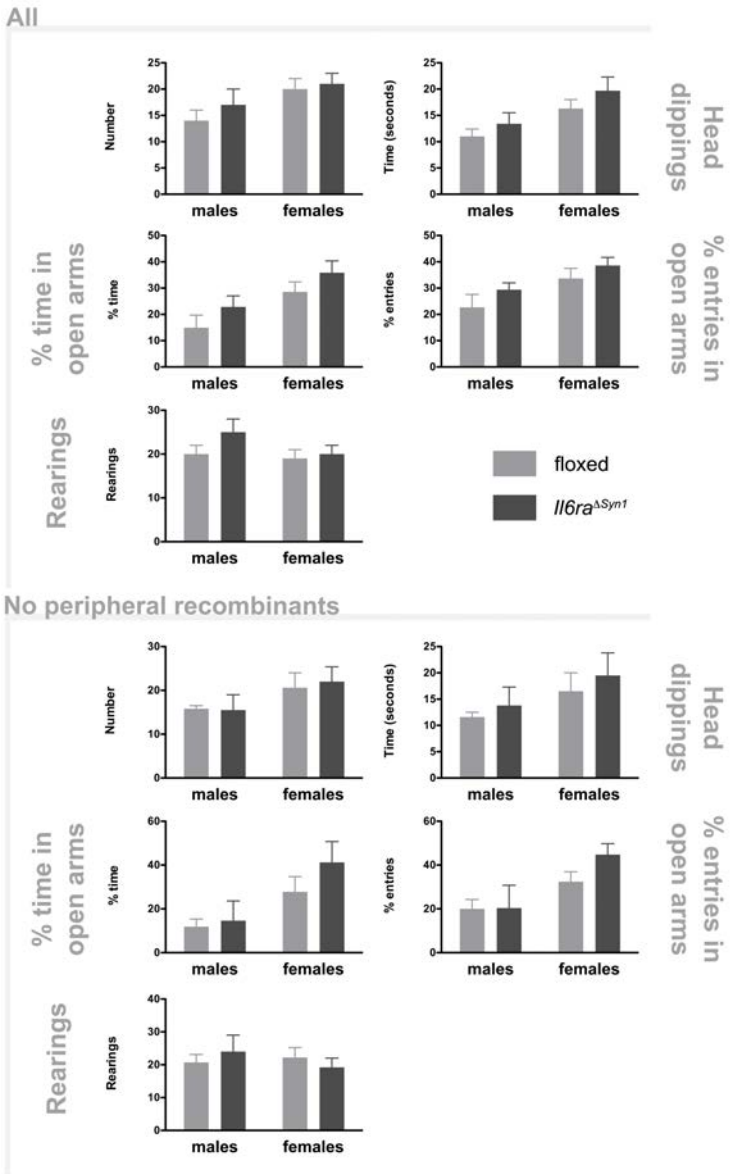

Figure 64. Elevated plus maze. No differences were detected between genotypes in any of the variables. N= 9-18 (all); n=2-6 (no peripheral recombinants).

6 DISCUSSION

6.1 Recombination of floxed genes

Extensive checks for recombination of *Il6* and *Il6ra* in non-target tissues (according to the used promoters, *GFAP* and *Syn1*) showed that an important percentage of the experimental animals had deleted exon 2 (in *Il6*) or exons 4-6 (in *Il6ra*). The problem existed with both *Cre* lines, even though the original publications for both of them claimed that no recombination (or expression of a reporter gene) was detected in peripheral tissues such as liver, heart, lung, kidney or intestine (Zhu et al. 2001; Bajenaru et al. 2002). However, upon uncovering our issue, a thorough literature review evidenced that this recombination is a prevalent phenomenon in *Cre* lines that may nevertheless remain underestimated (Rempe et al. 2006; Zhang et al. 2013). The problem with reporter genes (such as lacZ) might be that only one crossing is carried out, lowering the chances of recombination. In our case, an initial crossing is performed to unite the *Cre* gene and the floxed allele, and then a second one to obtain the experimental animals. In addition, spontaneous leaked Cre activity in any given generation can occur in the germ-line (Rempe et al. 2006) and then give rise to a hemizygous offspring, explaining why some floxed mice had the recombined allele in the tail. Wild-type animals (lox/wt) never had a recombined allele because their floxed one always comes from the *Il6* or *Il6ra* floxed line, which are never derived from a *Cre*-positive animal.

Recombination was more extensive in the crossings derived from *Syn1-Cre*, probably because the promoter is less specific and has more germ-line recombination, which we observed in both male and female progenitors, unlike previously reported results (Rempe et al. 2006).

This rather late discovery had a major impact on sample sizes of finished experiments once the assessment was performed (when possible). Nevertheless,

the effect of hemizygosis of IL-6 or IL-6R seems negligible in most cases since the results for the complete group and the one with exclusion of mice with peripheral recombination are mostly identical. The lack of statistical significance or major changes in very specific variables, is probably due to the drastic reduction in sample size. The similar trends in the complete group and the one excluding peripheral recombinants mirror the lack of some of these phenotypes in systemic IL-6KO mice, possibly because in these mice compensatory mechanisms (Kamiński et al. 2009; Gomez et al. 2010) are more necessary and appear during development, since no other sources of IL-6 exist. Also, one allele, in case it does not suffer somatic recombination due to leaked Cre activity, could produce enough protein for many functions (Bethin et al. 2000; McFarland-Mancini et al. 2010; Mandal et al. 2011).

6.1.1 Expression of IL-6 or IL-6R in conditional knock-outs

Recombination PCRs for the *Il6* or *Il6ra* gene consistently showed the recombined (delta) band in the brain of $Il6^{\Delta Gfap}$, $Il6^{\Delta Syn1}$ and $Il6ra^{\Delta Syn1}$ mice without recombination in peripheral tissues. The specificity of the $Il6^{\Delta Gfap}$ model had already been shown (Erta et al. 2015), and given the phenotypic differences with the neuronal model we assume that at least the recombination is not happening in the same cells. Certainly, further attempts must be carried out to determine the specificity of the recombination.

However, when expression was measured in the whole hypothalamus by qPCR, no genotype differences were seen in either of the conditions assessed (control, HFD, 48-hour fast or LPS). In one instance, an effect of the floxed *Il6* gene was seen, which meant a reduction in expression of both floxed and $Il6^{\Delta Syn1}$ mice when compared to wt, but coincidentally, in that diet experiment wt and floxed mice weights were very similar. In the case of the receptor, administration of LPS

increased its expression as expected (Vallières and Rivest 1999), but its deficit in neurons could not be proved.

Several approaches were taken to specifically measure IL-6 (in the neuronal IL-6 knock-out line) or IL-6R (in the neuronal IL-6Rα knock-out line) in the CNS, such as primary cell cultures of astrocytes and neurons and double immunofluorescence, but all failed to provide reliable results so they have been excluded from this dissertation. Primary cultures of neurons or astrocytes (as a control) were stimulated as previously described, with either KCl or forskolin in neurons (Sallmann et al. 2000), or LPS in astrocytes (Erta et al. 2015). However, IL-6, as measured by ELISA, was undetectable. Also, double immunofluorescence of IL-6R and NeuN showed what seemed specific signal of the receptor in neurons of both floxed and *Il6ra*$^{\Delta Syn1}$ mice.

The lack of clear expression differences between floxed and conditional knock-out mice is disappointing, but the clear phenotypes observed do point to a cell-specific effect of IL-6, and to a lesser extent, of its receptor in neurons. There are several possibilities to explain the absent differences 1) in basal conditions the levels are too low to discriminate a slight reduction due to a specific cell type, 2) there is a dilution effect due to the other IL-6-producing cells in the brain and 3) the effects took place in the developmental stages and permanent changes occurred that are not due to transient changes in cytokine or receptor expression. This latter option is based on certain differences between the phenotype of IL-6KO mice and the inhibition of IL-6 signaling using antibodies in adults (Zahs et al. 2013). Therefore, it will be critical to also study inducible systems in future experiments.

6.2 Weaning frequencies

Previous results from our group found that *Il6*$^{\Delta Gfap/wt}$ and even more *Il6*$^{\Delta Gfap}$ were underrepresented at weaning (Quintana et al. 2013), an effect that was less prominent with further backcrossing into the C57BL/6OlaHsd background (Erta et al. 2015). This was attributed to a pro-survival role of IL-6, despite being contrary to results with systemic IL-6KO mice, which have normal mendelian ratios in two independent models (Kopf et al. 1994; Dalrymple et al. 1995). Here we have corroborated the same trend with an increased number of mice, which partially included some of those in the published data. And again, *Il6*$^{\Delta Gfap}$ offspring was reduced compared to *Il6*$^{\Delta Gfap/wt}$.

Furthermore, we have shown that *Il6*$^{\Delta Syn1}$ and *Il6*$^{\Delta Syn1/wt}$ are also weaned at reduced ratios, but this was only detected when the two genes were analyzed separately, instead of the four final genotypes. Nevertheless, it hints towards a deleterious effect, albeit to a lesser extent, of the lack of neuronal IL-6.

However, given the discrepancy with the total knock-out, the possibility of Cre-dependent toxicity must be considered (Loonstra et al. 2001; Bersell et al. 2013; Lexow et al. 2013). Frequency analysis of a total of 277 of our *GFAP*-Cre, and 190 of our *Syn1-Cre* progenitor mice (described in sections *4.2.3* and *4.2.4*) showed a significant underrepresentation of *GFAP-Cre*$^{+/-}$ mice (104 *GFAP-Cre*$^{+/-}$ vs 173 *GFAP-Cre*$^{-/-}$, expected N 138.5, χ^2 17.188, $p<0.05$), while *Syn1-Cre* had similar frequencies at weaning (101 *Syn1*-Cre$^{+/-}$ vs 89 *Syn1*-Cre$^{-/-}$, expected N 95, χ^2 0.758, $p>0.05$). Therefore, it seems that part of the reduction in conditional knock-out mice derived from the *GFAP-Cre* line might be due to Cre itself, while in the *Syn1-Cre*-derived line there is only the IL-6-specific effect.

A pro-survival role of neuronal or astrocytic IL-6 would not be so surprising, since the cytokine has been shown to promote neural stem cell differentiation into neurons and astrocytes through its soluble receptor (Islam et al. 2009). It has also been associated with improving survival of neurons (Thier et

al. 1999) and neurite growth (Wu and Bradshaw 1996) *in vitro*, and astrocyte-derived IL-6, specifically, increased the differentiation of a hippocampal neuronal line (Oh et al. 2010).

Mutation of gp130, the common signal transducer for IL-6 and related cytokines, has severe consequences in embryonic development, with death occurring between day 12.5 post-coitum and birth (Yoshida et al. 1996). Furthermore, Stat3-deficient mice show embryonic lethality (Takeda et al. 1997). The fact that they die by E7.0 evidences the more widespread implication of the transcription factor, since our models start expressing *Cre* at E12.5 (*Syn1*) or E14.5 (*GFAP*) and therefore the lack of the cytokine would appear later and have a more discrete effect.

6.3 Linear growth

Il6$^{\Delta Gfap}$ mice of both sexes had longer tibiae, suggesting a greater size, which in females, was accompanied by increased IGF-1 levels. IGF-1, along with growth hormone (GH), is a critical element in postnatal growth and directly determines bone growth and density (Lupu et al. 2001; Yakar et al. 2002). It is produced both in the liver (endocrine effects) and in every tissue (paracrine/autocrine effects). Its circulating levels come primarily from the liver after GH stimulation (Le Roith et al. 2001) so the connection to the CNS could come from regulating GH in the adenohypophysis or above. However, i*n vitro* results regarding stimulation of GH regulation by IL-6 generally point to no effect of the cytokine in either GHRH or GH secretion. In hypothalamic explants or normal rat pituitary cells, it has no effect; and only in GH3 cells, a rat pituitary tumor cell line, does it stimulate GH secretion (Honegger et al. 1991; Artz et al. 1993).

In the blood, IGF-1 forms a complex with IGFBP-3 and the acid labile subunit (ALS), which increases its half-life (Jones and Clemmons 1995). IGFBP-1, which can also bind circulating IGF-1, has been shown to inhibit its actions on fetal and postnatal growth, adipocyte proliferation and modulation of the hypoglycemic activity of unbound IGF-1 (Lewitt et al. 1991; Rajkumar et al. 1995; Siddals et al. 2002). However, we observed no changes in IGFBP-3 or -1.

Neuronal IL-6 deficiency had the opposite effect on linear growth. Both nose-rump distance and tibial length were reduced in 12-15-week-old *Il6*$^{\Delta Syn1}$ mice of both sexes, even though IGF-1 was unaffected. Lack of IGF-1 involvement and the fact that the deficient cells are neurons suggests that, in this case, CNS involvement might be more related to SNS control of bone homeostasis. It has been known for some time now that the SNS innervates bone tissue, reaching the bone marrow space, the periosteum and cortical bone (Duncan and Shim 1977; Hohmann et al. 1986; Hill and Elde 1991). Some of these sympathetic neurons express different neuropeptides (e.g. NPY and vasoactive intestinal peptide, VIP) and they have been linked to the regulation of blood flow to the bone, as well as to the general regulation of growth through trophic effects. For example, *in vitro* studies have shown an interference of NPY with parathyroid hormone and NE by counteracting their induction of cAMP (Bjurholm et al. 1988). These neurons are innervated in turn by others in the PVN and other hypothalamic nuclei, beside others at lower levels (Dénes et al. 2005). Therefore, it is a possibility that lack of IL-6 in sympathetic or autonomic premotor neurons in the PVN affects regulation of these circuits, thus altering bone metabolism.

A GFAP-IL6 line with high IL-6 expression and NSE/hIL6 mice, two models of neuroinflammation with transgenic expression of IL-6 in the CNS (in astrocytes and neurons, respectively), display stunted growth (Campbell et al. 1993; De Benedetti et al. 1997), although the GFAP-IL6 line with moderate expression has been shown to have a normal body length and similar-to-control levels of IGF-1 (Señarís et al. 2011). Inflammation has been consistently associated with growth

retardation (Li and Tsutsui 2000; Prendergast et al. 2014), but the specific mechanisms are not well defined. In the case of NSE/hIL6 mice, it seems to be mediated by a decrease in IGFBP-3 which increases IGF-1 clearance. Another mechanism could be the stimulation of somatostatin (somatotropin release inhibiting hormone, SRIH) by interleukin-1β (Honegger et al. 1991), a cytokine that is upregulated in GFAP-IL6 mice (Chiang et al. 1994). In these models, source of IL-6 seems irrelevant, probably because it increases so dramatically that a more generalized effect can be seen, whereas in the case of our conditional knock-out a more focalized autocrine/paracrine effect is probably more relevant.

A study with different models of altered gp130 signaling pathways (Sims et al. 2004) showed that mice with impaired gp130 signaling through STAT1/3 also have mild dwarfism due to premature growth plate closure, but normal trabecular bone volume. Conversely, in mice where the mutation is specific to the SHP2/ras/MAPK pathway, increased osteoclast activity reduced trabecular bone volume, leaving length unaffected. In the latter model, complete lack of IL-6 (by crossing it with IL-6KO mice) resulted in a worsening of the phenotype suggesting that IL-6 acts through STATs to increase osteoblast proliferation. These models, however, are difficult to integrate with ours since in this case osteoblast IL-6 deficiency probably confounds a possible central effect, and also, all gp130-family cytokines will have defective signaling, not just IL-6.

A role of IL-6 in the VMH should also be considered, since leptin acts on this area to activate sympathetic signaling and elicit its anti-osteogenic effects (Takeda et al. 2002). A recent study has found that IL-6 increases leptin sensitivity in neurons of this nucleus, but the authors later linked it to a microglial source (Le Foll et al. 2015; Larsen et al. 2016). Further studies with conditional microglial knock-outs, currently under-way in our group, might shed more light on this source-specific effects.

Il6ra$^{\Delta Syn1}$ mice had a similar phenotype to *Il6*$^{\Delta Syn1}$ mice regarding tibial length, but in this case IGF-1 also correlated to bone length (in males).

Taken together, results from the three models highlight the importance of the cellular source of IL-6 and its autocrine/paracrine effects and they suggest a network of astrocytes and neurons that regulates bone metabolism. Gliotransmitters are likely candidates to mediate the effect of astrocytes on neurons (Stern and Filosa 2013). For example, given that presympathetic neurons originating in the PVN are under a $GABA_A$–mediated tonic inhibitory tone by astrocytes, which influences their excitability (Park et al. 2007; Park et al. 2009), maybe astrocytic IL-6 potentiates this inhibition. Information on the bone length of *Il6ra*$^{\Delta Gfap}$, which at present we lack, will be needed to support whether this is an autocrine phenomenon. The role in neurons might be complicated by the subpopulations implicated in the central regulation of bone metabolism and their opposing roles. Potentially, both sympathetic and *Cart*-expressing neurons could express IL-6 and be dependent on autocrine signaling to maintain their respective positive or negative effect on osteoclast differentiation (Elefteriou et al. 2005), so other intermediate regulators are likely to participate. In addition, it should be taken into consideration that bone length and density are differentially regulated, so it will be very interesting to also evaluate bone density in our models in the future. Furthermore, microglial cells may also contribute to the regulation (Stern and Filosa 2013), and studies with conditional microglial knock-outs might shed light on this point.

6.4 Energy intake and HFD-induced obesity

6.4.1 Basal weight

We observed a reduced weight of weaned male and female *Il6*$^{\Delta Gfap}$ mice compared to wt, and also against floxed in males without peripheral recombination. Nevertheless, this initial difference dissipated with age, which contrasts with initial results from our group, that found no differences at weaning

but also that *Il6*$^{\Delta Gfap}$ were heavier on a control diet (Quintana et al. 2013). However, those results were obtained from earlier backcrossings, so the genetic background was less homogeneous. Further backcrossing found that the effect of astrocytic IL-6 deficiency on basal weight was subtler, delayed to age 25 weeks, and appeared only in males (Erta 2014). This would be in line with the results obtained here, since mice were studied up to age 22 weeks approximately. The shift in weight differences from weaning to adulthood likely reflexes a developmental effect of astrocytic IL-6 that then is no longer relevant in the adult.

Results in neuronal IL-6 conditional knock-outs were generally opposed to those observed in the astrocyte model. These mice had no weight differences at weaning, but soon thereafter, and up to 11 weeks of age, their weight was consistently lower than floxed controls. Further monitoring during the diet experiment (up to 24 weeks approximately) showed mixed results, as removal of mice with peripheral recombination greatly reduced the sample size and it probably was insufficient to detect the small variation seen before.

6.4.2 HFD-induced obesity

As expected, HFD caused obesity in wt and floxed mice in all three long-term HFD experiments, although the latter were more sensitive to the diet and gained more weight. Weight gain was clearly due to an increase in fat pads, with WAT Sc being the most significant one since it best mirrored the variations in body weight.

Lack of astrocytic IL-6, in the absence of additional recombination, caused a more prominent weight gain in both males and females, which in males was primarily due to the WAT Sc depot. Also, increased body weight related to increased liver weight, possibly because of hepatic steatosis (Yaqoob et al. 1995; Eccleston et al. 2011). These results align with previous results from our group using GFAP-IL6 mice, which are resistant to HFD-induced obesity and with

females having a clearer phenotype (Hidalgo et al. 2010). In our short-term experiment, we could not see these weight differences, in line with previous data where they appeared after approximately 5 weeks (Hidalgo et al. 2010).

Worth mentioning here is the fact that, even though the GFAP promoter has been extensively used to drive astrocyte-specific expression of different genes (Campbell et al. 1993; Bajenaru et al. 2002; Gan et al. 2012), other cells in the CNS, such as non-myelinating Schwann cells and reactive retinal Müller cells, can also express it (Brenner et al. 1994). In our case, this is probably irrelevant. However, GFAP-positive glial cells have been identified in the enteric nervous system (Jessen and Mirsky 1983), and, at least in *in vitro* rat cultures, they are capable of synthesizing IL-6 after an immune challenge (Rühl et al. 2001). This is certainly an interesting topic that could have implications in the absorptive capacities of the gut, or the microbiota present, which has recently been uncovered as a promising field in obesity research (Das 2010).

It should also be noted that *Il6*$^{\Delta Gfap}$ showed reduced weaning weight and this has been correlated in humans to the development of obesity and type 2 diabetes in the adult (Barker et al. 1993), probably by epigenetic mechanisms. In rats, calorie-restricted dams had smaller offspring that showed hyperphagia, which was exacerbated on a HFD (Vickers et al. 2000). Since this resembles our model, we speculate that it could also be related to the intrauterine mortality of *Il6*$^{\Delta Gfap}$ mice, and mean that a fetal or early postnatal deficit of astrocytic IL-6 determines adult susceptibility to HFD-induced obesity.

In general, it seems that astrocytic IL-6 acts as a brake on body weight increase, especially after a challenge such as a HFD. Further evidence supporting this role comes from the decrease in body fat after ICV administration of IL-6 to rats (Wallenius et al. 2002a), and the mature-onset obesity of the systemic IL-6KO model (Wallenius et al. 2002b; Navia et al. 2014).

Conversely, lack of neuronal IL-6 dramatically protected female mice from developing HFD-induced obesity, while in males the effect was milder. The lower

body weight was clear in both the subcutaneous and gonadal WAT depots in females, and only in the former in males. Liver weight was also less affected by HFD, again probably due to the lower lipid accumulation. These results are very interesting, since they may point to a change in sympathetic outflow to adipose tissue and liver due to the lack of neuronal IL-6. The white adipose tissue is innervated by the SNS (Bowers et al. 2004), NE stimulation on β2-adrenergic receptors is known to promote lipolysis (Carpéné et al. 1998), and a mutation on that receptor has been linked to obesity in women (Large et al. 1997). Therefore, our model might have increased sympathetic outflow that would decrease fat deposition. This is in line with our results on bone length, which also suggested increased sympathetic activity.

Comparison of either model with IL-6KO mice is complicated, since despite the evidence of mature-onset obesity (Wallenius et al. 2002b; Navia et al. 2014), other studies have found no differences (Di Gregorio et al. 2004); and feeding these mice a HFD shows either no effect (Ellingsgaard et al. 2008) or a slightly lower weight gain (Di Gregorio et al. 2004; Ellingsgaard et al. 2008). Nevertheless, the case of the total knock-out is bound to be more complex, since all sources of IL-6 are abolished and each one, peripheral or central, might have a distinct effect as shown both here and previously with conditional IL-6 knock-outs in muscle (Ferrer et al. 2014) or adipose tissue (Navia et al. 2014).

Regarding glucose homeostasis, it was not surprising that it remained normal in the *Il6*$^{\Delta Gfap}$ experiment since the most altered fat depot was the WAT Sc one, and this is not the most relevant in insulin resistance (Shoelson et al. 2007). So, despite fasting blood glucose being raised in all genotypes on the HFD, they all displayed similar curves after insulin or glucose administration. Of note, the global genotype effect seen in the ITT of male, which could not be attributed to a specific group, might be due to the less prominent obesity of wt animals.

However, in the *Il6*$^{\Delta Syn1}$ experiment, floxed mice were somewhat less sensitive to insulin than floxed mice of the *Il6*$^{\Delta Gfap}$ experiment, despite showing

similar weight gain and feed efficiency, and these were especially evident when mice with peripheral recombination were removed.

Also, despite the resistance to increased body weight of *Il6*$^{\Delta Syn1}$ mice with a HFD, they had raised blood glucose levels (after a 4-hour fast) but were able to respond to insulin or glucose much better than floxed mice, maybe because they were after all leaner than them. This could be related to an inhibition of the IKKβ/NF-κB pathway in ARC neurons, which has been shown to attenuate several traits of HFD-induced obesity (Benzler et al. 2015). However, since other authors linked this phenomenon to an IL-6-mediated activation of IL-10, which would in turn inhibit IKKβ (Ropelle et al. 2010), it is an unlikely mechanism in our model; but would agree with the phenotype of CNS transgenic IL-6 mice.

6.4.3 Energy homeostasis

Variations in body weight are due to an imbalance in energy intake and/or expenditure. Indeed, mice on the HFD had a higher energy intake (despite eating less grams of food), and this, combined with the higher feed efficiency of this diet (more weight gain per energy unit), explains their weight increase. It has been already shown that a HFD, even when calorie-matched to a low-fat *ad libitum*, leads to more fat deposition (Petro et al. 2004). A proposed mechanism for this "effectiveness" of HFD is a deficit in the central response to adiposity signals like insulin, due to accumulation of saturated CoA species and the activation of local inflammatory signals, such as IKKβ, in hypothalamic neurons (Posey et al. 2009; Benzler et al. 2015). Lack of astrocytic IL-6 did not affect feed efficiency, suggesting that the cytokine from astrocytes does not participate in this regulation, and that putative IL-6 deficiency in enteric glia (as mentioned before) is probably irrelevant. However, neuronal deficit dramatically reduced feed efficiency in females, which had the clearest resistance to obesity. It will now be interesting to study whether this action of IL-6 occurs on the neurons themselves,

in an autocrine fashion, or rather if it acts in a paracrine way, and to what extent trans-signaling might be involved (Timper et al. 2017).

Regarding the effect of IL-6 on food intake, conflicting results exist, ranging from absence, to very limited, to effective both when injected ICV or IP. GFAP-IL6 mice show no apparent alterations in food intake with either a control or HFD (Hidalgo et al. 2010), and neither do NSE-IL-6 mice on a control diet (De Benedetti et al. 1997). ICV administration of IL-6 in rats causes a slight decrease in average food intake over 2 weeks (Wallenius et al. 2002a), as does IP administration in mice (De Benedetti et al. 1997); but ICV injection in control- and HFD-fed mice immediately decreases (after 2 hours) food intake in fasted animals (Timper et al. 2017). The range of results may reflect differences in dose, though it is difficult to determine how ICV injections compare to transgenic levels; a very time-sensitive effect, or the fact that physiological levels lack a major effect. The present results go in the line of no effect in the fed state, with no apparent differences in energy intake in either single-housed *Il6*$^{\Delta Gfap}$ mice or group-housed *Il6*$^{\Delta Syn1}$ mice. The higher intake seen in grouped floxed males (from the first *Il6*$^{\Delta Gfap}$ experiment) is likely an artifact, since feed efficiency shows a corresponding decrease and in females, where the weight difference is higher, no such difference is observed.

One-day fasting, however, had mixed effects regarding IL-6 deficiency. In *Il6*$^{\Delta Gfap}$ individualized males fed a control diet, it was associated with a lower compensatory intake, maybe due to their lower weight loss, while on grouped-housed animals, the differences in weight loss were inexistent and intake was only barely lower. *Il6*$^{\Delta Gfap}$ females, on the other hand, despite losing more weight when isolated, showed no changes in energy intake on the control diet, maybe pointing to an insufficient defense of body weight. Neuronal IL-6 deficit was associated with a lower compensatory intake in grouped males throughout the refeeding and more discretely in females, which had lost more weight during the fast. Regarding the receptor, isolated *Il6ra*$^{\Delta Syn1}$ females ate less when refed despite

having lost more weight during the fast. In this case, both sources of IL-6 seem to go in the same direction and to be acting on neurons, suggesting that the role of the cytokine may vary according to the type of caloric challenge. Variations between single- and group-housed mice could be due to different sensitivity to an additional stressor such as fasting when isolated, as has been shown for psychological stressors (Bartolomucci et al. 2003). The reduced weight loss might suggest a protective effect from starvation of lack of astrocytic IL-6 in males. However, our current data on the HPA axis, which shows no alterations of either *Crh* (basal or after a 48-hour fast) or corticosterone (basal), does not allow us to make such an affirmation, since it comes exclusively from grouped-housed animals (Erta et al. 2015).

The other arm of energy homeostasis is energy expenditure, and it can be modified by differences in activity. *Il6*$^{\Delta Gfap}$ mice do indeed ambulate less on a HB and EPM (Quintana et al. 2013; Erta et al. 2015), so their energy expenditure would be reduced and could therefore explain their increased weight gain. In addition, a decreased metabolism can also contribute to the conservation of energy. In a recent doctoral dissertation from our group, male *Il6*$^{\Delta Gfap}$ mice tended to present a lower rectal temperature than floxed littermates and also failed to display LPS-induced fever (Erta 2014). Unfortunately, we have been unable to perform indirect calorimetry on these mice to further corroborate this hypothesis.

Il6$^{\Delta Syn1}$ mice, on the other hand, show consistently higher activity than floxed littermates (see *6.5 Behavior* for discussion), which would align with their lower weight phenotype, even when HFD decreases some variables (Lavin et al. 2011).

6.4.3.1 Hypothalamic neuropeptides

In general, the only significant changes observed in hypothalamic neuropeptides pertained to the orexigenic *Npy* and *Agrp*. Female *Il6*$^{\Delta Gfap}$

consistently showed lower expression of these neuropeptides, either on a control diet, and after a HFD or a fast. This was surprising, given that NPY and AgRP increase food intake and decrease energy expenditure, and that female *Il6*$^{\Delta Gfap}$ mice are more susceptible to HFD-induced obesity. Therefore, if this ARC population were implicated in causing the phenotype, it would be expected that they had increased expression of orexigenic neuropeptides. Moreover, *Il6*$^{\Delta Gfap}$ females lost more weight after a fast, a fact that did not further increase their *Npy* and *Agrp* levels. In this case, the lower levels could correlate with an increased energy expenditure that would explain the greater weight loss. Males, on the other hand, were capable of raising *Npy* and *Agrp* as a consequence of the fast. Interpretation, however, is difficult given that floxed males failed to show a significant increase of these neuropeptides. Combination of these data with the refeeding experiment suggests that fasted males on a control diet eat less despite having increased orexigenic neuropeptides. Comparison however, might not be so straightforward since fasting time may cause different expression profiles. To further complicate the interpretation of these results, GFAP-IL6 have been previously shown to have decreased levels of *Npy* and *Agrp* in control diet females (Señarís et al. 2011), even though in the experiment included here no basal differences were observed. The lower expression could be the cause of their leaner phenotype, which in our case was not apparent yet, characterized by lower fat and leptin levels, where IL-6 action at the hypothalamic level, might enhance leptin sensitivity (Sadagurski et al. 2010).

Il6$^{\Delta Syn1}$ females have increased *Agrp* expression both with the control and HFD, an opposite pattern of the orexigenic neuropeptide to the astrocytic model. In the HFD group, this is likely just a consequence of their lower feed efficiency and a signal to either increase intake, which we do not see, or conserve energy, for which indirect calorimetry would be a valuable indicator. In the control diet group, however, the increased levels of *Agrp* are indicative of an inherent difference in regulation of these neuropeptides, and would agree with the increased weight gain seen in *Il6*$^{\Delta Syn1}$ females. Given that no differences are seen in

absolute body weight over the whole experiment, this is probably a catch-up increase consequence of the lower weight they displayed for the first 8 weeks after weaning. The opposed phenotype to *Il6*$^{\Delta Gfap}$ mice might be explained by an interplay of astrocytes and neurons, where astrocytic IL-6 stimulates production of neuronal IL-6, which in turn would inhibit AgRP neurons, either directly or via activation of an intermediary inhibitory cell.

In the systemic IL-6KO model, the obese phenotype of old mice has been associated to decreased *Crh* levels in the hypothalamus (Benrick et al. 2009) that would suggest a lower sympathetic tone. Indeed, they present a reduced heart rate during stress and impaired cold-induced thermogenesis (Wernstedt et al. 2006). Our *Il6*$^{\Delta Gfap}$ mice, however, have no overt alterations of *Crh* expression (as mentioned before in relation to stress) that would explain a decreased sympathetic activity. GFAP-IL6 mice also show conflicting results, since males tend to have defective thermogenesis, associated with increased mortality, despite having increased *Crh* expression (Hidalgo et al. 2010).

The lack of dramatic effects in *Il6*$^{\Delta Gfap}$ mice is perhaps not so surprising if we consider another member of the IL-6 family, CNTF. This cytokine reduces food intake and counteracts obesity due to leptin deficiency, but is unable to reverse fasting-induced changes in hypothalamic neuropeptides (Gloaguen et al. 1997).

Also, sex-dependent variations have already been observed in other conditional *Il6* knock-outs in our group. Male and female muscular or adipose tissue *Il6* conditional knock out mice respond differently to a HFD with subsequent variations in hypothalamic neuropeptides (Navia et al. 2014; Ferrer et al. 2014). Estradiol has been shown to affect POMC neuron circuitry in the ARC (Gao et al. 2007), and the estrogen receptor inhibits *Il6* expression through NF-κB (Stein and Yang 1995), so it is unsurprising that sex hormones might add an extra layer of complexity to our models.

Quantification of expression of hypothalamic neuropeptides in the second diet experiment will add more information to this complicated scenario.

Taken together, it would seem that NPY/AgRP neurons are differentially regulated, and in a sex-dependent manner, by astrocytic or neuronal IL-6, and this manifests with diverse challenges such as starvation and excess calories.

6.4.3.2 Hypothalamic inflammation

The current view in the field of obesity proposes hypothalamic inflammation as a cause to defective leptin and insulin signaling in hypothalamic neurons. Some evidence exists of this phenomenon after a short-term HFD (Thaler et al. 2012; Waise et al. 2015), but our experiment with GFAP-IL6 mice failed to show any significant inflammation in the hypothalamus of wt mice, maybe due to different fat composition or the start of remission after the initial inflammation.

In the *Il6*$^{\Delta Syn1}$ long-term HFD experiment, however, mice on the fat-rich diet did show certain signs of inflammation, such as astrogliosis (increased *Gfap*) and microgliosis (increased *Mac1*), which seems to be reduced in the leaner *Il6*$^{\Delta Syn1}$ HFD-fed females, although the presence of mice with peripheral recombination confounds the interpretation of the results.

In vitro studies suggest a mechanism by which astrocytes could, via TLR-4 and maybe after microglial stimulation, respond to saturated fatty acids by producing IL-6 and TNF-α (Gupta et al. 2012), which would in turn interfere with leptin signaling in nearby hypothalamic neurons. Our present results with *Il6*$^{\Delta Gfap}$ mice do not support this hypothesis, since lack of IL-6 production by astrocytes would then mean the prevention, to a certain degree at least, of impaired leptin signaling and resistance to HFD-induced obesity. Rather, they would align more with results showing an enhancement of leptin signaling by IL-6 (Sadagurski et al. 2010), which would also explain the phenotype of GFAP-IL6 mice.

HFD-induced inflammation also induces apoptosis of hypothalamic neurons (Moraes et al. 2009), which is detectable both at the mRNA and protein level in several apoptosis markers. In the *Il6*$^{\Delta Syn1}$ HFD experiment, we assessed *Casp3* as representative of apoptosis and only found an increase due to HFD in males, but no genotype differences that could align with the weight phenotype.

Interestingly, neuronal deficiency of IL-6 in females, which leads to resistance to the HFD, was associated with decreased *Socs3* expression, which otherwise increased with that diet. This could be interpreted either as a consequence of the reduced adipose tissue, and presumably leptin levels, causing less expression of the negative regulator *Socs3* (Banks et al. 2000) or rather, as the reason why these mice are resistant, having an inherently better sensitivity to leptin, insulin or IL-6 (Howard et al. 2004; Mori et al. 2004). Regarding the cytokine, it is also produced in the muscle in response to contraction (Steensberg et al. 2002) and moderate exercise has been shown to protect from HFD-induced hypothalamic inflammation (Yi et al. 2012). Given that *Il6*$^{\Delta Syn1}$ mice have increased activity, even when fed a HFD, increased sensibility to peripheral IL-6 might be related to their phenotype.

Fasting has been associated with an anti-inflammatory effect in the brain (Lavin et al. 2011), as the counterpoint to the caloric excess of HFD. Our present results seem to go along the same lines, since we also observed a decrease in a microglia/macrophage marker, in our case *Mac1*, and an increase in *Il6* (possibly a reflection of its more anti-inflammatory effects), though only in males.

Nevertheless, conditional knock-outs that are not inducible, such as these ones, have the caveat of affecting developmental stages in an uncontrolled way, so compensatory mechanisms could be in place. For example, microglial cells, which also secrete cytokines in response to fatty acids (Milanski et al. 2009), might play a relevant role. Further studies with a conditional and inducible microglial IL-6 knock-out are currently under way in our group and they are bound to add to our understanding of this point.

Taken together, these results add the **source of the cytokine** as a critical factor to the already stablished dichotomy of hypothalamic inflammation, whereby high levels of inflammatory cytokines promote a negative energy balance (De Benedetti et al. 1997; Hidalgo et al. 2010; Arruda et al. 2011), in line with endotoxemia-induced anorexia or cancer cachexia; while low-grade inflammation has the reverse effect (Münzberg et al. 2004; Arruda et al. 2011).

6.5 Behavior

In order to further characterize the role of the different sources of IL-6 in the CNS, the aim here was to complete our group's previous results using *Il6*$^{\Delta Gfap}$ mice with *Il6*$^{\Delta Syn1}$ and *Il6ra*$^{\Delta Syn1}$ mice.

6.5.1 Locomotor activity

Spontaneous locomotor activity was evaluated specifically in the OF, but also as an additional measure in the HB.

It had been previously shown that mice with astrocytic deficiency of IL-6 or its receptor display a significant decrease in activity in the HB, especially in female mice (Quintana et al. 2013; Erta et al. 2015). In contrast, *Il6*$^{\Delta Syn1}$ mice showed the opposite phenotype, with higher ambulation rates in the OF and HB, being the effect more robust in male mice.

Since astrocytic deletion of the membrane IL-6 receptor (by using *Il6ra*$^{\Delta Gfap}$ mice) showed a similar phenotype than that observed in *Il6*$^{\Delta Gfap}$ mice, it was logical to suggest that astrocytic IL-6 act in an autocrine or paracrine (on neighboring astrocytes) way to control this behavioral trait. Therefore, it was also tempting to speculate that neuronal IL-6 should act preferentially on neurons (and/or cells other than astrocytes) to regulate ambulation, since the phenotype

of *Il6*$^{\Delta Syn1}$ mice is opposed to that of *Il6*$^{\Delta Gfap}$ mice. However, the lack of neuronal IL-6Rα has shown a much less dramatic phenotype than *Il6*$^{\Delta Syn1}$ mice, with only increased activity in the external areas of the HB in females.

Regardless of the exact targets, it is clear that astrocytic IL-6 increases locomotor activity in mice, whereas neuronal IL-6 inhibits it. Opposing roles of astrocytic and neuronal IL-6 may be at the root of the discrepancies observed with IL-6KO mice in several studies. With this model, depending on the production of IL-6 by each cell type (which might be affected by a wide range of factors) a different outcome could be obtained. Our group had previously observed a decreased activity of systemic IL-6KO mice in the HB (Armario et al. 1998), whereas others found the opposite in the OF (Butterweck et al. 2003). Other studies, however, showed normal behavior in the novel cage and OF paradigms (Chourbaji et al. 2006), or in an hour-long OF in sham-operated animals (Ley et al. 2011). Also, in a different genetic background, IL-6 deficiency did not alter activity in home and novel cages and in an OF (Swiergiel and Dunn 2006). On the other hand, central injection of IL-6 left ambulatory behavior unchanged in the OF (Sukoff Rizzo et al. 2012), but an increase was observed when a chronic viral approach was used (Wei et al. 2012). Perinatal subdural administration of hyper IL-6 (a fusion protein of human IL-6 and IL-6Rα) also causes an early increase in locomotion and earlier emergence of some activity-related behaviors, but they later dissipate (Brunssen et al. 2013). Moreover, peripheral administration of IL-6 increased activity and exploratory behavior in mice (Zalcman et al. 1998). Therefore, astrocytic *vs* neuronal and central *vs* peripheral sources of IL-6 may underlie the discrepancies between different studies reported so far regarding the role of this cytokine on general activity of rodents.

6.5.2 Exploration

Rearings and head dippings are considered measures of exploratory behavior (File and Wardill 1975; Lever et al. 2006). *Il6*$^{\Delta Syn1}$ males consistently showed increased rearings, while females had the same tendency but depending on the test the difference was not significant. In *Il6ra*$^{\Delta Syn1}$ mice however, only females showed increased rearings in the OF and HB. Head dippings in the HB were increased in *Il6*$^{\Delta Syn1}$ males and unaffected in females, and no apparent differences were observed in *Il6ra*$^{\Delta Syn1}$ mice. The same behavior in the EPM was also increased, despite the different nature of the two apparatuses. In *Il6*$^{\Delta Gfap}$ mice, a similar pattern was seen in the HB and EPM, suggestive of a detrimental role of astrocytic IL-6 in exploration (Quintana et al. 2013).

Sex differences could be related to the more prominent effect of neuronal IL-6 deficiency observed in male mice in ambulation, since it may be correlated with measures of exploration (Lalonde and Strazielle 2008), but then the results for *Il6*$^{\Delta Gfap}$ mice do not completely fit with this hypothesis. What is clear, however, is that combined, the results for exploratory behavior do not support opposed roles of astrocytic and neuronal sources of IL-6 as was the case for activity. Thus, one should expect a more robust phenotype in total IL-6 KO mice; however, they showed decreased rearings and head-dippings in the HB or OF (Armario et al. 1998; Butterweck et al. 2003), which is contrary to expectations based on the effects of astrocytic and neuronal IL-6 deficiencies. Clearly, much still remains to be understood in this regard.

6.5.3 Anxiety-like behavior

We have found that lack of neuronal IL-6 decreases anxiety-like behavior in male mice (as assessed by relative open arm entries and time in the EPM), which is not clearly recapitulated with lack of the neuronal receptor despite there being a trend in the same sense.

Systemic IL-6KO mice have increased anxiety as indicated by their behavior in the EPM, where they enter less and spend less time in the open arms (Armario et al. 1998; Butterweck et al. 2003). Some studies, however, do not find increased anxiety levels in normal conditions (Swiergiel and Dunn 2006), but do after either a forced-swim test, suggesting a greater susceptibility to the anxiogenic effect of stress (Baier et al. 2009). In agreement with these EPM results, the time spent in the lit compartment of the dark-light box was decreased in systemic IL-6KO mice, supporting increased anxiety levels (Chourbaji et al. 2006). Interestingly, increased CNS IL-6 production by infection with an adenovirus decreased anxiety in the EPM in mice (Wei et al. 2012); and in rats bred for extremes in anxiety-related behavior, those with high anxiety have lower circulating IL-6 levels than those with low anxiety (Salome et al. 2008). It was therefore surprising to find that male *Il6*$^{\Delta Syn1}$ mice showed a prominent decrease of anxiety levels in the EPM. A similar, albeit subtler, trend had been observed in *Il6*$^{\Delta Gfap}$ male mice (Quintana et al. 2013). Thus, similarly to exploration and contrary to activity, neuronal and astrocytic IL-6 seem to exert similar effects on the control of anxiety, but the greater phenotype of *Il6*$^{\Delta Syn1}$ mice suggests a more prominent role of the neuronal source. Why these are the opposite to those observed in systemic IL-6KO mice remains to be established. The lack of clear effects of the deficit of either membrane receptor might point to a role of trans-signaling in regulating anxiety-like behavior. Indeed, blockade of trans-signaling prevents the stress-induced IL-6-dependent postsynaptic inhibition that normally shifts the balance towards excitation (Garcia-Oscos et al. 2012).

6.5.4 Spatial learning

Hippocampus-dependent learning was assessed in *Il6*$^{\Delta Syn1}$ mice in the MWM (Vorhees and Williams 2006), but no learning alterations were evidenced by lack of neuronal IL-6. This was quite surprising, since previous results suggested a deleterious role of IL-6. *In vitro* treatment with IL-6 or transgenic expression of IL-6 (in GFAP-IL6 mice) impaired long-term potentiation (LTP) and different kinds of hippocampus-dependent learning (Bellinger et al. 1995; Heyser et al. 1997; Li et al. 1997; Samuelsson et al. 2006). Conversely, application of a neutralizing anti-IL6 antibody significantly improved LTP and spatial alternation learning and long-term memory in rats (Balschun et al. 2004). However, more recent results with systemic IL-6KO mice suggest otherwise; these mice displayed a clear impairment both in the performance in the MWM (Baier et al. 2009), and in the novel object recognition memory test, which is hippocampus-independent (Hryniewicz et al. 2007; Baier et al. 2009), pointing to a beneficial role of IL-6 instead. In line with this, *Il6*$^{\Delta Gfap}$ and *Il6ra*$^{\Delta Gfap}$ mice also had impaired spatial learning in the MWM (Erta et al. 2015). The discrepancy with the direct effect of IL-6 might be an example of the previously mentioned developmental effects of the deficiency *vs* activity in the adult.

Therefore, IL-6 clearly has a role in spatial learning which seems to rely more on that produced by astrocytes, acting in an autocrine way. Future studies with other conditional knock-outs (such as microglial) and *Il6ra*$^{\Delta Syn1}$ might help paint a more complete picture of the producer and target cells implicated.

In general, the phenotypic differences between *Il6*$^{\Delta Syn1}$ and *Il6*$^{\Delta Gfap}$ mice clearly demonstrate that the source of IL-6 is critical for understanding its roles, and that autocrine and/or paracrine actions of IL-6, rather than more conventional endocrine actions, are of critical importance in the CNS.

7 CONCLUSIONS

In this work, we have used conditional IL-6 and IL6-Rα knock-out mice in astrocytes or neurons, as well as the GFAP-IL6 chronic neuroinflammation mouse model, in order to characterize the role of CNS-produced IL-6 in the regulation of body weight and behavior.

In light of our results we can conclude that:

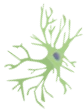

Astrocytic IL-6:

1. has a pro-survival and growth-promoting *in utero* effect, evidenced by the underrepresentation and reduced body weight of astrocytic conditional knock-out mice at the moment of weaning.
2. inhibits longitudinal bone growth, which in females could be mediated by IGF-1 given the correlation of tibial length with serum IGF-1 levels, although earlier measures would be required to consolidate this possibility.
3. inhibits obesity in a situation of chronic caloric excess, without affecting energy intake, but has no effect on glucose homeostasis.
4. shows no effect on inflammatory markers in the hypothalamus in a short-term high-fat diet.

Neuronal IL-6:

5. also has a pro-survival *in utero* effect, evidenced by the reduced weaning frequency of neuronal conditional knock-out mice at weaning.
6. promotes longitudinal bone growth, in principle independently of IGF-1, although earlier effects should not be disregarded.
7. promotes obesity, with a secondary affectation of glucose homeostasis, in a situation of chronic caloric excess, possibly by affecting activity rather than

energy intake; even though, in a context of caloric deficit it is necessary for the compensatory food intake, especially in males.

8. restricts spontaneous locomotor activity and exploration and facilitates anxiety-like behavior, though it lacks an effect on spatial learning and memory.

Neuronal IL-6Rα:

9. is necessary to mediate the positive autocrine effect of IL-6 on bone length, given that lack of the receptor and the cytokine in neurons yield a similar phenotype.
10. mediates the effect of IL-6 in compensatory food intake after a fast in females, suggesting that autocrine action of IL-6 is more relevant in this sex.
11. does not seem to mediate the effects of either astrocytic or neuronal IL-6 on locomotor activity, exploration, or anxiety-like behavior.

In general,

12. leaked Cre recombinase activity depends on the promoter and is a prevalent phenomenon that must be carefully accounted for.
13. hemizygosity of *Il6* due to off-target recombination is not critical for the observed phenotypes, suggesting that they are specific to the conditional knock-out.
14. sex differences depending on genetic model or intervention reinforce the importance of working with males and females.
15. IL-6 likely participates in the development of brain circuitry, given the many phenotypes observed in conditional knock-outs but failure to detect differential *Il6* expression in the adult brain.

16. the **cellular source of IL-6 in the CNS**, being it astrocytes or neurons, is **critical for determining its effects**, as evidenced by the, in many cases, opposed phenotypes of the two conditional knock-out models. Thus, the source differentially affects the response to a caloric challenge, general locomotion, and linear growth; whilst having similar actions on *in utero* survival, exploration and anxiety.

8 REFERENCES

Abizaid A, Liu ZW, Andrews ZB, Shanabrough M, Borok E, Elsworth JD, Roth RH, Sleeman MW, Picciotto MR, Tschöp MH, Gao XB, Horvath TL (2006) Ghrelin modulates the activity and synaptic input organization of midbrain dopamine neurons while promoting appetite. J Clin Invest 116:3229–3239. doi: 10.1172/JCI29867

Ahn JD, Dubern B, Lubrano-Berthelier C, Clement K, Karsenty G (2006) Cart overexpression is the only identifiable cause of high bone mass in melanocortin 4 receptor deficiency. Endocrinology 147:3196–3202. doi: 10.1210/en.2006-0281

Akaneya Y, Takahashi M, Hatanaka H (1995) Interleukin-1β enhances survival and interleukin-6 protects against MPP+ neurotoxicity in cultures of fetal rat dopaminergic neurons. Exp. Neurol. 136:44–52.

Akira S, Hirano T, Taga T, Kishimoto T (1990) Biology of multifunctional cytokines: IL 6 and related molecules (IL 1 and TNF). FASEB J 4:2860–2867.

Aniszewska A, Chłodzińska N, Bartkowska K, Winnicka MM, Turlejski K, Djavadian RL (2015) The expression of interleukin-6 and its receptor in various brain regions and their roles in exploratory behavior and stress responses. J Neuroimmunol 284:1–9. doi: 10.1016/j.jneuroim.2015.05.001

Arenas MC, Daza-Losada M, Vidal-Infer A, Aguilar MA, Miñarro J, Rodríguez-Arias M (2014) Capacity of novelty-induced locomotor activity and the hole-board test to predict sensitivity to the conditioned rewarding effects of cocaine. Physiol Behav 133:152–160. doi: 10.1016/j.physbeh.2014.05.028

Arletti R, Benelli A, Bertolini A (1990) Oxytocin inhibits food and fluid intake in rats. Physiol Behav 48:825–830. doi: 10.1016/0031-9384(90)90234-U

Armario A, Hernández J, Bluethmann H, Hidalgo J (1998) IL-6 deficiency leads to increased emotionality in mice: evidence in transgenic mice carrying a null mutation for IL-6. J Neuroimmunol 92:160–169. doi: 10.1016/S0165-5728(98)00199-4

Arruda AP, Milanski M, Coope A, Torsoni AS, Ropelle E, Carvalho DP, Carvalheira JB, Velloso LA (2011) Low-grade hypothalamic inflammation leads to defective thermogenesis, insulin resistance, and impaired insulin secretion. Endocrinology 152:1314–1326. doi: 10.1210/en.2010-0659

Artz E, Buric R, Stelzer G, Stalla J, Sauer J, Renner U, Stalla GK (1993) Interleukin involvement in anterior pituitary cell growth regulation: effects of IL-2 and IL-6. Endocrinology 132:459–467.

Asnicar MA, Smith DP, Yang DD, Heiman ML, Fox N, Chen Y-F, Hsiung HM, Köster A (2001) Absence of cocaine- and amphetamine-regulated transcript results in obesity in mice fed a high caloric diet. Endocrinology 142:4394–4400. doi: 10.1210/endo.142.10.8416

Atreya R, Mudter J, Finotto S, Müllberg J, Jostock T, Wirtz S, Schütz M, Bartsch B, Holtmann M, Becker C, Strand D, Czaja J, Schlaak JF, Lehr HA, Autschbach F, Schürmann G, Nishimoto N, Yoshizaki K, Ito H, Kishimoto T, Galle PR, Rose-John S, Neurath MF (2000) Blockade of interleukin 6 trans signaling suppresses T-cell resistance against apoptosis in chronic intestinal inflammation: evidence in Crohn disease and experimental colitis in vivo. Nat Med 6:583–588. doi: 10.1038/nm1110-1341

Bai D, Ueno L, Vogt PK (2009) Akt-mediated regulation of NFκB and the essentialness of NFκB for the oncogenicity of PI3K and Akt. Int J Cancer 125:2863–2870. doi: 10.1002/ijc.24748

Baier PC, May U, Scheller J, Rose-John S, Schiffelholz T (2009) Impaired hippocampus-dependent and -independent learning in IL-6 deficient mice. Behav Brain Res 200:192–196. doi:

10.1016/j.bbr.2009.01.013

Bailey ART, Von Englehardt N, Leng G, Smith RG, Dickson SL (2000) Growth hormone secretagogue activation of the arcuate nucleus and brainstem occurs via a non-noradrenergic pathway. J Neuroendocrinol 12:191–197. doi: 10.1046/j.1365-2826.2000.00398.x

Bajenaru ML, Zhu Y, Hedrick NM, Donahoe J, Parada LF, Gutmann DH (2002) Astrocyte-specific inactivation of the neurofibromatosis 1 gene (NF1) is insufficient for astrocytoma formation. Mol Cell Biol 22:5100–5113. doi: 10.1128/MCB.22.14.5100-5113.2002

Balschun D, Wetzel W, del Rey A, Pitossi F, Schneider H, Zuschratter W, Besedovsky HO (2004) Interleukin-6: a cytokine to forget. FASEB J 18:1788–1790. doi: 10.1096/fj.04-1625fje

Banks AS, Davis SM, Bates SH, Myers MG (2000) Activation of downstream signals by the long form of the leptin receptor. J Biol Chem 275:14563–14572. doi: 10.1074/jbc.275.19.14563

Banks WA, Jaspan JB, Huang W, Kastin AJ (1997) Transport of insulin across the blood-brain barrier: saturability at euglycemic doses of insulin. Peptides 18:1423–1429. doi: 10.1016/S0196-9781(97)00231-3

Banks WA, Kastin AJ, Gutierrez EG (1994) Penetration of IL-6 across the murine blood-brain barrier. Neurosci Lett 179:53–56. doi: 10.1016/0304-3940(94)90933-4

Banks WA, Kastin AJ, Huang W, Jaspan JB, Maness LM (1996) Leptin enters the brain by a saturable system independent of insulin. Peptides 17:305–311. doi: 10.1016/0196-9781(96)00025-3

Barker DJP, Hales CN, Fall CHD, Smond CO, Phipps K, Clark PMS (1993) Type 2 (non-insulin-dependent) diabetes mellitus, hypertension and hyperlipidaemia (syndrome X): relation to reduced fetal growth. Diabetologia 36:62–67. doi: 10.1007/BF00399095

Bartolomucci A, Palanza P, Sacerdote P, Ceresini G, Chirieleison A, Panerai AE, Parmigiani S (2003) Individual housing induces altered immuno-endocrine responses to psychological stress in male mice. Psychoneuroendocrinology 28:540–558. doi: 10.1016/S0306-4530(02)00039-2

Bastard JP, Maachi M, Van Nhieu JT, Jardel C, Bruckert E, Grimaldi A, Robert JJ, Capeau J, Hainque B (2002) Adipose tissue IL-6 content correlates with resistance to insulin activation of glucose uptake both in vivo and in vitro. J Clin Endocrinol Metab 87:2084–2089. doi: 10.1210/jc.87.5.2084

Basterzi AD, Aydemir Ç, Kisa C, Aksaray S, Tuzer V, Yazici K, Göka E (2005) IL-6 levels decrease with SSRI treatment in patients with major depression. Hum Psychopharmacol Clin Exp 20:473–476. doi: 10.1002/hup.717

Bauer J, Lengyel G, Bauer TM, Acs G, Gerok W (1989) Regulation of interleukin-6 receptor expression in human monocytes and hepatocytes. FEBS Lett 249:27–30. doi: 10.1016/0014-5793(89)80008-0

Baufeld C, Osterloh A, Prokop S, Miller KR, Heppner FL (2016) High-fat diet-induced brain region-specific phenotypic spectrum of CNS resident microglia. Acta Neuropathol 132:361–375. doi: 10.1007/s00401-016-1595-4

Baumann H, Gauldie J (1994) The acute phase response. Immunol Today 15:74–80. doi: 10.1016/0167-5699(94)90137-6

Bazan JF (1990) Structural design and molecular evolution of a cytokine receptor superfamily. Proc Natl Acad Sci 87:6934–6938. doi: 10.1073/pnas.87.18.6934

Bazin R, Lemieux R (1987) Role of the macrophage-derived hybridoma growth factor in the in vitro and in vivo proliferation of newly formed B cell hybridomas. J Immunol 139:780–787.

Belda X, Daviu N, Nadal R, Armario A (2012) Acute stress-induced sensitization of the pituitary-adrenal response to heterotypic stressors: Independence of glucocorticoid release and

activation of CRH1 receptors. Horm Behav 62:515–524. doi: 10.1016/j.yhbeh.2012.08.013

Bellinger FP, Madamba SG, Campbell IL, Siggins GR (1995) Reduced long-term potentiation in the dentate gyrus of transgenic mice with cerebral overexpression of interleukin-6. Neurosci Lett 198:95–98. doi: 10.1016/0304-3940(95)11976-4

Benoit SC, Air EL, Coolen LM, Strauss R, Jackman A, Clegg DJ, Seeley RJ, Woods SC (2002) The catabolic action of insulin in the brain is mediated by melanocortins. J Neurosci 22:9048–9052.

Benrick A, Schéle E, Pinnock SB, Wernstedt-Asterholm I, Dickson SL, Karlsson-Lindahl L, Jansson J-O (2009) Interleukin-6 gene knockout influences energy balance regulating peptides in the hypothalamic paraventricular and supraoptic nuclei. J Neuroendocrinol 21:620–628. doi: 10.1111/j.1365-2826.2009.01879.x

Benveniste EN, Sparacio SM, Norris G, Grenett HE, Fuller GM (1990) Induction and regulation of interleukin-6 gene expression in rat astrocytes. J Neuroimmunol 30:201–212. doi: 10.1016/0165-5728(90)90104-U

Benzler J, Ganjam GK, Pretz D, Oelkrug R, Koch CE, Legler K, Stöhr S, Culmsee C, Williams LM, Tups A (2015) Central inhibition of IKKβ/NF-κB signaling attenuates high-fat diet-induced obesity and glucose intolerance. Diabetes 64:2015–2027. doi: 10.2337/db14-0093

Bersell K, Choudhury S, Mollova M, Polizzotti BD, Ganapathy B, Walsh S, Wadugu B, Arab S, Kühn B (2013) Moderate and high amounts of tamoxifen in αMHC-MerCreMer mice induce a DNA damage response, leading to heart failure and death. Dis Model Mech 6:1459–69. doi: 10.1242/dmm.010447

Bethin KE, Vogt SK, Muglia LJ (2000) Interleukin-6 is an essential, corticotropin-releasing hormone-independent stimulator of the adrenal axis during immune system activation. Proc Natl Acad Sci 97:9317–9322. doi: 10.1073/pnas.97.16.9317

Betz UA, Müller W (1998) Regulated expression of gp130 and IL-6 receptor alpha chain in T cell maturation and activation. Int Immunol 10:1175–1184. doi: 10.1093/intimm/10.8.1175

Billington CJ, Briggs JE, Harker S, Grace M, Levine AS (1994) Neuropeptide Y in hypothalamic paraventricular nucleus: a center coordinating energy metabolism. Am J Physiol 266:R1765-1770.

Bjurholm A, Kreicbergs A, Schultzberg M, Lerner UH (1988) Parathyroid hormone and noradrenaline-induced enhancement of cyclic AMP in a cloned osteogenic sarcoma cell line (UMR 106) is inhibited by neuropeptide Y. Acta Physiol Scand 134:451–452. doi: 10.1111/j.1748-1716.1988.tb08515.x

Boissier JR, Simon P (1962) La réaction d'exploration chez la souris. Therapie 17:1225–1232.

Bolin LM, Verity AN, Silver JE, Shooter EM, Abrams JS (1995) Interleukin-6 production by Schwann cells and induction in sciatic nerve injury. J Neurochem 64:850–858. doi: 10.1046/j.1471-4159.1995.64020850.x

Boulanger MJ, Chow D, Brevnova EE, Garcia KC (2003) Hexameric structure and assembly of the interleukin-6/IL-6 alpha-receptor/gp130 complex. Science 300:2101–2104. doi: 10.1126/science.1083901

Boulant JA (2000) Role of the preoptic-anterior hypothalamus in thermoregulation and fever. Clin Infect Dis 31:S157-161. doi: 10.1086/317521

Bowers RR, Festuccia WTL, Song CK, Shi H, Migliorini RH, Bartness TJ (2004) Sympathetic innervation of white adipose tissue and its regulation of fat cell number. Am J Physiol 286:R1167–R1175. doi: 10.1152/ajpregu.00558.2003

REFERENCES

Braida D, Sacerdote P, Panerai AE, Bianchi M, Aloisi AM, Iosuè S, Sala M (2004) Cognitive function in young and adult IL (interleukin)-6 deficient mice. Behav Brain Res 153:423–429. doi: 10.1016/j.bbr.2003.12.018

Bray GA (2000) Reciprocal relation of food intake and sympathetic activity: experimental observations and clinical implications. Int J Obes 24:S8-17.

Brenner M, Kisseberth WC, Su Y, Besnard F, Messing A (1994) GFAP promoter directs astrocyte-specific expression in transgenic mice. J Neurosci 14:1030–1037.

Bristow A, Mosley K, Poole S (1991) Interleukin-1 beta production in vivo and in vitro in rats and mice measured using specific immunoradiometric assays. J Mol Endocrinol 7:1–7.

Broberger C, de Lecea L, Sutcliffe JG, Hökfelt T (1998) Hypocretin/orexin- and hormone-expressing cells form distinct populations in the rodent lateral hypothalamus: relationship to the neuropeptide Y and agouti gene-related protein systems. J Comp Neurol 402:460–474.

Brown GR, Nemes C (2008) The exploratory behaviour of rats in the hole-board apparatus: Is head-dipping a valid measure of neophilia? Behav Processes 78:442–448. doi: 10.1016/j.beproc.2008.02.019

Brunssen SH, Moy SS, Toews AD, McPherson CA, Harry GJ (2013) Interleukin-6 (IL-6) receptor/IL-6 fusion protein (Hyper IL-6) effects on the neonatal mouse brain: possible role for IL-6 trans-signaling in brain development and functional neurobehavioral outcomes. Brain Behav Immun 27:42–53. doi: 10.1016/j.bbi.2012.08.017

Buckman LB, Hasty AH, Flaherty DK, Buckman CT, Thompson MM, Matlock BK, Weller K, Ellacott KLJ (2014) Obesity induced by a high-fat diet is associated with increased immune cell entry into the central nervous system. Brain Behav Immun 35:33–42. doi: 10.1016/j.bbi.2013.06.007

Buckman LB, Thompson MM, Moreno HN, Ellacott KLJ (2013) Regional astrogliosis in the mouse hypothalamus in response to obesity. J Comp Neurol 521:1322–33. doi: 10.1002/cne.23233

Butterweck V, Prinz S, Schwaninger M (2003) The role of interleukin-6 in stress-induced hyperthermia and emotional behaviour in mice. Behav Brain Res 144:49–56. doi: 10.1016/S0166-4328(03)00059-7

Cabeza de Vaca S, Carr KD (1998) Food restriction enhances the central rewarding effect of abused drugs. J Neurosci 18:7502–7510.

Cadman ED, Witte DG, Lee CM (1994) Regulation of the release of interleukin-6 from human astrocytoma cells. J Neurochem 63:980–987.

Campbell IL, Abraham CR, Masliah E, Kemper P, Inglis JD, Oldstone MB, Mucke L (1993) Neurologic disease induced in transgenic mice by cerebral overexpression of interleukin 6. Proc Natl Acad Sci 90:10061–10065.

Campbell IL, Cutri A, Wilson A, Harrison LC (1989) Evidence for IL-6 production by and effects on the pancreatic beta-cell. J Immunol 143:1188–91.

Campbell IL, Erta M, Lim SL, Frausto R, May U, Rose-John S, Scheller J, Hidalgo J (2014) Trans-signaling is a dominant mechanism for the pathogenic actions of interleukin-6 in the brain. J Neurosci 34:2503–2513. doi: 10.1523/JNEUROSCI.2830-13.2014

Campbell IL, Hobbs M V, Kemper P, Oldstone MB (1994) Cerebral expression of multiple cytokine genes in mice with lymphocytic choriomeningitis. J Immunol 152:716–723.

Caro JF, Kolaczynski JW, Nyce MR, Ohannesian JP, Opentanova I, Goldman WH, Lynn RB, Pei-Li Z, Sinha MK, Considine R V (1996) Decreased cerebrospinal-fluid/serum leptin ratio in obesity: a possible mechanism for leptin resistance. Lancet 348:159–161.

Carpéné C, Bousquet-Mélou A, Galitzky J, Berlan M, Lafontan M (1998) Lipolytic effects of β1-, β2-,

and β3-adrenergic agonists in white adipose tissue of mammals. Ann N Y Acad Sci 839:186–189. doi: 10.1111/j.1442-9993.2007.01825.x

Carpenter LL, Heninger GR, Malison RT, Tyrka AR, Price LH (2004) Cerebrospinal fluid interleukin (IL)-6 in unipolar major depression. J Affect Disord 79:285–289. doi: 10.1016/S0165-0327(02)00460-3

Carson MJ, Doose JM, Melchior B, Schmid CD, Ploix CC (2006) CNS immune privilege: hiding in plain sight. Immunol Rev 213:48–65. doi: 10.1111/j.1600-065X.2006.00441.x.CNS

Catar R, Witowski J, Zhu N, Lücht C, Derrac Soria A, Uceda Fernandez J, Chen L, Jones SA, Fielding CA, Rudolf A, Topley N, Dragun D, Jörres A (2016) IL-6 trans-signaling links inflammation with angiogenesis in the peritoneal membrane. J Am Soc Nephrol 28:ahead of print. doi: 10.1681/ASN.2015101169

Chai Z, Gatti S, Toniatti C, Poli V, Bartfai T (1996) Interleukin (IL)-6 gene expression in the central nervous system is necessary for fever response to lipopolysaccharide or IL-1β: a study on IL-6-deficient mice. J Exp Med 183:311–316. doi: 10.1084/jem.183.1.311

Chalaris A, Rabe B, Paliga K, Lange H, Laskay T, Fielding CA, Jones SA, Rose-John S, Scheller J (2007) Apoptosis is a natural stimulus of IL6R shedding and contributes to the proinflammatory trans-signaling function of neutrophils. Blood 110:1748–1755. doi: 10.1182/blood-2007-01-067918

Chambers AP, Sandoval DA, Seeley RJ (2013) Integration of satiety signals by the central nervous system. Curr Biol 23:R379–R388. doi: 10.1016/j.cub.2013.03.020

Chen G, Castro WL, Chow H, Reichlin S, College A (1997) Clearance of 125 I-labeled interleukin-6 from brain into blood following intracerebroventricular injection in rats. Endocrinology 138:4830–4836.

Chiang CS, Stalder A, Samimi A, Campbell IL (1994) Reactive gliosis as a consequence of interleukin-6 expression in the brain: studies in transgenic mice. Dev Neurosci 16:212–221. doi: 10.1159/000112109

Chikuma T, Yoshimoto T, Ohba M, Sawada M, Kato T, Sakamoto T, Hiyama Y, Hojo H (2009) Interleukin-6 induces prostaglandin E2 synthesis in mouse astrocytes. J Mol Neurosci 39:175–184.

Chomarat P, Banchereau J, Davoust J, Palucka AK (2000) IL-6 switches the differentiation of monocytes from dendritic cells to macrophages. Nat Immunol 1:510–514. doi: 10.1038/82763

Chomczynski P, Sacchi N (1987) Single-step method of RNA isolation by acid guanidinium thiocyanate-phenol-chloroform extraction. Anal Biochem 162:156–159. doi: 10.1016/0003-2697(87)90021-2

Chourbaji S, Urani A, Inta I, Sanchis-Segura C, Brandwein C, Zink M, Schwaninger M, Gass P (2006) IL-6 knockout mice exhibit resistance to stress-induced development of depression-like behaviors. Neurobiol Dis 23:587–594. doi: 10.1016/j.nbd.2006.05.001

Clark JT, Kalra PS, Crowley WR, Kalra SP (1984) Neuropeptide Y and human Pancreatic polypeptide stimulate feeding behavior in rats. Endocrinology 115:427–429. doi: 10.1017/CBO9781107415324.004

Codeluppi S, Fernandez-Zafra T, Sandor K, Kjell J, Liu Q, Abrams M, Olson L, Gray NS, Svensson CI, Uhlén P (2014) Interleukin-6 secretion by astrocytes is dynamically regulated by PI3K-mTOR-calcium signaling. PLoS One 9:e92649. doi: 10.1371/journal.pone.0092649

Cone RD (2005) Anatomy and regulation of the central melanocortin system. Nat Neurosci 8:571–578. doi: 10.1038/nn1455

REFERENCES

Cone RD, Cowley MA, Butler AA, Fan W, Marks DL, Low MJ (2001) The arcuate nucleus as a conduit for diverse signals relevant to energy homeostasis. Int J Obes 25:S63–S67. doi: 10.1038/sj.ijo.0801913

Cowley MA, Smart JL, Rubinstein M, Cerdán MG, Diano S, Horvath TL, Cone RD, Low MJ (2001) Leptin activates anorexigenic POMC neurons through a neural network in the arcuate nucleus. Nature 411:480–484. doi: 10.1038/35078085

Cowley MA, Smith RG, Diano S, Tschöp M, Pronchuk N, Grove KL, Strasburger CJ, Bidlingmaier M, Esterman M, Heiman ML, Garcia-Segura LM, Nillni EA, Mendez P, Low MJ, Sotonyi P, Friedman JM, Liu H, Pinto S, Colmers WF, Cone RD, Horvath TL (2003) The distribution and mechanism of action of ghrelin in the CNS demonstrates a novel hypothalamic circuit regulating energy homeostasis. Neuron 37:649–661. doi: 10.1016/S0896-6273(03)00063-1

Cressman DE, Greenbaum LE, DeAngelis RA, Ciliberto G, Furth EE, Poli V, Taub R (1996) Liver failure and defective hepatocyte regeneration in interleukin-6-deficient mice. Science 274:1379–1383. doi: 10.1126/science.274.5291.1379

Cross DA, Alessi DR, Cohen P, Andjelkovich M, Hemmings BA (1995) Inhibition of glycogen synthase kinase-3 by insulin mediated by protein kinase B. Nature 378:785–789. doi: 10.1038/378785a0

Curnow SJ, Scheel-Toellner D, Jenkinson W, Raza K, Durrani OM, Faint JM, Rauz S, Wloka K, Pilling D, Rose-John S, Buckley CD, Murray PI, Salmon M (2004) Inhibition of T cell apoptosis in the aqueous humor of patients with uveitis by IL-6/soluble IL-6 receptor trans-signaling. J Immunol 173:5290–7. doi: 10.4049/jimmunol.173.8.5290

Dalrymple SA, Lucian LA, Slattery R, McNeil T, Aud DM, Fuchino S, Lee F, Murray R (1995) Interleukin-6-deficient mice are highly susceptible to Listeria monocytogenes infection: correlation with inefficient neutrophilia. Infect Immun 63:2262–2268.

Dantzer R (2001) Cytokine-induced sickness behavior: mechanisms and implications. Ann N Y Acad Sci 933:222–234. doi: 10.1016/S0889-1591(02)00077-6

Dantzer R, Kelley KW (2007) Twenty years of research on cytokine-induced sickness behavior. Brain Behav Immun 21:153–160. doi: 10.1016/j.bbi.2006.09.006

Dantzer R, Wollman EE, Vitkovic L, Yirmiya R (1999) Cytokines and depression: fortuitous or causative association? Mol Psychiatry 4:328–32. doi: 10.1007/978-0-585-37970-8_17

Das UN (2010) Obesity: Genes, brain, gut, and environment. Nutrition 26:459–473. doi: 10.1016/j.nut.2009.09.020

Date Y, Murakami N, Toshinai K, Matsukura S, Niijima A, Matsuo H, Kangawa K, Nakazato M (2002) The role of the gastric afferent vagal nerve in ghrelin-induced feeding and growth hormone secretion in rats. Gastroenterology 123:1120–1128. doi: 10.1053/gast.2002.35954

Davis S, Aldrich TH, Stahl N, Pan L, Taga T, Kishimoto T, Ip NY, Yancopoulos GD (1993) LIFR beta and gp130 as heterodimerizing signal transducers of the tripartite CNTF receptor. Science 260:1805–1808. doi: 10.1126/science.8390097

De Benedetti F, Alonzi T, Moretta A, Lazzaro D, Costa P, Poli V, Martini A, Ciliberto G, Fattori E (1997) Interleukin 6 causes growth impairment in transgenic mice through a decrease in insulin-like growth factor-I. A model for stunted growth in children with chronic inflammation. J Clin Invest 99:643–650. doi: 10.1172/JCI119207

de Bock F, Dornand J, Rondouin G (1996) Release of TNF alpha in the rat hippocampus following epileptic seizures and excitotoxic neuronal damage. Neuroreport 7:1125–1129.

De Souza CT, Araujo EP, Bordin S, Ashimine R, Zollner RL, Boschero AC, Saad MJA, Velloso LA (2005) Consumption of a fat-rich diet activates a proinflammatory response and induces insulin

resistance in the hypothalamus. Endocrinology 146:4192–4199. doi: 10.1210/en.2004-1520

Del Fattore A, Cappariello A, Capulli M, Rucci N, Muraca M, De Benedetti F, Teti A (2014) An experimental therapy to improve skeletal growth and prevent bone loss in a mouse model overexpressing IL-6. Osteoporos Int 25:681–692. doi: 10.1007/s00198-013-2479-2

Della-Zuana O, Presse F, Ortola C, Duhault J, Nahon JL, Levens N (2002) Acute and chronic administration of melanin- concentrating hormone enhances food intake and body weight in Wistar and Sprague – Dawley rats. Int J Obes 26:1289–1295. doi: 10.1038/sj.ijo.0802079

Dénes Á, Boldogkoi Z, Uhereczky G, Hornyák Á, Rusvai M, Palkovits M, Kovács KJ (2005) Central autonomic control of the bone marrow: Multisynaptic tract tracing by recombinant pseudorabies virus. Neuroscience 134:947–963. doi: 10.1016/j.neuroscience.2005.03.060

Derouet D, Rousseau F, Alfonsi F, Froger J, Hermann J, Barbier F, Perret D, Diveu C, Guillet C, Preisser L, Dumont A, Barbado M, Morel A, DeLapeyrière O, Gascan H, Chevalier S (2004) Neuropoietin, a new IL-6-related cytokine signaling through the ciliary neurotrophic factor receptor. Proc Natl Acad Sci 101:4827–4832. doi: 10.1073/pnas.0306178101

Di Gregorio GB, Hensley L, Lu T, Ranganathan G, Kern PA (2004) Lipid and carbohydrate metabolism in mice with a targeted mutation in the IL-6 gene: absence of development of age-related obesity. Am J Physiol Endocrinol Metab 287:E182–E187. doi: 10.1152/ajpendo.00189.2003

Dittrich E, Renfrew Haft C, Muys L, Heinrich PC, Graeve L (1996) A di-leucine motif and an upstream serine in the interleukin-6 (IL-6) signal transducer gp130 mediate ligand-induced endocytosis and down-regulation of the IL-6 receptor. J Biol Chem 271:5487–5494. doi: 10.1074/jbc.271.10.5487

Dittrich E, Rose-John S, Gerhartz C, Müllberg J, Stoyan T, Yasukawa K, Heinrich PC, Graeve L (1994) Identification of a region within the cytoplasmic domain of the interleukin-6 (IL-6) signal transducer gp130 important for ligand-induced endocytosis of the IL-6 receptor. J Biol Chem 269:19014–19020.

Diveu C, Lagrue Lak-Hal AH, Froger J, Ravon E, Grimaud L, Barbier F, Hermann J, Gascan H, Chevalier S (2004) Predominant expression of the long isoform of GP130-like (GPL) receptor is required for interleukin-31 signaling. Eur Cytokine Netw 15:291–302.

Dominitzki S, Fantini MC, Neufert C, Nikolaev A, Galle PR, Scheller J, Monteleone G, Rose-John S, Neurath MF, Becker C (2007) Cutting edge: trans-signaling via the soluble IL-6R abrogates the induction of FoxP3 in naive CD4+CD25- T cells. J Immunol 179:2041–2045. doi: 10.4049/jimmunol.179.4.2041

Ducy P, Amling M, Takeda S, Priemel M, Schilling AF, Beil FT, Shen J, Vinson C, Rueger JM, Karsenty G (2000) Leptin inhibits bone formation through a hypothalamic relay: a central control of bone mass. Cell 100:197–207. doi: 10.1016/S0092-8674(00)81558-5

Duncan CP, Shim S-S (1977) The autonomic nerve supply of bone. An experimental study of the intraosseous adrenergic nervi vasorum in the rabbit. J Bone Jt Surg 59:323–330. doi: 10.1159/000140455

Eccleston HB, Andringa KK, Betancourt AM, King AL, Mantena SK, Swain TM, Tinsley HN, Nolte RN, Nagy TR, Abrams GA, Bailey SM (2011) Chronic exposure to a high-fat diet induces hepatic steatosis, impairs nitric oxide bioavailability, and modifies the mitochondrial proteome in mice. Antioxid Redox Signal 15:447–459. doi: 10.1089/ars.2010.3395

Egawa M, Yoshimatsu H, Bray GA (1990) Effect of corticotropin releasing hormone and neuropeptide Y on electrophysiological activity of sympathetic nerves to interscapular brown adipose tissue. Neuroscience 34:771–775. doi: 10.1016/0306-4522(90)90181-3

Elefteriou F, Ahn JD, Takeda S, Starbuck M, Yang X, Liu X, Kondo H, Richards WG, Bannon TW, Noda M, Clement K, Vaisse C, Karsenty G (2005) Leptin regulation of bone resorption by the

sympathetic nervous system and CART. Nature 434:514–520. doi: 10.1038/nature03398

Ellingsgaard H, Ehses J a, Hammar EB, Van Lommel L, Quintens R, Martens G, Kerr-Conte J, Pattou F, Berney T, Pipeleers D, Halban P a, Schuit FC, Donath MY (2008) Interleukin-6 regulates pancreatic alpha-cell mass expansion. Proc Natl Acad Sci 105:13163–13168. doi: 10.1073/pnas.0801059105

Erta M (2014) Role of astrocytic IL-6 and IL-6R in normal physiology and neuroinflammation. Universitat Autònoma de Barcelona

Erta M, Giralt M, Esposito FL, Fernandez-Gayol O, Hidalgo J (2015) Astrocytic IL-6 mediates locomotor activity, exploration, anxiety, learning and social behavior. Horm Behav 73:64–74. doi: 10.1016/j.yhbeh.2015.06.016

Erta M, Giralt M, Jiménez S, Molinero A, Comes G, Hidalgo J (2016) Astrocytic IL-6 Influences the Clinical Symptoms of EAE in Mice. Brain Sci 6:15. doi: 10.3390/brainsci6020015

Erta M, Quintana A, Hidalgo J (2012) Interleukin-6, a major cytokine in the central nervous system. Int J Biol Sci 8:1254–1266. doi: 10.7150/ijbs.4679

Eulenfeld R, Dittrich A, Khouri C, Müller PJ, Mütze B, Wolf A, Schaper F (2012) Interleukin-6 signalling: More than Jaks and STATs. Eur J Cell Biol 91:486–495. doi: 10.1016/j.ejcb.2011.09.010

Eulenfeld R, Schaper F (2009) A new mechanism for the regulation of Gab1 recruitment to the plasma membrane. J Cell Sci 122:55–64. doi: 10.1242/jcs.037226

Fan J, Molina PE, Gelato MC, Lang CH (1994) Differential tissue regulation of insulin-like growth factor-1 content and binding proteins after endotoxin. Endocrinology 134:1685–1692.

Farooqi IS, Yeo GSH, Keogh JM, Aminian S, Jebb SA, Butler G, Cheetham T, Rahilly SO (2000) Dominant and recessive inheritance of morbid obesity associated with melanocortin 4 receptor deficiency. J Clin Invest 106:271–279. doi: 10.1172/JCI9397

Fattori E, Lazzaro D, Musiani P, Modesti A, Alonzi T, Ciliberto G (1995) IL-6 expression in neurons of transgenic mice causes reactive astrocytosis and increase in ramified microglial cells but no neuronal damage. Eur J Neurosci 7:2441–2449. doi: 10.1111/j.1460-9568.1995.tb01042.x

Fei H, Okano HJ, Li C, Lee G-H, Zhao C, Darnell R, Friedman JM (1997) Anatomic localization of alternatively spliced leptin receptors (Ob-R) in mouse brain and other tissues. Proc Natl Acad Sci 94:7001–7005. doi: 10.1073/pnas.94.13.7001

Fekete C, Mihály E, Luo LG, Kelly J, Clausen JT, Mao Q, Rand WM, Moss LG, Kuhar M, Emerson CH, Jackson IM, Lechan RM (2000) Association of cocaine- and amphetamine-regulated transcript-immunoreactive elements with thyrotropin-releasing hormone-synthesizing neurons in the hypothalamic paraventricular nucleus and its role in the regulation of the hypothalamic-pituitary-thyroid a. J Neurosci 20:9224–9234.

Fenselau H, Campbell JN, Verstegen AMJ, Madara JC, Xu J, Shah BP, Resch JM, Yang Z, Mandelblat-Cerf Y, Livneh Y, Lowell BB (2017) A rapidly acting glutamatergic ARC→PVH satiety circuit postsynaptically regulated by α-MSH. Nat Neurosci 20:42–51. doi: 10.1038/nn.4442

Ferguson-Smith AC, Chen Y-F, Newman MS, May LT, Sehgal PB, Ruddle FH (1988) Regional localization of the interferon-β2/B-cell stimulatory factor 2/hepatocyte stimulating factor gene to human chromosome 7p15-p21. Genomics 2:203–208. doi: 10.1016/0888-7543(88)90003-1

Fernández-Alonso A, Benamar K, Sancibrián M, López-Valpuesta F, Miñano F (1996) Role of interleukin-1 beta, interleukin-6 and macrophage inflammatory protein-1 beta in prostaglandin-E2-induced hyperthermia in rats. Life Sci 59:185–190. doi: 10.1016/0024-3205(96)00410-9

Fernandez-Botran R (1991) Soluble cytokine receptors: their role in immunoregulation. FASEB J 5:2567–2574.

Fernandez-Gayol O (2015) Using the wrMTrck plugin to analyze the Morris Water maze in mice. Poster Present. 2015 ImageJ User Dev. Conf. Sep 3-4; Madison, WI, USA.

Ferrer B, Navia B, Giralt M, Comes G, Carrasco J, Molinero A, Quintana A, Señarís RM, Hidalgo J (2014) Muscle-specific interleukin-6 deletion influences body weight and body fat in a sex-dependent manner. Brain Behav Immun 40:121–130. doi: 10.1016/j.bbi.2014.03.001

Figlewicz DP, Bennett J, Evans SB, Kaiyala K, Sipols AJ, Benoit SC, Evans B, Da R, Mh RO (2004) Intraventricular insulin and leptin reverse place preference conditioned with high-fat diet in rats. Behav Neurosci 118:479–487. doi: 10.1037/0735-7044.118.3.479

Figlewicz DP, Evans SB, Murphy J, Hoen M, Baskin DG (2003) Expression of receptors for insulin and leptin in the ventral tegmental area / substantia nigra (VTA/SN) of the rat. Brain Res 964:107–115. doi: 10.1016/j.brainres.2015.12.041

Figlewicz DP, Higgins MS, Ng-Evans SB, Havel PJ (2001) Leptin reverses sucrose-conditioned place preference in food-restricted rats. Physiol Behav 73:229–234. doi: 10.1016/S0031-9384(01)00486-3

File SE, Wardill AG (1975) Validity of head-dipping as a measure of exploration in a modified hole-board. Psychopharmacologia 44:53–59.

Franchimont N, Lambert C, Huynen P, Ribbens C, Relic B, Chariot A, Bours V, Piette J, Merville MP, Malaise M (2005) Interleukin-6 receptor shedding is enhanced by interleukin-1 beta and tumor necrosis factor alfa and is partially mediated by tumor necrosis factor alfa-converting enzyme in osteoblast-like cells. Arthritis Rheum 52:84–93. doi: 10.1002/art.20727

Franklin KBJ, Paxinos G (2007) The mouse brain in stereotaxic coordinates, 3rd edn. Academic Press

Frei K, Malipiero U V, Leist TP, Zinkernagel RM, Schwab ME, Fontana a (1989) On the cellular source and function of interleukin 6 produced in the central nervous system in viral diseases. Eur J Immunol 19:689–694. doi: 10.1002/eji.1830190418

Fried SK, Bunkin DA, Greenberg AS (1998) Omental and subcutaneous adipose tissues of obese subjects release interleukin-6: depot difference and regulation by glucocorticoid. J Clin Endocrinol Metab 83:847–850. doi: 10.1210/jc.83.3.847

Fujita T, Tozaki-Saitoh H, Inoue K (2009) P2Y1 receptor signaling enhances neuroprotection by astrocytes against oxidative stress via IL-6 release in hippocampal cultures. Glia 57:244–257. doi: 10.1002/glia.20749

Fukada T, Hibi M, Yamanaka Y, Takahashi-Tezuka M, Fujitani Y, Yamaguchi T, Nakajima K, Hirano T (1996) Two signals are necessary for cell proliferation induced by a cytokine receptor gp130: involvement of STAT3 in anti-apoptosis. Immunity 5:449–460. doi: 10.1016/S1074-7613(00)80501-4

Gadient RA, Otten U (1994a) Expression of interleukin-6 (IL-6) and interleukin-6 receptor (IL-6R) mRNAs in rat brain during postnatal development. Brain Res 637:10–14.

Gadient RA, Otten U (1996) Postnatal expression of interleukin-6 (IL-6) and IL-6 receptor (IL-6R) mRNAs in rat sympathetic and sensory ganglia. Brain Res 724:41–46. doi: 10.1016/0006-8993(96)00264-8

Gadient RA, Otten U (1994b) Identification of interleukin-6 (IL-6)-expressing neurons in the cerebellum and hippocampus of normal adult rats. Neurosci Lett 182:243–246.

Gan L, Vargas MR, Johnson DA, Johnson JA (2012) Astrocyte-specific overexpression of Nrf2 delays motor pathology and synuclein aggregation throughout the CNS in the alpha-synuclein mutant

(A53T) mouse model. J Neurosci 32:17775–87. doi: 10.1523/JNEUROSCI.3049-12.2012

Gantz I, Miwa H, Konda Y, Shimoto Y, Tashiro T, Watson SJ, DelValle J, Yamada T (1993) Molecular cloning, expression, and gene localization of a fourth melanocortin receptor. J Biol Chem 268:15174–15179.

Gao K, Wang CR, Jiang F, Wong AYK, Su N, Jiang JH, Chai RC, Vatcher G, Teng J, Chen J, Jiang YW, Yu ACH (2013) Traumatic scratch injury in astrocytes triggers calcium influx to activate the JNK/c-Jun/AP-1 pathway and switch on GFAP expression. Glia 61:2063–2077. doi: 10.1002/glia.22577

Gao Q, Mezei G, Nie Y, Rao Y, Choi CS, Bechmann I, Leranth C, Toran-Allerand D, Priest C a, Roberts JL, Gao X-B, Mobbs C, Shulman GI, Diano S, Horvath TL (2007) Anorectic estrogen mimics leptin's effect on the rewiring of melanocortin cells and Stat3 signaling in obese animals. Nat Med 13:89–94. doi: 10.1038/nm1525

Garbers C, Spudy B, Aparicio-Siegmund S, Waetzig GH, Sommer J, Hölscher C, Rose-John S, Grötzinger J, Lorenzen I, Scheller J (2013) An lnterleukin-6 receptor-dependent molecular switch mediates signal transduction of the IL-27 cytokine subunit p28 (IL-30) via a gp130 protein receptor homodimer. J Biol Chem 288:4346–4354. doi: 10.1074/jbc.M112.432955

Garcia-Oscos F, Salgado H, Hall S, Thomas F, Farmer GE, Bermeo J, Galindo LC, Ramirez RD, D'Mello S, Rose-John S, Atzori M (2012) The stress-induced cytokine interleukin-6 decreases the inhibition/excitation ratio in the rat temporal cortex via trans-signaling. Biol Psychiatry 71:574–582. doi: 10.1016/j.biopsych.2011.11.018

Gauldie J, Northemann W, Fey GH (1990) IL-6 functions as an exocrine hormone in inflammation. Hepatocytes undergoing acute phase responses require exogenous IL-6. J Immunol 144:3804–3808.

Gauldie J, Richards C, Harnish D, Lansdorp P, Baumann H (1987) Interferon beta 2/B-cell stimulatory factor type 2 shares identity with monocyte-derived hepatocyte-stimulating factor and regulates the major acute phase protein response in liver cells. Proc Natl Acad Sci 84:7251–7255. doi: 10.1073/pnas.84.20.7251

Gearing DP, Comeau MR, Friend DJ, Gimpel SD, Thut CJ, McGourty J, Brasher KK, King JA, Gillis S, Mosley B, Ziegler SF, Cosman D (1992) The IL-6 signal transducer, gp130: an oncostatin M receptor and affinity converter for the LIF receptor. Science 255:1434–1437. doi: 10.1126/science.1542794

Gearing DP, Thut CJ, VandeBos T, Gimpel SD, Delaney PB, King J, Price V, Cosman D, Beckmann MP (1991) Leukemia inhibitory factor receptor is structurally related to the IL-6 signal transducer, gp130. EMBO J 10:2839–2848.

Gerhartz C, Heesel B, Hemmann U, Landgraf C, Schneider-Mergener J, Horn F, Heinrich PC, Graeve L (1996) Differential activation of acute phase response factor/STAT3 and STAT1 via the cytoplasmic domain of the interleukin 6 signal transducer gp130. J Biol Chem 271:12991–12998.

Ghamari-Langroudi M, Srisai D, Cone RD (2011) Multinodal regulation of the arcuate/paraventricular nucleus circuit by leptin. Proc Natl Acad Sci 108:355–360. doi: 10.1073/pnas.1016785108

Ghamari-Langroudi M, Vella KR, Srisai D, Sugrue ML, Hollenberg AN, Cone RD (2010) Regulation of thyrotropin-releasing hormone-expressing neurons in paraventricular nucleus of the hypothalamus by signals of adiposity. Mol Endocrinol 24:2366–2381. doi: 10.1210/me.2010-0203

Giralt M, Ramos R, Quintana A, Ferrer B, Erta M, Castro-Freire M, Comes G, Sanz E, Unzeta M, Pifarré P, García A, Campbell IL, Hidalgo J (2013) Induction of atypical EAE mediated by transgenic

production of IL-6 in astrocytes in the absence of systemic IL-6. Glia 61:587–600. doi: 10.1002/glia.22457

Gitter BD, Regoli D, Howbert JJ, Glasebrook AL, Waters DC (1994) Interleukin-6 secretion from human astrocytoma cells induced by substance P. J Neuroimmunol 51:101–108.

Gloaguen I, Costa P, Demartis A, Lazzaro D, Di Marco A, Graziani R, Paonessa G, Chen F, Rosenblum CI, Van der Ploeg LH, Cortese R, Ciliberto G, Laufer R (1997) Ciliary neurotrophic factor corrects obesity and diabetes associated with leptin deficiency and resistance. Proc Natl Acad Sci 94:6456–6461. doi: 10.1073/pnas.94.12.6456

Göke R, Larsen PJ, Mikkelsen JD, Sheikh SP (1995) Distribution of GLP-1 binding sites in the rat brain: evidence that exendin-4 is a ligand of brain GLP-1 binding sites. - PubMed - NCBI. Eur J Neurosci 7:2294–2300.

Gomez CR, Karavitis J, Palmer JL, Faunce DE, Ramirez L, Nomellini V, Kovacs EJ (2010) Interleukin-6 contributes to age-related alteration of cytokine production by macrophages. Mediators Inflamm 2010:Article ID 475139. doi: 10.1155/2010/475139

Gong J, Zhang J-P, Li B, Zeng C, You K, Chen M-X, Yuan Y, Zhuang S-M (2012) MicroRNA-125b promotes apoptosis by regulating the expression of Mcl-1, Bcl-w and IL-6R. Oncogene 3071–3079. doi: 10.1038/onc.2012.318

Gopinathan G, Milagre C, Pearce OMT, Reynolds LE, Hodivala-Dilke K, Leinster DA, Zhong H, Hollingsworth RE, Thompson R, Whiteford JR, Balkwill F (2015) Interleukin-6 stimulates defective angiogenesis. Cancer Res 75:3098–3107. doi: 10.1158/0008-5472.CAN-15-1227

Goto M, Arima H, Watanabe M, Hayashi M, Banno R, Sato I, Nagasaki H, Oiso Y (2006) Ghrelin increases neuropeptide Y and agouti-related peptide gene expression in the arcuate nucleus in rat hypothalamic organotypic cultures. Endocrinology 147:5102–5109. doi: 10.1210/en.2006-0104

Gottschall PE, Tatsuno I, Arimura A (1994) Regulation of interleukin-6 (IL-6) secretion in primary cultured rat astrocytes: synergism of interleukin-1 (IL-1) and pituitary adenylate cyclase activating polypeptide (PACAP). Brain Res 637:197–203.

Grill HJ (2006) Distributed neural control of energy balance: contributions from hindbrain and hypothalamus. Obesity 14:216S–221S. doi: 10.1038/oby.2006.312

Grötzinger J, Kernebeck T, Kallen KJ, Rose-John S (1999) IL-6 type cytokine receptor complexes: Hexamer, tetramer or both? Biol Chem 380:803–813. doi: 10.1515/BC.1999.100

Grötzinger J, Kurapkat G, Wollmer A, Kalai M, Rose-John S (1997) The family of the IL-6-type cytokines: specificity and promiscuity of the receptor complexes. Proteins Struct Funct Genet 27:96–109. doi: 10.1002/(SICI)1097-0134(199701)27:1<96::AID-PROT10>3.0.CO;2-D

Guan X-M, Yu H, Palyha OC, McKee KK, Feighner SS, Sirinathsinghji DJS, Smith RG, Van der Ploeg LHT, Howard AD (1997) Distribution of mRNA encoding the growth hormone secretagogue receptor in brain and peripheral tissues. Mol Brain Res 48:23–29. doi: 10.1016/S0169-328X(97)00071-5

Gupta S, Knight AG, Gupta S, Keller JN, Bruce-Keller AJ (2012) Saturated long-chain fatty acids activate inflammatory signaling in astrocytes. J Neurochem 120:1060–1071. doi: 10.1111/j.1471-4159.2012.07660.x

Hama T, Kushima Y, Miyamoto M, Kubota M, Takei M, Hatanaka H (1991) Interleukin-6 improves the survival of mesencephalic catecholamines and septal cholinergic neurons from postnatal, two-week-old rats in cultures. Neuroscience 40:445–452.

Hama T, Miyamoto M, Tsukui H, Nishio C, Hatanaka H (1989) Interleukin-6 as a neurotrophic factor for promoting the survival of cultured basal forebrain cholinergic neurons from postnatal rats.

Neurosci Lett 104:340–344. doi: 10.1016/0304-3940(89)90600-9

Hammacher A, Richardson RT, Layton JE, Smith DK, Angus LJL, Hilton DJ, Nicola NA, Wijdenes J, Simpson RJ (1998) The immunoglobulin-like module of gp130 is required for signaling by interleukin-6, but not by leukemia inhibitory factor. J Biol Chem 273:22701–22707. doi: 10.1074/jbc.273.35.22701

Hamrick MW, Pennington C, Newton D, Xie D, Isales C (2004) Leptin deficiency produces contrasting phenotypes in bones of the limb and spine. Bone 34:376–383. doi: 10.1016/j.bone.2003.11.020

Hans VH, Kossmann T, Joller H, Otto V, Morganti-Kossmann MC (1999) Interleukin-6 and its soluble receptor in serum and cerebrospinal fluid after cerebral trauma. Neuroreport 10:409–412.

Harden LM, du Plessis I, Poole S, Laburn HP (2006) Interleukin-6 and leptin mediate lipopolysaccharide-induced fever and sickness behavior. Physiol Behav 89:146–155. doi: 10.1016/j.physbeh.2006.05.016

Harris M, Aschkenasi C, Elias CF, Chandrankunnel A, Nillni EA, Bjørbæk C, Elmquist JK, Flier JS, Hollenberg AN (2001) Transcriptional regulation of the thyrotropin-releasing hormone gene by leptin and melanocortin signaling. J Clin Invest 107:111–120. doi: 10.1172/JCI10741

Haskell-Luevano C, Monck EK (2001) Agouti-related protein functions as an inverse agonist at a constitutively active brain melanocortin-4 receptor. Regul Pept 99:1–7. doi: 10.1016/S0167-0115(01)00234-8

Heink S, Yogev N, Garbers C, Herwerth M, Aly L, Gasperi C, Husterer V, Croxford AL, Möller-Hackbarth K, Bartsch HS, Sotlar K, Krebs S, Regen T, Blum H, Hemmer B, Misgeld T, Wunderlich TF, Hidalgo J, Oukka M, Rose-John S, Schmidt-Supprian M, Waisman A, Korn T (2016) Trans-presentation of IL-6 by dendritic cells is required for the priming of pathogenic TH17 cells. Nat Immunol. doi: 10.1038/ni.3632

Heinrich PC, Behrmann I, Haan S, Hermanns HM, Müller-Newen G, Schaper F (2003) Principles of interleukin (IL)-6-type cytokine signalling and its regulation. Biochem J 374:1–20. doi: 10.1042/BJ20030407

Heinrich PC, Behrmann I, Müller-Newen G, Schaper F, Graeve L (1998) Interleukin-6-type cytokine signalling through the gp130/Jak/STAT pathway 1. Biochem J 334:297–314. doi: 9716487

Heyser CJ, Masliah E, Samimi A, Campbell IL, Gold LH (1997) Progressive decline in avoidance learning paralleled by inflammatory neurodegeneration in transgenic mice expressing interleukin 6 in the brain. Proc Natl Acad Sci 94:1500–1505. doi: 10.1073/pnas.94.4.1500

Hibi M, Murakami M, Saito M, Hirano T, Taga T, Kishimoto T (1990) Molecular cloning and expression of an IL-6 signal transducer, gp130. Cell 63:1149–1157. doi: 10.1016/0092-8674(90)90411-7

Hidalgo J, Florit S, Giralt M, Ferrer B, Keller C, Pilegaard H (2010) Transgenic mice with astrocyte-targeted production of interleukin-6 are resistant to high-fat diet-induced increases in body weight and body fat. Brain Behav Immun 24:119–126. doi: http://dx.doi.org/10.1016/j.bbi.2009.09.002

Hill EE, Zack E, Battaglini C, Viru M, Viru A, Hackney AC (2008) Exercise and circulating cortisol levels: the intensity threshold effect. J Endocrinol Invest 31:587–591.

Hill EL, Elde R (1991) Distribution of CGRP-, VIP-, DβH-, SP-, and NPY-immunoreactive nerves in the periosteum of the rat. Cell Tissue Res 264:469–480. doi: 10.1007/BF00319037

Hirano T, Taga T, Nakano N, Yasukawa K, Kashiwamura S, Shimizu K, Nakajima K, Pyun KH, Kishimoto T (1985) Purification to homogeneity and characterization of human B-cell differentiation factor (BCDF or BSFp-2). Proc Natl Acad Sci 82:5490–5494. doi:

10.1073/pnas.82.16.5490

Hirata Y, Taga T, Hibi M, Nakano N, Hirano T, Kishimoto T (1989) Characterization of IL-6 receptor expression by monoclonal and polyclonal antibodies. J Immunol 143:2900–2906.

Hirota H, Kiyama H, Kishimoto T, Taga T (1996) Accelerated nerve regeneration in mice by upregulated expression of interleukin (IL) 6 and IL-6 receptor after trauma. J Exp Med 183:2627–2634. doi: 10.1084/jem.183.6.2627

Hohmann EL, Elde RP, Rysavy JA, Einzig S, Gebhard RL (1986) Innervation of periosteum and bone by sympathetic vasoactive intestinal peptide-containing nerve fibers. Science 232:868–871. doi: 10.1126/science.3518059

Holm S (1979) A simple sequentially rejective multiple test procedure. Scand J Stat 6:65–70.

Holm TH, Draeby D, Owens T (2012) Microglia are required for astroglial toll-like receptor 4 response and for optimal TLR2 and TLR3 response. Glia 60:630–638. doi: 10.1002/glia.22296

Holmes AG, Watt MJ, Carey AL, Febbraio MA (2004) Ionomycin, but not physiologic doses of epinephrine, stimulates skeletal muscle Interleukin-6 mRNA expression and protein release. Metabolism 53:1492–1495. doi: 10.1016/j.metabol.2004.05.015

Honegger J, Spagnoli A, D'Urso R, Navarra P, Tsagarakis S, Besser GM, Grossman AB (1991) Interleukin-1beta modulates the acute release of growth hormone-releasing hormone and somatostatin from rat hypothalamus in vitro, whereas tumor necrosis factor and interleukin-6 have no effect. Endocrinology 129:1275–1282. doi: 10.1210/endo-129-3-1275

Horii Y, Muraguchi A, Suematsu S, Matsuda T, Yoshizaki K, Hirano T, Kishimoto T (1988) Regulation of BSF-2/IL-6 production by Macrophage-dependent synthesis of BSF-2/IL-6 by T cells. J Immunol 141:1529–1535.

Horiuchi S, Koyanagi Y, Zhou Y, Miyamoto H, Tanaka Y, Waki M, Matsumoto A, Yamamoto M, Yamamoto N (1994) Soluble interleukin-6 receptors released from T cell or granulocyte/macrophage cell lines and human peripheral blood mononuclear cells are generated though an alterantive splicing mechanism. Eur J Immunol 24:1945–1948.

Hotamisligil GS, Peraldi P, Budavari A, Ellis R, White MF, Spiegelman BM (1996) IRS-1-mediated inhibition of insulin receptor tyrosine kinase activity in TNF-α- and obesity-induced insulin resistance. Science 271:665–668.

Howard JK, Cave BJ, Oksanen LJ, Tzameli I, Bjørbæk C, Flier JS (2004) Enhanced leptin sensitivity and attenuation of diet-induced obesity in mice with haploinsufficiency of Socs3. Nat Med 10:734–738. doi: 10.1038/nm1072

Howren MB, Lamkin DM, Suls J (2009) Associations of depression with C-reactive protein, IL-1, and IL-6: a meta-analysis. Psychosom Med 71:171–186. doi: 10.1097/PSY.0b013e3181907c1b

Hryniewicz A, Bialuk I, Kamiński KA, Winnicka MM (2007) Impairment of recognition memory in interleukin-6 knock-out mice. Eur J Pharmacol 577:219–220. doi: 10.1016/j.ejphar.2007.08.046

Huang S-P, Wu M-S, Shun C-T, Wang H-P, Lin M-T, Kuo M-L, Lin J-T (2004) Interleukin-6 increases vascular endothelial growth factor and angiogenesis in gastric carcinoma. J Biomed Sci 11:517–527. doi: 10.1159/000077902

Hunter CA, Jones SA (2015) IL-6 as a keystone cytokine in health and disease. Nat Immunol 16:448–457. doi: 10.1038/ni.3153

Hurst SM, Wilkinson TS, McLoughlin RM, Jones S, Horiuchi S, Yamamoto N, Rose-John S, Fuller GM, Topley N, Jones SA (2001) IL-6 and its soluble receptor orchestrate a temporal switch in the pattern of leukocyte recruitment seen during acute inflammation. Immunity 14:705–714. doi:

10.1016/S1074-7613(01)00151-0

Huszar D, Lynch CA, Fairchild-Huntress V, Dunmore JH, Fang Q, Berkemeier LR, Gu W, Kesterson RA, Boston BA, Cone RD, Smith FJ, Campfield LA, Burn P, Lee F (1997) Targeted disruption of the melanocortin-4 receptor results in obesity in mice. Cell 88:131–141. doi: 10.1016/S0092-8674(00)81865-6

Ihara S, Iwamatsu A, Fujiyoshi T, Komi A, Yamori T, Fukui Y (1996) Identification of interleukin-6 as a factor that induces neurite outgrowth by PC12 cells primed with NGF. J Biochem 120:865–868.

Ihara S, Nakajima K, Fukada T, Hibi M, Nagata S, Hirano T, Fukui Y (1997) Dual control of neurite outgrowth by STAT3 and MAP kinase in PC12 cells stimulated with interleukin-6. EMBO J 16:5345–5352. doi: 10.1093/emboj/16.17.5345

Ikebuchi K, Wong GG, Clark SC, Ihle JN, Hirai Y, Ogawa M (1987) Interleukin 6 enhancement of interleukin 3-dependent proliferation of multipotential hemopoietic progenitors. Proc Natl Acad Sci 84:9035–9039. doi: 10.1073/pnas.84.24.9035

Ishimi Y, Miyaura C, Jin CH, Akatsu T, Abe E, Nakamura Y, Yamaguchi A, Yoshiki S, Matsuda T, Hirano T (1990) IL-6 is produced by osteoblasts and induces bone resorption. J Immunol 145:3297–3303.

Islam O, Gong X, Rose-John S, Heese K (2009) Interleukin-6 and Neural Stem Cells: More Than Gliogenesis. Mol Biol Cell 20:188–199. doi: 10.1091/mbc.E08

Israel PA, Park CR, Schwartz MW, Green PK, Sipols AJ, Woods SC, Porte Jr D, Figlewicz DP (1993) Effect of diet-induced obesity and experimental hyperinsulinemia on insulin uptake into CSF of the rat. Brain Res Bull 30:571–575.

Isshiki H, Akira S, Tanabe O, Nakajima T, Shimamoto T, Hirano T, Kishimoto T (1990) Constitutive and interleukin-1 (IL-1)-inducible factors interact with the IL-1-responsive element in the IL-6 gene. Mol Cell Biol 10:2757–2764. doi: 10.1128/MCB.10.6.2757

Jankord R, Zhang R, Flak JN, Solomon MB, Albertz J, Herman JP (2010) Stress activation of IL-6 neurons in the hypothalamus. Am J Physiol Regul Integr Comp Physiol 299:R343–R351. doi: 10.1152/ajpregu.00131.2010

Jessen KR, Mirsky R (1983) Astrocyte-like glia in the peripheral nervous system: an immunohistochemical study of enteric glia. J Neurosci 3:2206–2218.

Johnson RW (2002) The concept of sickness behavior: a brief chronological account of four key discoveries. Vet Immunol Immunopathol 87:443–450. doi: 10.1016/S0165-2427(02)00069-7

Joly-Amado A, Denis RGP, Castel J, Lacombe A, Cansell C, Rouch C, Kassis N, Dairou J, Cani PD, Ventura-Clapier R, Prola A, Flamment M, Foufelle F, Magnan C, Luquet S (2012) Hypothalamic AgRP-neurons control peripheral substrate utilization and nutrient partitioning. EMBO J 31:4276–4288. doi: 10.1038/emboj.2012.250

Jones JI, Clemmons DR (1995) Insulin-like growth factors and their binding proteins: biological actions. Endocr Rev 16:3–34. doi: 10.1210/er.16.1.3

Jostock T, Müllberg J, Özbek S, Atreya R, Blinn G, Voltz N, Fischer M, Neurath MF, Rose-John S (2001) Soluble gp130 is the natural inhibitor of soluble interleukin-6 receptor transsignaling responses. Eur J Biochem 268:160–167. doi: 10.1046/j.1432-1327.2001.01867.x

Kamiński KA, Kożuch M, Bonda TA, Stepaniuk MM, Waszkiewicz E, Chyczewski L, Musiał WJ, Winnicka MM (2009) Effect of interleukin 6 deficiency on the expression of Bcl-2 and Bax in the murine heart. Pharmacol Reports 61:504–513. doi: 10.1016/S1734-1140(09)70093-3

Kayakabe K, Kuroiwa T, Sakurai N, Ikeuchi H, Kadiombo AT, Sakairi T, Matsumoto T, Maeshima A,

Hiromura K, Nojima Y (2012) Interleukin-6 promotes destabilized angiogenesis by modulating angiopoietin expression in rheumatoid arthritis. Rheumatology 51:1571–1579. doi: 10.1093/rheumatology/kes093

Keller C, Steensberg A, Hansen AK, Fischer CP, Plomgaard P, Pedersen BK (2005) Effect of exercise, training, and glycogen availability on IL-6 receptor expression in human skeletal muscle. J Appl Physiol 99:2075–2079. doi: 10.1152/japplphysiol.00590.2005.

Keller C, Steensberg A, Pilegaard H, Osada T, Saltin B, Pedersen BK, Neufer PD (2001) Transcriptional activation of the IL-6 gene in human contracting skeletal muscle: influence of muscle glycogen content. FASEB J 15:2748–2750. doi: 10.1096/fj.01-0507fje

Kim MS, Rossi M, Abusnana S, Sunter D, Morgan DGA, Small CJ, Edwards CMB, Heath MM, Stanley SA, Seal LJ, Bhatti JR, Smith DM, Ghatei MA, Bloom SR (2000) Hypothalamic Localization of the Feeding E ffect of Agouti-Related Peptide and -Melanocyte – Stimulating Hormone. Diabetes 49:177–182.

Kiriyama Y, Murayama T, Tokumitsu Y, Nomura Y (1997) Protein kinase A-dependent IL-6 production induced by calcitonin in human glioblastoma A172 cells. J Neuroimmunol 76:139–144. doi: 10.1016/S0165-5728(97)00044-1

Kishimoto T, Akira S, Narazaki M, Taga T (1995) Interleukin-6 family of cytokines and gp130. Blood 86:1243–1254.

Kishimoto T, Yoshizaki K, Kimoto M, Okada M, Kuritani T, Kikutani H, Shimizu K, Nakagawa T, Nakagawa N, Miki Y, Kishi H, Fukunaga K, Yoshikubo T, Taga T (1984) B cell growth and differentiation factors. Immunol Rev 78:97–118. doi: 10.1111/j.1600-065X.1984.tb00478.x

Kitamura H, Konno A, Morimatsu M, Jung BD, Kimura K, Saito M (1997) Immobilization stress increases hepatic IL-6 expression in mice. Biochem Biophys Res Commun 238:707–711. doi: 10.1006/bbrc.1997.7368

Kleinridders A, Schenten D, Könner AC, Belgardt BF, Mauer J, Okamura T, Wunderlich FT, Medzhitov R, Brüning JC (2009) MyD88 signaling in the CNS is required for development of fatty acid-induced leptin resistance and diet-induced obesity. Cell Metab 10:249–259. doi: 10.1016/j.cmet.2009.08.013

Klir JJ, McClellan JL, Kluger MJ (1994) Interleukin-1 beta causes the increase in anterior hypothalamic interleukin-6 during LPS-induced fever in rats. Am J Physiol Regul Integr Comp Physiol 266:R1845–R1848.

Klir JJ, Roth J, Szelényi Z, McClellan JL, Kluger MJ (1993) Role of hypothalamic interleukin-6 and tumor necrosis factor-α in LPS fever in rat. Am J Physiol Regul Integr Comp Physiol 265:R512–R517.

Kohase M, May LT, Tamm I, Vilcek J, Sehgal PB (1987) A cytokine network in human diploid fibroblasts: interactions of beta-interferons, tumor necrosis factor, platelet-derived growth factor, and interleukin-1. Mol Cell Biol 7:273–280.

Koike K, Nakahata T, Takagi M, Kobayashi T, Ishiguro A, Tsuji K, Naganuma K, Okano A, Akiyama Y, Akabane T (1988) Synergism of BSF-2/interleukin 6 and interleukin 3 on development of multipotential hemopoietic progenitors in serum-free culture. J Exp Med 168:879–890.

Kojima M, Hosoda H, Date Y, Nakazato M, Matsuo H, Kangawa K (1999) Ghrelin is a growth-hormone-releasing acylated peptide from stomach. Nature 402:656–660. doi: 10.1038/45230

Kopf M, Baumann H, Freer G, Freudenberg M, Lamers M, Kishimoto T, Zinkernagel R, Bluethmann H, Köhler G, Kohler G, Köhler G (1994) Impaired immune and acute-phase responses in interleukin-6-deficient mice. Nature 368:339–342. doi: 10.1038/368339a0

Kotz CM, Grace MK, Briggs J, Levine AS, Billington CJ (1995) Effects of opioid antagonists naloxone

and naltrexone on neuropeptide Y-induced feeding and brown fat thermogenesis in the rat neural site of action. J Clin Invest 96:163–170.

Krady JK, Lin H-W, Liberto CM, Basu A, Kremlev SG, Levison SW (2008) Ciliary Neurotrophic Factor and Interleukin-6 Differentially Activate Microglia. J Neurosci Res 86:1538–1547. doi: 10.1002/jnr.21620

Krahn DD, Gosnell BA, Levine AS, Morley JE (1988) Behavioral effects of corticotropin-releasing factor: localization and characterization of central effects. Brain Res 443:63–69.

Kristensen P, Judge ME, Thim L, Ribel U, Christjansen KN, Wulff BS, Clausen JT, Jensen PB, Madsen OD, Vrang N, Larsen PJ, Hastrup S (1998) Hypothalamic CART is a new anorectic peptide regulated by leptin. Nature 393:72–76. doi: 10.1038/29993

Kurotani R, Yasuda M, Oyama K, Egashira N, Sugaya M, Teramoto A, Osamura RY (2001) Expression of interleukin-6, interleukin-6 receptor (gp80), and the receptor's signal-transducing subunit (gp130) in human normal pituitary glands and pituitary adenomas. Mod Pathol 14:791–797. doi: 10.1038/modpathol.3880392

Lalonde R, Strazielle C (2008) Relations between open-field, elevated plus-maze, and emergence tests as displayed by C57/BL6J and BALB/c mice. J Neurosci Methods 171:48–52. doi: 10.1016/j.jneumeth.2008.02.003

Langub MC, Koszewski NJ, Turner H V, Monier-Faugere MC, Geng Z, Malluche HH (1996) Bone resorption and mRNA expression of IL-6 and IL-6 receptor in patients with renal osteodystrophy. Kidney Int 50:515–520. doi: 10.1038/ki.1996.343

Large V, Hellström L, Reynisdottir S, Lönnqvist F, Eriksson P, Lannfelt L, Arner P (1997) Human beta-2 adrenoceptor gene polymorphisms are highly frequent in obesity and associate with altered adipocyte beta-2 adrenoceptor function. J Clin Invest 100:3005–3013. doi: 10.1172/JCI119854

Larsen L, Le Foll C, Dunn-Meynell AA, Levin BE (2016) IL-6 ameliorates defective leptin sensitivity in DIO Ventromedial Hypothalamic Nucleus neurons. Am J Physiol Regul Integr Comp Physiol ajpregu.00258.2016. doi: 10.1152/ajpregu.00258.2016

Lavin DN, Joesting JJ, Chiu GS, Moon ML, Meng J, Dilger RN, Freund GG (2011) Fasting induces an anti-inflammatory effect on the neuroimmune system which a high-fat diet prevents. Obesity 19:1586–1594. doi: 10.1038/oby.2011.73

Le Foll C, Johnson MD, Dunn-Meynell AA, Boyle CN, Lutz TA, Levin BE (2015) Amylin-induced central IL-6 production enhances ventromedial hypothalamic leptin signaling. Diabetes 64:1621–1631. doi: 10.2337/db14-0645

Le Roith D, Bondy C, Yakar S, Liu J-L, Butler A (2001) The Somatomedin Hypothesis: 2001. Endocr Rev 22:53–74.

Lechan RM, Segerson TP (1989) Pro-TRH gene expression and precursor peptides in rat brain. Observations by hybridization analysis and immunocytochemistry. Ann N Y Acad Sci 553:29–59.

Lehmann U, Schmitz J, Weissenbach M, Sobota RM, Hörtner M, Friederichs K, Behrmann I, Tsiaris W, Sasaki A, Schneider-Mergener J, Yoshimura A, Neel BG, Heinrich PC, Schaper F (2003) SHP2 and SOCS3 contribute to Tyr-759-dependent attenuation of interleukin-6 signaling through gp130. J Biol Chem 278:661–671. doi: 10.1074/jbc.M210552200

Lehtimäki KA, Keränen T, Huhtala H, Hurme M, Ollikainen J, Honkaniemi J, Palmio J, Peltola J (2004) Regulation of IL-6 system in cerebrospinal fluid and serum compartments by seizures: The effect of seizure type and duration. J Neuroimmunol 152:121–125. doi: 10.1016/j.jneuroim.2004.01.024

LeMay LG, Otterness IG, Vander AJ, Kluger MJ (1990a) In vivo evidence that the rise in plasma IL 6 following injection of a fever-inducing dose of LPS is mediated by IL 1β. Cytokine 2:199–204. doi: 10.1016/1043-4666(90)90016-M

LeMay LG, Vander AJ, Kluger MJ (1990b) The effects of psychological stress on plasma interleukin-6 activity in rats. Physiol Behav 47:957–961. doi: 10.1016/0031-9384(90)90024-X

Lenczowski MJP, Bluthé RM, Roth J, Rees GS, Rushforth DA, van Dam A-MM, Tilders FJH, Dantzer R, Rothwell NJ, Luheshi GN, Bluthe R-M, Roth J, Rees GS, Rushforth DA, van Dam A-MM, Tilders FJH, Dantzer R, Rothwell NJ, Luheshi GN (1999) Central administration of rat IL-6 induces HPA activation and fever but not sickness behavior in rats. Am J Physiol Regul Integr Comp Physiol 276:R652–R658.

Leonard BE (2001) Changes in the immune system in depression and dementia: causal or co-incidental effects? Int J Dev Neurosci 19:305–312. doi: 10.1016/S0736-5748(01)00014-4

Lever C, Burton S, O'Keefe J (2006) Rearing on hind legs, environmental novelty, and the hippocampal formation. Rev Neurosci 17:111–133. doi: 10.1515/REVNEURO.2006.17.1-2.111

Levine AS, Morley JE (1984) Neuropeptide Y: a potent inducer of consummatory behavior in rats. Peptides 5:1025–1029. doi: 10.1016/0196-9781(84)90165-7

Levine J, Barak Y, Chengappa KN, Rapoport A, Rebey M, Barak V (1999) Cerebrospinal cytokine levels in patients with acute depression. Neuropsychobiology 40:171–176. doi: 10.1159/000026615

Levine SJ (2004) Mechanisms of soluble cytokine receptor generation. J Immunol 283:5343–5348. doi: 10.1074/jbc.R700052200

Lewitt MS, Denyer GS, Cooney GJ, Baxter RC (1991) Insulin-like growth factor-binding protein-1 modulates blood glucose levels. Endocrinology 129:2254–2256.

Lexow J, Poggioli T, Sarathchandra P, Santini MP, Rosenthal N (2013) Cardiac fibrosis in mice expressing an inducible myocardial-specific Cre driver. Dis Model Mech 6:1470–1476. doi: 10.1242/dmm.010470

Ley EJ, Clond MA, Singer MB, Shouhed D, Salim A (2011) IL-6 deficiency affects function after traumatic brain injury. J Surg Res 170:253–256. doi: 10.1016/j.jss.2011.03.006

Li A-J, Katafuchi T, Oda S, Hori T, Oomura Y (1997) Interleukin-6 inhibits long-term potentiation in rat hippocampal slices. Brain Res 748:30–38. doi: 10.1016/S0006-8993(96)01283-8

Li R-Y, Tsutsui Y (2000) Growth retardation and microcephaly induced in mice by placental infection with murine cytomegalovirus. Teratology 62:79–85. doi: 10.1002/1096-9926(200008)62:2<79::AID-TERA3>3.0.CO;2-S

Libermann TA, Baltimore D (1990) Activation of interleukin-6 gene expression through the NF-kappa B transcription factor. Mol Cell Biol 10:2327–2334. doi: 10.1128/MCB.10.5.2327.Updated

Lindqvist D, Janelidze S, Hagell P, Erhardt S, Samuelsson M, Minthon L, Hansson O, Björkqvist M, Träskman-Bendz L, Brundin L (2009) Interleukin-6 is elevated in the cerebrospinal fluid of suicide attempters and related to symptom severity. Biol Psychiatry 66:287–292. doi: 10.1016/j.biopsych.2009.01.030

Ling E-A, Wong W-C (1993) The origin and nature of ramified and amoeboid microglia: A historical review and current concepts. Glia 7:9–18.

Loonstra A, Vooijs M, Beverloo HB, Allak BA, van Drunen E, Kanaar R, Berns A, Jonkers J (2001) Growth inhibition and DNA damage induced by Cre recombinase in mammalian cells. Proc Natl Acad Sci 98:9209–9214. doi: 10.1073/pnas.161269798

REFERENCES

Lotz M, Jirik F, Kabouridis P, Tsoukas C, Hirano T, Kishimoto T, Carson DA (1988) B cell stimulating factor 2/interleukin 6 is a costimulant for human thymocytes and T lymphocytes. J Exp Med 167:1253–1258.

Lotz M, Zuraw BL, Carson DA, Jirik FR (1989) Hepatocytes produce interleukin-6. Ann N Y Acad Sci 557:509–511. doi: 10.1111/j.1749-6632.1989.tb24048.x

Louveau A, Harris TH, Kipnis J (2015) Revisiting the mechanisms of CNS immune privilege. Trends Immunol 36:569–577. doi: 10.1016/j.it.2015.08.006

Lucas S-M, Rothwell NJ, Gibson RM (2006) The role of inflammation in CNS injury and disease. Br J Pharmacol 147:S232–S240. doi: 10.1038/sj.bjp.0706400

Lupu F, Terwilliger JD, Lee K, Segre G V, Efstratiadis A (2001) Roles of growth hormone and insulin-like growth factor 1 in mouse postnatal growth. Dev Biol 229:141–162. doi: 10.1006/dbio.2000.9975

Lust J, Donovan KA, Kline MP, Greipp PR, Kyle RA, Maihle NJ (1992) Isolation of an mRNA encoding a soluble form of the human interleukin-6 receptor. Cytokine 4:96–100. doi: 10.1016/1043-4666(92)90043-Q

Lütticken C, Wegenka UM, Yuan J, Buschmann J, Schindler C, Ziemiecki A, Harpur a G, Wilks a F, Yasukawa K, Taga T (1994) Association of transcription factor APRF and protein kinase Jak1 with the interleukin-6 signal transducer gp130. Science 263:89–92. doi: 10.1126/science.8272872

Lutz TA, Althaus J, Rossi R, Scharrer E (1998) Anorectic effect of amylin is not transmitted by capsaicin-sensitive nerve fibers. Am J Physiol Regul Integr Comp Physiol 274:R1777–R1782.

Lyson K, McCann SM (1991) The effect of interleukin-6 on pituitary hormone release in vivo and in vitro. Neuroendocrinology 54:262–266.

Maes M, Meltzer HY, Bosmans E, Bergmans R, Vandoolaeghe E, Ranjan R, Desnyder R (1995a) Increased plasma concentrations of interleukin-6, soluble interleukin-6, soluble interleukin-2 and transferrin receptor in major depression. J Affect Disord 34:301–309. doi: 10.1016/0165-0327(95)00028-L

Maes M, Smith R, Simon S (1995b) The monocyte-T-lymphocyte hypothesis of major depression. Psychoneuroendocrinology 20:111–116. doi: 10.1016/0306-4530(94)00066-J

Maes M, Song C, Lin a, De Jongh R, Van Gastel a, Kenis G, Bosmans E, De Meester I, Benoy I, Neels H, Demedts P, Janca a, Scharpé S, Smith RS (1998) The effects of psychological stress on humans: increased production of pro-inflammatory cytokines and a Th1-like response in stress-induced anxiety. Cytokine 10:313–318. doi: 10.1006/cyto.1997.0290

Maier B, Schwerdtfeger K, Mautes A, Holanda M, Müller M, Steudel WI, Marzi I (2001) Differential release of interleukines 6, 8, and 10 in cerebrospinal fluid and plasma after traumatic brain injury. Shock 15:421–426.

Maimone D, Cioni C, Rosa S, Macchia G, Aloisi F, Annunziata P (1993) Norepinephrine and vasoactive intestinal peptide induce IL-6 secretion by astrocytes: Synergism with IL-1β and TNFα. J Neuroimmunol 47:73–81. doi: 10.1016/0165-5728(93)90286-8

Mandal M, Marzouk AC, Donnelly R, Ponzio NM (2011) Maternal immune stimulation during pregnancy affects adaptive immunity in offspring to promote development of TH17 cells. Brain Behav Immun 25:863–871. doi: 10.1016/j.bbi.2010.09.011

Manning B, Cantley L (2007) AKT/PKB Signaling: navigating downstream. Cell 129:1261–1274. doi: 10.1016/j.cell.2007.06.009.AKT/PKB

Manso Y, Carrasco J, Comes G, Adlard PA, Bush AI, Hidalgo J (2012) Characterization of the role of

the antioxidant proteins metallothioneins 1 and 2 in an animal model of Alzheimer's disease. Cell Mol Life Sci 69:3665–3681. doi: 10.1007/s00018-012-1045-y

Marin V, Montero-Julian FA, Grès S, Bongrand P, Farnarier C, Kaplanski G (2002) Chemoktactic agents induce IL-6Rα shedding from polymorphonuclear cells: involvement of a metalloprotease of the TNF-α-converting enzyme (TACE) type. Eur J Immunol 32:2965–2972.

Marks JL, Porte D, Stahl WL, Baskin DG (1990) Localization of insulin receptor mRNA in rat brain by in situ hybridization. Endocrinology 127:3234–3236. doi: 10.1210/endo-127-6-3234

März P, Cheng J-G, Gadient RA, Patterson PH, Stoyan T, Otten U, Rose-John S (1998) Sympathetic neurons can produce and respond to interleukin 6. Proc Natl Acad Sci 95:3251–3256.

März P, Gadient RA, Otten U (1996) Expression of interleukin-6 receptor (IL-6R) and gp130 mRNA in PC12 cells and sympathetic neurons: modulation by tumor necrosis factor α (TNF-α). Brain Res 706:71–79. doi: 10.1016/0006-8993(95)01210-9

März P, Heese K, Dimitriades-Schmutz B, Rose-John S, Otten U (1999) Role of interleukin-6 and soluble IL-6 receptor in region-specific induction of astrocytic differentiation and neurotrophin expression. Glia 26:191–200. doi: 10.1002/(SICI)1098-1136(199905)26:3<191::AID-GLIA1>3.0.CO;2-#

März P, Herget T, Lang E, Otten U, Rose-John S (1997) Activation of gp130 by IL-6/soluble IL-6 receptor induces neuronal differentiation. Eur J Neurosci 10:2765–2773.

Matsuguchi T, Okamura S, Kawasaki C, Niho Y (1990) Production of interleukin 6 from human liver cell lines: production of interleukin 6 is not concurrent with the production of α-fetoprotein. Cancer Res 50:7457–7459.

Matsusaka T, Fujikawa K, Nishio Y, Mukaida N, Matsushima K, Kishimoto T, Akira S (1993) Transcription factors NF-IL6 and NF-κB synergistically activate transcription of the inflammatory cytokines, interleukin 6 and interleukin 8. Proc Natl Acad Sci 90:10193–10197. doi: 10.1073/pnas.90.21.10193

Matthews V, Schuster B, Schütze S, Bussmeyer I, Ludwig A, Hundhausen C, Sadowski T, Saftig P, Hartmann D, Kallen K-J, Rose-John S (2003) Cellular cholesterol depletion triggers shedding of the human interleukin-6 receptor by ADAM10 and ADAM17 (TACE). J Biol Chem 278:38829–38839. doi: 10.1074/jbc.M210584200

May LT, Ghrayeb J, Santhanam U, Tatter SB, Sthoeger Z, Helfgott DC, Chiorazzi N, Grieninger G, Sehgal PB (1988a) Synthesis and secretion of multiple forms of beta 2-interferon/B-cell differentiation factor 2/hepatocyte-stimulating factor by human fibroblasts and monocytes. J Biol Chem 263:7760–7766.

May LT, Santhanam U, Tatter SB, Bhardwaj N, Ghrayeb J, Sehgal PB (1988b) Phosphorylation of secreted forms of human beta 2-interferon/hepatocyte stimulating factor/interleukin-6. Biochem Biophys Res Commun 152:1144–1150. doi: 10.1016/S0006-291X(88)80404-2

McFarland-Mancini MM, Funk HM, Paluch AM, Zhou M, Giridhar PV, Mercer CA, Kozma SC, Drew AF (2010) Differences in wound healing in mice with deficiency of IL-6 versus IL-6 receptor. J Immunol 184:7219–7128. doi: 10.4049/jimmunol.0901929

McLoughlin RM, Jenkins BJ, Grail D, Williams AS, Fielding C a, Parker CR, Ernst M, Topley N, Jones S a (2005) IL-6 trans-signaling via STAT3 directs T cell infiltration in acute inflammation. Proc Natl Acad Sci 102:9589–9594. doi: 10.1073/pnas.0501794102

McLoughlin RM, Witowski J, Robson RL, Wilkinson TS, Hurst SM, Williams AS, Williams JD, Rose-John S, Jones SA, Topley N (2003) Interplay between IFN-γ and IL-6 signaling governs neutrophil trafficking and apoptosis during acute inflammation. J Clin Invest 112:598–607. doi: 10.1172/JCI200317129

REFERENCES

Medawar PB (1948) Immunity to homologous grafted skin. III The fate of skin homografts transplanted to the brain, to subcutaneous tissue, and to the anterior chamber of the eye. Br J Exp Pathol 58–69.

Mihara M, Hashizume M, Yoshida H, Suzuki M, Shiina M (2012) IL-6/IL-6 receptor system and its role in physiological and pathological conditions. Clin Sci 122:143–159. doi: 10.1042/CS20110340

Milanski M, Degasperi G, Coope A, Morari J, Denis R, Cintra DE, Tsukumo DML, Anhe G, Amaral ME, Takahashi HK, Curi R, Oliveira HC, Carvalheira JBC, Bordin S, Saad MJ, Velloso LA (2009) Saturated fatty acids produce an inflammatory response predominantly through the activation of TLR4 signaling in hypothalamus: implications for the pathogenesis of obesity. J Neurosci 29:359–370. doi: 10.1523/JNEUROSCI.2760-08.2009

Minami M, Kuraishi Y, Satoh M (1991) Effects of kainic acid on messenger RNA levels of IL-1 beta, IL-6, TNF alpha and LIF in the rat brain. Biochem Biophys Res Commun 176:593–598. doi: 10.1006/cyto.1998.0426

Miyaura C, Jin CH, Yamaguchi Y, Tomida M, Hozumi M, Matsuda T, Hirano T, Kishimoto T, Suda T (1989) Production of interleukin-6 and its relation to the macrophage differentiation of mouse myeloid leukemia cells (M1) treated with differentiation-inducing factor and 1α,25-dihydroxyvitamin D3. Biochem Biophys Res Commun 158:660–666.

Mock BA, Nordan RP, Justice MJ, Kozak C, Jenkins NA, Copeland NG, Clark SC, Wong GG, Rudikoff S (1989) The murine Il-6 gene maps to the proximal region of chromosome 5. J Immunol 142:1372–1376.

Mohamed-Ali V, Flower L, Sethi J, Hotamisligil G, Gray R, Humphries S, York D, Pinkney J (2001) β-adrenergic regulation of IL-6 release from adipose tissue: in vivo and in vitro studies. J Clin Endocrinol Metab 86:5864–5869.

Mohamed-Ali V, Goodrick S, Rawesh A, Katz DR, Miles JM, Yudkin JS, Klein S, Coppack SW (1997) Subcutaneous adipose tissue releases interleukin-6, but not tumor necrosis factor-alfa, in vivo. J Clin Endocrinol Metab 82:4196–4200. doi: 10.1210/jcem.82.12.4450

Monje FJ, Cabatic M, Divisch I, Kim EJ, Herkner KR, Binder BR, Pollak DD (2011) Constant darkness induces IL-6-dependent depression-like behavior through the NF-kappaB signaling pathway. J Neurosci 31:9075–9083. doi: 10.1523/JNEUROSCI.1537-11.2011

Moraes JC, Coope A, Morari J, Cintra DE, Roman EA, Pauli JR, Romanatto T, Carvalheira JB, Oliveira ALR, Saad MJ, Velloso LA (2009) High-fat diet induces apoptosis of hypothalamic neurons. PLoS One 4:e5045. doi: 10.1371/journal.pone.0005045

Morello G, Imperatore R, Palomba L, Finelli C, Labruna G, Pasanisi F, Sacchetti L, Buono L, Piscitelli F, Orlando P, Di Marzo V, Cristino L (2016) Orexin-A represses satiety-inducing POMC neurons and contributes to obesity via stimulation of endocannabinoid signaling. Proc Natl Acad Sci 113:4759–4764. doi: 10.1073/pnas.1521304113

Mori H, Hanada R, Hanada T, Aki D, Mashima R, Nishinakamura H, Torisu T, Chien KR, Yasukawa H, Yoshimura A (2004) Socs3 deficiency in the brain elevates leptin sensitivity and confers resistance to diet-induced obesity. Nat Med 10:739–743. doi: 10.1038/nm1071

Morris R (1984) Developments of a water-maze procedure for studying spatial learning in the rat. J Neurosci Methods 11:47–60. doi: 10.1016/0165-0270(84)90007-4

Morris RGM (1981) Spatial localization does not require the presence of local cues. Learn Motiv 12:239–260. doi: 10.1016/0023-9690(81)90020-5

Morrison CD, Morton GJ, Niswender KD, Gelling RW, Schwartz MW (2005) Leptin inhibits hypothalamic Npy and Agrp gene expression via a mechanism that requires phosphatidylinositol 3-OH-kinase signaling. Am J Physiol Endocrinol Metab 289:E1051–

E1057. doi: 10.1152/ajpendo.00094.2005

Morrow LE, McClellan JL, Conn CA, Kluger MJ (1993) Glucocorticoids alter fever and IL-6 responses to psychological stress and to lipopolysaccharide. Am J Physiol Regul Integr Comp Physiol 264:R1010–R1016.

Morton GJ, Cummings DE, Baskin DG, Barsh GS, Schwartz MW (2006) Central nervous system control of food intake and body weight. Nature 443:289–295. doi: 10.1038/nature05026

Motro B, Itin A, Sachs L, Keshet E (1990) Pattern of interleukin 6 gene expression in vivo suggests a role for this cytokine in angiogenesis. Proc Natl Acad Sci 87:3092–3096. doi: 10.1073/pnas.87.8.3092

Müllberg J, Dittrich E, Graeve L, Gerhartz C, Yasukawa K, Taga T, Kishimoto T, Heinrich PC, Rose-John S (1993a) Differential shedding of the two subunits of the interleukin-6 receptor. FEBS Lett 332:174–178. doi: 10.1016/0014-5793(93)80507-Q

Müllberg J, Schooltink H, Stoyan T, Günther M, Graeve L, Buse G, Mackiewicz A, Heinrich PC, Rose-John S (1993b) The soluble interleukin-6 receptor is generated by shedding. Eur J Immunol 23:473–480. doi: 10.1002/eji.1830230226

Müllberg J, Schooltink H, Stoyan T, Heinrich PC, Rose-John S (1992) Protein kinase C activity is rate limiting for shedding of the interleukin-6 receptor. Biochem Biophys Res Commun 189:794–800.

Münzberg H, Flier JS, Bjørbæk C (2004) Region-specific leptin resistance within the hypothalamus of diet-induced obese mice. Endocrinology 145:4880–4889. doi: 10.1210/en.2004-0726

Muraguchi A, Kishimoto T, Miki Y, Kuritani T, Kaieda T, Yoshizaki K, Yamamura Y (1981) T cell-replacing factor (TRF)-induced IgG secretion in a human B blastoid cell line and demonstration of acceptors for TRF. J Immunol 127:412–416.

Murakami M, Hibi M, Nakagawa N, Nakagawa T, Yasukawa K, Yamanishi K, Taga T, Kishimoto T (1993) IL-6-induced homodimerization of gp130 and associated activation of a tyrosine kinase. Science 260:1808–1810.

Nadal R, Escorihuela RM, Armario A (2006) The elevated plus-maze test of anxiety: methodological considerations. In: Tasks and Techniques: A Sampling of the Methodologies for the Investigation of Animal Learning, Behavior and Cognition. ova Science Publishers, Inc.,

Naitoh Y, Fukata J, Tominaga T, Nakai Y, Tamai S, Mori K, Imura H (1988) Interleukin-6 stimulates the secretion of adrenocorticotropic hormone in conscious, freely-moving rats. Biochem Biophys Res Commun 155:1459–1463.

Nakagawa A, Satake H, Nakabayashi H, Nishizawa M, Furuya K, Nakano S, Kigoshi T, Nakayama K, Uchida K (2004) Receptor gene expression of glucagon-like peptide-1, but not glucose-dependent insulinotropic polypeptide, in rat nodose ganglion cells. Auton Neurosci 110:36–43. doi: 10.1016/j.autneu.2003.11.001

Nakamura K (2011) Central circuitries for body temperature regulation and fever. Am J Physiol Regul Integr Comp Physiol 301:R1207–R1228. doi: 10.1152/ajpregu.00109.2011

Narazaki M, Yasukawa K, Saito T, Ohsugi Y, Fukui H, Koishihara Y, Yancopoulos GD, Taga T, Kishimoto T (1993) Soluble forms of the interleukin-6 signal-transducing receptor component gp130 in human serum possessing a potential to inhibit signals through membrane-anchored gp130. Blood 82:1120–1126.

Natsuka S, Akira S, Nishio Y, Hashimoto S, Sugita T, Isshiki H, Kishimoto T (1992) Macrophage differentiation-specific expression of NF-IL6, a transcription factor for interleukin-6. Blood 79:460–466.

REFERENCES

Navarra P, Tsagarakis S, Faria MS, Rees LH, Besser GM, Grossman AB (1991) Interleukins-1 and -6 stimulate the release of corticotropin-releasing hormone-41 from rat hypothalamus in vitro via the eicosanoid cyclooxygenase pathway. Endocrinology 128:37–44. doi: 10.1210/endo-128-1-37

Navia B, Ferrer B, Giralt M, Comes G, Carrasco J, Molinero a., Quintana a., Leclerc J, Viollet B, Señarís RM, Hidalgo J (2014) Interleukin-6 deletion in mice driven by aP2-Cre-ERT2 prevents against high-fat diet-induced gain weight and adiposity in female mice. Acta Physiol 211:585–596. doi: 10.1111/apha.12328

Nechemia-Arbely Y, Shriki A, Denz U, Drucker C, Scheller J, Raub J, Pappo O, Rose-John S, Galun E, Axelrod JH (2011) Early hepatocyte DNA synthetic response posthepatectomy is modulated by IL-6 trans-signaling and PI3K/AKT activation. J Hepatol 54:922–929. doi: 10.1016/j.jhep.2010.08.017

Nijenhuis WAJ, Oosterom J, Adan RAH (2001) AgRP(83-132) acts as an inverse agonist on the human-melanocortin-4 receptor. Mol Endocrinol 15:164–171. doi: 10.1210/me.15.1.164

Nilsson MB, Armaiz-Pena G, Takahashi R, Lin YG, Trevino J, Li Y, Jennings N, Arevalo J, Lutgendorf SK, Gallick GE, Sanguino AM, Lopez-Berestein G, Cole SW, Sood AK (2007) Stress hormones regulate interleukin-6 expression by human ovarian carcinoma cells through a Src-dependent mechanism. J Biol Chem 282:29919–29926. doi: 10.1074/jbc.M611539200

Nimmerjahn A, Kirchhoff F, Helmchen F (2005) Resting microglial cells are highly dynamic surveillants of brain parenchyma in vivo. Science 308:1314–1318. doi: 10.1126/science.1110647

Norris CA, He M, Kang LI, Ding MQ, Radder JE, Haynes MM, Yang Y, Paranjpe S, Bowen WC, Orr A, Michalopoulos GK, Stolz DB, Mars WM (2014) Synthesis of IL-6 by hepatocytes is a normal response to common hepatic stimuli. PLoS One 9:e96053. doi: 10.1371/journal.pone.0096053

Norris JG, Benveniste EN (1993) Interleukin-6 production by astrocytes: Induction by the neurotransmitter norepinephrine. J Neuroimmunol 45:137–145. doi: 10.1016/0165-5728(93)90174-W

Northemann W, Braciak TA, Hattori M, Lee F, Fey GH (1989) Structure of the rat interleukin-6 gene and its expression in macrophage-derived cell lines. J Biol Chem 264:16072–16082.

Nussbaum-Krammer CI, Neto MF, Brielmann RM, Pedersen JS, Morimoto RI (2015) Investigating the Spreading and Toxicity of Prion-like Proteins Using the Metazoan Model Organism C. elegans. J vis Exp e52321. doi: doi:10.3791/52321

Oh J, McCloskey MA, Blong CC, Bendickson L, Nilsen-Hamilton M, Sakaguchi DS (2010) Astrocyte-derived interleukin-6 promotes specific neuronal differentiation of neural progenitor cells from adult hippocampus. J Neurosci Res 88:2798–2809. doi: 10.1002/jnr.22447

Ollmann MM, Wilson BD, Yang Y-K, Kerns JA, Chen Y, Gantz I, Barsh GS (1997) Antagonism of central melanocortin receptors in vitro and in vivo by agouti-related protein. Science 278:135–138. doi: 10.1126/science.278.5335.135

Ørskov C, Puolsen S, Møller M, Holst JJ (1996) Glucagon-like peptide 1 receptors in the subformical organ and the area postrema are accessible to circulating glucagon-like peptide 1. Diabetes 45:832–835. doi: 10.2337/diabetes.45.6.832

Palmqvist P, Persson E, Conaway HH, Lerner UH (2002) IL-6, leukemia inhibitory factor, and oncostatin M stimulate bone resorption and regulate the expression of receptor activator of NF-κB ligand, osteoprotegerin, and receptor activator of NF-κB in mouse calvariae. J Immunol 169:3353–3362. doi: 10.4049/jimmunol.169.6.3353

Paonessa G, Graziani R, De Serio A, Savino R, Ciapponi L, Lahm A, Salvati AL, Toniatti C, Ciliberto G (1995) Two distinct and independent sites on IL-6 trigger gp 130 dimer formation and

signalling. EMBO J 14:1942–1951.

Park HS, Park JY, Yu R (2005) Relationship of obesity and visceral adiposity with serum concentrations of CRP, TNF-α and IL-6. Diabetes Res Clin Pract 69:29–35. doi: 10.1016/j.diabres.2004.11.007

Park JB, Jo JY, Zheng H, Patel KP, Stern JE (2009) Regulation of tonic GABA inhibitory function, presympathetic neuronal activity and sympathetic outflow from the paraventricular nucleus by astroglial GABA transporters. J Physiol 587:4645–4660. doi: 10.1113/jphysiol.2009.173435

Park JB, Skalska S, Son S, Stern JE (2007) Dual GABAA receptor-mediated inhibition in rat presympathetic paraventricular nucleus neurons. J Physiol 582:539–551. doi: 10.1113/jphysiol.2007.133223

Pasare C, Medzhitov R (2003) Toll pathway-dependent blockade of CD4+CD25+ T cell-mediated suppression by dendritic cells. Science 299:1033–1036. doi: 10.1126/science.1078231

Päth G, Scherbaum W a, Bornstein SR (2000) The role of interleukin-6 in the human adrenal gland. Eur J Clin Invest 30:91–95.

Penkowa M, Giralt M, Carrasco J, Hadberg H, Hidalgo J (2000) Impaired inflammatory response and increased oxidative stress and neurodegeneration after brain injury in interleukin-6-deficient mice. Glia 32:271–285.

Pennica D, King KL, Shaw KJ, Luis E, Rullamas J, Luoh S-M, Darbonne WC, Knutzon DS, Yen R, Chien KR, Baker JB, Wood WI (1995) Expression cloning of cardiotrophin 1, a cytokine that induces cardiac myocyte hypertrophy. Proc Natl Acad Sci 92:1142–1146. doi: 10.1073/pnas.92.4.1142

Perry W, Minassian A, Lopez B, Maron L, Lincoln A (2007) Sensorimotor gating deficits in adults with autism. Biol Psychiatry 61:482–486. doi: 10.1016/j.biopsych.2005.09.025

Peters BM, Schirmacher P, Goldschmitt J, Odenthal M, Peschel C, Fattori E, Ciliberto G, Dienes H-P, Meyer zum Büschenfelde K-H, Rose-John S (1997) Extramedullary expansion of hematopoietic progenitor cells in interleukin (IL)-6-sIL-6R double transgenic mice. J Exp Med 185:755–766.

Petro AE, Cotter J, Cooper DA, Peters JC, Surwit SJ, Surwit RS (2004) Fat, carbohydrate, and calories in the development of diabetes and obesity in the C57BL/6J mouse. Metabolism 53:454–457. doi: 10.1016/j.metabol.2003.11.018

Pfaffl MW (2001) A new mathematical model for relative quantification in real-time RT-PCR. Nucleic Acids Res 29:e45. doi: 10.1093/nar/29.9.e45

Pflanz S, Kurth I, Grötzinger J, Heinrich PC, Müller-Newen G (2000) Two different epitopes of the signal transducer gp130 sequentially cooperate on IL-6-induced receptor activation. J Immunol 165:7042–7049. doi: 10.4049/jimmunol.165.12.7042

Plata-Salamán CR (1996) Anorexia induces by activators of the signal transducer gp130. Neuroreport 7:841–844.

Poli V, Balena R, Fattori E, Markatos A, Yamamoto M, Tanaka H, Ciliberto G, Rodan GA, Costantini F (1994) Interleukin-6 deficient mice are protected from bone loss caused by estrogen depletion. EMBO J 13:1189–1196.

Posey KA, Clegg DJ, Printz RL, Byun J, Morton GJ, Vivekanandan-Giri A, Pennathur S, Baskin DG, Heinecke JW, Woods SC, Schwartz MW, Niswender KD (2009) Hypothalamic proinflammatory lipid accumulation , inflammation , and insulin resistance in rats fed a high-fat diet. Am J Physiol Endocrinol Metab 296:E1003–E1012. doi: 10.1152/ajpendo.90377.2008.

Poupart P, Vandenabeele P, Cayphas S, Van Snick J, Haegeman G, Kruys V, Fiers W, Content J (1987)

B cell growth modulating and differentiating activity of recombinant human 26-kd protein (BSF-2, HuIFN-beta 2, HPGF). EMBO J 6:1219–1224.

Prendergast AJ, Rukobo S, Chasekwa B, Mutasa K, Ntozini R, Mbuya MNN, Jones A, Moulton LH, Stoltzfus RJ, Humphrey JH (2014) Stunting is characterized by chronic inflammation in zimbabwean infants. PLoS One 9:e86928. doi: 10.1371/journal.pone.0086928

Quintana A, Erta M, Ferrer B, Comes G, Giralt M, Hidalgo J (2013) Astrocyte-specific deficiency of interleukin-6 and its receptor reveal specific roles in survival, body weight and behavior. Brain Behav Immun 27:162–173. doi: 10.1016/j.bbi.2012.10.011

Quintana FJ (2016) Old dog, new tricks: IL-6 cluster signaling promotes pathogenic TH17 cell differentiation. Nat Immunol 18:8–10. doi: 10.1038/ni.3637

Rajkumar K, Barron D, Lewitt MS, Murphy LJ (1995) Growth retardation and hyperglycemia in insulin-like growth factor binding protein-1 transgenic mice. Endocrinology 136:4029–4034.

Ray A, Tatter SB, Santhanam U, Helfgott DC, May LT, Sehgal PB (1989) Regulation of expression of interleukin-6. Molecular and clinical studies. Ann N Y Acad Sci 557:353–362.

Rempe D, Vangeison G, Hamilton J, Li Y, Jepson M, Federoff HJ (2006) Synapsin I Cre transgene expression in male mice produces germline recombination in progeny. genesis 44:44–49. doi: 10.1002/gene.20183

Ringheim GE, Burgher KL, Heroux JA (1995) Interleukin-6 mRNA expression by cortical neurons in culture: evidence for neuronal sources of interleukin-6 production in the brain. J Neuroimmunol 63:113–123. doi: 10.1016/0165-5728(95)00134-4

Ritchie DG, Fuller GM (1983) Hepatocyte-stimulating factor: a monocyte-derived acute-phase regulatory protein. Ann N Y Acad Sci 408:490–502.

Roman CW, Derkach VA, Palmiter RD (2016) Genetically and functionally defined NTS to PBN brain circuits mediating anorexia. Nat Commun 7:11905. doi: 10.1038/ncomms11905

Ropelle ER, Flores MB, Cintra DE, Rocha GZ, Pauli JR, Morari J, de Souza CT, Moraes JC, Prada PO, Guadagnini D, Marin RM, Oliveira AG, Augusto TM, Carvalho HF, Velloso LA, Saad MJA, Carvalheira JBC (2010) IL-6 and IL-10 anti-inflammatory activity links exercise to hypothalamic insulin and leptin sensitivity through IKKbeta and ER stress inhibition. PLoS Biol 8:e1000465. doi: 10.1371/journal.pbio.1000465

Rose-John S, Schooltink H, Lenz D, Hipp E, Dufhues G, Schmitz H, Schiel X, Hirano T, Kishimoto T, Heinrich PC (1990) Studies on the structure and regulation of the human hepatic interleukin-6 receptor. Eur J Biochem Biochem 190:79–83.

Roselli-Rehfuss L, Mountjoy KG, Robbins LS, Mortrud MT, Low MJ, Tatro JB, Entwistlet ML, Simerly RB, Cone RD (1993) Identification of a receptor for gamma melanotropin and other proopiomelanocortin peptides in the hypothalamus and limbic system. Proc Natl Acad Sci 90:8856–8860. doi: 10.1073/pnas.90.19.8856

Rothwell NJ, Busbridge NJ, Lefeuvre R a, Hardwick a J, Gauldie J, Hopkins SJ (1991) Interleukin-6 is a centrally acting endogenous pyrogen in the rat. Can J Physiol Pharmacol 69:1465–1469.

Rott O, Tontsch U, Fleischer B, Cash E (1993) Interleukin-6 production in "normal" and HTLV-1 tax-expressing brain-specific endothelial cells. Eur J Immunol 23:1987–1991.

Rühl A, Franzke S, Collins SM, Stremmel W (2001) Interleukin-6 expression and regulation in rat enteric glial cells. Am J Physiol Gastrointest Liver Physiol 280:G1163–G1171.

Sabio G, Das M, Mora A, Zhang Z, Yun JY, Ko HJ, Barrett T, Kim JK, Davis RJ (2008) A stress signaling pathway in adipose tissue regulates hepatic insulin resistance. Science 1539–1543.

Sadagurski M, Norquay L, Farhang J, D'Aquino K, Copps K, White MF (2010) Human IL6 enhances

leptin action in mice. Diabetologia 53:525–535. doi: 10.1007/s00125-009-1580-8

Sakurai T, Amemiya A, Ishii M, Matsuzaki I, Chemelli RM, Tanaka H, Williams SC, Richardson JA, Kozlowski GP, Wilson S, Arch JRS, Buckingham RE, Haynes AC, Carr SA, Annan RS, Mcnulty DE, Liu W, Terrett JA, Elshourbagy NA, Bergsma DJ, Yanagisawa M (1998) Orexins and orexin receptors: a family of hypothalamic neuropeptides and G protein-coupled receptors that regulate feeding behavior. Cell 92:573–585.

Salas MA, Evans SW, Levell MJ, Whicher JT (1990) Interleukin-6 and ACTH act synergistically to stimulate the release of corticosterone from adrenal gland cells. Clin Exp Immunol 79:470–473.

Sallmann S, Jüttler E, Prinz S, Petersen N, Knopf U, Weiser T, Schwaninger M (2000) Induction of Interleukin-6 by depolarization of neurons. J Neurosci 20:8637–8642.

Samoilova EB, Horton JL, Hilliard B, Liu T-S, Chen Y (1998) IL-6-deficient mice are resistant to experimental autoimmune encephalomyelitis: roles of IL-6 in the activation and differentiation of autoreactive T cells. J Immunol 161:6480–6486.

Samuelsson A-M, Jennische E, Hansson H-A, Holmäng A (2006) Prenatal exposure to interleukin-6 results in inflammatory neurodegeneration in hippocampus with NMDA/GABA(A) dysregulation and impaired spatial learning. Am J Physiol Regul Integr Comp Physiol 290:R1345–R1356. doi: 10.1152/ajpregu.00268.2005

Sanz E, Yang L, Su T, Morris DR, McKnight GS, Amieux PS (2009) Cell-type-specific isolation of ribosome-associated mRNA from complex tissues. Proc Natl Acad Sci 106:13939–13944. doi: 10.1073/pnas.0907143106

Sasayama D, Hattori K, Wakabayashi C, Teraishi T, Hori H, Ota M, Yoshida S, Arima K, Higuchi T, Amano N, Kunugi H (2013) Increased cerebrospinal fluid interleukin-6 levels in patients with schizophrenia and those with major depressive disorder. J Psychiatr Res 47:401–406. doi: 10.1016/j.jpsychires.2012.12.001

Satoh T, Nakamura S, Taga T, Matsuda T, Hirano T, Kishimoto T, Kaziro Y (1988) Induction of neuronal differentiation in PC12 cells by B-cell stimulatory factor 2/interleukin 6. Mol Cell Biol 8:3546–3549. doi: 10.1128/MCB.8.8.3546

Sawada M, Suzumura A, Marunouchi T (1992) TNFα induces IL-6 production by astrocytes but not by microglia. Brain Res 583:296–299. doi: 10.1016/S0006-8993(10)80037-X

Schaper F, Gendo C, Eck M, Schmitz J, Grimm C, Anhuf D, Kerr IM, Heinrich PC (1998) Activation of the protein tyrosine phosphatase SHP2 via the interleukin-6 signal transducing receptor protein gp130 requires tyrosine kinase Jak1 and limits acute-phase protein expression. Biochem J 335:557–65. doi: 10.1042/bj3350557

Schaper F, Rose-John S (2015) Interleukin-6: Biology, signaling and strategies of blockade. Cytokine Growth Factor Rev 26:475–487. doi: 10.1016/j.cytogfr.2015.07.004

Scheller J, Chalaris A, Schmidt-Arras D, Rose-John S (2011) The pro- and anti-inflammatory properties of the cytokine interleukin-6. Biochim Biophys Acta 1813:878–888. doi: 10.1016/j.bbamcr.2011.01.034

Schiemann WP, Bartoe JL, Nathanson NM (1997) Box 3-independent signaling mechanisms are involved in leukemia inhibitory factor receptor α- and gp130-mediated stimulation of mitogen activated protein kinase. J Biol Chem 272:16631–16636.

Schirmacher P, Peters M, Ciliberto G, Blessing M, Lotz J, Meyer zum Büschenfelde KH, Rose-John S (1998) Hepatocellular hyperplasia, plasmacytoma formation, and extramedullary hematopoiesis in interleukin (IL)-6/soluble IL-6 receptor double-transgenic mice. Am J Pathol 153:639–648. doi: 10.1016/S0002-9440(10)65605-2

REFERENCES

Schneider CA, Rasband WS, Eliceiri KW (2012) NIH Image to ImageJ: 25 years of image analysis. Nat Methods 9:671–675. doi: 10.1038/nmeth.2089

Schöbitz B, de Kloet ER, Sutanto W, Holsboer F (1993) Cellular localization of interleukin 6 mRNA and interleukin 6 receptor mRNA in rat brain. Eur J Neurosci 5:1426–1435. doi: 10.1111/j.1460-9568.1993.tb00210.x

Schöbitz B, Pzeshki G, Pohl T, Hemmann U, Heinrich PC, Holsboer F, Reul JMHM (1995) Soluble interleukin-6 (IL-6) receptor augments central effects of IL-6 in vivo. FASEB J 6:659–664.

Schoester M, Heinrich PC, Graeve L (1994) Regulation of interleukin-6 receptor expression by interleukin-6 in human monocytes - a re-examination. FEBS Lett 345:131–134. doi: 10.1016/0014-5793(94)00416-1

Schwaninger M, Neher M, Viegas E, Schneider A, Spranger M (1997) Stimulation of interleukin-6 secretion and gene transcription in primary astrocytes by adenosine. J Neurochem 69:1145–1150.

Schwaninger M, Sallmann S, Petersen N, Schneider A, Prinz S, Libermann TA, Spranger M (1999) Bradykinin induces interleukin-6 expression in astrocytes through activation of nuclear factor-κB. J Neurochem 73:1461–1466. doi: 10.1046/j.1471-4159.1999.0731461.x

Schwartz MW, Seeley RJ, Woods SC, Weigle DS, Campfield LA, Burn P, Baskin DG (1997) Leptin increases hypothalamic pro-opiomelanocortin mRNA expression in the rostral arcuate nucleus. Diabetes 46:2119–2123.

Seeley RJ, Yagaloff KA, Fisher SL, Burn P, Thiele TE, van Dijk G, Baskin DG, Schwartz MW (1997) Melanocortin receptors in leptin effects. Nature 390:349. doi: 10.1038/37016

Sehgal PB, May LT, Tamm I, Vilcek J (1987) Human ß2 interferon and B-cell differentiation factor BSF-2 are identical. Science 235:731–732. doi: 10.1126/science.3492764

Sehgal PB, Zilberstein A, Ruggieri RM, May LT, Ferguson-Smith A, Slate DL, Revel M, Ruddle FH (1986) Human chromosome 7 carries the ß2 interferon gene. Proc Natl Acad Sci 83:5219–5222.

Selmaj KW, Farooq M, Norton WT, Raine CS, Brosnan CF (1990) Proliferation of astrocytes in vitro in response to cytokines. A primary role for tumor necrosis factor. J Immunol 144:129–135.

Senaldi G, Varnum BC, Sarmiento U, Starnes C, Lile J, Scully S, Guo J, Elliott G, McNinch J, Shaklee CL, Freeman D, Manu F, Simonet WS, Boone T, Chang M-S (1999) Novel neurotrophin-1/B cell-stimulating factor-3: a cytokine of the IL-6 family. Proc Natl Acad Sci 96:11458–11463. doi: 10.1073/pnas.96.20.11458

Senn JJ, Klover PJ, Nowak IA, Mooney RA (2002) Interleukin-6 induces cellular insulin resistance in hepatocytes. Diabetes 51:3391–3399.

Señarís RM, Trujillo ML, Navia B, Comes G, Ferrer B, Giralt M, Hidalgo J (2011) Interleukin-6 regulates the expression of hypothalamic neuropeptides involved in body weight in a gender-dependent way. J Neuroendocrinol 23:675–686. doi: 10.1111/j.1365-2826.2011.02158.x

Shabo Y, Lotem J, Sachs L (1989) Autoregulation of interleukin 6 and granulocyte-macrophage colony-stimulating factor in the differentiation of myeloid leukemic cells. Mol Cell Biol 9:4109–4112.

Shah BP, Vong L, Olson DP, Koda S, Krashes MJ, Ye C, Yang Z, Fuller PM, Elmquist JK, Lowell BB (2014) MC4R-expressing glutamatergic neurons in the paraventricular hypothalamus regulate feeding and are synaptically connected to the parabrachial nucleus. Proc Natl Acad Sci 111:13193–13198. doi: 10.1073/pnas.1407843111

Shalev U, Yap J, Shaham Y (2001) Leptin attenuates acute food deprivation-induced relapse to

heroin seeking. J Neurosci 21:RC129.

Shatz CJ (2009) MHC Class I: An unexpected role in neuronal plasticity. Neuron 64:40–45. doi: 10.1016/j.neuron.2009.09.044

Shimada M, Tritos NA, Lowell BB, Flier JS, Maratos-Flier E (1998) Mice lacking melanin-concentrating hormone are hypophagic and lean. Nature 396:670–674. doi: 10.1038/25341

Shimizu E, Tang Y-P, Rampon C, Tsien JZ (2000) NMDA receptor-dependent synaptic reinforcement as a crucial process for memory consolidation. Science 290:1170–1174. doi: 10.1126/science.290.5494.1170

Shoelson SE, Herrero L, Naaz A (2007) Obesity, inflammation, and insulin resistance. Gastroenterology 132:2169–2180. doi: 10.1053/j.gastro.2007.03.059

Siddals KW, Westwood M, Gibson JM, White A (2002) IGF-binding protein-1 inhibits IGF effects on adipocyte function: Implications for insulin-like actions at the adipocyte. J Endocrinol 174:289–297. doi: 10.1677/joe.0.1740289

Simpson RJ, Moritz RL (1988) Characterization of a recombinant murine interleukin-6: assignment of disulfide bonds. Biochem Biophys Res Commun 157:364–372.

Simpson RJ, Moritz RL, Rubira MR, Van Snick J (1988) Murine hybridoma/plasmacytoma growth factor. Complete amino-acid sequence and relation to human interleukin-6. FEBS J 176:187–197. doi: 10.1111/j.1432-1033.1988.tb14268.x

Sims NA, Jenkins BJ, Quinn JMW, Nakamura A, Glatt M, Gillespie MT, Ernst M, Martin TJ (2004) Glycoprotein 130 regulates bone turnover and bone size by distinct downstream signaling pathways. J Clin Invest 113:379–389. doi: 10.1172/JCI200419872

Smith G. P., Jerome C., Cushin B. J., Eterno R., Simansky K. J. (1981) Abdominal vagotomy blocks the satiety effect of cholecystokinin in the rat. Science 213:1036–1037. doi: 10.1126/science.7268408

Smith SEP, Li J, Garbett K, Mirnics K, Patterson PH (2007) Maternal immune activation alters fetal brain development through interleukin-6. J Neurosci 27:10695–10702. doi: 10.1523/JNEUROSCI.2178-07.2007

Snyers L, De Wit L, Content J (1990) Glucocorticoid up-regulation of high-affinity interleukin 6 receptors on human epithelial cells. Proc Natl Acad Sci 87:2838–2842. doi: 10.1073/pnas.87.7.2838

Somers W, Stahl M, Seehra JS (1997) 1.9 Å crystal structure of interleukin 6: Implications for a novel mode of receptor dimerization and signaling. EMBO J 16:989–997. doi: 10.1093/emboj/16.5.989

Soszynski D, Kozak W, Conn CA, Rudolf K, Kluger MJ (1996) Beta-adrenoreceptor antagonists suppress elevation in body temperature and increase in plasma IL-6 in rats exposed to open field. Neuroendocrinology 63:459–467.

Spangelo BL, Judd AM, Isakson PC, MacLeod RM (1989) Interleukin-6 stimulates anterior pituitary hormone release in vitro. Endocrinology 125:575–577.

Sparkman NL, Buchanan JB, Heyen JR, Chen J, Beverly JL, Johnson RW (2006) Interleukin-6 facilitates lipopolysaccharide-induced disruption in working memory and expression of other proinflammatory cytokines in hippocampal neuronal cell layers. J Neurosci 26:10709–10716. doi: 10.1523/JNEUROSCI.3376-06.2006

Späth-Schwalbe E, Born J, Schrezenmeier H, Bornstein SR, Stromeyer P, Drechsler S, Fehm HL, Porzsolt F (1994) Interleukin-6 stimulates the hypothalamus-pituitary-adrenocortical axis in man. J Clin Endocrinol Metab 79:1212–1214. doi: 10.1210/jcem.79.4.7962296

REFERENCES

Sriram K, Benkovic SA, Hebert MA, Miller DB, O'Callaghan JP (2004) Induction of gp130-related cytokines and activation of JAK2/STAT3 Pathway in astrocytes precedes up-regulation of glial fibrillary acidic protein in the 1-methyl-4-phenyl-1, 2, 3, 6-tetrahydropyridine model of neurodegeneration. Key signaling pathway for . J Biol Chem 279:19936–19947. doi: 10.1074/jbc.M309304200

Stahl N, Boulton TG, Farruggella T, Ip NY, Davis S, Witthuhn BA, Quelle FW, Silvennoinen O, Barbieri G, Pellegrini S, Ihle JN, Yancopoulos GD (1994) Association and activation of Jak-Tyk kinases by CNTF-LIF-OSM-IL-6 beta receptor components. Science 263:92–95. doi: 10.1126/science.8272873

Stahl N, Farruggella TJ, Boulton TG, Zhong Z, Darnell JE, Yancopoulos GD (1995) Choice of STATs and other substrates specified by modular tyrosine-based motifs in cytokine receptors. Science 267:1349–1353. doi: 10.1126/science.7871433

Stanley BG, Leibowitz SF (1984) Neuropeptide Y: stimulation of feeding and drinking by injection into the paraventricular nucleus. Life Sci 35:2635–2642.

Steensberg A, Keller C, Starkie RL, Osada T, Febbraio MA, Pedersen BK (2002) IL-6 and TNF-α expression in, and release from, contracting human skeletal muscle. Am J Physiol Endocrinol Metab 283:E1272–E1278. doi: 10.1152/ajpendo.00255.2002

Stein B, Yang M (1995) Repression of the interleukin-6 promoter by estrogen receptor is mediated by NF-kappa B and C/EBP beta. Mol Cell Biol 15:4971–4979. doi: 10.1128/MCB.15.9.4971

Stenlöf K, Wernstedt I, Fjällman T, Wallenius V, Wallenius K, Jansson J-O (2003) Interleukin-6 levels in the central nervous system are negatively correlated with fat mass in overweight/obese subjects. J Clin Endocrinol Metab 88:4379–4383. doi: 10.1210/jc.2002-021733

Stephan AH, Barres BA, Stevens B (2012) The Complement System: an unexpected role in synaptic pruning during development and disease. Annu Rev Neurosci 35:369–389. doi: 10.1146/annurev-neuro-061010–113810

Stern JE, Filosa JA (2013) Bidirectional neuro-glial signaling modalities in the hypothalamus: Role in neurohumoral regulation. Auton Neurosci Basic Clin 175:51–60. doi: 10.1016/j.autneu.2012.12.009

Sternberg N, Hamilton D (1981) Bacteriophage P1 site-specific recombination. J Mol Biol 150:467–486. doi: 10.1016/0022-2836(81)90375-2

Sterneck E, Kaplan DR, Johnson PF (1996) Interleukin-6 induces expression of peripherin and cooperates with Trk receptor signaling to promote neuronal differentiation in PC12 cells. J Neurochem 67:1365–1374. doi: 10.1046/j.1471-4159.1996.67041365.x

Stübner S, Schön T, Padberg F, Teipel SJ, Schwarz MJ, Haslinger A, Buch K, Dukoff R, Lasser R, Müller N, Sunderland T, Rapoport SI, Möller HJ, Hampel H (1999) Interleukin-6 and the soluble IL-6 receptor are decreased in cerebrospinal fluid of geriatric patients with major depression: no alteration of soluble gp130. Neurosci Lett 259:145–148. doi: 10.1016/S0304-3940(98)00916-1

Sukoff Rizzo SJ, Neal SJ, Hughes ZA, Beyna M, Rosenzweig-Lipson S, Moss SJ, Brandon NJ (2012) Evidence for sustained elevation of IL-6 in the CNS as a key contributor of depressive-like phenotypes. Transl Psychiatry 2:e199. doi: 10.1038/tp.2012.120

Sullivan CN, Raboin SJ, Gulley S, Sinzobahamvya NT, Green GM, Reeve JR, Sayegh AI (2007) Endogenous cholecystokinin reduces food intake and increases Fos-like immunoreactivity in the dorsal vagal complex but not in the myenteric plexus by CCK1 receptor in the adult rat. Am J Physiol Regul Integr Comp Physiol 292:R1071–R1080. doi: 10.1152/ajpregu.00490.2006

Swartz KR, Liu F, Sewell D, Schochet T, Campbell I, Sandor M, Fabry Z (2001) Interleukin-6 promotes post-traumatic healing in the central nervous system. Brain Res 896:86–95.

Swiergiel AH, Dunn AJ (2006) Feeding, exploratory, anxiety- and depression-related behaviors are not altered in interleukin-6-deficient male mice. Behav Brain Res 171:94–108. doi: 10.1016/j.bbr.2006.03.024

Taga T, Hibi M, Hirata Y, Yamasaki K, Yasukawa K, Matsuda T, Hirano T, Kishimoto T (1989) Interleukin-6 triggers the association of its receptor with a possible signal transducer, gp130. Cell 58:573–581. doi: 10.1016/0092-8674(89)90438-8

Takahashi-Tezuka M, Yoshida Y, Fukada T, Ohtani T, Yamanaka Y, Nishida K, Nakajima K, Hibi M, Hirano T (1998) Gab1 acts as an adapter molecule linking the cytokine receptor gp130 to ERK mitogen-activated protein kinase. Mol Cell Biol 18:4109–4117. doi: 10.1128/MCB.18.7.4109

Takaki A, Huang Q-H, Somogyvári-Vigh A, Arimura A (1994) Immobilization stress may increase plasma interleukin-6 via central and peripheral catecholamines. Neuroimmunomodulation 1:335–342.

Takeda K, Noguchi K, Shi W, Tanaka T, Matsumoto M, Yoshida N, Kishimoto T, Akira S (1997) Targeted disruption of the mouse Stat3 gene leads to early embryonic lethality. Proc Natl Acad Sci 94:3801–3804.

Takeda S, Elefteriou F, Levasseur R, Liu X, Zhao L, Parker KL, Armstrong D, Ducy P, Karsenty G (2002) Leptin regulates bone formation via the sympathetic nervous system. Cell 111:305–317. doi: 10.1016/S0092-8674(02)01049-8

Tamura T, Udagawa N, Takahashi N, Miyaura C, Tanaka S, Yamada Y, Koishihara Y, Ohsugi Y, Kumaki K, Taga T, Kishimoto T, Suda T (1993) Soluble interleukin-6 receptor triggers osteoclast formation by interleukin 6. Proc Natl Acad Sci 90:11924–11928. doi: 10.1073/pnas.90.24.11924

Tanabe O, Akira S, Kamiya T, Wong GG, Hirano T, Kishimoto T (1988) Genomic structure of the murine IL-6 gene. High degree conservation of potential regulatory sequences between mouse and human. J Immunol 141:3875–3881.

Tarassishin L, Suh HS, Lee SC (2014) LPS and IL-1 differentially activate mouse and human astrocytes: Role of CD14. Glia 62:999–1013. doi: 10.1002/glia.22657

Thaler JP, Schwartz MW (2010) Minireview: Inflammation and obesity pathogenesis: the hypothalamus heats up. Endocrinology 151:4109–4115. doi: 10.1210/en.2010-0336

Thaler JP, Yi C, Schur EA, Guyenet SJ, Hwang BH, Dietrich MO, Zhao X, Sarruf DA, Izgur V, Maravilla KR, Nguyen HT, Fischer JD, Matsen ME, Wisse BE, Morton GJ, Horvath TL, Baskin DG, Tschöp MH, Schwartz MW (2012) Obesity is associated with hypothalamic injury in rodents and humans. J Clin Invest 122:153–162. doi: 10.1172/JCI59660.adjacent

Thier M, März P, Otten U, Weis J, Rose-John S (1999) Interleukin-6 (IL-6) and its soluble receptor support survival of sensory neurons. J Neurosci Res 55:411–422. doi: 10.1002/(SICI)1097-4547(19990215)55:4<411::AID-JNR2>3.0.CO;2-D

Tilders FJH, DeRuk RH, Van Dam AM, Vincent VAM, Schotanus K, Persoons JHA (1994) Activation of the hypothalamus-pituitary-adrenal axis by bacterial endotoxins: routes and intermediate signals. Psychoneuroendocrinology 19:209–232. doi: 10.1016/0306-4530(94)90010-8

Timper K, Denson JL, Steculorum SM, Heilinger C, Engström-Ruud L, Wunderlich CM, Rose-John S, Wunderlich FT, Brüning JC (2017) IL-6 improves energy and glucose homeostasis in obesity via enhanced central IL-6 trans-signaling. Cell Rep 19:267–280. doi: 10.1016/j.celrep.2017.03.043

Tokita K, Armstrong WE, St John SJ, Boughter Jr. JD (2014) Activation of lateral hypothalamus-projecting parabrachial neurons by intraorally delivered gustatory stimuli. Front Neural Circuits 8:article 86. doi: 10.3389/fncir.2014.00086

REFERENCES

Toni R, Jackson IM, Lechan RM (1990) Neuropeptide-Y-immunoreactive innervation of thyrotropin-releasing hormone-synthesizing neurons in the rat hypothalamic paraventricular nucleus. Endocrinology 126:2444–2453.

Trautwein C, Rakemann T, Niehof M, Rose-John S, Manns MP (1996) Acute-phase response factor, increased binding, and target gene transcription during liver regeneration. Gastroenterology 110:1854–1862. doi: 10.1053/gast.1996.v110.pm8964411

Tschöp M, Smiley DL, Heiman ML (2000) Ghrelin induces adiposity in rodents. Nature 407:908–913. doi: 10.1038/35038090

Turton MD, O'Shea D, Gunn I, Beak SA, Edwards CM, Meeran K, Choi SJ, Taylor GM, Heath MM, Lambert PD, Wilding JP, Smith DM, Ghatei MA, Herbert J, Bloom SR (1996) A role for glucagon-like peptide-1 in the central regulation of feeding. Nature 379:69–72.

Udagawa N, Takahashi N, Katagiri T, Tamura T, Wada S, Findlay DM, Martin TJ, Hirota H, Taga T, Kishimoto T, Suda T (1995) Interleukin-6 induction of osteoclast differentiation depends on IL-6 receptors expressed on osteoblastic cells but not on osteoclast progenitors. J Exp Med 182:1461–1468.

Ueki K, Kondo T, Kahn CR (2004) Suppressor of cytokine signaling 1 (SOCS-1) and SOCS-3 cause insulin resistance through inhibition of tyrosine phosphorylation of insulin receptor substrate proteins by discrete mechanisms. Mol Cell Biol 24:5434–5446. doi: 10.1128/MCB.24.12.5434

Utsuyama M, Hirokawa K (2002) Differential expression of various cytokine receptors in the brain after stimulation with LPS in young and old mice. Exp Gerontol 37:411–420. doi: 10.1016/S0531-5565(01)00208-X

Valkanova V, Ebmeier KP, Allan CL (2013) CRP, IL-6 and depression: A systematic review and meta-analysis of longitudinal studies. J Affect Disord 150:736–744. doi: 10.1016/j.jad.2013.06.004

Vallières L, Rivest S (1997) Regulation of the genes encoding interleukin-6, its receptor, and gp130 in the rat brain in response to the immune activator lipopolysaccharide and the proinflammatory cytokine interleukin-1 beta. J Neurochem 69:1668–1683.

Vallières L, Rivest S (1999) Interleukin-6 is a needed proinflammatory cytokine in the prolonged neural activity and transcriptional activation of corticotropin-releasing factor during endotoxemia. Endocrinology 140:3890–3903. doi: 10.1210/endo.140.9.6983

van Dam M, Müllberg J, Schooltink H, Stoyan T, Brakenhoff JPJ, Graeve L, Heinrich PC, Rose-John S (1993) Structure-function analysis of interleukin-6 utilizing human/murine chimeric molecules: Involvement of two separate domains in receptor binding. J Biol Chem 268:15285–15290.

Van Damme J, Cayphas S, Van Snick J, Conings R, Put W, Lenaerts JP, Simpson RJ, Billiau A (1987) Purification and characterization of human fibroblast-derived hybridoma growth factor identical to T-cell-derived B-cell stimulatory factor-2 (interleukin-6). FEBS J 168:543–550. doi: 10.1111/j.1432-1033.1987.tb13452.x

van der Meijden M, Gage J, Breen EC, Taga T, Kishimoto T, Martínez-Maza O (1998) IL-6 receptor (CD126'IL-6R') expression is increased on monocytes and B lymphocytes in HIV infection. Cell Immunol 190:156–166. doi: 10.1006/cimm.1998.1387

Van Snick J, Cayphas S, Szikora J-P, Renauld J-C, Roost E Van, Boon T, Simpson RJ (1988) cDNA cloning of murine interleukin-HP1: homology with human interleukin 6. Eur J Immunol 18:193–197. doi: 10.1002/eji.1830180202

Van Snick J, Cayphast S, Vinkt A, Uyttenhove C, Pierre G, Rubirat MR, Simpson RJ (1986) Purification and NH2-terminal amino acid sequence of a T-cell-derived lymphokine with growth factor activity for B-cell hybridomas. Proc Natl Acad Sci 83:9679–9683.

Van Tubergen E, Vander Broek R, Lee J, Wolf G, Carey T, Bradford C, Prince M, Kirkwood KL, D'Silva NJ (2011) Tristetraprolin regulates interleukin-6, which is correlated with tumor progression in patients with head and neck squamous cell carcinoma. Cancer 117:2677–2689. doi: 10.1002/cncr.25859

Van Wagoner NJ, Oh JW, Repovic P, Benveniste EN (1999) Interleukin-6 (IL-6) production by astrocytes: autocrine regulation by IL-6 and the soluble IL-6 receptor. J Neurosci 19:5236–5244.

Vickers MH, Breier BH, Cutfield WS, Hofman PL, Gluckman PD (2000) Fetal origins of hyperphagia, obesity, and hypertension and postnatal amplification by hypercaloric nutrition. Am J Physiol Endocrinol Metab 279:E83–E87. doi: 10.1210/jcem-72-2-277

Voorhees JL, Tarr AJ, Wohleb ES, Godbout JP, Mo X, Sheridan JF, Eubank TD, Marsh CB (2013) Prolonged restraint stress increases IL-6, reduces IL-10, and causes persistent depressive-like behavior that is reversed by recombinant IL-10. PLoS One 8:e58488. doi: 10.1371/journal.pone.0058488

Vorhees C V, Williams MT (2006) Morris water maze: procedures for assessing spatial and related forms of learning and memory. Nat Protoc 1:848–858. doi: 10.1038/nprot.2006.116.Morris

Waage A, Slupphaug G, Shalaby R (1990) Glucocorticoids inhibit the production of IL6 from monocytes, endothelial cells and fibroblasts. Eur J Immunol 20:2439–2443. doi: 10.1002/eji.1830201112

Waise TZ, Toshinai K, Naznin F, NamKoong C, Moin ASM, Sakoda H, Nakazato M (2015) One-day high-fat diet induces inflammation in the nodose ganglion and hypothalamus of mice. Biochem Biophys Res Commun 464:1157–1162. doi: 10.1016/j.bbrc.2015.07.097

Walev I, Vollmer P, Palmer M, Bhakdi S, Rose-John S (1996) Pore-forming toxins trigger shedding of receptors for interleukin 6 and lipopolysaccharide. Proc Natl Acad Sci 93:7882–7887. doi: 10.1073/pnas.93.15.7882

Wallenius K, Wallenius V, Sunter D, Dickson SL, Jansson J-O (2002a) Intracerebroventricular interleukin-6 treatment decreases body fat in rats. Biochem Biophys Res Commun 293:560–565. doi: 10.1016/s0006-291x(02)00230-9

Wallenius V, Wallenius K, Ahrén B, Rudling M, Carlsten H, Dickson SL, Ohlsson C, Jansson J-O (2002b) Interleukin-6-deficient mice develop mature-onset obesity. Nat Med 8:75–79. doi: 10.1038/nm0102-75

Wang M, Orci L, Ravazzola M, Unger RH (2005) Fat storage in adipocytes requires inactivation of leptin's paracrine activity: Implications for treatment of human obesity. Proc Natl Acad Sci 102:18011–18016. doi: 10.1073?pnas.0509001102

Wang Z, Zhou Y-T, Kakuma T, Lee Y, Kalra SP, Kalra PS, Pan W, Unger RH (2000) Leptin resistance of adipocytes in obesity: role of suppressors of cytokine signaling. Biochem Biophys Res Commun 277:20–26. doi: 10.1006/bbrc.2000.3615

Ward LD, Howlett GJ, Discolo G, Yasukawa K, Hammacher A, Moritz RL, Simpson RJ (1994) High affinity interleukin-6 receptor is a hexameric complex consisting of two molecules each of interleukin-6, interleukin-6 receptor, and gp-130. J Biol Chem 269:23286–23289.

Wei H, Chadman KK, McCloskey DP, Sheikh AM, Malik M, Brown WT, Li X (2012) Brain IL-6 elevation causes neuronal circuitry imbalances and mediates autism-like behaviors. Biochim Biophys Acta 1822:831–842. doi: 10.1016/j.bbadis.2012.01.011

Wernstedt I, Edgley A, Berndtsson A, Fäldt J, Bergström G, Wallenius V, Jansson J-O (2006) Reduced stress- and cold-induced increase in energy expenditure in interleukin-6-deficient mice. Am J Physiol Regul Integr Comp Physiol 291:R551–R557. doi: 10.1152/ajpregu.00514.2005

REFERENCES

Werther GA, Hogg A, Oldfield BJ, McKinley MJ, Figdor R, Allen AM, Mendelsohn FAO (1987) Localization and characterization of insulin receptors in rat brain and pituitary gland using in vitro autoradiography and computerized densitometry. Endocrinology 121:1562–1570. doi: 10.1210/endo-121-4-1562

Whitham M, Chan MHS, Pal M, Matthews VB, Prelovsek O, Lunke S, El-Osta A, Broenneke H, Alber J, Brüning JC, Wunderlich FT, Lancaster GI, Febbraio MA (2012) Contraction-induced interleukin-6 gene transcription in skeletal muscle is regulated by c-Jun terminal kinase/activator protein-1. J Biol Chem 287:10771–10779. doi: 10.1074/jbc.M111.310581

WHO (2017) Obesity and overweight. http://www.who.int/mediacentre/factsheets/fs311/en/. Accessed 11 Feb 2016

Wichers MC, Kenis G, Leue C, Koek G, Robaeys G, Maes M (2006) Baseline immune activation as a risk factor for the onset of depression during interferon-alpha treatment. Biol Psychiatry 60:77–79. doi: 10.1016/j.biopsych.2005.11.024

Wiesinger MY, Haan S, Wüller S, Kauffmann ME, Recker T, Küster A, Heinrich PC, Müller-Newen G (2009) Development of an IL-6 inhibitor based on the functional analysis of murine IL-6Rα. Chem Biol 16:783–794. doi: 10.1016/j.chembiol.2009.06.010

Will MJ, Franzblau EB, Kelley AE (2004) The amygdala is critical for opioid-mediated binge eating of fat. Neuroreport 15:1857–1860.

Woolley JD, Lee BS, Fields HL (2006) Nucleus accumbens opioids regulate flavor-based preferences in food consumption. Neuroscience 143:309–317. doi: 10.1016/j.neuroscience.2006.06.067

Wu Q, Palmiter RD (2011) GABAergic signaling by AgRP neurons prevents anorexia via a melanocortin-independent mechanism. Eur J Pharmacol 660:21–27. doi: 10.1016/j.ejphar.2010.10.110

Wu YY, Bradshaw RA (1996) Induction of neurite outgrowth by interleukin-6 is accompanied by activation of Stat3 signaling pathway in a variant PC12 cell (E2) line. J Biol Chem 271:13023–13032. doi: 10.1074/jbc.271.22.13023

Wynn JK, Dawson ME, Schell AM, McGee M, Salveson D, Green MF (2004) Prepulse facilitation and prepulse inhibition in schizophrenia patients and their unaffected siblings. Biol Psychiatry 55:518–523. doi: 10.1016/j.biopsych.2003.10.018

Xu H, Barnes GT, Yang Q, Tan G, Yang D, Chou CJ, Sole J, Nichols A, Ross JS, Tartaglia LA, Chen H (2003) Chronic inflammation in fat plays a crucial role in the development of obesity-related insulin resistance. J Clin Invest 112:1821–1830. doi: 10.1172/jci19451

Yakar S, Rosen CJ, Beamer WG, Ackert-Bicknell CL, Wu Y, Liu J-L, Ooi GT, Setser J, Frystyk J, Boisclair YR, LeRoith D (2002) Circulating levels of IGF-1 directly regulate bone growth and density. J Clin Invest 110:771–781. doi: 10.1172/JCI200215463

Yamabe T, Dhir G, Cowan EP, Wolf AL, Bergey GK, Krumholz A, Barry E, Hoffman PM, Dhib-Jalbut S (1994) Cytokine-gene expression in measles-infected adult human glial cells. J Neuroimmunol 49:171–179. doi: 10.1016/0165-5728(94)90193-7

Yamagata K, Matsumura K, Inoue W, Shiraki T, Suzuki K, Yasuda S, Sugiura H, Cao C, Watanabe Y, Kobayashi S (2001) Coexpression of microsomal-type prostaglandin E synthase with cyclooxygenase-2 in brain endothelial cells of rats during endotoxin-induced fever. J Neurosci 21:2669–2677.

Yamasaki K, Taga T, Hirata Y, Yawata H, Kawanishi Y, Seed B, Taniguchi T, Hirano T, Kishimoto T (1988) Cloning and expression of the human interleukin-6 (BSF-2/IFN beta 2) receptor. Science 241:825–828.

Yan HQ, Banos MA, Herregodts P, Hooghe R, Hooghe-Peters EL (1992) Expression of interleukin

(IL)-1 beta, IL-6 and their respective receptors in the normal rat brain and after injury. Eur J Immunol 22:2963–2971. doi: 10.1002/eji.1830221131

Yang R, Lin Q, Gao HB, Zhang P (2014) Stress-related hormone norepinephrine induces interleukin-6 expression in GES-1 cells. Brazilian J Med Biol Res 47:101–109. doi: 10.1590/1414-431X20133346

Yaqoob P, Sherrington EJ, Jeffery NM, Sanderson P, Harvey DJ, Newsholme EA, Calder PC (1995) Comparison of the effects of a range of dietary lipids upon serum and tissue lipid composition in the rat. Int J Biochem Cell Biol 27:297–310.

Yasukawa K, Hirano T, Watanabe Y, Muratani K, Matsuda T, Nakai S, Kishimoto T (1987) Structure and expression of human B cell stimulatory factor-2 (BSF-2/IL-6) gene. EMBO J 6:2939–2945. doi: 10.1002/ajh.2830310408

Yi C-X, Al-Massadi O, Donelan E, Lehti M, Weber J, Ress C, Trivedi C, Müller TD, Woods SC, Hofmann SM (2012) Exercise protects against high-fat diet-induced hypothalamic inflammation. Physiol Behav 106:485–490. doi: 10.1016/j.physbeh.2012.03.021

Yin T, Taga T, Tsang ML, Yasukawa K, Kishimoto T, Yang YC (1993) Involvement of IL-6 signal transducer gp130 in IL-11-mediated signal transduction. J Immunol 151:2555–2561. doi: 0022-1 767/93/1515-2555$02.00/0

Yoshida K, Taga T, Saito M, Suematsu S, Kumanogoh A, Tanaka T, Fujiwara H, Hirata M, Yamagami T, Nakahata T, Hirabayashi T, Yoneda Y, Tanaka K, Wang WZ, Mori C, Shiota K, Yoshida N, Kishimoto T (1996) Targeted disruption of gp130, a common signal transducer for the interleukin 6 family of cytokines, leads to myocardial and hematological disorders. Proc Natl Acad Sci 93:407–411. doi: 10.1073/pnas.93.1.407

Zahs A, Bird MD, Ramirez L, Choudhry MA, Kovacs EJ (2013) Anti-IL-6 antibody treatment but not IL-6 knockout improves intestinal barrier function and reduces inflammation after binge ethanol exposure and burn injury. Shock 39:373–379. doi: 10.1097/SHK.0b013e318289d6c6

Zalcman S, Murray L, Dyck DG, Greenberg AH, Nance DM (1998) Interleukin-2 and -6 induce behavioral-activating effects in mice. Brain Res 811:111–121. doi: 10.1016/S0006-8993(98)00904-4

Zeng H, Horie K, Madisen L, Pavlova MN, Gragerova G, Rohde AD, Schimpf BA, Liang Y, Ojala E, Kramer F, Roth P, Slobodskaya O, Dolka I, Southon E a, Tessarollo L, Bornfeldt KE, Gragerov A, Pavlakis GN, Gaitanaris GA (2008) An inducible and reversible mouse genetic rescue system. PLoS Genet 4:e1000069. doi: 10.1371/journal.pgen.1000069

Zhang J-M, An J (2007) Cytokines, inflammation, and pain. Int Anesthesiol Clin 45:27–37. doi: 10.1097/AIA.0b013e318034194e.Cytokines

Zhang J, Dublin P, Griemsmann S, Klein A, Brehm R, Bedner P, Fleischmann BK, Steinhäuser C, Theis M (2013) Germ-line recombination activity of the widely used hGFAP-Cre and nestin-Cre transgenes. PLoS One 8:e82818. doi: 10.1371/journal.pone.0082818

Zhang X, Zhang G, Zhang H, Karin M, Bai H, Cai D (2008) Hypothalamic IKKβ/NF-κB and ER stress link overnutrition to energy imbalance and obesity. Cell 135:61–73. doi: 10.1016/j.cell.2008.07.043

Zhang Y, Riesterer C, Ayrall A-M, Sablitzky F, Littlewood TD, Reth M (1996) Inducible site-directed recombination in mouse embryonic stem cells. Nucleic Acids Res 24:543–548. doi: 10.1093/nar/24.4.543

Zhong Z, Wen Z, Darnell JE (1994) Stat3: a STAT family member activated by tyrosine phosphorylation in response to epidermal growth factor and interleukin-6. Science 264:95–98. doi: 10.1126/science.8140422

REFERENCES

Zhou D, Kusnecov AW, Shurin MR, DePaoli M, Rabin BS (1993) Exposure to physical and psychological stressors elevates plasma interleukin 6: relationship to the activation of hypothalamic-pituitary-adrenal axis. Endocrinology 133:2523–2530.

Zhu Y, Romero MI, Ghosh P, Ye Z, Charnay P, Rushing EJ, Marth JD, Parada LF (2001) Ablation of NF1 function in neurons induces abnormal development of cerebral cortex and reactive gliosis in the brain. Genes Dev 15:859–876. doi: 10.1101/gad.862101

Zilberstein A, Ruggieri R, Korn JH, Revel M (1986) Structure and expression of cDNA and genes for human interferon-beta-2, a distinct species inducible by growth-stimulatory cytokines. EMBO J 5:2529–2537.